RÉPUBLIQUE FRANÇAISE
Liberté Égalité Fraternité

Université de Toulouse

Doctorat de l'Université de Toulouse

préparé à l'INSA Toulouse

Comprendre et exploiter le métabolisme d'overflow en biotechnologie

Thèse présentée et soutenue, le 23 septembre 2025 par

Thomas GOSSELIN

École doctorale
SEVAB - Sciences Ecologiques, Vétérinaires, Agronomiques et Bioingenieries

Spécialité
Ingénieries microbienne et enzymatique

Unité de recherche
TBI - Toulouse Biotechnology Institute, Bio & Chemical Engineering

Thèse dirigée par
Stéphanie HEUX et Pierre MILLARD

Composition du jury
M. Stéphane GUILLOUET, Président, INSA Toulouse
M. Benjamin PFEUTY, Rapporteur, CNRS Hauts-de-France
Mme Sophie COLOMBIE, Rapporteure, INRAE Nouvelle-Aquitaine-Bordeaux
M. Manish KUSHWAHA, Rapporteur, INRAE Île-de-France - Jouy-en-Josas - Antony
Mme Carole CAMARASA, Examinatrice, INRAE Occitanie-Montpellier
Mme Stéphanie HEUX, Directrice de thèse, INRAE Occitanie-Toulouse
M. Pierre MILLARD, Co-directeur de thèse, INRAE Occitanie-Toulouse

Membres invités
Mme Nathalie POUPIN, INRAE Occitanie-Toulouse

“Living matter evades the decay to equilibrium”

— **Erwin Schrödinger, What is Life?**

Abstract

Overflow metabolism is a highly conserved phenomenon that refers to the production of partially oxidized metabolites (such as acetate, ethanol, or lactate) by microbial cells grown on glycolytic substrates, even under aerobic conditions. Long considered wasteful by-products, overflow metabolites are increasingly recognized as part of a regulated and adaptive response to nutrient-rich environments.

In this thesis, we propose a general conceptual framework to investigate overflow metabolism across species. Drawing on thermodynamic constraints, metabolic control theory, and systems-level observations, we identify general principles that govern the onset and regulation of overflow metabolism. Central to this framework is the notion that the accumulation of extracellular by-products (such as ethanol or acetate), along with the interplay between glycolysis and overflow pathways, regulates the flux of overflow metabolites and may led to their co-utilization with glycolytic substrates. The reversibility of this flux is accompanied by beneficial effects on cell physiology: acetate (and ethanol), far from being merely toxic waste, can in fact enhance microbial growth under glycolytic limitations.

We tested the robustness and universality of this framework by comparing three evolutionarily distant model organisms: *Escherichia coli*, a bacterium that excretes acetate; *Saccharomyces cerevisiae*, a Crabtree-positive yeast that excretes ethanol; and *Komagataella phaffii*, a Crabtree-negative yeast that produces significantly less ethanol. Despite differences in cellular architecture and regulatory mechanisms, all these organisms exhibit overflow metabolism that appears to be governed by similar underlying principles. Our results demonstrate a remarkable conservation of metabolic functioning across domains of life.

Finally, we explored the implications of these findings for industrial biotechnology. Overflow metabolism often limits product yields in microbial cell factories, yet better understanding its functioning and regulation opens new avenues for metabolic engineering. By modulating the parameters that govern overflow, it is possible to redirect fluxes toward desired products, enhance bioprocess efficiency, and improve robustness under production conditions. Our work thus contributes both to the fundamental understanding of cellular metabolism and to its rational manipulation for biotechnological innovation.

Résumé

Le métabolisme d'overflow est un phénomène hautement conservé qui désigne la production de métabolites partiellement oxydés (tels que l'acétate, l'éthanol ou le lactate) par des cellules microbiennes cultivées sur des substrats glycolytiques, même en conditions aérobies. Longtemps considérés comme des sous-produits inutiles, les métabolites d'overflow sont de plus en plus reconnus comme faisant partie d'une réponse régulée et adaptative à des environnements riches en nutriments.

Dans cette thèse, nous proposons un cadre conceptuel générique pour étudier le métabolisme d'overflow de différentes espèces. En nous appuyant sur les contraintes thermodynamiques, la théorie du contrôle métabolique et des observations à l'échelle des systèmes, nous identifions des principes généraux qui gouvernent l'apparition et la régulation du métabolisme d'overflow. Ce cadre repose notamment sur l'idée que l'accumulation de sous-produits extracellulaires (comme l'éthanol ou l'acétate), combinée à l'interaction entre la glycolyse et les voies d'overflow, régule le flux de métabolites d'overflow et peut conduire à leur co-utilisation avec les substrats glycolytiques. La réversibilité de ce flux s'accompagne d'effets bénéfiques sur la physiologie cellulaire : l'acétate (et l'éthanol), loin d'être de simples déchets toxiques, peuvent en réalité favoriser la croissance microbienne en conditions de limitation glycolytique.

Nous avons testé la robustesse et l'universalité de ce cadre en étudiant des organismes modèles évolutivement éloignés : *Escherichia coli*, une bactérie qui excrète de l'acétate ; *Saccharomyces cerevisiae*, une levure Crabtree-positive qui excrète de l'éthanol ; et *Komagataella phaffii*, une levure Crabtree-négative qui produit nettement moins d'éthanol. Malgré des différences d'architecture cellulaire et de mécanismes de régulation, tous ces organismes présentent un métabolisme d'overflow régi par des principes sous-jacents similaires. Nos résultats révèlent une remarquable conservation du fonctionnement métabolique à travers les domaines du vivant.

Enfin, nous avons exploré les implications de ces résultats pour la biotechnologie industrielle. Le métabolisme d'overflow limite souvent les rendements des produits dans les bioraffineries microbiennes, mais une meilleure compréhension de son fonctionnement et de sa régulation ouvre de nouvelles perspectives pour l'ingénierie métabolique. En modulant les paramètres qui gouvernent l'overflow, il devient possible de rediriger les flux vers des produits d'intérêt, d'améliorer l'efficacité des bioprocédés et d'accroître la robustesse en conditions de production. Notre travail contribue ainsi à la fois à la compréhension fondamentale du métabolisme cellulaire et à sa manipulation rationnelle pour l'innovation biotechnologique.

Remerciements

Cette thèse n'aurait pas pu voir le jour si bon nombre de personnes n'auraient pas été là pour me soutenir, moralement comme scientifiquement.

A Stéphanie Heux, ma directrice de thèse, je tiens à te remercier pour la patience et la présence dont tu as su faire part au cours de ces trois années.

A Pierre Millard, mon co-encadrant de thèse, merci pour m'avoir donné la chance de faire mes preuves, m'avoir fait confiance sur ces 3 années et offert cette liberté qui a fait de ce travail ce beau travail dont nous pouvons être fier !

A Nico Classens, pour avoir bien voulu avec Carole Camarasa, m'aiguiller et participer à mon comité de suivi de thèse.

A Benjamin Pfeuty, Sophie Colombié et Manish Kushwaha pour avoir accepté d'être les rapporteurs de ce travail et à Carole Camarasa, Nathalie Poupin et Stéphane Guillouet pour avoir accepté de participer à ce jury.

A Gilles Truan, directeur du Toulouse Biotechnology Insitute (TBI, Toulouse), pour m'avoir accueilli au sein de son unité.

A l'INRAE et la région Occitanie pour m'avoir permis de réaliser ces travaux.

A l'EUR BioEco pour m'avoir permis de collaborer avec l'université de Bâle grâce à son programme de mobilité et à Mattia Zampieri pour son accueil au sein de son laboratoire. A Tobbia et Alexandra pour votre accueil et votre soutien au cours de ce séjour.

A la plateforme MetaToul (TBI, Toulouse) pour m'avoir offert la possibilité d'accéder à leurs ressources analytiques et à leur expertise.

A tous les membres de l'équipe MetaSys/I_2M et membres de la plateforme Metatoul, Denis Jallet, le fier magicien sombre du dieu de la biomol, disons que selon le sacrifice accordé, on peut s'accorder un 50/50. Sandrine pour ton soutien. Mais aussi à Edern Cahoreau, rotater or not rotater, the eternal question… Nina (tchinouuu), Floriant Belvert, Cécilia Bergès, Lindsay Peyriga, Maud Heuillet. Pour votre réactivité et votre aide sans faille. Ma stagiaire Chloé pour ton travail assidu et ton enthousiasme !

A Sara Castaño-Cerezo et Anthony, pour nos discussions sur le métabolisme des levures et sur la production de mévalonate.

A notre fier groupe d'EAD21, Yannick, Thibaut, Laura, Thomas pour nos discussions et nos rires partagés.

Brice Enjalbert, pour m'avoir permis de superviser des étudiants, une expérience qui m'a à la fois enrichi et peut-être engendré une vocation ! Mais aussi pour nos discussions sur les transitions carbonés !

Dorian Grégnagnin. Gregnangnin ragna…… Dorian, pour avoir supporté mes interruptions multiples, et mes craquages de fin de thèse !

A Jeanne Gallard, pour nos discussions aussi folles que divertissantes quand l'esprit craquelait.

A Lucie, Adilya, pour votre humour et votre soutien tant scientifiquement que moralement. Peut-être réussirons nous un jour à ce que Lucie dépasse la limite de 2 heures par repas ?

A Margaux & Quentin, pour ces soirées et découvertes ensemble !

Et un remerciement extrememement particulier pour une personne de toute première importance qui je ne sais pas quel miracle ne s'est retrouvé dans ces remerciements initialement, je parle bien sûr du grand, que dis-je, l'immense Loïc Legregam. Merci pour tout, notre soutien mutuel durant cette thèse a été un souffle d'oxygène quand il venait à manquer.. Merci pour avoir permis tous ces fits, comme on pourrait le dire : « Elle pourtant il fit », référence subtil à notre cher Galilée, ce qui te convient très bien je trouve. Bon courage pour la suite, puisse nos chemins se recroiser cher ami !

A mes frères et ma mère pour m'avoir soutenu sans limite depuis toujours, sans qui je ne serais pas là à écrire ces remerciements. Mimouche, nous sommes ton héritage…

Enfin à toi Camille, pour ton soutien sans faille, tes attentions et pour avoir supporté mon esprit occupé au cours de cette thèse

Table of Content

Abbreviations 5

List of figures 7

Contributions to side projects: 9

General context 11

Chapter 1 Introduction 13

1.1 The classical view of overflow metabolism emerging from diauxic growth 15

1.2 Overflow fluxes are controlled by overflow pathways, glycolysis, and the TCA cycle 16

1.3 The high reversibility of overflow metabolism uncouples carbon oxidation from nutrient uptake 20

1.4 Thermodynamic control of overflow fluxes can lead to co-consumption of overflow metabolites with glycolytic nutrients 22

1.5 Low uptake of glycolytic nutrients enhances co-utilization of overflow metabolites 23

1.6 Overflow metabolites are global regulators of cellular metabolism and physiology 24

1.7 Overflow metabolites are not toxic *per se* and can be beneficial to cells 25

1.8 Similar principles apply to other species and overflow by-products 26

1.9 Controlling overflow metabolism for biotechnology 27

1.10 Overflow metabolism in health and disease 29

1.11 Toward a general framework to investigate overflow metabolism 30

2. Thesis Outline 32

3. References 33

Chapter 2 Acetate is a beneficial nutrient for *E. coli* at low glycolytic flux 43

1. Introduction 44

2 Results 44

2.1 Model-driven hypotheses on the interplay between glucose and acetate metabolism in *Escherichia coli* 44

2.2 Enhanced acetate utilization at low glycolytic flux buffers carbon uptake 46

2.3 The glycolytic flux determines the acetate concentration threshold at which the acetate flux reverses. 48

2.4 The Acetate enhances *E. coli* growth at low glycolytic flux. 50

2.5 At low glycolytic flux, acetate activates *E. coli* metabolism and growth at the transcriptional level. 52

2.6 Acetate-enhances growth is supported by the Pta-AckA pathway. 53

2.7 Acetate boosts growth of *E. coli* on glycerol and galactose. 54

3. Discussion 55

4. Materials and Methods 60

4.1 Strains. 60
4.2 Growth conditions. 60
4.3 Transcriptomics experiments. 60
4.4 Metabolomics experiments. 60
4.5 Flux calculation. 60
4.6 Kinetic modeling. 60
4.7 Sensitivity analyses. 61
4.8 Statistical analyses. 61
5. References 62
Chapter 3 Acetate as a metabolic booster for *Escherichia coli*-based bioproduction, from fundamental knowledge to biotechnology application 65
1. Introduction 66
2. Results 67
2.1 Model-guided strategy to evaluate acetate's effect on bioproduction 67
2.2 Predictions for an acetyl-CoA-sensitive production pathway 68
2.3 Validation using mevalonate production 69
2.4 Predictions for an acetyl-CoA-insensitive production pathway 72
2.5 Validation with 3-hydroxypropionate production 73
3. Discussion 75
4. Materials and Methods 77
4.1 Strains construction 77
4.2. Cultivations 77
4.3 Metabolomics 78
4.3.1 Exometabolome analysis 78
4.3.2 Intraceullar acetyl-CoA quantification 78
4.3.3 Isotopic analyses of mevalonate 78
4.3.4 Extracellular flux calculations 79
4.3.5 Kinetic modeling 79
4.4 Statistical analyses 79
5. References 80
Chapter 4 Ethanol overflow of yeast: Toward the control of Crabtree effect? 83
1. Introduction 84
2. Results 85
2.1 Is ethanol flux thermodynamically controlled by its extracellular concentration? 85
2.2 Is the switch from ethanol production to consumption governed by an interplay between glycolytic and overflow flux? 87

2.3 Under metabolic perturbations, can ethanol become beneficial for yeast growth? 88
2.4 Can we relate the principles proposed in Chapter 1 to the crabtree effect ? 89
3. Discussion 91
4. Materials and Methods 93
4.1 Strains, medium and cultivation conditions 93
4.2 Biomass and extracellular metabolite concentrations 93
4.3 Extracellular flux calculations 94
5. References 94
Chapter 5 Conclusion and Outlook 97
1. Chapter perspectives 98
2. General perspective: Towards a unified theory of overflow metabolism 102
3. References: 106
Annexes 111
Annex 1: MultiNMRFit: A software to fit 1D and pseudo-2D NMR spectra 113
Annex 2: Acetate promotes *Escherichia coli* metabolic adaptation 123
Annex 3: Support for International Mobility 2024 – Report 143

Abbreviations

3HP: 3-hydroxypropionate

2-DG: 2-deoxyglucose

AAD: Acetaldehyde

AcP: Acetyl-Phosphate

Ace: Acetate

acetyl-CoA/AcCoA/: Acetyl Coenzyme A

Acs: acetyl-CoA synthetase

AckA: acetate kinase

ACN: Acetonitril

Adh: Alcohol DeHydrogenase

αMG/aMG: α-methyl-glucose

ATP/ADP/AMP: Adenosine Tri/Di/MonoPhosphate

atoB: acetoacetyl-CoA thiolase

CHO: Chinese Hamster Ovaries cells

CO2: Carbon dioxyde

D2O: Deuterium Oxyde

DW/DCW: Dry Cellular Weight

E. coli: *Escherichia coli*

Eth: Ethanol

Glc: Glucose

HMGS: HMG-CoA synthase

IPTG: isopropyl β-D-1-thiogalactopyranoside

KM: Affinity constant

Lac: Lactose

LC: Liquid Chromatography

Ldh: Lactate DeHydrogenase

Mcr: malonyl-CoA reductase

MeOH: Methanol

MS: Mass spectrometry

NADH/NAD+: Nicotinamide adenine dinucleotide

NADPH: Nicotinamide adenine dinucleotide phosphate

NMR: Nuclear Magnetic Resonance

OD: Optical density

P. pastoris: *Pichia Pastoris*

Pdh: Pyruvate DeHydrogenase

PfkA: Phosphofructokinase A

Pgi: Phosphoglucoisomerase

Pta: phosphate acetyltransferase

PTS: phosphotransferase system

Pyr: Pyruvate

S. cerevisiae: *Saccharomyces cerevisiae*

SCFA: Short Chain Fatty Acid

TCA: TriCarboxylic Acid cycle

TF: Transcription Factor

TSP: (3-(trimethylsilyl)-1-propanesulfonic acid-tetra deuterated

Vmax: Maximal reaction speed

WT: Wild Type strain

List of figures

Chapter 1 - Introduction

Figure 1. Overflow metabolism induces diauxic shifts in yeast, bacterial and mammalian cells. 16

Figure 2. Identification of the pathways controlling overflow fluxes. 19

Figure 3. Isotope labeling experiments demonstrate the high reversibility of overflow pathways. 21

Figure 4. Overflow fluxes are thermodynamically controlled by the concentration of overflow metabolites..... 23

Figure 5. Impact of reducing the glycolytic flux on overflow fluxes. 24

Figure 6. Function and regulation of overflow metabolism (in green), roles of overflow metabolites (in blue) and applications (in orange). 31

Chapter 2 - Acetate is a beneficial nutrient for *E. coli* at low glycolytic flux

Figure 1. Predicted response of *Escherichia coli* to glycolytic and acetate perturbations.....46

Figure 2. Glycolytic control of *Escherichia coli* metabolism.....48

Figure 3. Acetate flux reversal is controlled by the glycolytic flux.....49

Figure 4. Effect of acetate on *Escherichia coli* growth on glucose.....51

Figure 5. Regulation of *Escherichia coli* transcriptome by acetate at high and low glycolytic flux.....53

Figure 6. Response of wild-type, Δpta, and Δacs strains of *E. coli* to acetate during growth on glucose (low glycolytic flux). 54

Figure 7. Response of *Escherichia coli* to acetate during growth on glycerol or galactose.....55

Figure 8. Change in pH of the cultivation medium of *E. coli* grown on glycolytic substrates plus different concentrations of αMG and acetate.....57

Figure 9. Response of *E. coli* to acetic acid.....58

Chapter 3 - Acetate as a metabolic booster for *Escherichia coli*-based bioproduction, from fundamental knowledge to biotechnology application

Figure 1. Representation (in Systems Biology Graphical Notation format, http://sbgn.org) of the glucose and acetate metabolism of a synthetic *E. coli* strain engineered for bioproduction of a product P, as implemented in the kinetic model used in the chapter.....67

Figure 2. Predicted response to glycolytic and acetate perturbations of an *Escherichia coli* strain with an acetyl-CoA-sensitive production pathway.....69

Figure 3. Impact of acetate on mevalonate production.....70

Figure 4. Predicted response to glycolytic and acetate perturbations of an *Escherichia coli* strain with an acetyl-CoA-insensitive production pathway……73

Figure 5. Impact of acetate on 3-hydroxypropionate production……..74

Figure 6. Impact of acetate with empty plasmid on (control experiment of figure 5)……75

Chapter 4 - Ethanol overflow of yeast: Toward the control of Crabtree effect?

Figure 1. *S. cerevisiae* response to ethanol exposure. (A) Ethanol flux, (B) Glucose uptake flux, (C) Growth rate, and (D) Total carbon uptake……..86

Figure 2. Glycolytic control of ethanol flux reversal. A, Ethanol flux or B, Glucose flux when BY 4741 is exposed to 40 mM of ethanol and/or 4 mM of 2DG……..87

Figure 3. Ethanol effect on *Δhxk2* growth……88

Figure 4. Impact of ethanol on *K. phaffi X33* strain……..90

Contributions to side projects:

In addition to the work detailed in the following chapters, I was also involved in several complementary projects during my PhD, which are briefly presented below.

In collaboration with the NMR Team of TBI, I have contributed to the development of a tool for versatile, open-source Python software for fitting 1D and pseudo-2D NMR spectra (i.e; MultiNMRFit). This tool supports multiple nuclei, includes models for common multiplets, allows custom signal modeling, and provides both a graphical user interface and a programmatic API. It enhances the accessibility and robustness of NMR analysis, facilitating its application in real-time metabolomics and isotope labeling studies. I contributed to the development of this tool by supplying multiple datasets for testing and validation, and by conducting software testing. I identified and reported several functional issues, which led to significant improvements in the tool's flexibility and usability. These contributions have been highlighted in a publication currently under revision. The initial article can be found in Annex 1 (MultiNMRFit: A software to fit 1D and pseudo-2D NMR spectra).

In collaboration with Loïc Legregam from the Metatoul Platform, we investigated the intracellular flux response of *Escherichia coli* to variations in glycolytic and acetate fluxes. To achieve this, we employed a high-throughput fluxomics workflow developed by L. Legregam. Together, we designed experiments and carried out bacterial cultivations, sampling, and analyses. This work was included in L. Legregam's PhD thesis and will be valorized in an upcoming publication.

In collaboration with Lucas Devlin, Brice Enjalbert, and Virginia Oudard (team PEEP @ TBI), we investigated how *Escherichia coli* adapts its metabolism during nutrient shifts, focusing on the lag phase following carbon source transitions. I contributed to the experimental design and conducted the metabolomic analyses. Our findings show that acetate—typically viewed as a by-product of high-glucose metabolism—can significantly reduce the duration of the lag phase, even at very low concentrations. This highlights a previously unrecognized role for acetate as a modulator of metabolic readiness in *E. coli*. The results will soon be validated in a publication. The initial draft of this article can be found in Annex 2 (Acetate promotes bacterial adaptation).

In collaboration with The Metatoul Platform, we studied the intracellular response of *E. coli* to acetate exposure, building on previous findings that acetate can act as a beneficial co-substrate rather than merely a toxic by-product. The aim was to explore in greater detail the timing and mechanisms of metabolic and transcriptional regulation. A novel method developed by Nina Lager-Lachaud (MetaToul Platfom) was used to simultaneously quantify intracellular metabolites and mRNAs from a single biological sample. This integrative approach enables rapid metabolic quenching and provides high-quality data, ideal for analyzing *E. coli*'s coordinated response to an acetate pulse. My contribution focused on analyzing the resulting omics data. I obtained EUR BioEco funding to carry out a research stay in Mattia Zampieri's lab at the University of Basel, where I was trained to use their omics data analysis tools. This allowed me to identify the dynamics of the transcriptional network over time, shedding light

on *E. coli*'s temporal adaptation mechanisms in response to acetate. The report of this work can be found in Annex 3 (Support for International Mobility 2024 – Report)

Publication accepted

- Millard P, Gosselin-Monplaisir T, Uttenweiler-Joseph S, Enjalbert B. Acetate is a beneficial nutrient for *E. coli* at low glycolytic flux. EMBO Journal. 2023 Aug 1;42(15):e113079. doi: 10.15252/embj.2022113079.

Publications in revision:

- Gosselin-Monplaisir T, Enjalbert B, Uttenweiler-Joseph S, Portais J-C, Heux S, Millard P. Overflow metabolism in bacterial, yeast, and mammalian cells: different names, same game. Submitted to Molecular Systems Biology.
- Millard P, Le Grégam L, Dubiley S, Gosselin-Monplaisir T, Lippens G, Charlier C. MultiNMRFit: A software to fit 1D and pseudo-2D NMR spectra. Submitted to Bioinformatics. (The initial article can be found in Annex 1)

Publications in preparation

- Devlin L, Oudard V, Barthe M, Gosselin-Monplaisir T, Cocaign-Bousquet M, Millard P and Enjalbert B. Acetate promotes bacterial adaptation. Will be submitted to EMBO Journal. (The draft paper can be found in Annex 2)
- Gosselin-Monplaisir T, Jallet D, Harscoet E, Uttenweiler-Joseph S, Heux S, Millard P. Acetate as a metabolic booster for glucose-based bioproduction in *Escherichia coli.* Will be submitted to Metabolic Engineering.

Oral presentations:

Acetate is a beneficial nutrient at low glycolytic flux (26 - 28 November 2024, Liverpool, United-Kingdom), awarded by the "best oral presentation".

From toxic waste to beneficial nutrient: acetate boosts *E. coli* growth at low glycolytic flux (19 to 21 July 2023, Biosynsys, Toulouse, France).

Poster:

Acetate is a beneficial nutrient at low glycolytic flux (30 of June to 3 of July 2024, Rotterdam, Netherlands, European Congress of Biotechnology).

General context

This work has been conducted in TBI, Toulouse Biotechnology Institute, Bio & Chemical Engineering (UMR792, UMR5504, CNRS, INRAE, INSA) which combines life sciences and engineering to pursue a multi-scale, multidisciplinary, and interdisciplinary scientific strategy. Its research addresses key challenges in the bioeconomy.

Microorganisms such as *Escherichia coli* and yeasts are central pillars of modern industrial biotechnology. They serve as robust, versatile platforms for the production of biofuels, pharmaceuticals, enzymes, and specialty chemicals. Their rapid growth, genetic tractability, and well-characterized metabolism make them ideal candidates for large-scale bioprocesses. However, despite decades of optimization, a major bottleneck persists across many production systems: the phenomenon of overflow metabolism.

When grown with high concentration of glycolytic substrates, cells often redirect excess flux into the excretion of partially oxidized metabolites, such as acetate in *E. coli* or ethanol in *S. cerevisiae*. While this strategy allows for rapid energy generation and growth under certain conditions, it is detrimental in biotechnological context. The accumulation of overflow by-products can inhibit cell growth, reduce product yield, complicate downstream processing, and destabilize engineered metabolic pathways. Consequently, controlling overflow metabolism remains one of the key challenges in the development of high-performance microbial factories.

The aim of this thesis is to better understand the mechanistic basis of overflow metabolism, with the goal of identifying generalizable principles that can be applied to metabolic engineering. By comparing model organisms that exhibit overflow profiles and integrating concepts from systems biology, thermodynamics, and metabolic regulation, this work seeks to uncover how overflow metabolism is triggered, maintained, and potentially mitigated. In doing so, it provides a conceptual framework for rational strain design and process optimization.

Beyond its implications for industrial biotechnology, overflow metabolism is also relevant to health and disease. In rapidly proliferating cells including cancer cells fermentation-like behavior reminiscent of microbial overflow has been observed, such as the Warburg effect. Understanding how and why cells adopt such strategies across different biological contexts may ultimately contribute to a more unified understanding of cellular growth control, with potential applications in both engineering and medicine.

Chapter 1
Introduction

This work has been submitted and is under review in Molecular Systems Biology and modifications have been introduced in the chapter below.

Contribution: In this work, I recovered the full paper corpus, contribute to the first and following versions of the manuscript, gathered data from papers, and performed data visualization.

Overflow metabolism refers to the phenomenon whereby cells excrete metabolic waste products in conditions where theoretically, they could completely oxidize nutrients such as glucose. This phenomenon is observed in virtually all living organisms. First reported by Pasteur in 1857 (although later named the Crabtree effect) for ethanol production by the yeast *Saccharomyces cerevisiae* (Pasteur, 1857), Harden observed the production of acetate by the bacterium *Escherichia coli* in 1901 (Harden, 1901), while the production of lactate by mammalian cells was elucidated in the 1920s and named the Warburg effect in cancer cells (Warburg and Minami, 1923). This ubiquitous overflow phenomenon represents a loss of carbon and energy for cells because the produced compounds are first excreted instead of being directly used for growth. Moreover, since overflow by-products inhibit cellular growth, they are traditionally considered toxic waste (Brown et al., 1981; Lao and Toth, 1997; Luli and Strohl, 1990). Understanding why cells produce self-inhibiting molecules instead of using glycolytic substrates more efficiently remains an intriguing question that has driven metabolic studies for more than a century.

Overflow metabolism also underlies a wide range of applications (Kiefer et al., 2021; Rabinowitz and Enerbäck, 2020; Van Der Hee and Wells, 2021; Zhang et al., 2022). Relevant overflow by-products in healthcare include lactate produced by host cells and short chain fatty acids (SCFAs, e.g., acetate, propionate) produced mainly by the gut microbiota (Cummings, 1981; Van Der Hee and Wells, 2021). Lactate, a circulating metabolite with a long-established reputation as a detrimental waste product, has in recent years been recognized as a major carbon and energy shuttle between organs (Rabinowitz and Enerbäck, 2020), and dysregulation of lactate metabolism is observed in cancer, obesity, and other diseases (Brooks, 2018). Similarly, dysregulation of microbiota-derived SCFA metabolism leads to microbiome-related disorders (Van Der Hee and Wells, 2021). Understanding overflow metabolite dynamics, as well as the roles and responses of host cells and of the gut microbiome to these dynamics, could significantly improve healthcare. In biotechnology, overflow metabolites are potential resources in renewable feedstocks (Kiefer et al., 2021; Zhang et al., 2022); however, their presence or accumulation in bioprocesses diminishes productivity by inhibiting growth and diverting carbon fluxes that could otherwise be used to synthesize biomass or valuable compounds (De Mey et al., 2007; Glacken et al., 1986; Luli and Strohl, 1990; Torres et al., 2018; Zhang et al., 2022). Alternatively, the co-utilization of overflow metabolites with glycolytic substrates may mitigate growth inhibition while recycling by-products (Mulukutla et al., 2012; Nam et al., 2024; Raamsdonk et al., 2001). Despite intensive efforts to limit their accumulation or increase their utilization, overflow by-products still pose a significant challenge in biotechnology (Torres et al., 2018; Zhang et al., 2022).

1.1 The classical view of overflow metabolism emerging from diauxic growth

The preferred carbon sources of most living organisms are glycolytic substrates (Görke and Stülke, 2008) which are taken up and converted into pyruvate through glycolytic pathways (Romano and Conway, 1996) including the canonical Embden-Meyerhof-Parnas pathway (i.e. glycolysis), the Entner-Doudoroff pathway, and the pentose phosphate pathway. Pyruvate can undergo further oxidation into CO_2 through the tricarboxylic acid (TCA) cycle and derivative pathways, sustaining the biosynthesis of cellular building blocks and providing energy for growth. Alternatively, pyruvate may undergo incomplete oxidation into different compounds, which are then excreted and accumulate in the medium (Figure 1A). In yeasts such as *S. cerevisiae* for example, pyruvate is converted into ethanol through pyruvate decarboxylase and various alcohol dehydrogenases (Adh); in mammalian cells, pyruvate is converted into lactate via different lactate dehydrogenases (Ldh); and in bacteria such as *E. coli*, pyruvate is converted into acetate through pyruvate dehydrogenase (Pdh), phosphate acetyltransferase (Pta) and acetate kinase (AckA). While acetate production involves the production of ATP, ethanol and lactate production enable the reoxidation of NADH into NAD^+, which can sustain glycolysis. Acetate, lactate, and ethanol are then excreted into the environment by diffusion and various transporters.

Overflow products are then reconsumed after depletion of glycolytic substrates (Figure 1B-D). This phenomenon, known respectively as the acetate switch, ethanol switch and lactate switch, is observed in bacteria (Holms, 1996; Wolfe, 2005), yeasts (Meyenburg, 1969), and mammalian cells (Ozturk et al., 1997). In *E. coli,* glucose exhaustion suppresses catabolite repression, leading to the expression of acetyl-CoA synthetase (Acs) (Holms, 1996; Valgepea et al., 2010; Wolfe, 2005), which converts acetate back into acetyl-CoA. Similarly, in *S. cerevisiae*, upon glycolytic exhaustion, the gene encoding for Adh2 is derepressed and ethanol is converted into acetaldehyde and ultimately acetyl-CoA (Ciriacy, 1975; Mohd Azhar et al., 2017; Wills, 1976). In mammalian cells, lactate reconsumption is thought to be caused by LdhC expression (Hartley et al., 2018; Torres et al., 2018).

Diauxic growth has significantly shaped the classical perspective that specific enzymes are responsible for the production of overflow by-products during glycolytic growth, while other enzymes are responsible for their utilization only after depletion of glycolytic substrates (Meyenburg, 1969; Ozturk et al., 1997; Wolfe, 2005). Substantiating this perspective, when catabolite repression is partially impaired or weakened, all enzymes are expressed, and both the producing and consuming pathways operate concurrently (Peebo et al., 2014). In this

situation, the rate of overflow product accumulation (i.e., the net contribution of both pathways) is notably reduced.

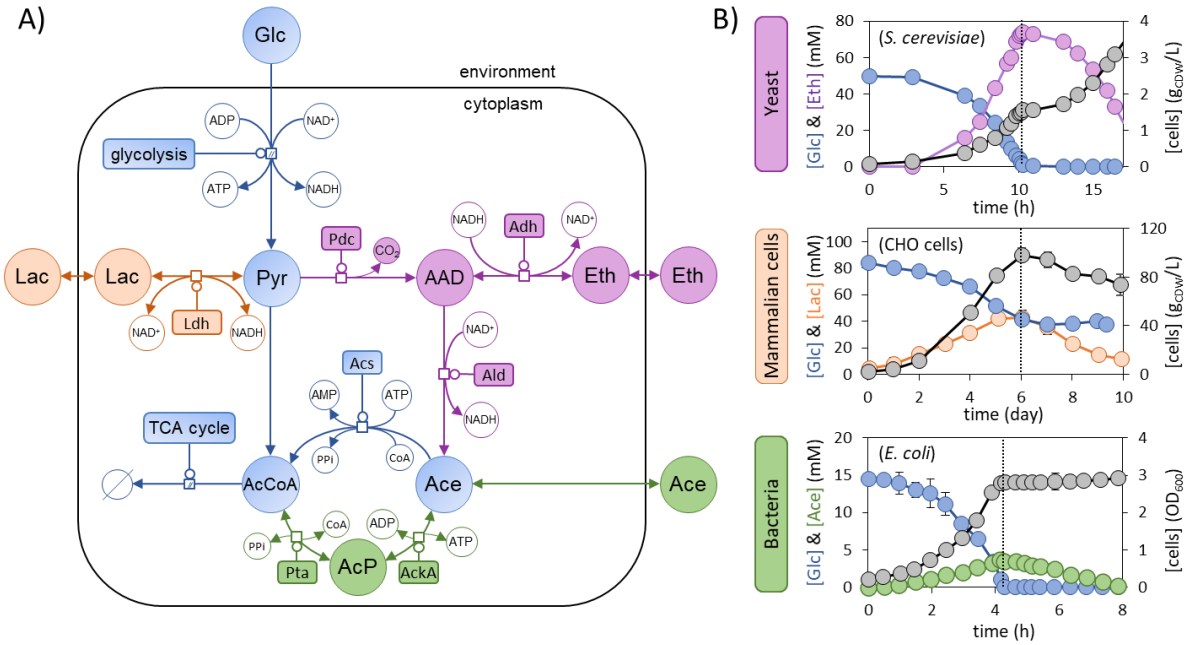


Figure 1. Overflow metabolism induces diauxic shifts in yeast, bacterial and mammalian cells.

A) Topology of conserved central metabolic reactions (in blue) and of the main overflow pathways in *S. cerevisiae* (in purple), CHO cells (in orange), and *E. coli* (in green). This network follows the Systems Biology Graphical Notation format (http://sbgn.org), with circles representing metabolites and rounded rectangles representing enzymes. B) Overflow by-products are produced during the glucose consumption phase and reconsumed once glucose is depleted or no longer consumed. The switch is highlighted in each case by a vertical dotted line. Experimental data were taken from (Enjalbert et al., 2013) for *E. coli*, from (Meyenburg, 1969) for *S. cerevisiae*, and from (Mulukutla et al., 2012) for CHO cells.

1.2 Overflow fluxes are controlled by overflow pathways, glycolysis, and the TCA cycle

While the topology of overflow pathways has long been established for all microorganisms (Romano and Conway, 1996), the factors determining overflow fluxes have only recently become clearer. A common pattern has emerged from metabolic control analysis, with the development of experimental or computational methods to quantify flux control (Fell, 2005). The typical approach involves measuring the flux response to a modulation of the activity of a

given reaction (i.e., Vmax). As outlined in this section, various experimental strategies have been used to modulate pathway activity, such as modulating the expression of a specific enzyme, iteratively deleting isoenzymes catalyzing a given reaction, using inhibitors, and employing different bioprocess strategies.

Early efforts to control the production of overflow products focused primarily on modulating the activity of enzymes catalyzing their biosynthesis (Figure 2). For example, deleting Adhs in yeast was found to reduce ethanol production (Smidt et al., 2012), and in *E. coli*, progressively increasing *pta* expression using an IPTG-inducible promoter was found to increase acetate accumulation (Sun-Gu and Liao, 2008). Indirectly modulating the activity of these enzymes via transcriptional (Schuurmans et al., 2008), translational (De Mets et al., 2019), or post-translational regulators (Castaño-Cerezo et al., 2014) was observed to produce the same metabolic response. Alternatively, artificially increasing the activity of enzymes with increased expression during the by-product utilization phase, such as Acs in *E. coli* (Peebo et al., 2014) or LdhC in CHO cells (Hartley et al., 2018; Torres et al., 2018), has also been shown to reduce by-product accumulation. These results are consistent with negative control of overflow fluxes by the enzymes involved in by-product utilization.

Other controlling pathways have also been identified. A notable reduction in by-product excretion has been observed in all microorganisms when the glycolytic flux is reduced by bioprocess or metabolic engineering (Figure 2). This was initially observed under carbon-limited conditions such as in fed-batch experiments (Aiba et al., 1976; Korz et al., 1995; Ljunggren and Häggström, 1994) and chemostat experiments (Hayter et al., 1993; Paalme et al., 1997; Van Hoek et al., 1998; Vergara et al., 2018). In carbon-limited chemostats, the relationship between the overflow flux and the dilution rate was first interpreted as a "growth rate dependence" of the overflow flux (Basan et al., 2015; Van Hoek et al., 1998). However, this interpretation is misleading: because the growth rate is a *consequence,* and not a *cause,* of the imposed restriction on the uptake rate of glycolytic substrates, these results should instead be understood as demonstrating a dependence of the overflow flux on the glycolytic flux rather than on the growth rate (Eiteman and Altman, 2006; Sonnleitner and Käppeli, 1986). Alternative metabolic engineering strategies targeting the glycolytic flux support this interpretation and confirm the positive control of overflow fluxes by glycolysis (Elbing et al., 2004; Tanner et al., 2018). Lowering the activity of enzymes involved in the transport of glycolytic nutrients (phosphotransferase and ABC transporters in *E. coli* (Fuentes et al., 2013) and hexose and maltose transporters in yeast (Elbing et al., 2004) and CHO cells (Wlaschin and Hu, 2007)), or in their utilization (e.g., phosphoglucose isomerase and phosphofructokinase in *E. coli* (Long and Antoniewicz, 2019), HXK2 in yeast (Raamsdonk et al., 2001)), reduces by-product accumulation. Glycolytic control of overflow fluxes is also apparent upon chemical inhibition of the glycolytic flux (H_2O_2 in yeast (Xiao et al., 2022), 2-deoxyglucose or 5-thioglucose (Naik et al., 2023; Niccoli et al., 2017) in CHO cells), as well as when using glycolytic substrates with a naturally low glycolytic flux, such as glycerol, fructose, or galactose

(Altamirano et al., 2006; Gerosa et al., 2015; Ostergaard et al., 1999). In all these experiments, lowering the glycolytic flux was found to limit by-product accumulation.

Overflow fluxes are also influenced by pyruvate and acetyl-CoA utilization pathways, primarily through the TCA cycle. In *E. coli*, overexpressing the global regulator ArcA represses the expression of TCA enzymes, thereby decreasing respiratory capacity and increasing acetate flux (Basan et al., 2017) (Figure 2). In contrast, deleting ArcA increases TCA activity and reduces acetate production (Peebo et al., 2014). Deleting *iclR* activates another acetyl-CoA consuming pathway, the glyoxylate shunt, and also reduces acetate accumulation (Liu et al., 2017). A similar response has been observed for lactate in CHO cells overexpressing *c-myc* (an activator of mitochondrial biogenesis; results for this *cMYC-OE* strain shown in Figure 2) (Kuystermans et al., 2010; Li et al., 2005) or *MDH2* (Chong et al., 2010). Ethanol production is also higher in "petite" yeast with disrupted mitochondrial activity (results for the *pet191*Δ strain shown in Figure 2) (Hutter and Oliver, 1998).

In tandem with these experimental approaches, the mathematical framework of metabolic control analysis and the increasing availability of kinetic models of overflow metabolism have contributed to a quantitative understanding of overflow flux regulation (Millard et al., 2021; Mulukutla et al., 2012). Experimental and modeling results both suggest there is no single "rate-limiting step", contrary to what has often been suggested. Instead, the control of overflow fluxes is widely distributed between three processes revolving around pyruvate oxidation: the overflow pathway itself, glycolysis, and the TCA cycle. This control pattern has been consistently observed across all organisms. For instance, flux measurements in seven yeast species have shown that combining low glycolytic fluxes with high TCA fluxes leads to higher growth rates and lower ethanol production (Christen and Sauer, 2011). While the same three pathways have been shown to control overflow fluxes to a similar extent in *E. coli* (Millard et al., 2021), the specific contributions of each pathway to overflow flux control remain to be quantified for yeast and mammalian cells.

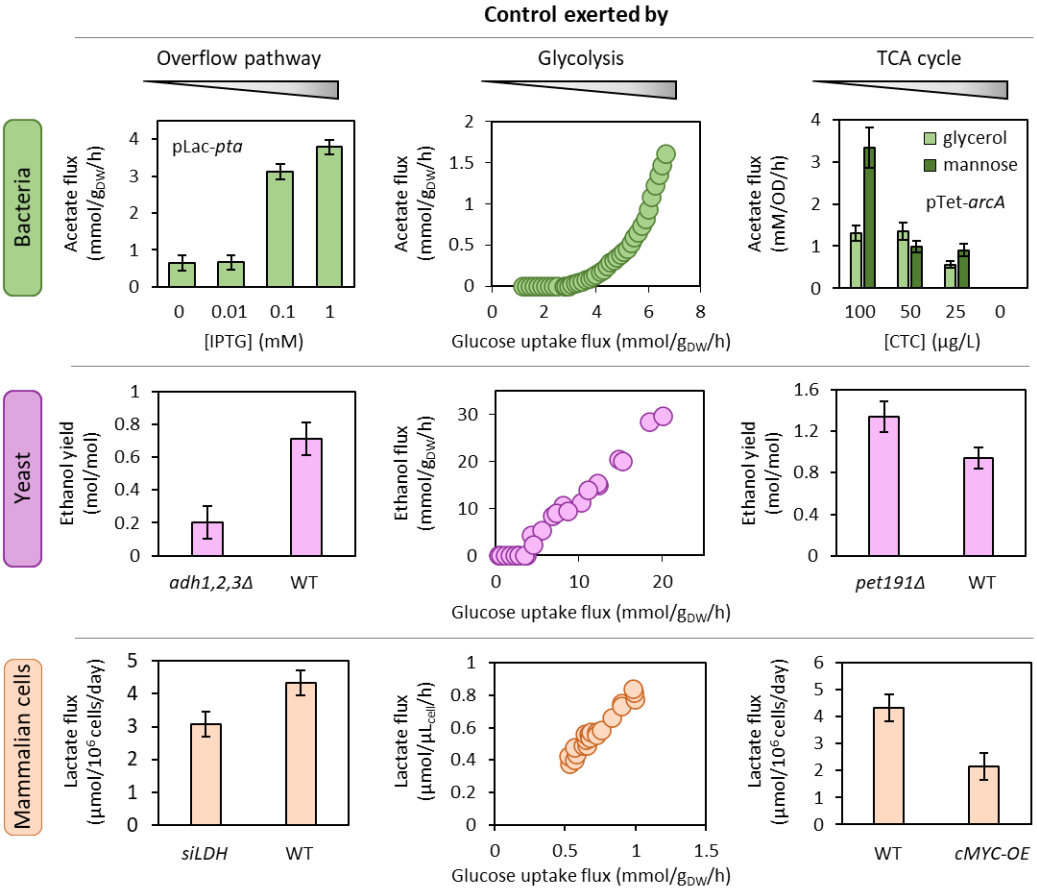


Figure 2. Identification of the pathways controlling overflow fluxes.

Overflow fluxes have been measured in response to modulations of the activity of enzymes in the overflow pathway (left column), glycolytic pathway (middle column), and TCA cycle (right column), in bacterial (*E. coli*, top row), yeast (*S. cerevisiae*, middle row) and mammalian cells (CHO cells, bottom row). The overflow flux depends on the activity of all three pathways, demonstrating that they all control overflow fluxes during growth on glycolytic substrates. The *E. coli* data are taken from (Sun-Gu and Liao, 2008) for the overflow pathway, from (Peebo et al., 2014) for glycolysis, and from (Basan et al., 2017) for the TCA cycle. The *S. cerevisiae* data are taken from (Smidt et al., 2012) for the overflow pathway, from (Christen and Sauer, 2011; Heyland et al., 2009; Van Hoek et al., 1998) for glycolysis, and from (Hutter and Oliver, 1998) for the TCA cycle. The CHO cell data are taken from (Noh et al., 2017) for the overflow pathway, from (Tanner et al., 2018) for glycolysis, and from (Kuystermans et al., 2010) for the TCA cycle.

1.3 The high reversibility of overflow metabolism uncouples carbon oxidation from nutrient uptake

While enzymes catalyzing the production of overflow products are reversible *in vitro* (Ganzhorn et al., 1987; Rose et al., 1954), the flux through these pathways has traditionally been considered irreversible because of the net accumulation of by-products and the expression of different genes during production and consumption (de Smidt et al., 2008; Hartley et al., 2018; Holms, 1996; Wolfe, 2005). However, the recent development of ^{13}C-fluxomics approaches(Ahn and Antoniewicz, 2013; Crown et al., 2016), combining isotope labeling experiments with mathematical models of metabolism (Figure 3A), has revealed that overflow fluxes are also reversible *in vivo*, even in conditions where catabolite repression is active (Chen et al., 2016; Enjalbert et al., 2017; Xiao et al., 2022).

Adding small amounts of ^{13}C-acetate to the extracellular medium during growth of *E. coli* on unlabeled glucose leads to an increase in the concentration of ^{12}C-acetate (produced from glucose) and to a decrease in the concentration of ^{13}C-acetate (Figure 3A) (Enjalbert et al., 2017). This demonstrates that acetate is constantly exchanged between *E. coli* cells and their environment and thus that the acetate flux is reversible. Carbon atoms from extracellular ^{13}C-acetate are likewise incorporated into intermediates of the TCA cycle, revealing the role of by-products in carbon nutrition. Similar results have been obtained in yeast (using ^{13}C-ethanol, Figure 3A) (Xiao et al., 2022), in adipocytes, glioma, and HeLa cells *in vitro* (using ^{13}C-lactate, Figure 3A) (Bouzier et al., 1998; Chen et al., 2016; Lagarde et al., 2021), and *in vivo* in mice (using intravenous infusion of ^{13}C-lactate) (Hui et al., 2020). These isotope labeling experiments showed significant incorporation of ^{13}C-by-products into TCA intermediates, amino acids and fatty acids in *E. coli*, yeast and mammalian cells (Figure 3A). Furthermore, growth of yeast or mammalian cells on unlabeled glucose plus ^{2}H-ethanol or ^{2}H-lactate led to the incorporation of ^{2}H isotopes into NAD(P)H, confirming the high reversibility of overflow pathways and revealing the contribution of overflow metabolites to redox metabolism (Hui et al., 2020; Xiao et al., 2022). ^{13}C-labeling experiments of *E. coli* mutant strains missing different acetate pathway enzymes have shown that those responsible for acetate production (Pta and AckA) are also simultaneously involved in acetate consumption (Enjalbert et al., 2017). Similarly, Ldh contributes to both lactate production and utilization in adipocytes (Lagarde et al., 2021). The contributions of different overflow pathway enzymes to bidirectionality have not been investigated in detail in yeast and CHO cells, but the producing enzymes may also be (at least partly) responsible for the simultaneous utilization of by-products.

Integration of isotopic data collected in ^{13}C- or ^{2}H-labeling experiments into isotopic models has enabled the quantification of individual production and consumption fluxes. While the exact flux values vary depending on the model and underlying assumptions, all *E. coli*, yeast and mammalian cell models converge on an exchange flux in the same range as glucose uptake and 2–4 times higher than the net overflow flux (Figure 3A) (Enjalbert et al., 2017; Lagarde et

al., 2021; Xiao et al., 2022). In all microorganisms therefore, the high reversibility of overflow pathways uncouples glucose utilization from glucose oxidation: glucose is primarily catabolized into extracellular overflow products, which are simultaneously taken up and used through the TCA cycle as carbohydrate fuels (Figure 3B-C). This uncoupling of glycolysis from the TCA cycle via overflow products is therefore a conserved feature of prokaryotic and eukaryotic metabolism.

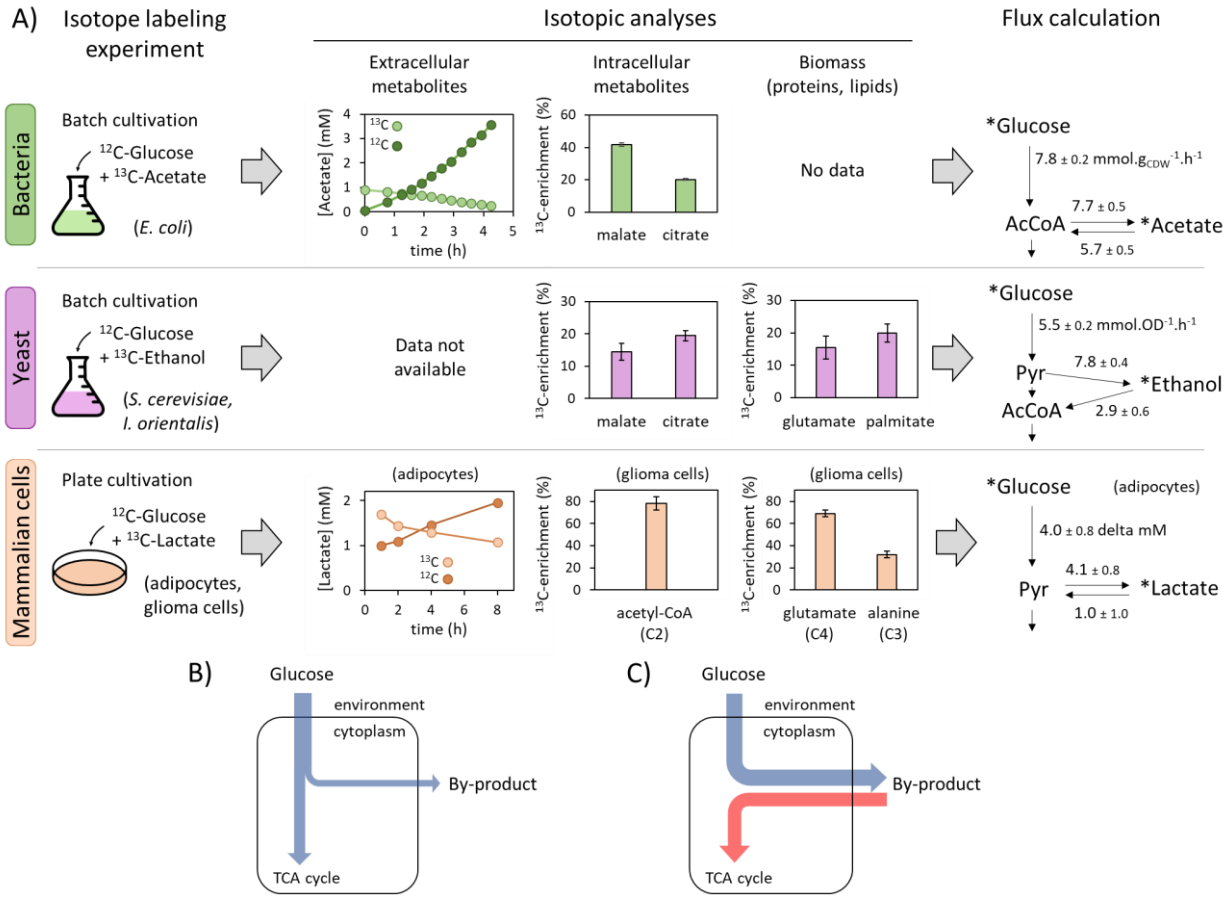


Figure 3. Isotope labeling experiments demonstrate the high reversibility of overflow pathways.

^{13}C-fluxomics allows the quantification of forward and reverse overflow fluxes, revealing the high reversibility of overflow fluxes in bacteria, yeast and mammalian cells (A). Isotope labeling experiments were performed by adding small amounts of ^{13}C-by-products during growth on glucose. The concentration dynamics of ^{12}C- and ^{13}C-by-products in the extracellular medium were monitored by NMR. ^{13}C-incorporation was also measured into central metabolites (malate, citrate, and acetyl-CoA are shown as examples) and biomass components (glutamate, alanine, and palmitate are shown as examples). Isotopic data from *E. coli* and *S. cerevisiae* were measured by MS and are expressed as the mean ^{13}C-enrichment

of metabolites, while data from glioma cells were measured by NMR and represent ^{13}C-enrichments at specific carbon atoms within the metabolites (with the carbon atom number indicated below the metabolite name). Fluxes were then quantified using isotopic models. The *E. coli* data are taken from (Enjalbert et al., 2017), the yeast data from (Xiao et al., 2022), and the mammalian data from (Bouzier et al., 1998; Lagarde et al., 2021). Complete datasets are available in the respective publications. In the flux maps, extracellular metabolites are denoted with stars; all other metabolites are intracellular. According to the traditional view of overflow metabolism, a fraction of glucose is excreted as a by-product, with the rest being oxidized through the TCA cycle (B). However, recent results indicate that the high reversibility of overflow pathways leads to an uncoupling of glucose uptake from glucose oxidation in the TCA cycle (C).

1.4 Thermodynamic control of overflow fluxes can lead to co-consumption of overflow metabolites with glycolytic nutrients

The recent discovery that overflow is a highly reversible process has led to the suggestion that increasing the extracellular concentration of by-products could modulate the thermodynamic driving force of overflow pathways and ultimately their flux. This hypothesis has been tested in detail in *E. coli* (Enjalbert et al., 2017). In line with the predictions obtained from a thermodynamic model of the Pta-AckA pathway, experimental data confirmed that increasing the acetate concentration progressively decreases the net acetate production flux, abolishing acetate accumulation at ~10 mM (Enjalbert et al., 2017) (Figure 4). Beyond this threshold, the net acetate flux reverses, leading to the co-utilization of acetate with glucose (Enjalbert et al., 2017). Analysis of *E. coli* mutant strains missing different enzymes in the acetate pathway has shown that co-utilization of acetate with glycolytic nutrients is supported solely by the Pta-AckA pathway (Enjalbert et al., 2017).

Thermodynamic control of overflow fluxes in yeast and CHO cells has yet to be studied in detail, but several observations suggests that similar principles apply to these organisms. CHO cells have been observed to consume lactate alongside glycolytic nutrients (glucose or galactose) (Altamirano et al., 2006; Martínez-Monge et al., 2019), and increasing the extracellular lactate concentration during growth on galactose has been shown to reverse the lactate flux (Altamirano et al., 2000; Torres et al., 2019) (Figure 4). In yeast grown on glucose, increasing the ethanol concentration enhances the incorporation of extracellular ^{13}C-ethanol into acetyl-CoA (Xiao et al., 2022) (Figure 4), indicating an increase in extracellular ethanol uptake. The net ethanol flux was not measured in these experiments, but co-consumption of glucose and ethanol has already been observed (Raamsdonk et al., 2001). These data support the hypothesis that overflow fluxes in all organisms are predominantly controlled at the thermodynamic level by the concentration of the respective by-products, as observed for

other nutrients in mammalian cells (Xiaoxuan Li et al., 2022). As demonstrated in detail for *E. coli* (Enjalbert et al., 2017) and suggested from published data for yeast and CHO cells, increasing the concentration of overflow metabolites does not only reduce their accumulation but may also lead to the reversal of overflow fluxes. The role of overflow metabolites as by-products or co-substrates of glycolytic nutrients is thus determined by this thermodynamic control mechanism.

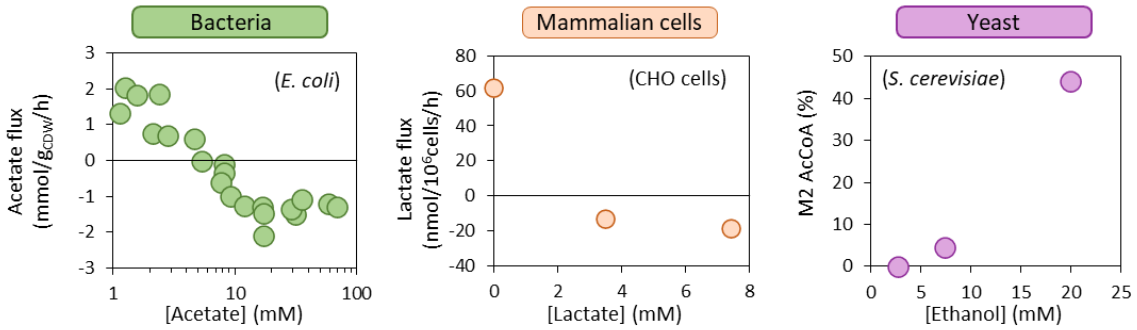


Figure 4. Overflow fluxes are thermodynamically controlled by the concentration of overflow metabolites.

In *E. coli* grown on glucose, the acetate flux decreases when the extracellular acetate concentration is increased (Enjalbert et al., 2017). In CHO cells grown on galactose, increasing the extracellular lactate concentration reverses the lactate flux (Altamirano et al., 2000; Torres et al., 2019). In *S. cerevisiae* grown on glucose, the contribution of ^{13}C-ethanol to acetyl-CoA biosynthesis increases with the extracellular ethanol concentration (Xiao et al., 2022). Although the net ethanol flux was not measured in these experiments, these results imply an increase in ethanol uptake.

1.5 Low uptake of glycolytic nutrients enhances co-utilization of overflow metabolites

Studies of glycolytic control of overflow fluxes have mostly been conducted in the absence of by-products. However, flux control is a local property that depends on the metabolic state of the organism, influenced in turn both by the glycolytic flux and the concentration of by-products. Co-consumption of lactate and glucose has indeed been observed in CHO cells, but only when the glucose uptake flux is low (Ahn and Antoniewicz, 2011; Torres et al., 2019) (Figure 5). Growing CHO cells on galactose, a nutrient with a naturally low glycolytic flux, also

leads to co-utilization of lactate (Altamirano et al., 2006). In yeast, simultaneous consumption of glucose and ethanol has been observed at low glycolytic flux in a *S. cerevisiae* strain lacking *HXK2*, the gene encoding the main glucose transporter (Raamsdonk et al., 2001) (Figure 5). Moreover, exposure of yeast to H_2O_2 also leads to a decrease in glycolytic flux (Shenton and Grant, 2003) and increases the contribution of ethanol to NADH regeneration (Xiao et al., 2022). The intricate interplay between glycolytic and overflow fluxes in the presence of acetate has been explored in detail in *E. coli* (Enjalbert et al., 2017; Millard et al., 2021). In yeast and CHO cells, several observations suggest that decreasing the glycolytic flux would reduce the overflow flux in the absence of by-products, but that the same perturbation would enhance overflow by-product utilization in the presence of by-products. These observations are consistent with the relationship between glucose and overflow metabolism suggesting that a similar control mechanism exists in yeast, bacteria and CHO cells. Though investigating the answer of *E. coli* to acetate when the glycolytic flux is modulated has not been studied yet.

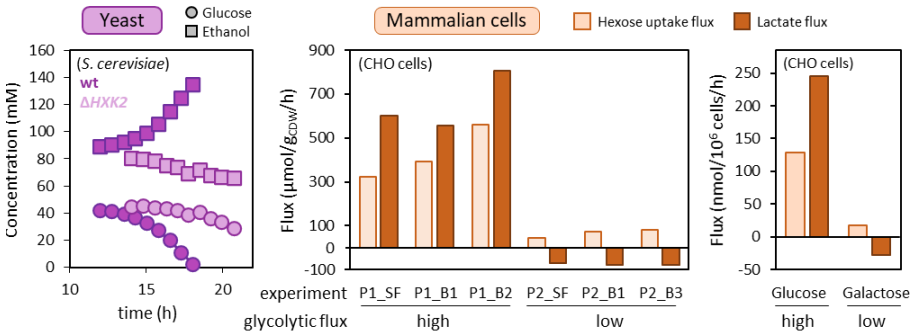


Figure 5. Impact of reducing the glycolytic flux on overflow fluxes.

In all microorganisms, lowering the glycolytic flux (either by deleting *HXK2* in *S. cerevisiae* (Raamsdonk et al., 2001), or by using different bioprocess conditions or carbon sources in CHO cells (Altamirano et al., 2006; Martínez-Monge et al., 2019)) reverses the overflow flux. The overflow flux switches from production (positive values) at high glycolytic flux to co-utilization (negative values) when the glycolytic flux is low.

1.6 Overflow metabolites are global regulators of cellular metabolism and physiology

Overflow metabolites fundamentally alter cellular physiology. Lactate, for example, is known to modulate growth, immunity, tumorigenesis, and tumor development (Brooks, 2018). Acetate influences growth, virulence, motility, carbon metabolism, biofilm formation, and peptide uptake (Castaño-Cerezo et al., 2014; Millard et al., 2021). Ethanol triggers a global response in yeast, impacting growth, cell viability, metabolism, cell structure, and membrane function (Sahana et al., 2024). Extensive research has been conducted to uncover the

underlying mechanisms. Acetate and lactate can disrupt the intracellular pH and the proton motive force through their uncoupling effect (Brooks, 2018; Pinhal et al., 2019). Ethanol disrupts yeast membrane bilayers, reduces water availability, affects enzymatic activity (Sahana et al., 2024), and denatures proteins. Lactate likewise alters protein stability (Xiaolu Li et al., 2022). In addition to these physicochemical effects, cells respond to overflow metabolites by reorganizing at all molecular levels, including the transcriptome (Barbieri et al., 2023; Millard et al., 2021; Sahana et al., 2024), proteome (Kirkpatrick et al., 2001; Sahana et al., 2024; Zhang et al., 2019), and metabolome and fluxome (Millard et al., 2021). The thermodynamic control of overflow pathways enables direct, system-wide control of fluxes and metabolite concentrations by the by-products themselves (Millard et al., 2021). Overflow metabolites modulate the expression of hundreds of genes involved in most cellular functions (metabolism, replication, motility, etc) (Brooks, 2018; Castaño-Cerezo et al., 2014; Sahana et al., 2024). Though a complete picture is still lacking, some sensing and signaling pathways have been identified. For instance, lactate is an agonist for the G-protein-coupled receptor GPR81 in neurons (Xiaolu Li et al., 2022), and acetate can be sensed by *E. coli* via the BarA/UvrY two component system (Alvarez et al., 2021). Lactate and acetate also modulate the activity of many proteins through epigenetic and post-translational modifications, respectively lactylation and acetylation (Xiaolu Li et al., 2022; Schastnaya et al., 2023). Several acetylation and lactylation targets involved in key cellular functions such as replication and metabolism have been identified (Wolfe, 2016; Xu et al., 2024), but here again a more global analysis is still needed. Despite extensive research and continuous progress on this topic, the complete list of targets and the detailed regulatory networks that sense and respond to overflow metabolites remain to be established.

Overflow metabolites are often referred to as "stress factors", but recognizing these compounds as global regulators is crucial to characterize the corresponding regulatory programs and the induced cellular responses. Importantly, the presence of these compounds in the extracellular medium means they can act as messengers between cells, and between organs in mammals, thereby influencing entire cell communities (Baker and Rutter, 2023).

1.7 Overflow metabolites are not toxic *per se* and can be beneficial to cells

Overflow products have long been considered toxic waste because of their detrimental effect on growth. Different theories have been proposed to explain this growth inhibition, but most cannot be generalized to all types of by-products (e.g. alcohols, acids, ketones). Acetate (Luli and Strohl, 1990), ethanol (Brown et al., 1981) and lactate (Lao and Toth, 1997) all hinder cellular membrane function either through their decoupling effect (Brooks, 2018; Pinhal et al., 2019), deleterious change in membrane fluidity, or osmotic stress. These by-products can also interfere with intracellular amino-acid pools such as methionine, glutamate and tryptophan

(Pinhal et al., 2019). Ethanol also promotes protein denaturation in yeast (Sahana et al., 2024). These long-known deleterious effects have contributed to the established perception of overflow metabolites as toxic compounds.

However, recent studies paint a very different picture, in which these molecules may in fact be beneficial for their producers. Lactate has recently been shown to be continuously used by mammalian cells, even under conditions of net lactate production, with many positive properties, such as i) being a source of pyruvate and energy (Hui et al., 2020), ii) being an energy redistribution shuttle between cells (Brooks, 2018; Rabinowitz and Enerbäck, 2020), iii) improving viability (Mulukutla et al., 2012), and iv) acting as an antioxidant (Groussard et al., 2000). In yeast, ethanol participates in carbon nutrition and is a major source of NADH and NADPH (Xiao et al., 2022), with its contribution augmented under oxidative stress conditions. Acetaldehyde, an intermediate of ethanol metabolism described as detrimental for growth (Jones, 1990), may instead promote growth and reduce lag in *S. cerevisiae* (Stanley et al., 1993; Walker-Caprioglio and Parks, 1987), even at high concentrations (up to 140 mM). In bacteria, acetate synthesis has been shown to be the most efficient pathway for energy production in *E. coli*, both in terms of spatial and protein cost efficiency. Moreover, It plays a crucial role in recycling cofactors like CoA, which are essential for glycolysis (Basan et al., 2015; Szenk et al., 2017; Zeng and Yang, 2019; Zhuang et al., 2011).

Although our degree of understanding of the impact of by-products varies between the three types of organisms, the parallels are striking. Overflow by-products tend to be increasingly viewed not merely as toxic waste but rather as beneficial co-substrates for individual cells and cell populations.

1.8 Similar principles apply to other species and overflow by-products

Overflow is a common feature of all living organisms, including bacterial, mammalian, fungal, and plant cells. It can also arise at virtually any step of the metabolic network, depending on the strain, cultivation conditions and experimental setup (e.g., carbon source, medium composition, temperature, pH, continuous or batch cultivation). It is therefore no surprise that overflow phenomena have been reported for a wide range of compounds, including sugars, amino acids, organic acids, and nucleotides (Paczia et al., 2012; Phégnon et al., 2024; Reaves et al., 2013; Ser et al., 2016). To list just a few examples, glucose overflow has been observed in engineered *S. cerevisiae* and *E. coli* strains grown on xylose (Diaz et al., 2019; Nijland et al., 2021), overflow of arabitol has been observed in *Pichia pastoris* grown on glycerol (Fina et al., 2021), and hemiterpenoid glycosides and acetate overflows have been observed in plants under stress conditions (Ward et al., 2011). Overflow has been observed in all species for most central metabolites, though at lower concentrations (Paczia et al., 2012), and does not

necessarily involve carbon compounds, with ammonium overflow having been observed during the growth of *E. coli* on mixtures of glycerol and ethanolamine (Jallet et al., 2024).

Several clues suggest that these principles may be generic and apply equally to most species and by-products. First, as observed for central metabolites and ammonia (Jallet et al., 2024; Paczia et al., 2012), overflow metabolites are typically re-consumed following the depletion of the primary nutrient. Second, the control of overflow fluxes is often shared between producing and consuming pathways, as shown for pyrimidine overflow in *E. coli* and poly-γ-glutamic acid overflow in *Bacillus licheniformis* (Li et al., 2021; Reaves et al., 2013), thereby reflecting the imbalance between the two pathways. Overflow typically occurs under conditions of nutrient excess (Paczia et al., 2012), characterized by high biosynthetic fluxes that cannot be supported by downstream pathways, while nutrient limitation favors the co-utilization of overflow metabolites (Paczia et al., 2012; Ward et al., 2011). Overflow also occurs when the uptake rates of different nutrients are imbalanced, with one nutrient limiting the downstream pathways required to incorporate the other. This has been observed in *E. coli* grown on a mixture of glycerol (used as carbon source) and ethanolamine (used as nitrogen source) (Jallet et al., 2024). Finally, overflow fluxes obey thermodynamic control, with high extracellular concentrations of metabolites limiting production and favoring (co-)utilization (Paczia et al., 2012; Pastoors et al., 2023). One of the most striking examples of the latter is perhaps the reversal of the TCA cycle in *Hippea maritima* at high CO_2 levels, enabling CO_2 fixation (Steffens et al., 2021).

1.9 Controlling overflow metabolism for biotechnology

Overflow metabolism is a central concern for two distinct bioprocess criteria. First, the excretion of common overflow by-products reduces productivity by diverting metabolic precursors and hindering growth (De Mey et al., 2007; Mohd Azhar et al., 2017; Xu et al., 2023). This type of overflow should be minimized and ideally reversed to enable the utilization of overflow metabolites as (co-)substrates and promote growth. Conversely, since the main objective of bioprocesses is to optimize the production of desired compounds, the flux of the corresponding overflow processes should be maximized.

Various strategies have been developed to limit the accumulation of overflow metabolites and redirect these compounds to serve as carbon and/or energy precursors for the products of interest. These strategies include specific process design, such as continuous culture and fed-batch approaches, and genetic interventions and adaptive laboratory evolution (De Mey et al., 2007; Mohd Azhar et al., 2017; Xu et al., 2023). However, these methods are not universally applicable in all production scenarios and can be challenging to implement at an industrial scale (Eiteman and Altman, 2006). An alternative strategy that is attracting growing

interest is to harness overflow products as valuable resources (Kiefer et al., 2021; Zhang et al., 2022). The surge in interest is being stimulated in part by the worldwide shift towards a sustainable, low-carbon bioeconomy, which has prompted an exploration of alternatives to sugars for biomanufacturing (Zhang et al., 2022). This shift is particularly appealing because industrial model organisms can co-consume overflow products with traditional nutrients (such as glucose or glycerol) under specific conditions, as observed for example in CHO cells with lactate (Altamirano et al., 2006; Li et al., 2012), in *S. cerevisiae* with ethanol (Zhang et al., 2022), and in *E. coli* with acetate (Nam et al., 2024). Research into these new feedstocks is therefore ongoing to optimize their utilization and improve yields (Charaniya et al., 2010; Mulukutla et al., 2012). Acetate, the most studied substrate, has proven to be a viable precursor in several bacteria and yeasts for various bio-based products including bioplastics, biofuels, biosurfactants, platform chemicals, amino acids, recombinants proteins, and fine chemicals (Kiefer et al., 2021). Acetate has been shown to be co-consumed with glycolytic nutrient when cells are exposed to it (Enjalbert et al., 2017), suggesting that it could possibly also improve productivity on glycolytic substrates. However, this putative positive effect on bioprocesses has yet to be explored (Zhang et al., 2022). Lactate, meanwhile, has predominantly been studied as a final product because of its interesting properties in bioplastic production, but its role as a feedstock is also beginning to be explored (Nduko and Taguchi, 2021). In combination with glycolytic substrates, lactate improves the viability of CHO cells and may enhance bioproduction (Mulukutla et al., 2012). Ethanol remains largely unexplored as a feedstock, primarily because of its historical role as a prototype for first-generation biofuels. However, recent studies have highlighted its potential, including as a precursor for artemisinin in *S. cerevisiae* and its efficient conversion into polyhydroxybutyrate or prenol in engineered strains of *E. coli* (Zhang et al., 2022).

As mentioned above, contrary to naturally produced overflow metabolites, the objective with desired overflow compounds is to maximize fluxes to optimize productivity. A generic understanding of overflow processes can be beneficial in this context too. For instance, thermodynamic control of overflow fluxes tends to reduce production fluxes when products accumulate, thereby limiting the final titer. Specific bioprocess methods have been developed for *in situ* product separation (such as membrane separation, adsorption, and crystallization) to increase thermodynamic gradients and enhance production fluxes (Fuchs et al., 2002; Pastoors et al., 2023), but the lack of a generic understanding of this phenomenon has limited their applicability. In the same vein, the fact that some end-products are reconsumed when the substrate becomes limiting and are likely subject to a continuous, bidirectional exchange even in the production phase has not generally been considered.

Rethinking overflow metabolism thus offers a practical framework in biotechnology to increase the utilization of abundant overflow metabolites and the production of a wide range of compounds.

1.10 Overflow metabolism in health and disease

Lactate overflow is a well-known feature of cancer (Warburg and Minami, 1923). Increased lactate production in ischemic tissues and stressed muscle has further reinforced the image of lactate as a marker of disease (Xiaolu Li et al., 2022). However, recent discoveries have highlighted the roles of lactate as a fuel and regulator, transforming our understanding of energy metabolism (Rabinowitz and Enerbäck, 2020). Lactate is now recognized as a major circulating nutrient that supplies energy to most organs and acts as a redox buffer, balancing the NADH/NAD^+ ratio across cells and tissues (DeBerardinis and Chandel, 2020).

While lactate is primarily produced by hosts, SCFAs, including acetate, butyrate and propionate, are primarily produced in large amounts by anaerobes in the colon by fermentation of dietary fibers and other carbohydrates. SCFAs are an important energy source for the microbiota and are essential for the establishment and persistence of a healthy gut flora (Dalile et al., 2019; Martinson and Walk, 2020). However, acetate and other SCFAs have long been considered toxic compounds for many microbial species (Luli and Strohl, 1990; Pinhal et al., 2019), raising questions as to their actual role in the gut as this environment is highly dynamic with alternance between high and low availability of glycolytic substrates and being acetate rich. No dedicated study has been performed to investigate the response of *E. coli* to acetate when glycolytic nutrients are limiting (Conway and Cohen, 2015). Lactate has been shown to increase the survival of *Pseudomonas aeruginosa* during macrophage infection (Florek et al., 2024). Furthermore, SCFAs appear to act as carbon shuttles, and likely messenger metabolites, between different gut microbiota species (Dalile et al., 2019; Parada Venegas et al., 2019; Xiao et al., 2020).

The role of SCFAs as circulating metabolites exchanged between host and microbiota is well established. The systemic effects of microbiota-produced SCFAs on immune function, liver function and lipid metabolism underscores their importance in healthcare (Brooks, 2018). Host-produced lactate is also converted into acetate by the gut microbiota. Besides their role as nutrients, overflow metabolites act as secondary messengers through their regulatory role, enabling crosstalk between organs. It is now clear that these compounds are key to gut-brain communication (Silva et al., 2020), and additional roles likely remain to be discovered.

Concentrations of lactate and other SCFAs vary depending on diet, gut microbiota composition, and overall health, with dysregulation of gut homeostasis being implicated in a wide spectrum of diseases from obesity to angiogenesis and immunodeficiency to mental illness (Brooks, 2018). Host and microbiota both influence the dynamics of this system, which remains to be fully characterized. Studies of individual cells may be helpful in this context, because they facilitate the identification of cellular processes involved in cell dynamics and of the underlying principles. Integrating this information into combined mathematical models of host and microbiota will likely lead to a quantitative, system-level understanding of their

overall dynamics, as developed in recent years for lactate (Xiaolu Li et al., 2022; Rabinowitz and Enerbäck, 2020).

1.11 Toward a general framework to investigate overflow metabolism

Despite extensive data on the universally observed phenomenon of overflow, no generic framework has yet been proposed to understand the determinants of overflow fluxes and the response of producing cells to the resulting by-products. However, the various observations from several fields in different organisms presented in this introduction points to the existence of universally conserved principles in both prokaryotes and eukaryotes (Figure 6): (i) overflow metabolism is a reversible process that uncouples carbon oxidation from nutrient uptake, (ii) overflow fluxes are regulated at the thermodynamic and metabolic levels, with metabolic control being distributed between several pathways, (iii) overflow metabolites can act as co-substrates for glycolytic nutrients, with (iv) their role as nutrient or by-product determined by their concentration and the uptake rate of other nutrients, (v) reducing the uptake of glycolytic nutrients could enhances the co-utilization of overflow metabolites (at least for mammalian and yeast cells, thus some work still need to be performed in *E. coli*), and (vi) overflow metabolites should not be considered stress factors but global regulators of metabolism with (vii) several dedicated regulatory programs and (viii) many positive roles for cells and populations. The proposed conceptualization explains and unifies previous observations, such as the co-utilization of ethanol and glucose by the *hxk2Δ* yeast mutant, the augmented contribution of ethanol to yeast metabolism in response to oxidative stress or when ethanol concentration is increased, and the reversal of lactate flux in CHO cells between different growth phases on glucose. It also sheds new light on overflow, traditionally viewed as a unidirectional process leading to the production and accumulation of compounds that are toxic to producing cells, whereas in fact the high reversibility of overflow fluxes enables their utilization as nutrients. By-products have several beneficial effects on carbon and energy metabolism, ultimately improving robustness to a range of environmental perturbations (such as nutrient limitation or oxidative stress). These exchanged metabolites should be considered valuable nutrients and messengers, allowing cells to shape their environments and share resources and information.

In biotechnology, the proposed principles can inform the development of more efficient strains, consortia and bioprocesses that maximize overflow fluxes for high-value products and minimize (or even reverse) fluxes for undesired compounds. Considering the nonlinear effects of by-products on growth is also essential for optimizing productivity. These principles should thus lead to more efficient and sustainable bioprocesses, mitigating the negative effects of by-products and enabling their efficient use as co-substrates. In healthcare, this understanding could help elucidate the roles and dynamics of overflow metabolites exchanged within the

microbiota, between organs, and between the host and its microbiota, with applications in diagnosis and therapy. Developing a generic conceptual framework for overflow metabolism – as universal as possible, as specific as necessary – is therefore crucial to advance both fundamental and applied science.

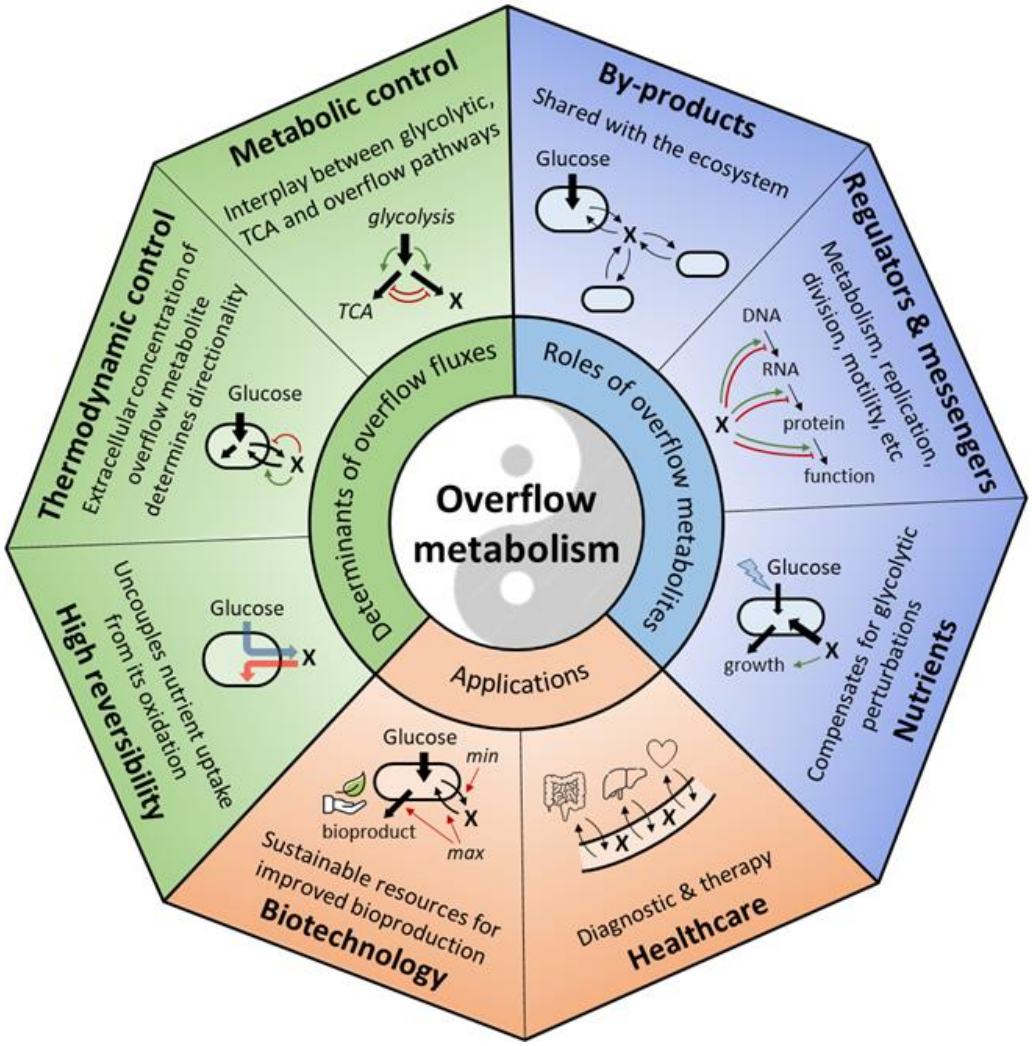


Figure 6. Function and regulation of overflow metabolism (in green), roles of overflow metabolites (in blue) and applications (in orange).

2. Thesis Outline

The main objective of my thesis, building on the previously presented framework, is to deepen our understanding of the control and regulation of overflow metabolism in living organisms and leverage this knowledge to develop more efficient biotechnological strategies.

To address this objective, I began my work with the most studied and widely used strain in biotechnology, *Escherichia coli*, focusing on its major overflow by-product, acetate.

Chapter 2 describes the intricate interplay between glucose metabolism, acetate metabolism and bacterial growth. In this chapter I aim to understand how *E. coli* responds to a modulation of both glycolysis and acetate flux using both model driven hypothesis and different experimental strategies. I demonstrated that, by decreasing the glycolytic flux and increasing the extracellular acetate concentration, acetate is co-consumed with glycolytic sources instead of being produced. Moreover, in this condition, acetate can boost bacterial growth. Results were published in the EMBO journal in 2023.

Chapter 3 illustrates how I apply the knowledge from Chapter 2 to enhance biotechnological processes involving *E. coli*. Here I show that the acetate supplementation increased the productivity of two acetyl-CoA derivated compounds by promoting biomass accumulation or increasing the specific production flux. Results will be submitted to Metabolic Engineering.

Given that overflow metabolism is conserved across living organisms, I further explore whether principles identified in *E. coli* could be apply to other microorganisms, particularly *Saccharomyces cerevisiae*, a key organism in biotechnology. Chapter 4 highlights the existence of a thermodynamic control of ethanol overflow in *S. cerevisiae* and *Komagataella phaffii* and a beneficial effect of ethanol on the growth rate when the glycolytic flux is lowered.

Chapter 5 provides the conclusions and future perspectives of this thesis.

This thesis follows a systems biology approach which is consistently applied throughout the various studies. It begins with modeling to generate hypotheses on the function, control, and regulation of overflow fluxes. These hypotheses are then tested experimentally NMR and MS spectroscopy, with data integration facilitated by software such as PhysioFit (Le Grégam et al., 2024) or MultiNMRfit. Experimental results either validate or refute the initial hypotheses, leading to iterative refinement and further testing.

3. References

Ahn, W.S., Antoniewicz, M.R., 2013. Parallel labeling experiments with [1,2-13C]glucose and [U-13C]glutamine provide new insights into CHO cell metabolism. Metab. Eng. 15, 34–47. https://doi.org/10.1016/j.ymben.2012.10.001

Ahn, W.S., Antoniewicz, M.R., 2011. Metabolic flux analysis of CHO cells at growth and non-growth phases using isotopic tracers and mass spectrometry. Metab. Eng. 13, 598–609. https://doi.org/10.1016/j.ymben.2011.07.002

Aiba, S., Nagai, S., Nishizawa, Y., 1976. Fed batch culture of *Saccharomyces cerevisiae* : A perspective of computer control to enhance the productivity in baker's yeast cultivation. Biotechnol. Bioeng. 18, 1001–1016. https://doi.org/10.1002/bit.260180712

Altamirano, C., Illanes, A., Becerra, S., Cairó, J.J., Gòdia, F., 2006. Considerations on the lactate consumption by CHO cells in the presence of galactose. J. Biotechnol. 125, 547–556. https://doi.org/10.1016/j.jbiotec.2006.03.023

Altamirano, C., Paredes, C., Cairó, J.J., Gòdia, F., 2000. Improvement of CHO cell culture medium formulation: simultaneous substitution of glucose and glutamine. Biotechnol. Prog. 16, 69–75. https://doi.org/10.1021/bp990124j

Alvarez, A.F., Rodríguez, C., González-Chávez, R., Georgellis, D., 2021. The *Escherichia. coli* two-component signal sensor BarA binds protonated acetate via a conserved hydrophobic-binding pocket. J. Biol. Chem. 297, 101383. https://doi.org/10.1016/j.jbc.2021.101383

Baker, S.A., Rutter, J., 2023. Metabolites as signalling molecules. Nat. Rev. Mol. Cell Biol. 24, 355–374. https://doi.org/10.1038/s41580-022-00572-w

Barbieri, L., Veliça, P., Gameiro, P.A., Cunha, P.P., Foskolou, I.P., Rullman, E., Bargiela, D., Johnson, R.S., Rundqvist, H., 2023. Lactate exposure shapes the metabolic and transcriptomic profile of CD8+ T cells. Front. Immunol. 14, 1101433. https://doi.org/10.3389/fimmu.2023.1101433

Basan, M., Hui, S., Okano, H., Zhang, Z., Shen, Y., Williamson, J.R., Hwa, T., 2015. Overflow metabolism in *Escherichia. coli* results from efficient proteome allocation. Nature 528, 99–104. https://doi.org/10.1038/nature15765

Basan, M., Hui, S., Williamson, J.R., 2017. ArcA overexpression induces fermentation and results in enhanced growth rates of E. coli. Sci. Rep. 7, 11866. https://doi.org/10.1038/s41598-017-12144-6

Bouzier, A.-K., Goodwin, R., De Gannes, F.M.-P., Valeins, H., Voisin, P., Canioni, P., Merle, M., 1998. Compartmentation of lactate and glucose metabolism in C6 glioma cells. J. Biol. Chem. 273, 27162–27169. https://doi.org/10.1074/jbc.273.42.27162

Brooks, G.A., 2018. The science and translation of lactate shuttle theory. Cell Metab. 27, 757–785. https://doi.org/10.1016/j.cmet.2018.03.008

Brown, S.W., Oliver, S.G., Harrison, D.E.F., Righelato, R.C., 1981. Ethanol inhibition of yeast growth and fermentation: Differences in the magnitude and complexity of the effect. Eur. J. Appl. Microbiol. Biotechnol. 11, 151–155. https://doi.org/10.1007/BF00511253

Castaño-Cerezo, S., Bernal, V., Post, H., Fuhrer, T., Cappadona, S., Sánchez-Díaz, N.C., Sauer, U., Heck, A.J., Altelaar, A.M., Cánovas, M., 2014. Protein acetylation affects acetate metabolism, motility and acid stress response in *Escherichia. coli*. Mol. Syst. Biol. 10, 762. https://doi.org/10.15252/msb.20145227

Charaniya, S., Le, H., Rangwala, H., Mills, K., Johnson, K., Karypis, G., Hu, W.-S., 2010. Mining manufacturing data for discovery of high productivity process characteristics. J. Biotechnol. 147, 186–197. https://doi.org/10.1016/j.jbiotec.2010.04.005

Chen, Y.-J., Mahieu, N.G., Huang, X., Singh, M., Crawford, P.A., Johnson, S.L., Gross, R.W., Schaefer, J., Patti, G.J., 2016. Lactate metabolism is associated with mammalian mitochondria. Nat. Chem. Biol. 12, 937–943. https://doi.org/10.1038/nchembio.2172

Chong, W.P.K., Reddy, S.G., Yusufi, F.N.K., Lee, D.-Y., Wong, N.S.C., Heng, C.K., Yap, M.G.S., Ho, Y.S., 2010. Metabolomics-driven approach for the improvement of Chinese hamster ovary cell growth: Overexpression of malate dehydrogenase II. J. Biotechnol. 147, 116–121. https://doi.org/10.1016/j.jbiotec.2010.03.018

Christen, S., Sauer, U., 2011. Intracellular characterization of aerobic glucose metabolism in seven yeast species by 13C flux analysis and metabolomics: Flux response to Crabtree effect in yeast species. FEMS Yeast Res. 11, 263–272. https://doi.org/10.1111/j.1567-1364.2010.00713.x

Ciriacy, M., 1975. Genetics of alcohol dehydrogenase inSaccharomyces cerevisiac: II. Two loci controlling synthesis of the glucose-repressible ADH II. Mol. Gen. Genet. MGG 138, 157–164. https://doi.org/10.1007/BF02428119

Conway, T., Cohen, P.S., 2015. Commensal and pathogenic *Escherichia coli* metabolism in the gut. Microbiol. Spectr. 3, 3.3.24. https://doi.org/10.1128/microbiolspec.MBP-0006-2014

Crown, S.B., Long, C.P., Antoniewicz, M.R., 2016. Optimal tracers for parallel labeling experiments and 13C metabolic flux analysis: A new precision and synergy scoring system. Metab. Eng. 38, 10–18. https://doi.org/10.1016/j.ymben.2016.06.001

Cummings, J., 1981. Short chain fatty acids in the human colon. Gut 22, 763–779.

Dalile, B., Van Oudenhove, L., Vervliet, B., Verbeke, K., 2019. The role of short-chain fatty acids in microbiota–gut–brain communication. Nat. Rev. Gastroenterol. Hepatol. 16, 461–478. https://doi.org/10.1038/s41575-019-0157-3

De Mets, F., Van Melderen, L., Gottesman, S., 2019. Regulation of acetate metabolism and coordination with the TCA cycle via a processed small RNA. Proc. Natl. Acad. Sci. 116, 1043–1052. https://doi.org/10.1073/pnas.1815288116

De Mey, M., De Maeseneire, S., Soetaert, W., Vandamme, E., 2007. Minimizing acetate formation in *E. coli* fermentations. J. Ind. Microbiol. Biotechnol. 34, 689–700. https://doi.org/10.1007/s10295-007-0244-2

de Smidt, O., du Preez, J.C., Albertyn, J., 2008. The alcohol dehydrogenases of *Saccharomyces cerevisiae* : a comprehensive review. FEMS Yeast Res. 8, 967–978. https://doi.org/10.1111/j.1567-1364.2008.00387.x

DeBerardinis, R.J., Chandel, N.S., 2020. We need to talk about the Warburg effect. Nat. Metab. 2, 127–129. https://doi.org/10.1038/s42255-020-0172-2

Diaz, C.A.C., Bennett, R.K., Papoutsakis, E.T., Antoniewicz, M.R., 2019. Deletion of four genes in Escherichia coli enables preferential consumption of xylose and secretion of glucose. Metab. Eng. 52, 168–177. https://doi.org/10.1016/j.ymben.2018.12.003

Eiteman, M.A., Altman, E., 2006. Overcoming acetate in Escherichia coli recombinant protein fermentations. Trends Biotechnol. 24, 530–536. https://doi.org/10.1016/j.tibtech.2006.09.001

Elbing, K., Larsson, C., Bill, R.M., Albers, E., Snoep, J.L., Boles, E., Hohmann, S., Gustafsson, L., 2004. Role of hexose transport in control of glycolytic flux in *Saccharomyces*

cerevisiae. Appl. Environ. Microbiol. 70, 5323–5330. https://doi.org/10.1128/AEM.70.9.5323-5330.2004
Enjalbert, B., Letisse, F., Portais, J.-C., 2013. Physiological and molecular timing of the glucose to acetate transition in *Escherichia. coli*. Metabolites 3, 820–837. https://doi.org/10.3390/metabo3030820
Enjalbert, B., Millard, P., Dinclaux, M., Portais, J.-C., Létisse, F., 2017. Acetate fluxes in *Escherichia. coli* are determined by the thermodynamic control of the Pta-AckA pathway. Sci. Rep. 7, 42135. https://doi.org/10.1038/srep42135
Fell, D.A., 2005. Metabolic Control Analysis, in: Alberghina, L., Westerhoff, H.V. (Eds.), Systems Biology, Topics in Current Genetics. Springer-Verlag, Berlin/Heidelberg, pp. 69–80. https://doi.org/10.1007/b137745
Fina, A., Brêda, G.C., Pérez-Trujillo, M., Freire, D.M.G., Almeida, R.V., Albiol, J., Ferrer, P., 2021. Benchmarking recombinant *Pichia pastoris* for 3-hydroxypropionic acid production from glycerol. Microb. Biotechnol. 14, 1671–1682. https://doi.org/10.1111/1751-7915.13833
Florek, L.C., Lin, X., Lin, Y.-C., Lin, M.-H., Chakraborty, A., Price-Whelan, A., Tong, L., Rahme, L., Dietrich, L.E.P., 2024. The L-lactate dehydrogenases of *Pseudomonas aeruginosa* are conditionally regulated but both contribute to survival during macrophage infection. https://doi.org/10.1101/2024.03.21.586142
Fuchs, C., Köster, D., Wiebusch, S., Mahr, K., Eisbrenner, G., Märkl, H., 2002. Scale-up of dialysis fermentation for high cell density cultivation of *Escherichia. coli*. J. Biotechnol. 93, 243–251. https://doi.org/10.1016/S0168-1656(01)00402-3
Fuentes, L.G., Lara, A.R., Martínez, L.M., Ramírez, O.T., Martínez, A., Bolívar, F., Gosset, G., 2013. Modification of glucose import capacity in *Escherichia. coli*: physiologic consequences and utility for improving DNA vaccine production. Microb. Cell Factories 12, 42. https://doi.org/10.1186/1475-2859-12-42
Ganzhorn, A.J., Green, D.W., Hershey, A.D., Gould, R.M., Plapp, B.V., 1987. Kinetic characterization of yeast alcohol dehydrogenases. Amino acid residue 294 and substrate specificity. J. Biol. Chem. 262, 3754–3761. https://doi.org/10.1016/S0021-9258(18)61419-X
Gerosa, L., Haverkorn van Rijsewijk, B.R.B., Christodoulou, D., Kochanowski, K., Schmidt, T.S.B., Noor, E., Sauer, U., 2015. Pseudo-transition analysis identifies the key regulators of dynamic metabolic adaptations from steady-state data. Cell Syst. 1, 270–282. https://doi.org/10.1016/j.cels.2015.09.008
Glacken, M.W., Fleischaker, R.J., Sinskey, A.J., 1986. Reduction of waste product excretion via nutrient control: Possible strategies for maximizing product and cell yields on serum in cultures of mammalian cells. Biotechnol. Bioeng. 28, 1376–1389. https://doi.org/10.1002/bit.260280912
Görke, B., Stülke, J., 2008. Carbon catabolite repression in bacteria: many ways to make the most out of nutrients. Nat. Rev. Microbiol. 6, 613–624. https://doi.org/10.1038/nrmicro1932
Groussard, C., Morel, I., Chevanne, M., Monnier, M., Cillard, J., Delamarche, A., 2000. Free radical scavenging and antioxidant effects of lactate ion: an in vitro study. J. Appl. Physiol. 89, 169–175. https://doi.org/10.1152/jappl.2000.89.1.169
Harden, A., 1901. LXIV.—The chemical action of *Bacillus coli communis* and similar organisms on carbohydrates and allied compounds. J. Chem. Soc. Trans. 79, 610–628. https://doi.org/10.1039/CT9017900610

Hartley, F., Walker, T., Chung, V., Morten, K., 2018. Mechanisms driving the lactate switch in Chinese hamster ovary cells: HARTLEY ET AL. Biotechnol. Bioeng. 115, 1890–1903. https://doi.org/10.1002/bit.26603

Hayter, P.M., Curling, E.M.A., Gould, M.L., Baines, A.J., Jenkins, N., Salmon, I., Strange, P.G., Bull, A.T., 1993. The effect of the dilution rate on CHO cell physiology and recombinant interferon-γ production in glucose-limited chemostat culture. Biotechnol. Bioeng. 42, 1077–1085. https://doi.org/10.1002/bit.260420909

Heyland, J., Fu, J., Blank, L.M., 2009. Correlation between TCA cycle flux and glucose uptake rate during respiro-fermentative growth of *Saccharomyces cerevisiae*. Microbiology 155, 3827–3837. https://doi.org/10.1099/mic.0.030213-0

Holms, H., 1996. Flux analysis and control of the central metabolic pathways in *Escherichia coli*. FEMS Microbiol. Rev. 19, 85–116. https://doi.org/10.1111/j.1574-6976.1996.tb00255.x

Hui, S., Cowan, A.J., Zeng, X., Yang, L., TeSlaa, T., Li, X., Bartman, C., Zhang, Z., Jang, C., Wang, L., Lu, W., Rojas, J., Baur, J., Rabinowitz, J.D., 2020. Quantitative Fluxomics of Circulating Metabolites. Cell Metab. 32, 676-688.e4. https://doi.org/10.1016/j.cmet.2020.07.013

Hutter, A., Oliver, S.G., 1998. Ethanol production using nuclear petite yeast mutants. Appl. Microbiol. Biotechnol. 49, 511–516. https://doi.org/10.1007/s002530051206

Jallet, D., Soldan, V., Shayan, R., Stella, A., Ismail, N., Zenati, R., Cahoreau, E., Burlet-Schiltz, O., Balor, S., Millard, P., Heux, S., 2024. Integrative *in vivo* analysis of the ethanolamine utilization bacterial microcompartment in *Escherichia coli*. mSystems 9, e00750-24. https://doi.org/10.1128/msystems.00750-24

Jones, R.P., 1990. Roles for Replicative Deactivation in Yeast-Ethanol Fermentations. Crit. Rev. Biotechnol. 10, 205–222. https://doi.org/10.3109/07388559009038208

Kiefer, D., Merkel, M., Lilge, L., Henkel, M., Hausmann, R., 2021. From acetate to bio-based products: underexploited potential for industrial biotechnology. Trends Biotechnol. 39, 397–411. https://doi.org/10.1016/j.tibtech.2020.09.004

Kirkpatrick, C., Maurer, L.M., Oyelakin, N.E., Yoncheva, Y.N., Maurer, R., Slonczewski, J.L., 2001. Acetate and formate stress: opposite responses in the proteome of *Escherichia coli*. J. Bacteriol. 183, 6466–6477. https://doi.org/10.1128/JB.183.21.6466-6477.2001

Korz, D.J., Rinas, U., Hellmuth, K., Sanders, E.A., Deckwer, W.-D., 1995. Simple fed-batch technique for high cell density cultivation of *Escherichia. coli*. J. Biotechnol. 39, 59–65. https://doi.org/10.1016/0168-1656(94)00143-Z

Kuystermans, D., Dunn, M.J., Al-Rubeai, M., 2010. A proteomic study of cMyc improvement of CHO culture. BMC Biotechnol. 10, 25. https://doi.org/10.1186/1472-6750-10-25

Lagarde, D., Jeanson, Y., Barreau, C., Moro, C., Peyriga, L., Cahoreau, E., Guissard, C., Arnaud, E., Galinier, A., Bouzier-Sore, A.-K., Pellerin, L., Chouchani, E.T., Pénicaud, L., Ader, I., Portais, J.-C., Casteilla, L., Carrière, A., 2021. Lactate fluxes mediated by the monocarboxylate transporter-1 are key determinants of the metabolic activity of beige adipocytes. J. Biol. Chem. 296, 100137. https://doi.org/10.1074/jbc.RA120.016303

Lao, M.-S., Toth, D., 1997. Effects of Ammonium and Lactate on Growth and Metabolism of a Recombinant Chinese Hamster Ovary Cell Culture. Biotechnol. Prog. 13, 688–691. https://doi.org/10.1021/bp9602360

Le Grégam, L., Guitton, Y., Bellvert, F., Heux, S., Jourdan, F., Portais, J.-C., Millard, P., 2024. PhysioFit: a software to quantify cell growth parameters and extracellular fluxes. Bioinformatics 40, btae488. https://doi.org/10.1093/bioinformatics/btae488

Li, B., Cai, D., Chen, S., 2021. Metabolic engineering of central carbon metabolism of bacillus licheniformis for enhanced production of poly-γ-glutamic acid. Appl. Biochem. Biotechnol. 193, 3540–3552. https://doi.org/10.1007/s12010-021-03619-4

Li, F., Wang, Y., Zeller, K.I., Potter, J.J., Wonsey, D.R., O'Donnell, K.A., Kim, J., Yustein, J.T., Lee, L.A., Dang, C.V., 2005. Myc stimulates nuclearly encoded mitochondrial genes and mitochondrial biogenesis. Mol. Cell. Biol. 25, 6225–6234. https://doi.org/10.1128/MCB.25.14.6225-6234.2005

Li, J., Wong, C.L., Vijayasankaran, N., Hudson, T., Amanullah, A., 2012. Feeding lactate for CHO cell culture processes: Impact on culture metabolism and performance. Biotechnol. Bioeng. 109, 1173–1186. https://doi.org/10.1002/bit.24389

Li, Xiaoxuan, Hui, S., Mirek, E.T., Jonsson, W.O., Anthony, T.G., Lee, W.D., Zeng, X., Jang, C., Rabinowitz, J.D., 2022. Circulating metabolite homeostasis achieved through mass action. Nat. Metab. 4, 141–152. https://doi.org/10.1038/s42255-021-00517-1

Li, Xiaolu, Yang, Y., Zhang, B., Lin, X., Fu, X., An, Y., Zou, Y., Wang, J.-X., Wang, Z., Yu, T., 2022. Lactate metabolism in human health and disease. Signal Transduct. Target. Ther. 7, 305. https://doi.org/10.1038/s41392-022-01151-3

Liu, M., Ding, Y., Chen, H., Zhao, Z., Liu, H., Xian, M., Zhao, G., 2017. Improving the production of acetyl-CoA-derived chemicals in Escherichia coli BL21(DE3) through iclR and arcA deletion. BMC Microbiol. 17, 10. https://doi.org/10.1186/s12866-016-0913-2

Ljunggren, J., Häggström, L., 1994. Catabolic control of hybridoma cells by glucose and glutamine limited fed batch cultures. Biotechnol. Bioeng. 44, 808–818. https://doi.org/10.1002/bit.260440706

Long, C.P., Antoniewicz, M.R., 2019. Metabolic flux responses to deletion of 20 core enzymes reveal flexibility and limits of *E. coli* metabolism. Metab. Eng. 55, 249–257. https://doi.org/10.1016/j.ymben.2019.08.003

Luli, G.W., Strohl, W.R., 1990. Comparison of growth, acetate production, and acetate inhibition of *Escherichia coli* strains in batch and fed-batch fermentations. Appl. Environ. Microbiol. 56, 1004–1011. https://doi.org/10.1128/aem.56.4.1004-1011.1990

Martínez-Monge, I., Comas, P., Triquell, J., Casablancas, A., Lecina, M., Paredes, C.J., Cairó, J.J., 2019. Concomitant consumption of glucose and lactate: A novel batch production process for CHO cells. Biochem. Eng. J. 151, 107358. https://doi.org/10.1016/j.bej.2019.107358

Martinson, J.N.V., Walk, S.T., 2020. *Escherichia coli* residency in the gut of healthy human adults. EcoSal Plus 9, ecosalplus.ESP-0003-2020. https://doi.org/10.1128/ecosalplus.ESP-0003-2020

Meyenburg, H.K.V., 1969. Energetics of the budding cycle of *Saccharomyces cerevisiae* during glucose limited aerobic growth. Arch Mikrobiol 289–303. https://doi.org/10.1007/BF00414585

Millard, P., Enjalbert, B., Uttenweiler-Joseph, S., Portais, J.-C., Létisse, F., 2021. Control and regulation of acetate overflow in Escherichia coli. eLife 10, e63661. https://doi.org/10.7554/eLife.63661

Mohd Azhar, S.H., Abdulla, R., Jambo, S.A., Marbawi, H., Gansau, J.A., Mohd Faik, A.A., Rodrigues, K.F., 2017. Yeasts in sustainable bioethanol production: A review. Biochem. Biophys. Rep. 10, 52–61. https://doi.org/10.1016/j.bbrep.2017.03.003

Mulukutla, B.C., Gramer, M., Hu, W.-S., 2012. On metabolic shift to lactate consumption in fed-batch culture of mammalian cells. Metab. Eng. 14, 138–149. https://doi.org/10.1016/j.ymben.2011.12.006

Naik, H.M., Kumar, S., Reddy, J.V., Gonzalez, J.E., O. McConnell, B., Gayatri Dhara, V., Wang, T., Yu, M., Antoniewicz, M., J. Betenbaugh, M., 2023. Chemical inhibitors of hexokinase-2 enzyme reduce lactate accumulation, alter glycosylation processing, and produce altered glycoforms in CHO cell cultures 1–19. https://doi.org/10.1002/bit.28417

Nam, S.H., Ye, D., Hwang, H.G., Jung, G.Y., 2024. Convergent synthesis of two heterogeneous fluxes from glucose and acetate for high-yield citramalate production 72, 5797–5804. https://doi.org/10.1021/acs.jafc.3c09466

Nduko, J.M., Taguchi, S., 2021. Microbial production of biodegradable lactate-based polymers and oligomeric building blocks from renewable and waste resources 8. https://doi.org/10.3389/fbioe.2020.618077

Niccoli, S., Boreham, D.R., Phenix, C.P., Lees, S.J., 2017. Non-radioactive 2-deoxy-2-fluoro-D-glucose inhibits glucose uptake in xenograft tumours and sensitizes HeLa cells to doxorubicin in vitro. PLOS ONE 12, e0187584. https://doi.org/10.1371/journal.pone.0187584

Nijland, J.G., Shin, H.Y., Dore, E., Rudinatha, D., de Waal, P.P., Driessen, A.J.M., 2021. D-glucose overflow metabolism in an evolutionary engineered high-performance D-xylose consuming *Saccharomyces cerevisiae* strain. FEMS Yeast Res. 21, foaa062. https://doi.org/10.1093/femsyr/foaa062

Noh, S.M., Park, J.H., Lim, M.S., Kim, J.W., Lee, G.M., 2017. Reduction of ammonia and lactate through the coupling of glutamine synthetase selection and downregulation of lactate dehydrogenase-A in CHO cells. Appl. Microbiol. Biotechnol. 101, 1035–1045. https://doi.org/10.1007/s00253-016-7876-y

Ostergaard, S., Roca, C., Rønnow, B., Nielsen, J., Olsson, L., 1999. Physiological studies in aerobic batch cultivations of *Saccharomyces cerevisiae* strains harboring the MEL1 gene 252–259. https://doi.org/10.1002/(sici)1097-0290(20000505)68:3<252::aid-bit3>3.0.co;2-k.

Ozturk, S.S., Jorjani, P., Taticek, R., Lowe, B., Shackleford, S., Ladehoff-Guiles, D., Thrift, J., Blackie, J., Naveh, D., 1997. Kinetics of glucose metabolism and utilization of lactate in mammalian cell cultures, in: Carrondo, M.J.T., Griffiths, B., Moreira, J.L.P. (Eds.), Animal Cell Technology. Springer Netherlands, Dordrecht, pp. 355–360. https://doi.org/10.1007/978-94-011-5404-8_56

Paalme, T., Elken, R., Kahru, A., Vanatalu, K., Vilu, R., 1997. The growth rate control in *Escherichia coli* at near to maximum growth rates: the A-stat approach. Antonie Van Leeuwenhoek 217–230. https://doi.org/10.1023/a:1000198404007

Paczia, N., Nilgen, A., Lehmann, T., Gätgens, J., Wiechert, W., Noack, S., 2012. Extensive exometabolome analysis reveals extended overflow metabolism in various microorganisms. Microb. Cell Factories 11, 122. https://doi.org/10.1186/1475-2859-11-122

Parada Venegas, D., De La Fuente, M.K., Landskron, G., González, M.J., Quera, R., Dijkstra, G., Harmsen, H.J.M., Faber, K.N., Hermoso, M.A., 2019. Short Chain Fatty Acids (SCFAs)-

mediated gut epithelial and immune regulation and its relevance for inflammatory bowel diseases. Front. Immunol. 10, 277. https://doi.org/10.3389/fimmu.2019.00277
Pasteur, L., 1857. Mémoire de L. Pasteur sur la fermentation alcoolique.
Pastoors, J., Deitert, A., Michel, C., Günster, K., Finger, M., Hofstede, J., Deischter, J., Biselli, A., Viell, J., Palkovits, R., Jupke, A., Büchs, J., 2023. In situ adsorption of itaconic acid from fermentations of Ustilago cynodontis improves bioprocess efficiency. Biotechnol. Biofuels Bioprod. 16, 181. https://doi.org/10.1186/s13068-023-02433-w
Peebo, K., Valgepea, K., Nahku, R., Riis, G., Õun, M., Adamberg, K., Vilu, R., 2014. Coordinated activation of PTA-ACS and TCA cycles strongly reduces overflow metabolism of acetate in *Escherichia coli*. Appl. Microbiol. Biotechnol. 98, 5131–5143. https://doi.org/10.1007/s00253-014-5613-y
Phégnon, L., Pérochon, J., Uttenweiler-Joseph, S., Cahoreau, E., Millard, P., Létisse, F., 2024. 6-Phosphogluconolactonase is critical for the efficient functioning of the pentose phosphate pathway. FEBS J. febs.17221. https://doi.org/10.1111/febs.17221
Pinhal, S., Ropers, D., Geiselmann, J., de Jong, H., 2019. Acetate metabolism and the inhibition of bacterial growth by acetate. J. Bacteriol. 201. https://doi.org/10.1128/JB.00147-19
Raamsdonk, L.M., Diderich, J.A., Kuiper, A., Van Gaalen, M., Kruckberg, A.L., Berden, J.A., Van Dam, K., 2001. Co-consumption of sugars or ethanol and glucose in aSaccharomyces cerevisiae strain deleted in theHXK2 gene. Yeast 18, 1023–1033. https://doi.org/10.1002/yea.746
Rabinowitz, J.D., Enerbäck, S., 2020. Lactate: the ugly duckling of energy metabolism. Nat. Metab. 2, 566–571. https://doi.org/10.1038/s42255-020-0243-4
Reaves, M.L., Young, B.D., Hosios, A.M., Xu, Y.-F., Rabinowitz, J.D., 2013. Pyrimidine homeostasis is accomplished by directed overflow metabolism. Nature 500, 237–241. https://doi.org/10.1038/nature12445
Romano, A.H., Conway, T., 1996. Evolution of carbohydrate metabolic pathways. Res. Microbiol. 147, 448–455. https://doi.org/10.1016/0923-2508(96)83998-2
Rose, I.A., Grunberg-Manago, M., Korey, S.R., Ochoa, S., 1954. ENZYMATIC PHOSPHORYLATION OF ACETATE. J. Biol. Chem. 211, 737–756. https://doi.org/10.1016/S0021-9258(18)71161-7
Sahana, G.R., Balasubramanian, B., Joseph, K.S., Pappuswamy, M., Liu, W.-C., Meyyazhagan, A., Kamyab, H., Chelliapan, S., Joseph, B.V., 2024. A review on ethanol tolerance mechanisms in yeast: Current knowledge in biotechnological applications and future directions. Process Biochem. 138, 1–13. https://doi.org/10.1016/j.procbio.2023.12.024
Schastnaya, E., Doubleday, P.F., Maurer, L., Sauer, U., 2023. Non-enzymatic acetylation inhibits glycolytic enzymes in Escherichia coli. Cell Rep. 42, 111950. https://doi.org/10.1016/j.celrep.2022.111950
Schuurmans, J.M., Rossell, S.L., Van Tuijl, A., Bakker, B.M., Hellingwerf, K.J., Teixeira De Mattos, M.J., 2008. Effect of *hxk2* deletion and *HAP4* overexpression on fermentative capacity in *Saccharomyces cerevisiae*. FEMS Yeast Res. 8, 195–203. https://doi.org/10.1111/j.1567-1364.2007.00319.x
Ser, Z., Gao, X., Johnson, C., Mehrmohamadi, M., Liu, X., Li, S., Locasale, J.W., 2016. Targeting one carbon metabolism with an antimetabolite disrupts pyrimidine homeostasis and induces nucleotide overflow. Cell Rep. 15, 2367–2376. https://doi.org/10.1016/j.celrep.2016.05.035

Shenton, D., Grant, C.M., 2003. Protein S-thiolation targets glycolysis and protein synthesis in response to oxidative stress in the yeast *Saccharomyces cerevisiae*. Biochem. J. 374, 513–519. https://doi.org/10.1042/bj20030414

Silva, Y.P., Bernardi, A., Frozza, R.L., 2020. The Role of Short-Chain Fatty Acids From Gut Microbiota in Gut-Brain Communication. Front. Endocrinol. 11, 25. https://doi.org/10.3389/fendo.2020.00025

Smidt, O., Du Preez, J.C., Albertyn, J., 2012. Molecular and physiological aspects of alcohol dehydrogenases in the ethanol metabolism of *Saccharomyces cerevisiae*. FEMS Yeast Res. 12, 33–47. https://doi.org/10.1111/j.1567-1364.2011.00760.x

Sonnleitner, B., Käppeli, O., 1986. Growth of *Saccharomyces cerevisiae* is controlled by its limited respiratory capacity: Formulation and verification of a hypothesis. Biotechnol. Bioeng. 28, 927–937. https://doi.org/10.1002/bit.260280620

Stanley, G.A., Douglas, N.G., Every, E.J., Tzanatos, T., Pamment, N.B., 1993. Inhibition and stimulation of yeast growth by acetaldehyde. Biotechnol. Lett. 15, 1199–1204. https://doi.org/10.1007/BF00130297

Steffens, L., Pettinato, E., M. Steiner, T., Mall, A., König, S., Eisenreich, W., A. Berg, I., 2021. High CO2 levels drive the TCA cycle backwards towards autotrophy 592, 784–788. https://doi.org/10.1038/s41586-021-03456-9

Sun-Gu, L., Liao, J.C., 2008. Control of acetate production rate in *Escherichia coli* by regulating expression of single-copy pta using lacIq in multicopy plasmid 18, 334–337. https://doi.org/18309280

Szenk, M., Dill, K.A., de Graff, A.M.R., 2017. Why Do Fast-Growing Bacteria Enter Overflow Metabolism? Testing the Membrane Real Estate Hypothesis. Cell Syst. 5, 95–104. https://doi.org/10.1016/j.cels.2017.06.005

Tanner, L.B., Goglia, A.G., Wei, M.H., Sehgal, T., Parsons, L.R., Park, J.O., White, E., Toettcher, J.E., Rabinowitz, J.D., 2018. Four Key Steps Control Glycolytic Flux in Mammalian Cells. Cell Syst. 7, 49-62.e8. https://doi.org/10.1016/j.cels.2018.06.003

Torres, M., Altamirano, C., Dickson, A.J., 2018. Process and metabolic engineering perspectives of lactate production in mammalian cell cultures. Curr. Opin. Chem. Eng. 22, 184–190. https://doi.org/10.1016/j.coche.2018.10.004

Torres, M., Berrios, J., Rigual, Y., Latorre, Y., Vergara, M., Dickson, A.J., Altamirano, C., 2019. Metabolic flux analysis during galactose and lactate co-consumption reveals enhanced energy metabolism in continuous CHO cell cultures. Chem. Eng. Sci. 205, 201–211. https://doi.org/10.1016/j.ces.2019.04.049

Valgepea, K., Adamberg, K., Nahku, R., Lahtvee, P.-J., Arike, L., Vilu, R., 2010. Systems biology approach reveals that overflow metabolism of acetate in Escherichia coli is triggered by carbon catabolite repression of acetyl-CoA synthetase. BMC Syst. Biol. 4, 166. https://doi.org/10.1186/1752-0509-4-166

Van Der Hee, B., Wells, J.M., 2021. Microbial regulation of host physiology by short-chain fatty acids. Trends Microbiol. 29, 700–712. https://doi.org/10.1016/j.tim.2021.02.001

Van Hoek, P., Van Dijken, J.P., Pronk, J.T., 1998. Effect of specific growth rate on fermentative capacity of baker's yeast. Appl. Environ. Microbiol. 64, 4226–4233. https://doi.org/10.1128/AEM.64.11.4226-4233.1998

Vergara, M., Torres, M., Müller, A., Avello, V., Acevedo, C., Berrios, J., Reyes, J.G., Valdez-Cruz, N.A., Altamirano, C., 2018. High glucose and low specific cell growth but not

mild hypothermia improve specific r-protein productivity in chemostat culture of CHO cells. PLOS ONE 13, e0202098. https://doi.org/10.1371/journal.pone.0202098
Walker-Caprioglio, H.M., Parks, L.W., 1987. Autoconditioning factor relieves ethanol-induced growth inhibition of *Saccharomyces cerevisiae*. Appl. Environ. Microbiol. 33–35. https://doi.org/10.1128/aem.53.1.33-35.1987
Warburg, O., Minami, S., 1923. Versuche an Überlebendem Carcinomgewebe. 2, 776–7. https://doi.org/doi: 10.1007/BF01712130
Ward, J.L., Baker, J.M., Llewellyn, A.M., Hawkins, N.D., Beale, M.H., 2011. Metabolomic analysis of *Arabidopsis* reveals hemiterpenoid glycosides as products of a nitrate ion-regulated, carbon flux overflow. Proc. Natl. Acad. Sci. 108, 10762–10767. https://doi.org/10.1073/pnas.1018875108
Wills, C., 1976. Production of yeast alcohol dehydrogenase isoenzymes by selection. Nature 261, 26–29. https://doi.org/10.1038/261026a0
Wlaschin, K.F., Hu, W.-S., 2007. Engineering cell metabolism for high-density cell culture via manipulation of sugar transport. J. Biotechnol. 131, 168–176. https://doi.org/10.1016/j.jbiotec.2007.06.006
Wolfe, A.J., 2005. The Acetate Switch. Microbiol. Mol. Biol. Rev. 69, 12–50. https://doi.org/10.1128/MMBR.69.1.12-50.2005
Wolfe, Alan.J., 2016. Bacterial protein acetylation: new discoveries unanswered questions. Curr. Genet. 62, 335–341. https://doi.org/10.1007/s00294-015-0552-4
Xiao, S., Jiang, S., Qian, D., Duan, J., 2020. Modulation of microbially derived short-chain fatty acids on intestinal homeostasis, metabolism, and neuropsychiatric disorder. Appl. Microbiol. Biotechnol. 104, 589–601. https://doi.org/10.1007/s00253-019-10312-4
Xiao, T., Khan, A., Shen, Y., Chen, L., Rabinowitz, J.D., 2022. Glucose feeds the tricarboxylic acid cycle via excreted ethanol in fermenting yeast. Nat. Chem. Biol. 18, 1380–1387. https://doi.org/10.1038/s41589-022-01091-7
Xu, K., Zhang, K., Wang, Y., Gu, Y., 2024. Comprehensive review of histone lactylation: Structure, function, and therapeutic targets. Biochem. Pharmacol. 225, 116331. https://doi.org/10.1016/j.bcp.2024.116331
Xu, W.-J., Lin, Y., Mi, C.-L., Pang, J.-Y., Wang, T.-Y., 2023. Progress in fed-batch culture for recombinant protein production in CHO cells. Appl. Microbiol. Biotechnol. 107, 1063–1075. https://doi.org/10.1007/s00253-022-12342-x
Zeng, H., Yang, A., 2019. Modelling overflow metabolism in Escherichia coli with flux balance analysis incorporating differential proteomic efficiencies of energy pathways. BMC Syst. Biol. 13, 3. https://doi.org/10.1186/s12918-018-0677-4
Zhang, C., Ottenheim, C., Weingarten, M., Ji, L., 2022. Microbial utilization of next-generation feedstocks for the biomanufacturing of value-added chemicals and food ingredients. Front. Bioeng. Biotechnol. 10, 874612. https://doi.org/10.3389/fbioe.2022.874612
Zhang, D., Tang, Z., Huang, H., Zhou, G., Cui, C., Weng, Y., Liu, W., Kim, S., Lee, S., Perez-Neut, M., Ding, J., Czyz, D., Hu, R., Ye, Z., He, M., Zheng, Y.G., Shuman, H.A., Dai, L., Ren, B., Roeder, R.G., Becker, L., Zhao, Y., 2019. Metabolic regulation of gene expression by histone lactylation. Nature 574, 575–580. https://doi.org/10.1038/s41586-019-1678-1
Zhuang, K., Vemuri, G.N., Mahadevan, R., 2011. Economics of membrane occupancy and respiro-fermentation. Mol. Syst. Biol. 7, 500. https://doi.org/10.1038/msb.2011.34

Chapter 2
Acetate is a beneficial nutrient for *E. coli* at low glycolytic flux

This work was published in "The EMBO journal" and only minor modifications have been introduced in the chapter below.

Full reference: Millard P, Gosselin-Monplaisir T, Uttenweiler-Joseph S, Enjalbert B. Acetate is a beneficial nutrient for *E. coli* at low glycolytic flux. EMBO J. 2023 Aug 1;42(15):e113079. doi: 10.15252/embj.2022113079.

Contribution: In this work, I have generated the deletion strains, designed and performed a significant part of the growth experiments**,** and contributed to review editing.

1. Introduction

As presented in Chapter 1, recent research suggests that acetate is not merely a metabolic waste product but also a co-substrate for glycolytic carbon sources such as glucose, fucose, and gluconate (Enjalbert et al., 2017; Millard et al., 2021). The balance between acetate production and consumption appears to be thermodynamically regulated by acetate concentration. Additionally, acetate functions as a global regulator of *E. coli* metabolism and physiology (Millard et al., 2021). However, these studies have focused on conditions of high glycolytic flux. But, *E. coli* frequently encounters environments with low glycolytic flux, both in its natural habitat the gut and in industrial bioprocesses (Cummings et al., 2001, 1987; De Graaf et al., 2010; Fabich et al., 2008; Jones et al., 2007; Kleman and Strohl, 1994; Macfarlane et al., 1992; Shen et al., 2012; Wolfe, 2005). The gut environment, in particular, is highly dynamic, alternating between nutrient abundance and scarcity while remaining rich in acetate. This raises key questions about how *E. coli* adapts to fluctuations in glycolytic and acetate availability and their combined influence on metabolic fluxes.

In this chapter, we used a systems biology approach to answer this question. By the use of a kinetic model of *E. coli* metabolism, we generated hypotheses on the relationships between glycolytic flux, acetate metabolism, and growth. These predictions were then experimentally validated to uncover the biochemical and regulatory mechanisms governing glucose metabolism. To extend our findings, we also examined other glycolytic substrates, providing a broader perspective on metabolic regulation.

2 Results

2.1 Model-driven hypotheses on the interplay between glucose and acetate metabolism in *Escherichia coli*.

We explored the functional relationship between glycolytic and acetate metabolism in *Escherichia coli* using a coarse-grained kinetic model coupling glucose and acetate metabolism with growth (Figure 1A) (Millard *et al.*, 2021). The model included two compartments, six compounds, and six reactions representing (i) glucose uptake and its conversion into acetyl-CoA by glycolysis, (ii) acetyl-CoA utilization in the TCA cycle and anabolic growth pathways, and (iii) the reversible conversion of acetyl-CoA into acetate via phosphotransacetylase (Pta), acetate kinase (AckA), and acetate exchange between the cell and its environment. Acetate utilization via acetylCoA synthetase (Acs), which is not active when glucose is present (Enjalbert *et al.*, 2017), was not included. The model also included two inhibitory terms representing on the one hand inhibition of glucose uptake and glycolysis, and on the other inhibition of the TCA cycle and growth, in line with the observed inhibition of catabolic and anabolic processes (Millard *et al.*, 2021). This model has been extensively validated and shown to have good predictive capabilities (Millard *et al.*, 2021). We used it to simulate the response

of glycolytic, acetate and growth fluxes to different degrees of glycolytic limitation by progressively reducing the activity (i.e. Vmax) of the glycolytic pathway – and thereby the glycolytic flux – from 100 % to 20 % of its initial value. Since glycolytic and acetate fluxes are both determined by the concentration of acetate (Enjalbert *et al*, 2017; Millard *et al*, 2021; Pinhal *et al*, 2019), these simulations were carried out over a broad range of acetate concentrations (from 0.1 to 100 mM).

The results obtained (Figure 1B-D) highlight the strong bidirectional interplay between glycolytic and acetate metabolism, which eventually modulate growth. Glucose uptake and acetate flux both respond nonlinearly to perturbations (Figure 1B-C). According to the model, increasing the acetate concentration inhibits glycolysis (Figure 1B) and reverses the acetate flux (Figure 1C) over the full range of glycolytic fluxes, as previously reported at the highest glucose uptake rate(Millard *et al*, 2021). The acetate concentration at which the flux reversal occurs appears to depend on the glycolytic flux (Figure 1C). Reducing the glycolytic flux lowers acetate production when acetate is a by-product of glucose metabolism, but seems to enhance acetate utilization when acetate is a co-substrate of glucose (Figure 1C). Finally, the glycolytic flux and the acetate concentration both have a strong, nonlinear effect on the growth rate (Figure 1D). At maximal glycolytic activity, the predictions of the model are consistent with the established deleterious effect of acetate on microbial growth (Figure 1D). However, despite the dual inhibition of catabolism and anabolism by acetate included in the model, it also predicts that at low glycolytic flux, increasing the acetate concentration should boost *E. coli* growth (Figure 1D). A global sensitivity analysis showed that the predictions of the model are robust to parameter uncertainty. We present these model-driven hypotheses in detail (including the sensitivity analysis results) in the following sections along with experimental results collected for validation. Note that none of the data obtained in this study were used to build or calibrate the model and therefore represent independent tests of its predictions and inferred hypotheses.

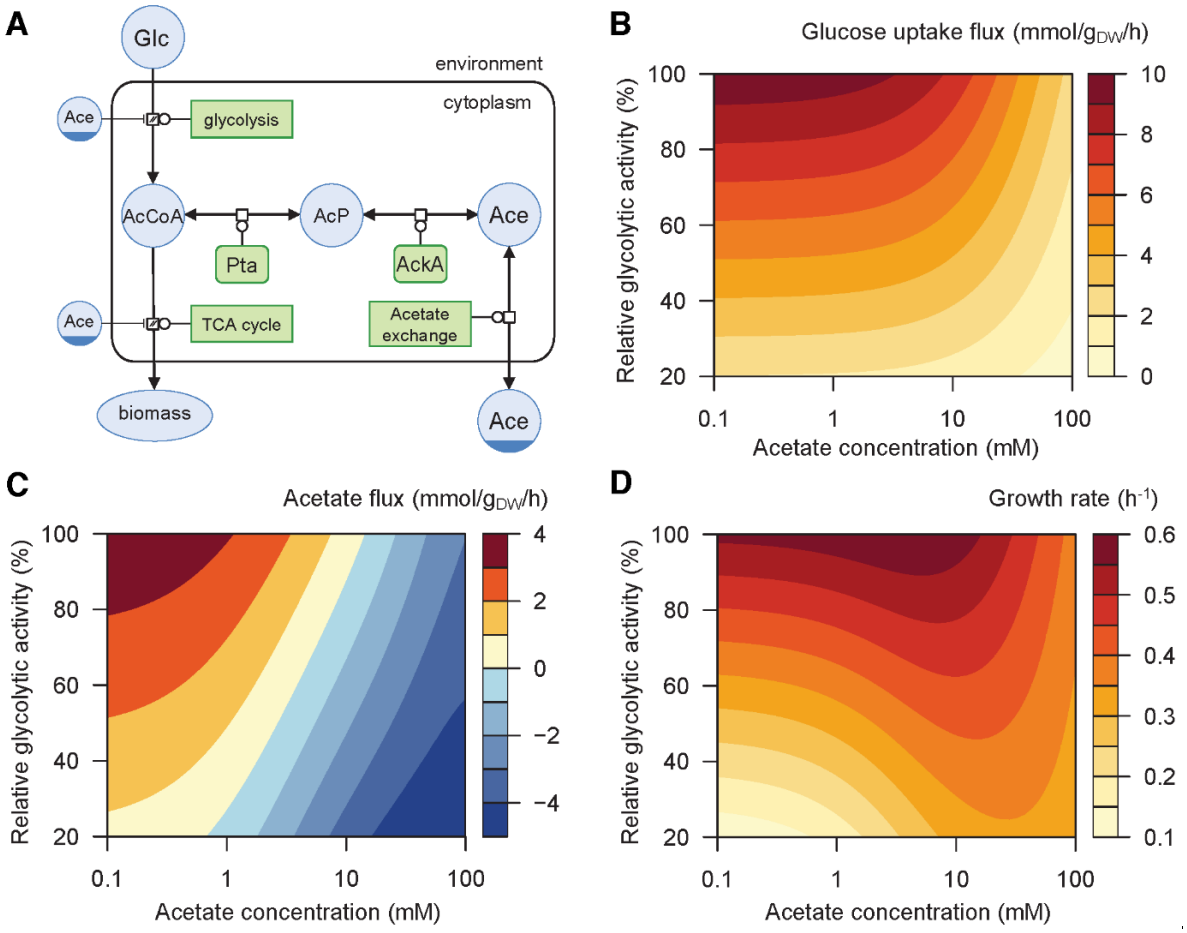


Figure 1. Predicted response of *Escherichia coli* to glycolytic and acetate perturbations.

A Representation (in Systems Biology Graphical Notation format, http://sbgn.org) of the glucose and acetate metabolism of *E. coli*, as implemented in the kinetic model used in the study (reproduced from Millard et al, 2021). B–D Glucose uptake flux (B), acetate flux (C), and growth rate (D) simulated over a broad range of glycolytic activity levels (from 20 to 100% of the initial Vmax) and acetate concentrations (from 0.1 to 100 mM).

2.2 Enhanced acetate utilization at low glycolytic flux buffers carbon uptake

We investigated the glycolytic control of *E. coli* metabolism by confronting the model predictions with experimental data (Figures 1 and 2). The simulations show that, at low acetate concentrations (0 mM in Figure 2A-D), acetate production is predicted to increase with the glycolytic flux, in line with the relationship observed in glucose-limited chemostat experiments (Renilla *et al*, 2012; Valgepea *et al*, 2010) and in a set of mutants with different levels of glucose uptake (Fuentes *et al*, 2013) (Fuentes *et al.*, 2013). In contrast, when the acetate concentration is high (30 mM in Figure 2A-D), such that it is co-consumed with glucose, acetate utilization is expected to increase when the glycolytic flux decreases. This response

implies, as suggested previously (Millard *et al.*, 2021) but never verified experimentally, that the control exerted by glycolysis on the acetate flux is non-monotonic.

To test this hypothesis, we measured growth, glucose uptake, and acetate fluxes in *E. coli* K-12 MG1655 grown on 15 mM glucose and increased the concentration of the glycolytic inhibitor methyl α-D-glucopyranoside (αMG, an analogue of glucose that is taken up and phosphorylated but not metabolized by glycolysis) (Negrete *et al*, 2010) (Figure 2E-H). Experiments were carried out without acetate or with 30 mM acetate for comparison with the predictions shown in Figure 2A-D. Results confirm that αMG inhibits glucose uptake under both conditions (Figure 2E). In the absence of acetate, the acetate (production) flux decreased when the αMG concentration was increased (Figure 2F), as expected based on the positive control exerted by glycolysis on the acetate flux. In contrast, in the presence of 30 mM acetate, increasing the αMG concentration increased the acetate uptake flux (Figure 2F). These results are consistent with the predictions of the model (Figure 2A-D) and demonstrate that glycolysis controls the acetate flux in a non-monotonic manner. The control exerted by glycolysis on acetate metabolism thus depends on the concentration of acetate itself.

The growth and total carbon uptake rates decreased when the αMG concentration was increased in the absence of acetate (Figure 2G-H), but were more stable in the presence of acetate despite a ~2-fold reduction in glucose uptake (between 5.7 and 3.3 $mmol \cdot g_{DW}^{-1} \cdot h^{-1}$ with 30 mM acetate; Figure 2E). Indeed, both the total carbon uptake and the growth rates were less sensitive to glycolytic perturbations in the presence of acetate than in the absence of acetate (Figure 2I-J), suggesting that acetate compensates for the drop in glucose uptake. Consistently, a strong, nonlinear relationship between glucose uptake and acetate flux was observed in all experiments (Figure 2K), which was reflected in the contribution of acetate to the total carbon uptake of *E. coli* (Figure 2L). At the maximal glucose uptake rate, acetate production represented a 10 % loss in carbon. However, when glucose uptake was below 7 $mmol.g_{DW}^{-1}.h^{-1}$, acetate was co-utilized with glucose and contributed positively to the carbon balance (up to 50 % at a glucose uptake rate of 3.3 $mmol \cdot g_{DW}^{-1} \cdot h^{-1}$; Figure 2L). These results highlight the coupling between glycolytic and acetate fluxes in *E. coli*, with acetate buffering carbon uptake at low glycolytic flux, thereby improving the robustness of *E. coli* to glycolytic perturbations.

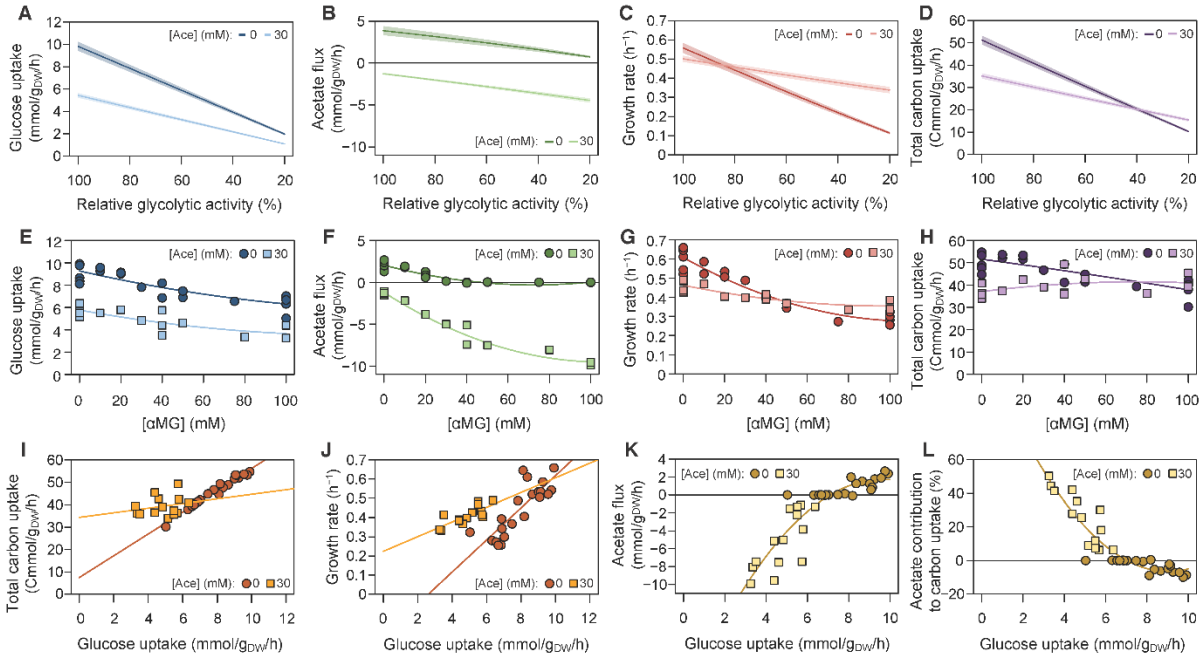


Figure 2. Glycolytic control of *Escherichia coli* metabolism.

A–D Predicted glucose uptake flux (A), acetate flux (B), growth rate (C), and total carbon uptake flux (D) of *E. coli* on glucose (15 mM) as a function of the glycolytic activity (20–100% of the maximal activity), at low (0 mM) and high (30 mM) acetate concentrations. Shaded areas correspond to ± 1 standard deviation on model predictions. E–H Experimental glucose uptake flux (E), acetate flux (F), and growth rate (G) of *E. coli* grown on glucose (15 mM) with different concentrations of aMG (0–100 mM), at low (0 mM) and high (30 mM) acetate concentrations. These data were used to quantify the total carbon uptake flux as a function of the aMG concentration (H). Each data point represents an independent biological replicate, and lines represent the best polynomial fits. I, J Total carbon uptake (I) and growth rate (J) as a function of the glucose uptake flux, at low (0 mM) and high (30 mM) acetate concentrations. Each data point represents an independent biological replicate, and lines represent the best linear fits. K, L Relationships between the acetate flux and glucose uptake (K), and between the contribution of acetate to carbon uptake and glucose uptake (L). Each data point represents an independent biological replicate, and lines represent the best polynomial fits.

2.3 The glycolytic flux determines the acetate concentration threshold at which the acetate flux reverses.

As already reported at maximal glucose uptake rates (Enjalbert *et al.*, 2017; Millard *et al.*, 2021), the acetate concentration threshold at which the acetate flux switches between production and consumption is about 10 mM. However, this threshold was predicted to depend on the glycolytic flux (Figures 1C and 3A-B). According to the model, the switch should occur at an acetate concentration of 3.8 mM when the glycolytic activity is 60 % of its maximum value, and at a concentration of just 0.6 mM when the glycolytic activity is reduced

to 20 % of the maximum. This suggests that the glycolytic flux determines the role of acetate as a co-substrate or by-product of glycolytic metabolism.

We tested this hypothesis by measuring acetate fluxes in *E. coli* grown on glucose (15 mM) plus acetate (from 0.1 to 100 mM) at different concentrations of αMG (0, 20, 40 or 100 mM, Figure 3C). As previously observed at full glycolytic activity (i.e., 0 mM αMG) (Beck *et al*, 2022; Enjalbert *et al*, 2017; Millard *et al*, 2021; Pinhal *et al*, 2019), acetate production decreased when the acetate concentration was increased (Figure 3C), and the acetate flux reversed at a concentration of 6 mM (Figure 3C-D), resulting in co-consumption of glucose and acetate. This threshold concentration gradually decreased when the glycolytic flux was reduced (from 2 mM acetate at 20 mM αMG to below 0.1 mM acetate at 40 or 100 mM αMG). Here again, the experimental profiles are qualitatively similar to the simulated profiles, albeit with quantitative differences. These results demonstrate that the acetate concentration threshold at which the acetate flux reverses depend on the glycolytic flux. It therefore follows that when the glycolytic flux is limited, acetate is utilized as a co-substrate at lower acetate concentrations. These results also confirm that inhibiting glycolysis enhances acetate utilization over the full range of acetate concentrations tested here, further validating the unusual control patterns identified above, and generalizing their functional relevance for acetate concentrations spanning three orders of magnitude.

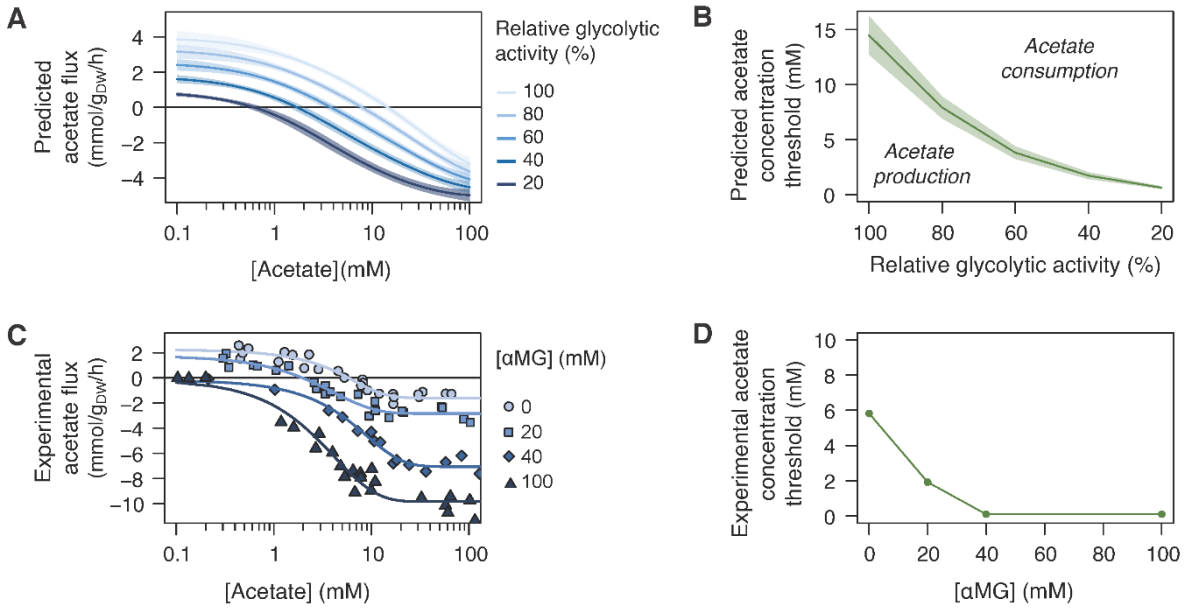


Figure 3. Acetate flux reversal is controlled by the glycolytic flux.

A Predicted acetate flux in *Escherichia coli* on glucose (15 mM) as a function of the acetate concentration at different values of glycolytic activity (from 20 to 100% of the maximal value). Shaded areas correspond to one standard deviation on model predictions. B Predicted acetate concentration threshold at which the acetate flux reverses as a function of the glycolytic activity, determined from the data shown in panel (A). Shaded areas correspond to 1 standard deviation on model predictions. C Experimental acetate flux of *E. coli* K-12 MG1655 grown on

glucose (15 mM) at different acetate concentrations in the presence of aMG (0, 20, 40, or 100 mM). The data measured in the absence of aMG are reproduced from (Enjalbert et al, 2017). Each data point represents an independent biological replicate, and the lines represent best fits using a logistic function. D Experimental acetate concentration threshold at which the acetate flux reverses as a function of the aMG concentration, determined from the best fits shown in panel (C).

2.4 The Acetate enhances *E. coli* growth at low glycolytic flux.

Acetate is considered toxic for microbial cells, but the model predicts this might not always be the case. At full glycolytic activity, the model predicts that maximal growth should occur at low acetate concentrations, with the growth rate remaining above 95 % of the maximum only at acetate concentrations below 12 mM (Figures 1D and 4A). In agreement with the reported toxicity of acetate, the growth rate then monotonously decreases for acetate concentrations above 12 mM. However, when the glycolytic flux is reduced, maximal growth is predicted to occur at high acetate concentrations (Figures 1D and 4A). For instance, when the glycolytic activity is reduced to 20 %, the growth rate is expected to be maximal at an acetate concentration of 28 mM, and should remain above 95 % of the maximum over a broad range of acetate concentrations (between 12 and 86 mM). According to the model therefore, acetate should enhance *E. coli* growth at low glycolytic flux.

To test this prediction, we measured the growth rate of *E. coli* on glucose (15 mM) with acetate (0.1 to 100 mM) in the presence of 100 mM αMG to inhibit glycolysis (Figure 4B). The data measured in the absence of αMG are shown for comparison. At maximal glycolytic flux, the growth rate decreased monotonically with the acetate concentration, but this relationship became non-monotonic when glycolysis was inhibited, which is qualitatively consistent with model predictions. In the presence of αMG, the growth rate was lower in the absence of acetate than at high acetate concentrations (0.28 ± 0.02 h^{-1} with acetate < 0.5 mM versus 0.34 ± 0.01 h^{-1} with 60 mM acetate, p-value = 8.10^{-3}). As predicted by the model therefore, acetate appears to be beneficial rather than toxic to *E. coli* when the glycolytic flux is reduced. The growth rate was slightly lower at 100 mM acetate (0.30 ± 0.03 h^{-1}) than at 60 mM acetate, but the similar growth rates observed across the concentration range demonstrate that acetate is not toxic when the glycolytic flux is low, even at high concentrations.

As an orthogonal, alternative strategy to the use of a glycolytic inhibitor, we tested the impact of acetate on the growth of mutant strains with low glycolytic flux, namely the *E. coli* K-12 BW25113 Δ*pgi* and Δ*pfkA* strains, where the glycolytic flux is 24 and 29 % that of the wild-type strain, respectively (Long & Antoniewicz, 2019). Their growth rates were measured on 15 mM glucose, with or without 10 mM acetate and the effect of acetate was quantified as the relative change in growth rate. The wild-type isogenic strain was grown in the absence and presence of αMG (100 mM) as a control. As expected, acetate reduced the growth rate of the wild-type strain in the absence of αMG (-6 ± 1 %, p-value = 4.10^{-5}) but increased its growth in the presence of 100 mM αMG ($+9 \pm 2$ %, p-value = 3.10^{-5}) (Figure 4C). The beneficial effect of

acetate on growth was also observed in the Δ*pgi* and Δ*pfkA* strains (Figure 4D), whose growth rate strongly increased despite the absence of αMG (Δ*pgi* : +60 ± 19 %, p-value = 3.10^{-2}; Δ*pfkA* : +117 ± 21 %, p-value = 1.10^{-2}). These results confirm that the beneficial effect of acetate is not due to the presence of αMG but is a consequence of the decrease in glycolytic flux.

Overall, all results are in line with the predictions of the model and demonstrate that acetate enhances *E. coli* growth when the glycolytic flux is reduced by either chemical or genetic perturbations.

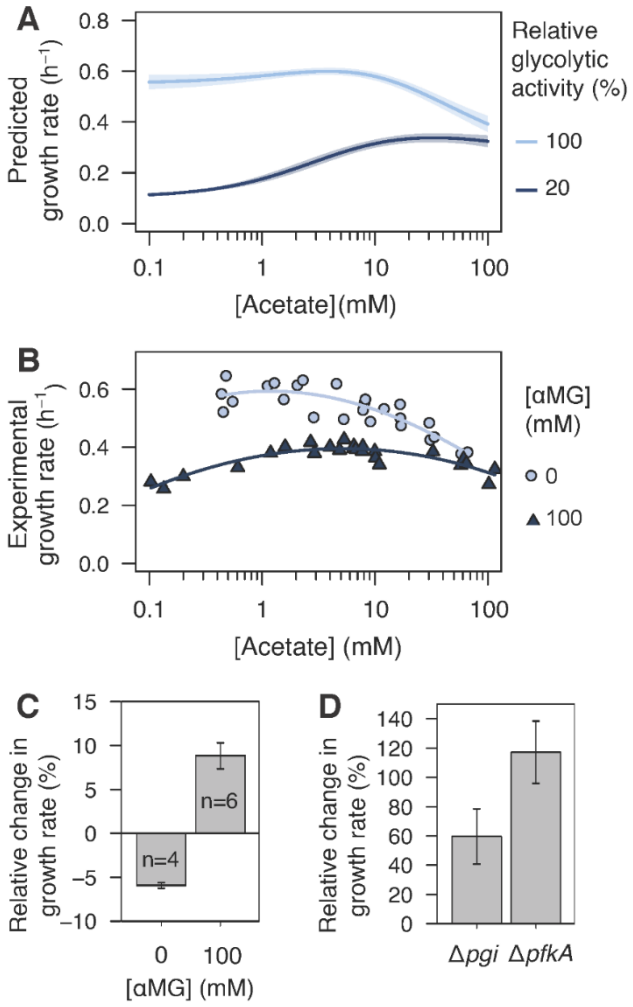


Figure 4. Effect of acetate on *Escherichia coli* growth on glucose.

A Predicted growth rate of *E. coli* on glucose (15 mM) as a function of the acetate concentration at 100 and 20% of the maximal glycolytic activity. Shaded areas correspond to 1 standard deviation on model predictions. B Experimental growth rate of *E. coli* K-12 MG1655 grown on glucose (15 mM) as a function of the acetate concentration at high (0 mM aMG, light blue, reproduced from Enjalbert et al, 2017) or low (100 mM aMG, dark blue) glycolytic flux. Each data point represents an independent biological replicate, and the lines represent best polynomial fits. C Relative change in the growth rate of *E. coli* K-12 BW25113 wild-type in the presence of 10 mM acetate at high (0 mM aMG) and low (100 mM aMG) glycolytic flux. Mean values standard deviations (error bars) were estimated from n independent biological

replicates, as indicated on the figure. D Relative change in the growth rates of *E. coli* K-12 BW25113 Δpgi and ΔpfkA strains in the presence of 10 mM acetate. Mean values standard deviations (error bars) were estimated from three independent biological replicates.

2.5 At low glycolytic flux, acetate activates *E. coli* metabolism and growth at the transcriptional level.

At high glycolytic flux, it has been proposed (Millard *et al.*, 2021) that the apparent "toxicity" of acetate is due to its inhibition of most metabolic genes – including those for the glucose phosphotransferase system (PTS), glycolysis and TCA cycle. Acetate also increases the expression of genes related to stress responses and downregulates genes related to transport, energy biosynthesis and mobility for instance. To determine if acetate has a similar regulatory effect at low glycolytic flux, we compared the transcriptomes of *E. coli* grown on glucose (15 mM) plus acetate (0, 10, 50 or 100 mM) in the presence of αMG (100 mM), with those measured in the absence of αMG at the same acetate concentrations (Millard *et al.*, 2021).

We observed that contrary to what occurs at maximal glycolytic flux (0 mM αMG) acetate did not trigger a stress response at low glycolytic flux (100 mM αMG) (Figure 5A). Conversely, acetate increased gene expression for the respiratory chain and some biosynthetic processes (ribonucleotide monophosphate biosynthesis, amino acid production). Other hallmarks of the effect of acetate at maximal glycolytic flux such as the inhibition of mobility-related gene expression were also not observed at low glycolytic flux. The activation of glutamate catabolism, the repression of transport related genes, and the repression of carbohydrate transport and catabolism were among the few similarities between the responses to acetate at high and low glycolytic flux.

At the metabolic level, acetate-driven inhibition of the expression of central metabolic genes (PTS, TCA and glycolytic enzymes) and growth machinery (ribosomal proteins) was not observed at low glycolytic flux (Figure 5B). In fact, expression of most of these genes (47/65) was slightly higher in the presence of 50 mM acetate and 100 mM αMG, whereas at maximal glycolytic flux it was lower at these acetate concentrations for a similar proportion (46/65). When the glycolytic flux was inhibited, *ptsG* expression, which controls glucose uptake (Rohwer *et al*, 2000), was 70 % higher at 10 and 50 mM acetate. The expression of most glycolytic genes was 15 to 110 % higher at 50 mM acetate, while the expression of TCA cycle genes remained stable. Regarding acetate metabolism, the expression of *pta* and *ackA* was slightly higher at 10 and 50 mM acetate, while alternative acetate utilization via Acs was inhibited by acetate (5-fold reduction in expression at 100 mM). Finally, expression of genes encoding ribosomal proteins (*rpl*, *rpm* and *rps* operons) was increased by 57 % on average at 50 mM acetate and 48 % on average at 100 mM acetate.

These results indicate that the stress response and lower metabolic activity triggered by acetate at high glycolytic flux do not occur at low glycolytic flux. In this situation, acetate enhances the expression of ribosomal and central metabolic genes, in line with its positive effect on growth. This is the opposite of what is observed at high glycolytic flux, demonstrating that the regulatory role of acetate is largely determined by the glycolytic flux.

A

αMG (mM)	0			100		
Acetate (mM)	10	50	100	10	50	100
response to stress	7.5E-03	1.2E-10	2.2E-14			
response to pH	1.4E-08	1.4E-07	1.7E-09			6.5E-03
response to oxidative stress		4.8E-04	4.8E-08			
response to osmotic stress	1.9E-03	4.7E-06	7.1E-07			5.5E-05
locomotion		5.8E-39	6.8E-30			
cytochrome assembly	8.8E-06	1.6E-03	8.8E-06			
ATP biosynthetic process			3.3E-09			
respiratory chain				1.0E-07	2.8E-10	
transport	9.1E-09	5.8E-12	6.5E-16		1.0E-07	3.8E-17
ion transport	2.5E-09	6.9E-10	1.1E-12			1.6E-04
peptide transport	8.5E-03	1.4E-05	4.9E-05			
carbohydrate transport	6.2E-03				4.3E-09	9.2E-25
catabolic process	6.2E-03		1.0E-03		7.9E-09	3.7E-10
glutamate catabolism	1.4E-04	1.4E-03	6.1E-03	4.5E-03	1.5E-04	8.0E-03
methionine biosynthesis					2.9E-07	3.1E-03
ribonucleoside biosynthesis					2.1E-03	5.1E-11
amino acid biosynthesis					2.2E-07	1.2E-04

B

	αMG (mM)	0				100			
	Acetate (mM)	0	10	50	100	0	10	50	100
Glc uptake	ptsG	1.0	0.6	0.4	0.2	1.0	1.8	1.6	1.2
	ptsH	1.0	0.7	0.5	0.4	1.0	1.2	1.1	1.0
	ptsI	1.0	0.9	0.7	0.7	1.0	1.1	0.9	0.8
	crr	1.0	1.0	0.8	0.7	1.0	1.2	1.0	0.8
	glk	1.0	0.7	0.6	0.6	1.0	1.4	1.1	0.6
Upper glycolysis	pgi	1.0	1.1	0.9	1.0	1.0	1.3	1.6	1.8
	pfkA	1.0	1.1	0.9	1.1	1.0	1.6	1.6	1.3
	pfkB	1.0	1.6	3.7	7.5	1.0	1.1	2.3	4.2
	fbaA	1.0	1.1	1.0	1.1	1.0	1.2	1.5	1.5
	fbaB	1.0	1.9	3.8	6.9	1.0	0.7	0.8	1.6
	tpiA	1.0	1.1	1.2	1.3	1.0	1.3	1.6	1.5
Lower glycolysis	gapA	1.0	0.9	0.9	0.6	1.0	2.2	1.9	1.5
	pgk	1.0	1.0	0.7	0.9	1.0	1.6	1.5	1.5
	gpmA	1.0	0.9	0.8	0.7	1.0	1.4	1.4	1.1
	eno	1.0	1.0	0.7	0.6	1.0	1.8	2.1	1.8
	pykA	1.0	1.0	0.9	1.1	1.0	1.4	1.2	0.8
	pykF	1.0	0.8	0.7	0.7	1.0	1.3	1.1	1.5
	aceE	1.0	0.8	0.8	0.7	1.0	1.3	1.8	0.9
	aceF	1.0	1.1	0.9	1.0	1.0	1.4	1.7	1.1
Anaplerotic	ppc	1.0	0.9	0.7	0.9	1.0	1.0	1.3	1.4
	pck	1.0	0.7	0.4	0.2	1.0	1.3	1.1	0.6
	maeA	1.0	1.0	1.0	1.1	1.0	1.0	2.1	1.9
	maeB	1.0	1.0	0.6	0.5	1.0	1.2	0.9	0.6

		0				100			
		0	10	50	100	0	10	50	100
Acetate	pta	1.0	1.0	1.1	1.1	1.0	1.5	1.4	1.2
	ackA	1.0	0.9	1.0	1.1	1.0	1.8	1.7	0.8
	acs	1.0	0.7	0.5	0.4	1.0	0.8	0.3	0.2
	poxB	1.0	2.8	2.6	8.1	1.0	0.7	1.1	1.9
TCA cycle and glyoxylate shunt	gltA	1.0	1.0	0.8	0.6	1.0	0.8	0.8	0.6
	acnA	1.0	1.2	1.5	2.2	1.0	1.0	1.0	1.3
	acnB	1.0	1.1	1.0	0.8	1.0	0.9	1.2	1.0
	icd	1.0	1.0	0.8	0.6	1.0	1.1	1.2	1.0
	lpd	1.0	1.0	0.8	0.7	1.0	0.9	1.2	1.1
	sucA	1.0	1.2	1.3	0.9	1.0	1.1	1.3	1.4
	sucB	1.0	1.0	1.0	0.6	1.0	1.1	1.3	1.2
	sucC	1.0	0.9	0.9	0.6	1.0	1.1	1.3	1.1
	sucD	1.0	0.9	0.8	0.5	1.0	1.1	1.2	1.0
	sdhA	1.0	1.0	0.9	0.7	1.0	0.8	0.9	0.9
	sdhB	1.0	0.9	0.7	0.5	1.0	0.8	0.9	0.8
	sdhC	1.0	1.0	0.8	0.5	1.0	0.8	1.0	1.0
	sdhD	1.0	0.9	0.8	0.5	1.0	0.8	0.9	1.0
	fumA	1.0	0.9	0.8	0.6	1.0	1.0	0.8	0.5
	fumB	1.0	1.2	1.4	1.3	1.0	1.0	1.1	1.0
	fumC	1.0	1.0	0.5	0.3	1.0	0.8	0.6	0.5
	mdh	1.0	1.0	0.5	0.6	1.0	1.2	1.3	1.1
	mqo	1.0	1.5	2.3	2.2	1.0	1.0	2.5	3.4
	aceA	1.0	1.1	0.7	0.9	1.0	1.2	1.0	0.9
	aceB	1.0	1.2	0.9	1.4	1.0	0.7	1.1	1.0

Figure 5. Regulation of *Escherichia coli* transcriptome by acetate at high and low glycolytic flux.

A, B Transcriptomic response of *E. coli* K-12 MG1655 to acetate (10, 50, or 100 mM versus 0 mM) at high (0 mM aMG) and low (100 mM aMG) glycolytic flux. The data obtained in the absence of aMG are reproduced from (Millard et al, 2021). The biological functions modulated by the presence of acetate (based on Gene Ontology analysis) are shown in part (A), with the corresponding P-values. The expression levels of central metabolic genes are shown in part (B). Gene expression is normalized to the value measured at the same aMG concentration but without acetate. Green and red indicate decreased and increased expression, respectively.

2.6 Acetate-enhances growth is supported by the Pta-AckA pathway.

According to the model (Figure 1A), the reversible Pta-AckA pathway (acetate consumption or production) explains by itself how acetate promotes *E. coli* growth, without the need for Acs (acetate consumption only). To confirm this hypothesis, we measured the growth rates of *E. coli* K-12 BW25113 wild-type and of Δ*pta* and Δ*acs* isogenic mutant strains cultivated on 15 mM glucose plus 100 mM αMG, with or without 10 mM acetate. The effect of acetate was quantified as the relative change in growth rate induced. Acetate had a similar, beneficial effect on the growth of the wild-type strain (+9 ± 2 %, p-value = 3.10^{-5}) and of the Δ*acs* strain

(+8 ± 1 %, p-value = 1.10^{-3}), but not for the Δ*pta* strain, whose growth rate decreased slightly but significantly (−6 ± 1 %, p-value = 7.10^{-3}). These results confirm that the beneficial effect of acetate on *E. coli* growth at low glycolytic flux is mediated by the Pta-AckA pathway, with no involvement of Acs in this phenomenon.

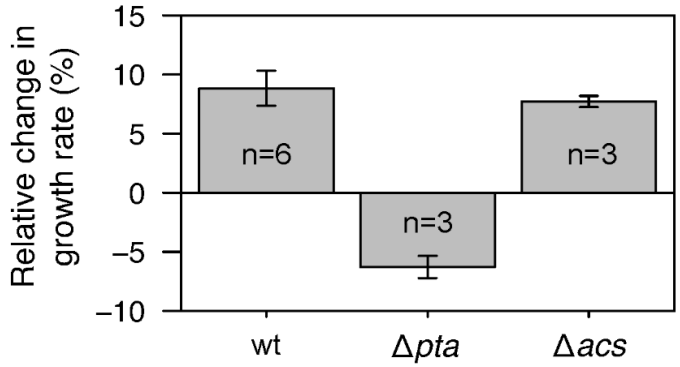


Figure 6. Response of wild-type, Δpta, and Δacs strains of *E. coli* to acetate during growth on glucose (low glycolytic flux).

Relative change in the growth rates of wild-type, Δ*pta*, and Δ*acs E. coli* K-12 BW25113 strains in the presence of 10 mM acetate at low glycolytic flux (100 mM aMG). Mean values and standard deviations (error bars) were estimated from n independent biological replicates, as indicated on the figure.

2.7 Acetate boosts growth of *E. coli* on glycerol and galactose.

Assuming that the beneficial impact of acetate on *E. coli* growth stems from the tight interplay of glycolytic and acetate fluxes, this should be independent of the nature of the carbon source, implying that acetate should boost *E. coli* growth on glycolytic substrates with low glycolytic flux, such as glycerol and galactose (Gerosa *et al*, 2015). And indeed, wild-type *E. coli* growth was enhanced on both glycerol (+7 ± 1 %, p-value = 1.10^{-2}, Figure 7A) and galactose (+52 ± 1 %, p-value = 2.10^{-4}, Figure 7B) in the presence of 10 mM acetate. Similar levels of enhancement were observed for the Δ*acs* strain (+8 ± 1 % on glycerol, p-value = 3.10^{-4}; +53 ± 5 % on galactose, p-value = 3.10^{-3}), but not for the Δ*pta* strain (−8 ± 2 % on glycerol, p-value = 1.10^{-2}; +2 ± 12 % on galactose, p-value = 0.70) (Figure 7). These results demonstrate that acetate promotes *E. coli* growth on galactose and glycerol. As observed for glucose, the growth enhancement is mediated exclusively by the Pta-AckA pathway, with no involvement of Acs. These results extend and generalize our findings to glycolytic carbon sources other than glucose and support our findings in more physiological conditions, i.e. without an inhibitor or deletion of metabolic genes.

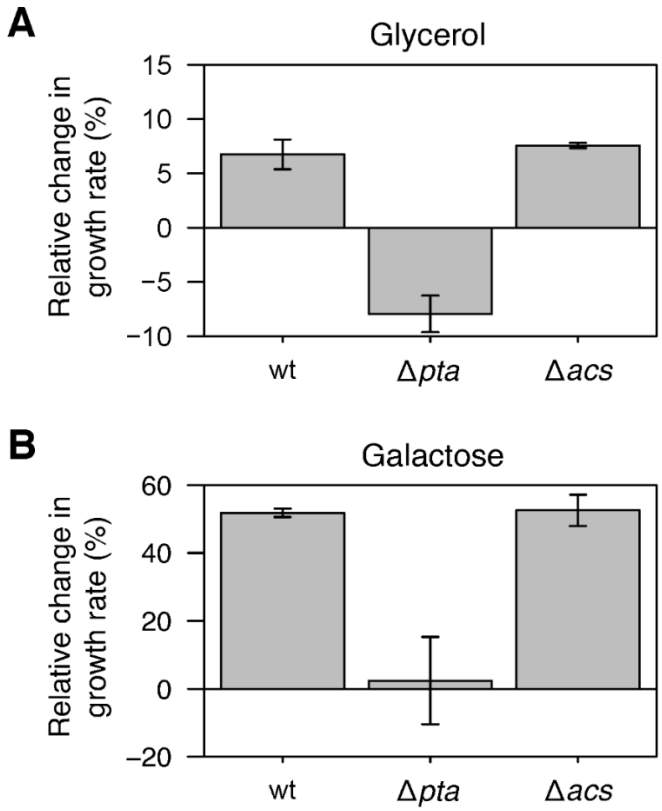


Figure 7. Response of *Escherichia coli* to acetate during growth on glycerol or galactose.

A, B Impact of the presence of 10 mM acetate on the growth rate of wildtype, Δpta, and Δacs *E. coli* K-12 BW25113 strains grown on (A) 30 mM glycerol and (B) 15 mM galactose. Mean values and standard deviations (error bars) were estimated from three independent biological replicates.

3. Discussion

Following a systems biology approach, we used a kinetic model of *E. coli* metabolism to generate a comprehensive map of the functional relationship between glycolytic and acetate metabolisms and predict their combined impact on *E. coli* growth. In agreement with the predictions of the model, experimental results revealed a strong interplay between acetate and glycolytic fluxes in *E. coli*, with wide-ranging physiological consequences for the cells. Despite its established toxicity for microbial growth, we found that acetate improves the robustness of *E. coli* to glycolytic perturbations, and even boosts growth when the glycolytic flux is low.

Previous studies of the glycolytic control of acetate metabolism were carried out in the absence of acetate. In this situation, as observed here, glycolysis as a positive effect on acetate production. However, our results also reveal that in the presence of acetate, glycolysis negatively affects acetate utilization. Glycolytic control of the acetate flux is thus determined

by the concentration of acetate itself. Because of this non-monotonous control pattern, reduced glycolytic flux increases acetate uptake and lowers the acetate concentration threshold at which acetate is co-consumed with glucose, with the overall effect of increasing acetate utilization by *E. coli*. This demonstrates that the metabolic status of acetate as a by-product or co-substrate of glycolytic carbon sources is determined both by the concentration of acetate (Enjalbert *et al.*, 2017; Millard *et al.*, 2021) and the glycolytic flux, and thus by the availability of glycolytic nutrients. This mechanism is exclusively mediated by the Pta-AckA pathway and its role and activity are determined by the nutritional conditions experienced by *E. coli*. The Pta-AckA pathway can therefore be seen as a metabolic valve that integrates information on the nutritional environment of the cells to rapidly adjust the acetate flux depending on the availability of glycolytic substrates and acetate. Our results indicate that these properties, which emerge simply from the distribution of control throughout the network, buffers the total carbon uptake flux and makes *E. coli* more robust to changes in the nutritional environment.

When the glycolytic flux is low, enhanced acetate utilization promotes *E. coli* growth, demonstrating that acetate can be beneficial to *E. coli*, even at high concentrations. Whereas 60 mM acetate has been shown to inhibit growth by ~35 % at maximal glucose uptake rates (Enjalbert *et al*, 2017; Luli & Strohl, 1990; Pinhal *et al*, 2019), the same concentration of acetate had a positive effect on growth at low glucose uptake rates (+21 % in presence of 100 mM αMG). We confirmed the beneficial effect of acetate on *E. coli* growth using three different strategies to reduce the glycolytic flux: i) chemical inhibition of glucose uptake with αMG, ii) mutant strains deleted for glycolytic genes, and iii) glycolytic substrates with a naturally low glycolytic flux (glycerol and galactose). Since the impact of acetate on growth is partly determined by the glycolytic flux, this metabolic by-product is not toxic *per se*. Importantly, these results also weaken several hypotheses that have been proposed to explain the apparent “toxicity” of acetate for microbial growth. Indeed, perturbations of the proton gradient, of the anion composition of the cell, or of methionine biosynthesis, would have a monotonic impact on growth. The slight but global activating effect of acetate on the transcriptome at low glycolytic flux, which correlates with the growth response, also contrasts with its inhibitory effect at high glycolytic flux. The results of this study indicate that mechanisms that only explain growth inhibition at high glycolytic flux are inadequate. Likewise, the recent suggestion that gluconeogenic substrates such as acetate enhance *E. coli* growth on glycolytic substrates (as observed for mixtures of oxaloacetate with glycerol, xylose or fucose) (Okano *et al*, 2020) also fails to capture the non-monotonic growth response of *E. coli* to acetate. The regulatory effect of acetate on *E. coli* metabolism, which depends both on the acetate concentration and on the glycolytic flux, is therefore more complex than previously suggested (Millard *et al.*, 2021) and should be investigated further.

Previous reports have shown that the “toxicity” of acetate for *E. coli* growth depends on the pH (Lawford & Rousseau, 1993; Orr *et al*, 2019; Pinhal *et al*, 2019). In our experiments, the pH was initially set to 7.0 but was not adjusted during growth. Nevertheless, the high buffer capacity of the M9 cultivation medium ensured that the pH remained stable in the exponential growth phase where growth rates and extracellular fluxes were measured, with changes of

less than 0.3 pH unit in all experiments (Figure 8). Therefore, the metabolic and physiological responses of *E. coli* to acetate highlighted in this study are not due to changes in pH. Another potential issue is that the effect of acetate might also depend on the concentration of salts (Bae & Lee, 2017; Lee *et al*, 2010). The effect of acetate added as sodium salt may differ from its effect when added as acetic acid. However, repeat experiments performed with acetic acid instead of sodium acetate showed that the beneficial effect of acetate on *E. coli* growth on glucose, galactose and glycerol was maintained (Figure 9B).

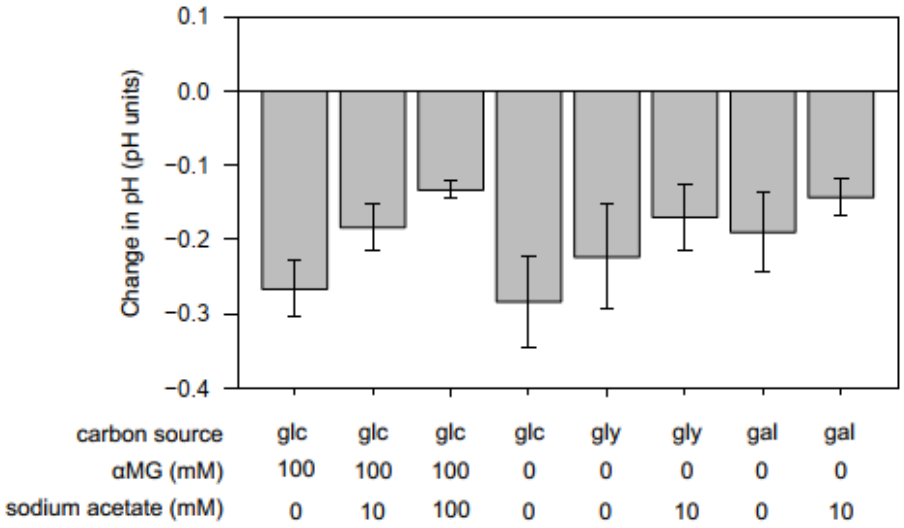


Figure 8. Change in pH of the cultivation medium of *E. coli* grown on glycolytic substrates plus different concentrations of αMG and acetate.

Change in pH of the cultivation medium during growth of *E. coli* K-12 BW25113 on glucose, glycerol or galactose plus different concentrations of αMG and acetate. Change in pH was measured in the exponential growth phase where growth rates and extracellular fluxes were measured (OD between ~0.1 and ~1.5). Mean values and standard deviations (error bars) were estimated from three independent biological replicates.

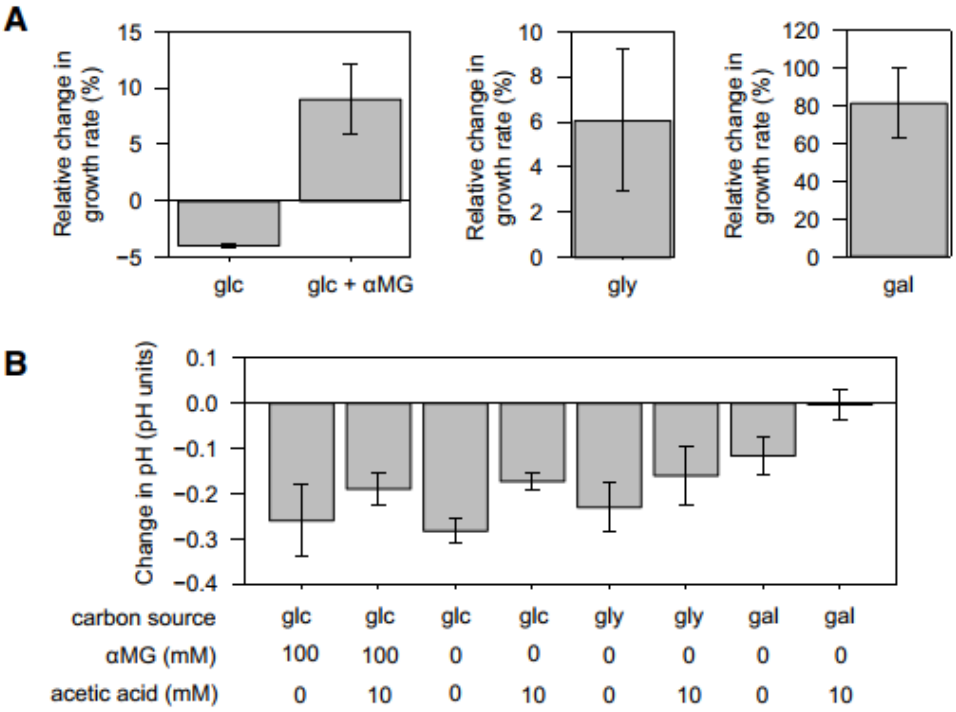


Figure 9. Response of *E. coli* to acetic acid.

A Relative change in the growth rate of *E. coli* K-12 BW25113 wild-type induced by the presence of 10 mM acetic acid during growth on glucose (without or with 100 mM αMG), glycerol or galactose. Mean values and standard deviations (error bars) were estimated from three independent biological replicates.

B Change in pH of the cultivation medium during growth of *E. coli* K-12 BW25113 wild-type on glucose, glycerol or galactose plus different concentrations of αMG and acetic acid. Change in pH was measured in the exponential growth phase where growth rates were measured (OD between ~0.1 and ~1.5). Mean values and standard deviations (error bars) were estimated from three independent biological replicates.

The measured responses of *E. coli* to a broad range of perturbations of the glycolytic and acetate metabolisms were qualitatively consistent with model predictions, though quantitative differences were observed. These differences may stem from the data used to construct and calibrate the model, which were obtained exclusively at maximal glycolytic flux. Therefore, although it was not initially developed to address the questions of this study, the kinetic model used here successfully predicts the observed interplay between glycolytic and acetate metabolisms, as well as the beneficial effect of acetate on *E. coli* growth at low glycolytic flux. Since the model does not account for the activation by acetate of the expression of glucose uptake, glycolytic, and ribosomal genes, this suggests that transcriptional activation by acetate may not be crucial for the flux response of *E. coli*. The metabolic network may indeed directly sense and integrate the availability of glucose and acetate to coordinate glucose and acetate fluxes, as already reported for the coordination other metabolic processes (Doucette *et al*, 2011; Millard *et al*, 2017; Yuan *et al*, 2009). In keeping with this hypothesis, our results support the concept of acetate flux being

thermodynamically controlled by acetate itself, as detailed in (Enjalbert *et al.*, 2017), and we show that the thermodynamically-driven flux reversal is also controlled by the glycolytic flux. The reduction in glucose-derived acetyl-CoA is counterbalanced by an increased contribution of acetate, which sustains growth. Metabolic regulation is thus (at least partly) responsible for the interplay between acetate and glycolytic flux. The precise regulatory program driven by acetate remains to be identified.

Acetate concentrations in the gut range from 30 to 100 mM (Cummings *et al*, 1987; Macfarlane *et al*, 1992; Cummings & Macfarlane, 1991; Macfarlane *et al*, 1992) and glycolytic nutrients, such as glycerol and galactose (Fabich *et al.*, 2008; Matamouros *et al*, 2018; Snider *et al*, 2009), are generally scarce. Given the established inhibition of microbial growth by acetate, these high acetate levels were considered detrimental to *E. coli* colonization. Our results indicate that acetate, far from being toxic, may in fact be beneficial to *E. coli* in this environment. Acetate enhances *E. coli* growth when glycolytic substrates are limiting and may therefore facilitate its colonization and survival in the gut. Moreover, acetate stabilizes growth when the glycolytic flux is perturbed by temporary nutrient shortages, which are frequent in the gut. We suggest that the underlying regulatory mechanism may therefore be optimal for *E. coli* in its natural environment. Our results also call for the role of acetate in the gut to be reconsidered, since it represents a valuable and abundant resource that may benefit *E. coli* and other microorganisms.

In biotechnology, developing efficient strategies to overcome the negative effects of acetate requires understanding what controls the acetate flux and how in turn acetate controls microbial metabolism. By addressing these two needs, our findings should immediately help design bioprocesses with reduced acetate overflow and accelerate the development of mixed feed processes in which acetate is utilized alongside glucose or other glycolytic substrates. Current strategies are mainly based on increasing Acs activity to (re)use acetate present in the feedstock, provided as a co-substrate or produced by the Pta-AckA pathway. Given the Pta-AckA pathway produces one ATP and Acs consumes two ATPs, strategies based on activating the Pta-AckA-Acs cycle are highly energy-consuming (Valgepea *et al*, 2010). Strategies involving the Pta-AckA pathway alone are inherently less costly for the cell. Our results show that the Pta-AckA pathway enables efficient co-utilization of acetate and glycolytic substrates (glucose, glycerol, galactose) in *E. coli* by itself, with a positive effect on growth. The comprehensive understanding of the relationship between glycolytic and acetate metabolisms provided by this study may also represents a valuable guide to increase the productivity of valuable products synthesized from acetate-derived acetyl-CoA (Becker & Wittmann, 2015; Zhang *et al*, 2015).

In this chapter, we demonstrate that similarly to lactate and ethanol, acetate is not a deleterious waste product but a valuable nutrient that can be shuttled between cells. The reversible Pta-AckA pathway enables uncoupling of glycolysis from the TCA cycle, indicating that this evolutionarily conserved design principle of eukaryotic metabolism (Xiao *et al*, 2022) is also present in bacteria. As a nutrient and global regulator of microbial metabolism, acetate plays a major role in cellular, microbial community and host-level carbon and energy homeostasis.

4. Materials and Methods

4.1 Strains.

Escherichia coli K-12 MG1655 was chosen as the model wild-type strain. For experiments involving mutant strains, *E. coli* K-12 BW25113 was chosen as the reference wild-type strain, and its isogenic Δ*pta*, Δ*pgi* and Δ*pfkA* mutants were constructed from the KEIO collection (Baba *et al*, 2006) by removing the kanamycin cassette (Datsenko & Wanner, 2000). The Δ*acs* strain was constructed by CRISPR-Cas9 genome editing using the method and plasmids described in jiang et al. (Jiang *et al*, 2015). *pta* deletion was confirmed by genome sequencing and *acs*, *pgi* and *pfkA* deletions by PCR (with primers listed in Appendix Table S1).

4.2 Growth conditions.

E. coli was grown in M9 minimal media (Millard *et al*, 2014) supplemented with 15 mM glucose, 15 mM galactose, or 30 mM glycerol. Sodium acetate (prepared as a 1.2 M solution at pH 7.0 by addition of potassium hydroxide), acetic acid (prepared as a 1.2 M solution at pH 7.0 by addition of ammonium hydroxide) and methyl α-D-glucopyranoside (αMG, prepared as a 1.2 M solution) were added up to the required concentrations. The cells were grown in shake flasks at 37 °C and 200 rpm, in 50 mL of medium. Growth was monitored by measuring the optical density (OD) at 600 nm using a Genesys 6 spectrophotometer (Thermo, USA). Biomass concentrations were determined using a conversion factor of 0.37 g_{DW}/L/OD unit (Revelles *et al*, 2013).

4.3 Transcriptomics experiments.

Cells were grown in M9 medium with 15 mM glucose, 100 mM αMG, and 0, 10, 50, or 100 mM sodium acetate. Sample preparations and transcriptomics analyses were carried out as described previously (Millard *et al.*, 2021). Three independent replicates were analyzed for each condition. The transcriptomics data can be downloaded from the ArrayExpress database (www.ebi.ac.uk/arrayexpress) under accession number E-MTAB-11717. Transcriptomics data in the absence of glycolytic inhibition (ArrayExpress database accession number E-MTAB-9086 (Millard *et al.*, 2021)) were measured under the exact same conditions but without αMG.

4.4 Metabolomics experiments.

Extracellular concentrations of glucose and acetate were quantified in 180 µL of filtered broth (0.2 µm syringe filter, Sartorius, Germany) by 1D ^{1}H-NMR on a Bruker Avance 500 MHz spectrometer equipped with a 5-mm z-gradient BBI probe (Bruker, Germany), as described previously (Millard *et al.*, 2021).

4.5 Flux calculation.

Glucose uptake, acetate and growth rates were calculated from glucose, acetate and biomass concentration–time profiles using PhysioFit (v1.0.2, https://github.com/MetaSys-LISBP/PhysioFit) (Peiro *et al*, 2019).

4.6 Kinetic modeling.

We used a kinetic model of *E. coli* (Millard *et al.*, 2021) available from the Biomodels database (https://www.ebi.ac.uk/biomodels) (Chelliah *et al*, 2015) under identifier MODEL2005050001. Simulations were carried out as described in the main text, using COPASI

(Hoops *et al*, 2006) (v4.34) with the CoRC package (Förster *et al*, 2021) (COPASI R Connector v0.11, https://github.com/jpahle/CoRC) in R (v4.1.3, https://www.r-project.org). The R notebook used to perform the simulations and to generate the figures is provided at https://github.com/MetaSys-LISBP/glucose_acetate_interplay.

4.7 Sensitivity analyses.

We used a Monte-Carlo approach (Saa & Nielsen, 2017) to estimate the robustness of model predictions. Following the procedure detailed in (Millard *et al.*, 2021), 500 simulated sets of calibration data were generated with noise added according to experimental standard deviations. For each of these artificially noisy data sets, we estimated model parameters and ran all simulations from the optimal parameters values. We calculated the mean value and standard deviation of each flux from the distribution of values obtained for the 500 sets of parameters.

4.8 Statistical analyses.

Comparisons between strains or conditions were performed using Student's t-tests with two-tailed distributions. The R notebook used to perform the calculations is provided at https://github.com/MetaSys-LISBP/glucose_acetate_interplay.

5. References

Baba T, Ara T, Hasegawa M, Takai Y, Okumura Y, Baba M, Datsenko KA, Tomita M, Wanner BL & Mori H (2006) Construction of *Escherichia coli* K-12 in-frame, single-gene knockout mutants: the Keio collection. *Mol Syst Biol* 2: 2006.0008

Bae Y-M & Lee S-Y (2017) Effect of salt addition on acid resistance response of Escherichia coli O157:H7 against acetic acid. *Food Microbiol* 65: 74–82

Beck AE, Pintar K, Schepens D, Schrammeck A, Johnson T, Bleem A, Du M, Harcombe WR, Bernstein HC, Heys JJ, *et al* (2022) Environment Constrains Fitness Advantages of Division of Labor in Microbial Consortia Engineered for Metabolite Push or Pull Interactions. *mSystems* 7: e00051-22

Becker J & Wittmann C (2015) Advanced Biotechnology: Metabolically Engineered Cells for the Bio-Based Production of Chemicals and Fuels, Materials, and Health-Care Products. *Angew Chem Int Ed* 54: 3328–3350

Chelliah V, Juty N, Ajmera I, Ali R, Dumousseau M, Glont M, Hucka M, Jalowicki G, Keating S, Knight-Schrijver V, *et al* (2015) BioModels: ten-year anniversary. *Nucleic Acids Res* 43: D542–D548

Cummings JH & Macfarlane GT (1991) The control and consequences of bacterial fermentation in the human colon. *J Appl Bacteriol* 70: 443–459

Cummings JH, Macfarlane GT & Englyst HN (2001) Prebiotic digestion and fermentation. *Am J Clin Nutr* 73: 415s–420s

Cummings JH, Pomare EW, Branch WJ, Naylor CP & Macfarlane GT (1987) Short chain fatty acids in human large intestine, portal, hepatic and venous blood. *Gut* 28: 1221–1227

Datsenko KA & Wanner BL (2000) One-step inactivation of chromosomal genes in *Escherichia coli* K-12 using PCR products. *Proc Natl Acad Sci* 97: 6640–6645

De Graaf AA, Maathuis A, De Waard P, Deutz NEP, Dijkema C, De Vos WM & Venema K (2010) Profiling human gut bacterial metabolism and its kinetics using [U-^{13} C]glucose and NMR: PROFILING GUT BACTERIAL METABOLISM USING [U-^{13} C] GLUCOSE AND NMR. *NMR Biomed* 23: 2–12

Doucette CD, Schwab DJ, Wingreen NS & Rabinowitz JD (2011) α-ketoglutarate coordinates carbon and nitrogen utilization via enzyme I inhibition. *Nat Chem Biol* 7: 894–901

Enjalbert B, Millard P, Dinclaux M, Portais J-C & Létisse F (2017) Acetate fluxes in *Escherichia. coli* are determined by the thermodynamic control of the Pta-AckA pathway. *Sci Rep* 7: 42135

Fabich AJ, Jones SA, Chowdhury FZ, Cernosek A, Anderson A, Smalley D, McHargue JW, Hightower GA, Smith JT, Autieri SM, *et al* (2008) Comparison of Carbon Nutrition for Pathogenic and Commensal *Escherichia coli* Strains in the Mouse Intestine. *Infect Immun* 76: 1143–1152

Förster J, Bergmann FT & Pahle J (2021) CoRC: the COPASI R Connector. *Bioinformatics* 37: 2778–2779

Fuentes LG, Lara AR, Martínez LM, Ramírez OT, Martínez A, Bolívar F & Gosset G (2013) Modification of glucose import capacity in *Escherichia. coli*: physiologic consequences and utility for improving DNA vaccine production. *Microb Cell Factories* 12: 42

Gerosa L, Haverkorn van Rijsewijk BRB, Christodoulou D, Kochanowski K, Schmidt TSB, Noor E & Sauer U (2015) Pseudo-transition analysis identifies the key regulators of dynamic metabolic adaptations from steady-state data. *Cell Syst* 1: 270–282

Hoops S, Sahle S, Gauges R, Lee C, Pahle J, Simus N, Singhal M, Xu L, Mendes P & Kummer U (2006) COPASI—a COmplex PAthway SImulator. *Bioinformatics* 22: 3067–3074

Jiang Y, Chen B, Duan C, Sun B, Yang J & Yang S (2015) Multigene Editing in the Escherichia coli Genome via the CRISPR-Cas9 System. *Appl Environ Microbiol* 81: 2506–2514

Jones SA, Chowdhury FZ, Fabich AJ, Anderson A, Schreiner DM, House AL, Autieri SM, Leatham MP, Lins JJ, Jorgensen M, *et al* (2007) Respiration of *Escherichia coli* in the Mouse Intestine. *Infect Immun* 75: 4891–4899

Kleman GL & Strohl WR (1994) Acetate metabolism by Escherichia coli in high-cell-density fermentation. *Appl Environ Microbiol* 60: 3952–3958

Lawford HG & Rousseau JD (1993) Effects of pH and acetic acid on glucose and xylose metabolism by a genetically engineered ethanologenicEscherichia coli. *Appl Biochem Biotechnol* 39–40: 301–322

Lee SY, Rhee MS, Dougherty RH & Kang DH (2010) Antagonistic effect of acetic acid and salt for inactivating *Escherichia coli* O157:H7 in cucumber puree. *J Appl Microbiol* 108: 1361–1368

Long CP & Antoniewicz MR (2019) Metabolic flux responses to deletion of 20 core enzymes reveal flexibility and limits of *E. coli* metabolism. *Metab Eng* 55: 249–257

Luli GW & Strohl WR (1990) Comparison of growth, acetate production, and acetate inhibition of *Escherichia coli* strains in batch and fed-batch fermentations. *Appl Environ Microbiol* 56: 1004–1011

Macfarlane GT, Gibson GR & Cummings JH (1992) Comparison of fermentation reactions in different regions of the human colon. *J Appl Bacteriol* 72: 57–64

Millard P, Enjalbert B, Uttenweiler-Joseph S, Portais J-C & Létisse F (2021) Control and regulation of acetate overflow in *Escherichia coli*. *eLife* 10: e63661

Millard P, Massou S, Wittmann C, Portais J-C & Létisse F (2014) Sampling of intracellular metabolites for stationary and non-stationary ^{13}C metabolic flux analysis in *Escherichia coli*. *Anal Biochem* 465: 38–49

Millard P, Smallbone K & Mendes P (2017) Metabolic regulation is sufficient for global and robust coordination of glucose uptake, catabolism, energy production and growth in Escherichia coli. *PLOS Comput Biol* 13: e1005396

Negrete A, Ng W-I & Shiloach J (2010) Glucose uptake regulation in E. coli by the small RNA SgrS: comparative analysis of E. coli K-12 (JM109 and MG1655) and E. coli B (BL21). *Microb Cell Factories* 9: 75

Okano H, Hermsen R, Kochanowski K & Hwa T (2020) Regulation underlying hierarchical and simultaneous utilization of carbon substrates by flux sensors in *Escherichia coli*. *Nat Microbiol* 5: 206–215

Orr JS, Christensen DG, Wolfe AJ & Rao CV (2019) Extracellular Acidic pH Inhibits Acetate Consumption by Decreasing Gene Transcription of the Tricarboxylic Acid Cycle and the Glyoxylate Shunt. *J Bacteriol* 201

Peiro C, Millard P, De Simone A, Cahoreau E, Peyriga L, Enjalbert B & Heux S (2019) Chemical and Metabolic Controls on Dihydroxyacetone Metabolism Lead to Suboptimal Growth of Escherichia coli. *Appl Environ Microbiol* 85: e00768-19

Pinhal S, Ropers D, Geiselmann J & de Jong H (2019) Acetate metabolism and the inhibition of bacterial growth by acetate. *J Bacteriol* 201

Renilla S, Bernal V, Fuhrer T, Castaño-Cerezo S, Pastor JM, Iborra JL, Sauer U & Cánovas M (2012) Acetate scavenging activity in *Escherichia coli*: interplay of acetyl–CoA synthetase and the PEP–glyoxylate cycle in chemostat cultures. *Appl Microbiol Biotechnol* 93: 2109–2124

Revelles O, Millard P, Nougayrède J-P, Dobrindt U, Oswald E, Létisse F & Portais J-C (2013) The Carbon Storage Regulator (Csr) System Exerts a Nutrient-Specific Control over Central Metabolism in Escherichia coli Strain Nissle 1917. *PLoS ONE* 8: e66386

Rohwer JM, Meadow ND, Roseman S, Westerhoff HV & Postma PW (2000) Understanding Glucose Transport by the Bacterial Phosphoenolpyruvate:Glycose Phosphotransferase System on the Basis of Kinetic Measurements in Vitro. *J Biol Chem* 275: 34909–34921

Saa PA & Nielsen LK (2017) Formulation, construction and analysis of kinetic models of metabolism: A review of modelling frameworks. *Biotechnol Adv* 35: 981–1003

Shen Q, Zhao L & Tuohy KM (2012) High-level dietary fibre up-regulates colonic fermentation and relative abundance of saccharolytic bacteria within the human faecal microbiota in vitro. *Eur J Nutr* 51: 693–705

Valgepea K, Adamberg K, Nahku R, Lahtvee P-J, Arike L & Vilu R (2010) Systems biology approach reveals that overflow metabolism of acetate in *Escherichia coli* is triggered by carbon catabolite repression of acetyl-CoA synthetase. *BMC Syst Biol* 4: 166

Wolfe AJ (2005) The Acetate Switch. *Microbiol Mol Biol Rev* 69: 12–50

Xiao T, Khan A, Shen Y, Chen L & Rabinowitz JD (2022) Glucose feeds the tricarboxylic acid cycle via excreted ethanol in fermenting yeast. *Nat Chem Biol* 18: 1380–1387

Yuan J, Doucette CD, Fowler WU, Feng X, Piazza M, Rabitz HA, Wingreen NS & Rabinowitz JD (2009) Metabolomics-driven quantitative analysis of ammonia assimilation in *E. coli*. *Mol Syst Biol* 5: 302

Zhang H, Pereira B, Li Z & Stephanopoulos G (2015) Engineering *Escherichia coli* coculture systems for the production of biochemical products. *Proc Natl Acad Sci* 112: 8266–8271

Chapter 3
Acetate as a metabolic booster for *Escherichia coli*-based bioproduction, from fundamental knowledge to biotechnology application

This work is submitted in "Metabolic Engineering" and only minor modifications have been introduced in the chapter below.

Full reference: Thomas Gosselin-Monplaisir, Denis Jallet, Erwana Harscoet, Sandrine Uttenweiler-Joseph, Stéphanie Heux, Pierre Millard

Contribution: In this work, I conceptualized and performed most of the experimental part. For the redaction of the paper, I provided an initial plan and contributed actively to the review and editing of the different drafts to the final draft.

1. Introduction

In Chapter 2, we demonstrated that *Escherichia coli* can co-utilize acetate alongside glycolytic substrates such as glucose and glycerol (Enjalbert et al., 2017; Millard et al., 2021, 2023). This co-utilization can enhance the production of acetyl-CoA-derived compounds and potentially accelerate bioprocesses. Notably, we also showed that acetate is not inherently toxic during growth on glycolytic substrates. Under low glycolytic flux—conditions often encountered in industrial bioprocesses—acetate may even improve metabolic robustness and support growth (Millard et al., 2023).

These findings challenge the traditional view of acetate in biotechnology. While fast glycolytic growth in *E. coli* often leads to acetate accumulation, which has long been considered detrimental due to growth inhibition and carbon loss (De Mey et al., 2007; Eiteman and Altman, 2006), our results suggest that instead of trying to reduce acetate accumulation, we can use acetate beneficial effect on growth and glycolytic buffer ability to improve bioprocesses using *Escherichia coli*. This is especially relevant given *E. coli*'s central role in biotechnology. Thanks to its genetic tractability, rapid growth, and metabolic flexibility, *E. coli* remains a key microbial platform for the production of biofuels, bioplastics, pharmaceuticals, and industrial enzymes (Kim et al., 2025; Pontrelli et al., 2018; Vickers et al., 2012). Glycolytic carbon sources like glucose and glycerol are widely used due to their efficiency and availability (Martínez-Gómez et al., 2012; Wang et al., 2015), but acetate accumulation remains a challenge for process optimization.

Despite its negative effect on glycolytic-based bioprocess efficiency, acetate itself can also serve as a primary carbon source for *E. coli*, although its utilization as the sole carbon source results in slow growth and low productivity (Chong et al., 2013; Gong et al., 2022; Noh et al., 2018). Nevertheless, acetate is a promising feedstock, metabolic intermediate, and industrial precursor for biofuels, bioplastics, pharmaceuticals, and synthetic biology applications (Kiefer et al., 2021). Notably, acetate has a high potential for producing acetyl-CoA-derived compounds (Gong et al., 2022; Kiefer et al., 2021; Lama et al., 2021; Zhang et al., 2022), as acetyl-CoA is a highly versatile precursor positioned at the intersection of glycolytic and acetate metabolisms. Since acetate can be sourced from CO_2 (H. Wang et al., 2023) and various waste streams, including agricultural and industrial by-products, its role in carbon recycling and sustainable bioprocessing is gaining increasing attention in modern industrial biotechnology (Kiefer et al., 2021; Zhang et al., 2022).

In this chapter, I investigate how acetate can be used to improve the bioproduction of acetyl-CoA-derived compounds in *E. coli*, using glucose as the primary carbon source. Kinetic modeling was applied to predict metabolic responses, then I validated these predictions experimentally using mevalonate and 3-hydroxypropionate as representative bioproducts.

2. Results

2.1 Model-guided strategy to evaluate acetate's effect on bioproduction

We used kinetic modeling to systematically explore whether acetate can enhance *E. coli*-based bioproduction. Building on the extensively validated model of glucose and acetate metabolism from Millard et al. (Millard et al., 2023, 2021), we incorporated a production pathway that converts acetyl-CoA into a product P (Figure 1).

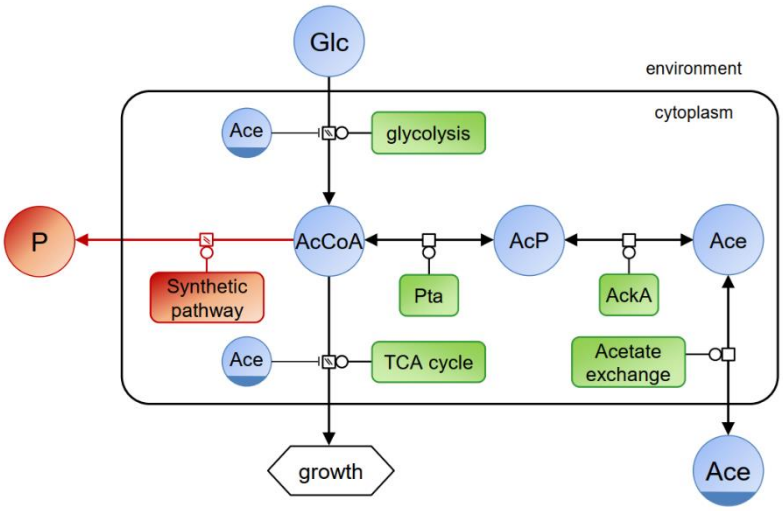


Figure 1. Representation (in Systems Biology Graphical Notation format, (http://sbgn.org) of the glucose and acetate metabolism of a synthetic *E. coli* strain engineered for bioproduction of a product P, as implemented in the kinetic model used in the chapter.

Native metabolism is shown in blue (metabolites) and green (enzymes), and the bioproduction pathway is shown in red.

Enzyme saturation is a key determinant of metabolic efficiency, shaping flux control, resource allocation, and pathway optimality (Noor and Liebermeister, 2024). To capture this essential feature, we modeled the production reaction as a Michaelis-Menten rate law, with V_{max} arbitrarily set to 10% of the maximal glucose uptake rate to reflect a bioproduction pathway with limited enzymatic capacity. The role of enzyme saturation, defined by the Michaelis constant (K_M), dictates how metabolic flux responds to intracellular metabolite levels (Castaño-Cerezo et al., 2024). At low substrate concentrations, the flux is responsive to substrate fluctuations, allowing for dynamic regulation but at the cost of inefficient enzyme utilization. Conversely, at high substrate concentrations, the pathway operates at maximum capacity, ensuring stable fluxes and optimal enzyme utilization, but with reduced flexibility and potential metabolic imbalances. This trade-off is critical in bioproduction, where balancing pathway flexibility and robustness is key to optimize process efficiency.

To capture these differences, we modeled two distinct configurations of the production pathway, differing in their degree of enzyme saturation. These two configurations were

simulated by adjusting the K_M of the production pathway. Given that the intracellular acetyl-CoA concentration in glucose-grown *E. coli* is typically between 0.02 and 0.6 mM (Bennett et al., 2009; Chohnan et al., 1998; Takamura et al., 1985), a high K_M (5 mM) simulated a pathway operating below substrate saturation, making it sensitive to changes in acetyl-CoA concentration, while a low K_M (5 µM) modeled a near-saturation state, where flux is largely independent of acetyl-CoA fluctuations. By tuning pathway saturation, we can strategically explore the trade-off between pathway flexibility with robustness and determine the impact of acetate on the balance between production and growth.

For each configuration, we simulated growth of *E. coli* on glucose (15 mM) across a wide range of acetate concentrations (0.1 to 100 mM) and glycolytic flux levels (20% to 100% of the maximal glycolytic flux). This allowed us to predict how acetate influences cell physiology (growth rate, acetate and glucose fluxes, intracellular acetyl-CoA levels) and bioprocess performance (product flux, yield, and productivity – three key metrics of bioprocess success). In the following sections, we present the simulation results for each configuration, along with a test case designed to evaluate the model's predictions.

2.2 Predictions for an acetyl-CoA-sensitive production pathway

We first explored the impact of acetate on an *E. coli* strain engineered with an acetyl-CoA-sensitive production pathway (K_M = 5 mM). The predicted glucose uptake rate (Figure 2A), acetate flux (Figure 2B), and growth rate (Figure 2C) in the different environmental conditions are similar to those observed in a non-producing *E. coli* strain, where: i) increasing acetate concentration inhibits glucose uptake and reverses the acetate flux, ii) the acetate concentration threshold at which flux reversal occurs depends on the glycolytic flux, and iii) acetate enhances growth at low glucose uptake flux. Additional details on these predictions, which have been experimentally validated in a non-producing *E. coli*, can be found in (Millard et al., 2023).

The model predicts that increasing acetate concentration could enhance the production flux (Figure 2D) due to an increase in intracellular acetyl-CoA concentration (Figure 2E). However, the full enzymatic capacity is not used, with significant variations of the production flux (0-0.6 mmol/g_{CDW}/h) which reaches only 60% of the maximal rate (V_{max} = 1 mmol/g_{CDW}/h). According to the model, acetate could improve the product yield (Figure 2F), which is predicted to be maximal at low glycolytic flux and high acetate concentration. Additionally, acetate could increase the volumetric productivity (Figure 2G), which is maximal at high glycolytic flux and medium acetate concentration (20-30 mM), as acetate enhances both production flux (Figure 2D) and growth rate (Figure 2C).

These predictions suggest that acetate could enhance bioproduction through the combined effects of three distinct mechanisms: i) reducing acetate production through the thermodynamic control of the Pta-AckA pathway, thereby minimizing carbon loss from the

biosynthetic pathway, ii) replenishing the acetyl-CoA pool, which can increase the bioproduction flux through the acetyl-CoA-sensitive pathway, iii) improving productivity by enhancing biomass accumulation. These mechanisms may work alone or synergistically to improve bioprocess efficiency.

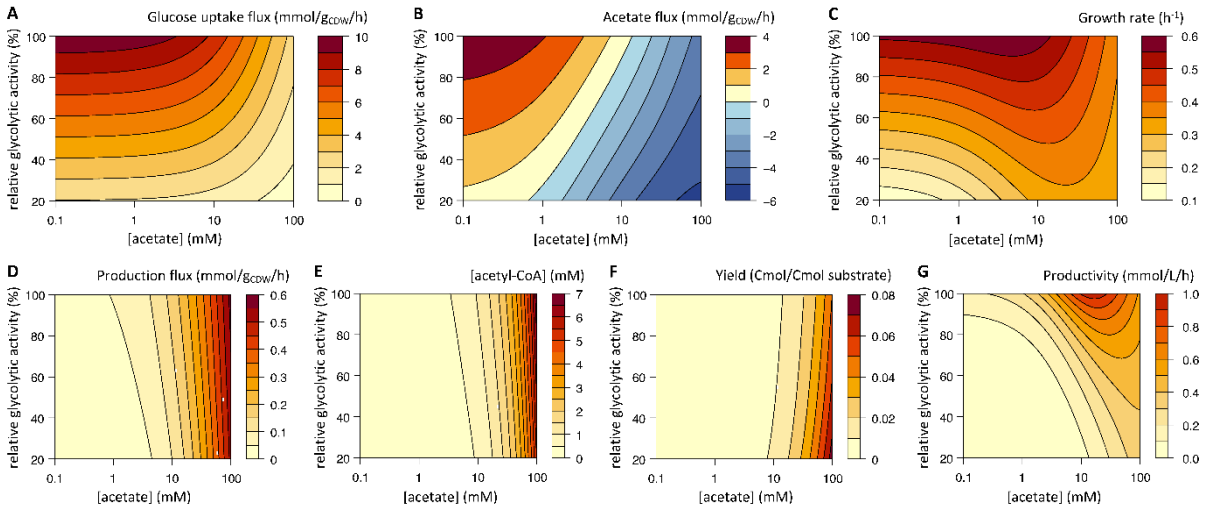


Figure 2. Predicted response to glycolytic and acetate perturbations of an Escherichia coli strain with an acetyl-CoA-sensitive production pathway.

Glucose uptake flux (A), acetate flux (B), growth rate (C), product flux (D), intracellular acetyl-CoA concentration (E), product yield (F) and volumetric productivity (G) simulated over a broad range of glycolytic activity levels (20 to 100% of the initial V_{max}) and acetate concentrations (0.1 to 100 mM).

2.3 Validation using mevalonate production

To evaluate model predictions, we selected as test case the production of mevalonate, a precursor for a broad range of high-value chemicals (e.g., carotenoids and steroids), pharmaceuticals (e.g., artemisinin), and biofuels (e.g., isoprenes) (C.-H. Wang et al., 2023). The mevalonate pathway is widely studied and well characterized, making it ideal for testing new strategies for bioprocess optimization that can be readily applied at the industrial scale (C.-H. Wang et al., 2023).

The first step of the mevalonate production pathway involves the conversion of acetyl-CoA into acetoacetyl-CoA by an acetoacetyl-CoA thiolase (Figure 3A). This enzyme has a relatively low affinity for acetyl-CoA (K_M = 0.47 mM, (Duncombe and Frerman, 1976)) in comparison to the intracellular acetyl-CoA concentration (0.02-0.6 mM). Therefore, the production flux should be responsive to the predicted increase of acetyl-CoA concentration caused by acetate supplementation (Figure 2E). Acetoacetyl-CoA is then converted into 3-hydroxy-3-methylglutaryl-CoA by HMG-CoA synthase, and finally into mevalonate by HMG-CoA reductase (Figure 3A). To test model predictions, we transformed *E. coli* K-12 BW25113 with

plasmid pMevT (Martin et al., 2003), which contains *atoB* (acetoacetyl-CoA thiolase), *HMGS* (HMG-CoA synthase), and *tHMGR* (truncated HMG-CoA reductase). We cultivated this strain on glucose, with or without acetate (30 mM), and we measured the growth rate, extracellular fluxes, and mevalonate bioproduction metrics.

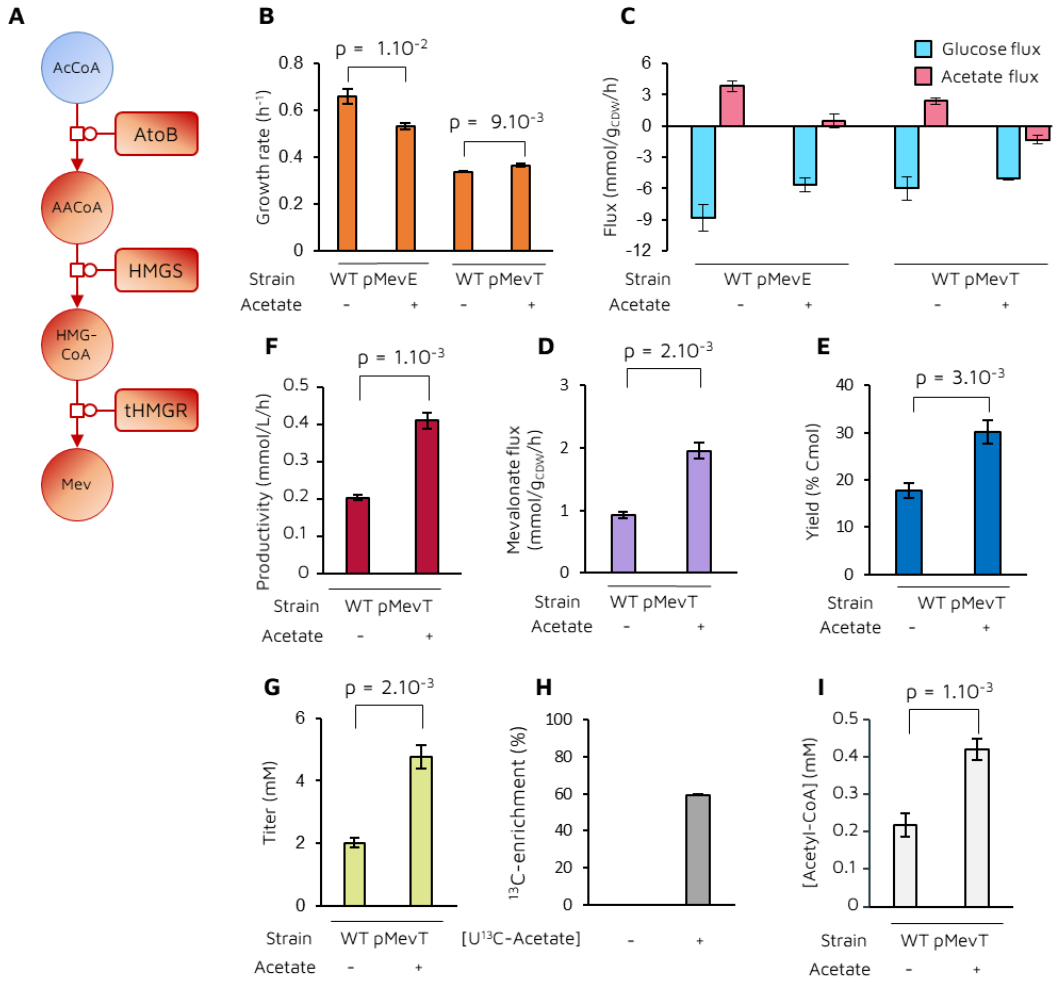


Figure 3. Impact of acetate on mevalonate production.

(A) Representation of the synthetic mevalonate production pathway implemented in *E. coli* K-12 BW25113 pMevT. Growth rate (B), glucose and acetate fluxes (C), mevalonate production flux (D), yield (E), productivity (F), and titer (G) measured during growth of *E. coli* on glucose (15 mM) with or without 30 mM acetate. (H) ^{13}C-enrichment on mevalonate produced on unlabeled glucose (15 mM) with or without 30 mM U-$^{13}C_2$-acetate. (I) Intracellular acetyl-CoA concentration measured in the producing strain during growth on glucose (15 mM) with or without 30 mM acetate. Mean values ± standard deviations (error bars) were estimated from three independent biological replicates.

In the absence of acetate, expression of the production pathway caused a 49% reduction in growth rate (from 0.66 to 0.33 h^{-1}, Figure 3B) while supporting a mevalonate production flux of 0.9 mmol/g_{CDW}/h (Figure 3D). The reduced growth rate can be caused by metabolic burden from heterologous protein expression (Snoeck et al., 2024), and by high mevalonate

production which diverts 15% of carbon away from anabolism. Additionally, acetate was produced at a rate of 2.4 mmol/g_{CDW}/h (13% of carbon uptake) in the production strain (Figure 3C), a level significantly lower than the parental strain with the empty plasmid (3.8 mmol/g_{CDW}/h).

The presence of 30 mM acetate reversed the acetate flux (Figure 3C), leading to co-consumption of acetate with glucose (-1.3 mmol/g_{CDW}/h), consistent with model predictions and results obtained in the non-producing parental strain under similar conditions (Millard et al., 2023). The glucose uptake rate decreased by 15% in the presence of acetate, in line with its known inhibitory effect on glucose uptake (Millard et al., 2021). Notably, mevalonate production increased significantly, with the production flux doubling from 0.9 to 2.0 mmol/g_{CDW}/h (+112%, Figure 3D) and leading to a similar increase in volumetric productivity (+102%, Figure 3F), and the titer increasing by 137% (Figure 3G). These results confirm that acetate enhances production flux, as predicted by the model. Furthermore, acetate supplementation improved growth (Figure 3B), with the growth rate slightly but significantly increasing from 0.33 to 0.36 h^{-1} (+8%), similar to effects observed with other glycolytic substrates such as glycerol (Millard et al., 2023). This result, also predicted by the model at low glycolytic flux, indicates that acetate partially alleviates metabolic burden associated with the synthetic pathway and carbon diversion.

The mevalonate flux on glucose alone represents 47% of the flux on glucose and acetate, suggesting that acetate is responsible for 53% of the mevalonate flux. To confirm acetate's contribution to mevalonate biosynthesis, we conducted a ^{13}C-labeling experiment, growing the mevalonate-producing strain on unlabeled glucose and U-$^{13}C_2$-acetate (Figure 3H). Under glucose-only conditions, ^{13}C enrichment of mevalonate was 0%, but in the presence of ^{13}C-labeled acetate, enrichment increased to 59%, with only 41% of mevalonate derived from glucose. These values closely align with the values estimated from the mevalonate flux measurements. Furthermore, the increase in mevalonate flux (from 0.9 to 2.0 mmol/g_{CDW}/h, representing a difference of 6.6 Cmmol/g_{CDW}/h) quantitatively matched the change in acetate balance (from +2.4 to –1.3 mmol/g_{CDW}/h, representing a difference of 7.4 Cmmol/g_{CDW}/h). These results demonstrate that the enhanced mevalonate flux was driven exclusively by acetate.

To verify model prediction that the flux increase was caused by an increase in intracellular acetyl-CoA level, we performed quantitative metabolomics experiments. Acetyl-CoA concentration increased from 0.22 mM in the absence of acetate to 0.42 mM in the presence of 30 mM acetate (Figure 3I), in agreement with model predictions. Given the *in vitro* K_M of acetoacetyl-CoA thiolase for acetyl-CoA (0.47 mM), this concentration increase should theoretically translate in a 68% flux increase. While qualitatively consistent with experimental flux measurements, the actual flux increase (+112%) exceeded this metabolomics-derived estimation. This suggests that the *in vivo* K_M of acetoacetyl-CoA thiolase could be higher than the *in vitro* measurement, as observed for other enzymes in a recent *in vivo* enzymology study (Castaño-Cerezo et al., 2024). Acetate could also enhance expression and thus activity of the heterologous pathway, as reported previously for the expression of the growth machinery (Millard et al., 2023).

These results highlight acetate's value for bioproduction using an acetyl-CoA-sensitive pathway, as simply adding 30 mM acetate increases the mevalonate production flux by 112%, productivity by 102%, and titer by 137%. The findings indicate that acetate enhances mevalonate production purely at the metabolic level, primarily through an acetate-induced increase in the acetyl-CoA pool. No acetate is produced, and virtually all acetate is converted into mevalonate, with a slight but significant increase in growth as a bonus.

2.4 Predictions for an acetyl-CoA-insensitive production pathway

Following the same strategy, we investigated an alternative scenario in which the production pathway operates under saturation (K_M = 5 µM) and is insensitive to changes in acetyl-CoA induced by acetate. In this case, the model predicts that the growth physiology of *E. coli* should respond to perturbations similarly to both the non-producing strain and the producing strain with an acetyl-CoA-sensitive pathway. However, the process efficiency metrics exhibit distinct profiles. The production flux (0.8-1 mmol/g_{CDW}/h, Figure 4D) remains close to the maximal enzyme capacity (V_{max} = 1 mmol/g_{CDW}/h), confirming optimal enzyme utilization, though the flux is less responsive to changes in acetyl-CoA concentrations (Figure 4E), as expected. Interestingly, the highest yield is observed at the lowest glucose uptake rate (Figure 4F), a trend commonly reported in production strains (Kyselova et al., 2018; Lim and Jung, 2017; Zhuang et al., 2013). However, acetate does not improve the product yield as strongly as for the acetyl-CoA sensitive pathway. Despite this, acetate still enhances productivity at all glycolytic activity levels (Figure 4G). Productivity should be maximal at medium acetate concentrations (5-10 mM), where acetate stimulates growth (Figure 4C).

These predictions suggest that even when using an acetyl-CoA-insensitive production pathway, acetate can still enhance bioproduction. While the two key benefits observed in acetyl-CoA-sensitive pathways resulting from the reduction of acetate overflow and increase in intracellular acetyl-CoA concentration are no longer present, acetate can still boost productivity by promoting biomass accumulation.

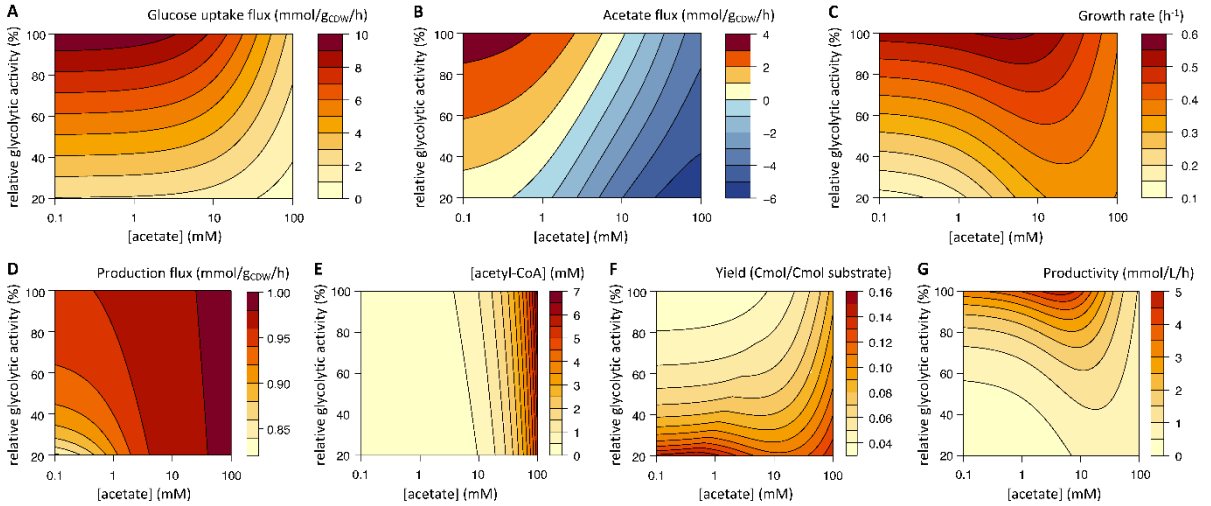


Figure 4. Predicted response to glycolytic and acetate perturbations of an Escherichia coli strain with an acetyl-CoA-insensitive production pathway.

Glucose uptake flux (A), acetate flux (B), growth rate (C), product flux (D), intracellular acetyl-CoA concentration (E), product yield (F) and volumetric productivity (G) simulated over a broad range of glycolytic activity levels (20 to 100% of the initial V_{max}) and acetate concentrations (0.1 to 100 mM).

2.5 Validation with 3-hydroxypropionate production

To test this scenario, we selected 3-hydroxypropionate (3HP) as test case, an important platform chemical in biotechnology with diverse applications in bioplastics (e.g., poly-3-hydroxypropionate), chemicals (e.g., acrylic acid and 1,3-propanediol), and pharmaceuticals (e.g., beta-lactones) (Vidra and Németh, 2017). The first step of the 3HP production pathway involves the conversion of acetyl-CoA into malonyl-CoA by a native acetyl-CoA carboxylase (Figure 5A). This enzyme has a high affinity for acetyl-CoA (K_M = 18 µM, (Soriano et al., 2006)) and is therefore expected to operate near saturation under physiological acetyl-CoA concentrations. Malonyl-CoA is then converted into 3HP by malonyl-CoA reductase (Figure 5A). To test this pathway, we constructed plasmid p3HP, which carries *mcr* (malonyl-CoA reductase).

We performed growth experiments using the parental *E. coli* K-12 BW25113 strain transformed with p3HP, cultured on glucose, with or without acetate. Based on model predictions that optimal productivity should be achieved at slightly lower acetate concentrations than for acetyl-CoA-sensitive production pathways, we chose an acetate concentration of 10 mM. Since malonyl-CoA reductase requires two NADPH molecules, we also conducted production experiments in a Δ*pgi* strain, which is expected to increase NADPH availability, thereby enhancing flux through NADPH-dependent biosynthetic pathways (Chemler et al., 2010).

In the absence of acetate, growth of the parental strain was not impacted by the introduction of the production pathway (Figure 5B-C, with control experiments shown in Supplementary Figure S1). Deletion of *pgi* reduced both growth and glucose uptake rates (-69 and -67%, respectively) and abolished acetate production (Figure 5B-C), consistent with previous reports (Long and Antoniewicz, 2019; Millard et al., 2023). Despite its negative impact on *E. coli* physiology, deletion of *pgi* increased 3HP production flux by 183% (Figure 5D), yield by 16-fold (Figure 5E), titer by 8-fold (Figure 5F), and volumetric productivity by 38% (Figure 5G), confirming that the Δ*pgi* strain is advantageous for the production of NADPH-dependent compounds.

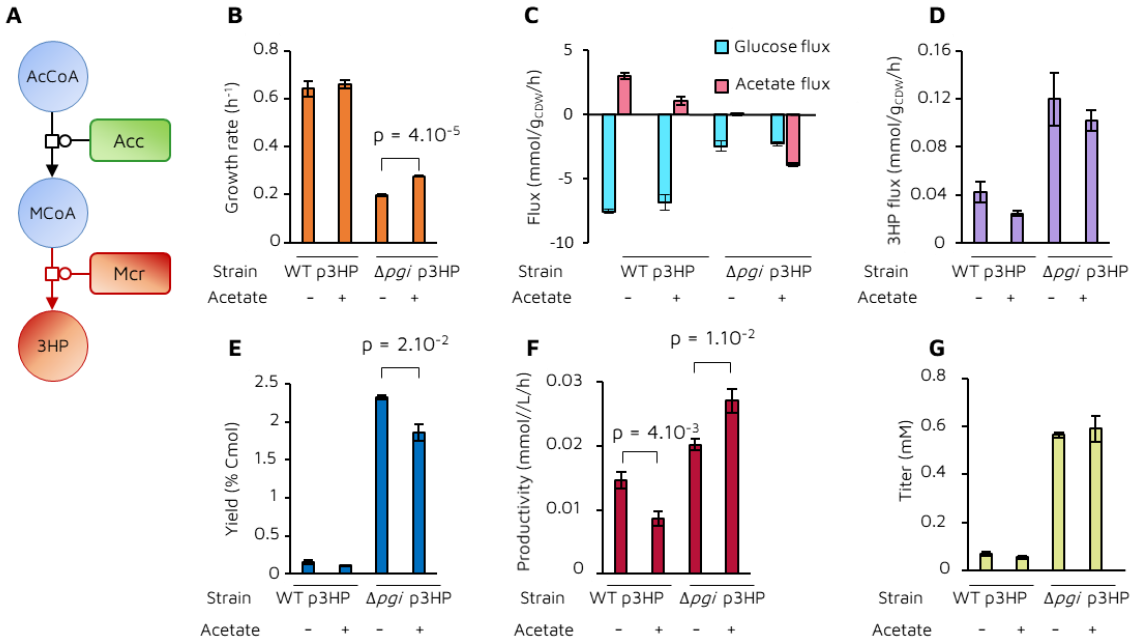


Figure 5. Impact of acetate on 3-hydroxypropionate production.

(A) Representation of the synthetic 3-hydroxypropionate production pathway implemented in *E. coli*. (B) Growth rate, (C) glucose and acetate fluxes, (D) 3-hydroxypropionate production flux, (E) yield, (F) volumetric productivity and (G) titer measured during growth of *E. coli* on glucose (15 mM) with or without 10 mM acetate. Mean values ± standard deviations (error bars) were estimated from three independent biological replicates.

In the parental producing strain, acetate supplementation reduced acetate production (-64%, Figure 5C), consistent with model predictions (Figure 4B). Moreover, 3HP production metrics declined, with production flux decreasing by 42%, yield by 26%, productivity by 41%, and titer by 20%, consistent with previous reported negative effects of acetate on bioproduction (Eiteman and Altman, 2006). Interestingly, the model had predicted a slight increase in these bioproduction metrics, indicating a reduced predictive accuracy under conditions of high glycolytic flux – at least in this specific context. In the acetate-supplemented Δ*pgi* strain, acetate supplementation leads to co-utilization of acetate with glucose, as previously reported (Millard et al., 2023). Moreover, acetate significantly enhanced growth (+40%) without affecting the production flux, in accordance with model predictions for a production pathway

operating at saturation and under low glycolytic flux. This increase in growth rate reduces the production yield (-20%, Figure 5E) since the extra carbon from acetate is used only by anabolism, as predicted by the model (Figure 4F). Moreover, faster biomass accumulation leads to a substantial increase in productivity (+34%, Figure 5F), as also predicted by the model (Figure 4G). Therefore, in the presence of acetate, the Δ*pgi* strain also exhibited higher productivity than the parental producing strain despite a strong reduction in growth rate.

These results demonstrate that acetate supplementation, by promoting biomass accumulation and overall productivity, also enhances the bioproduction of acetyl-CoA-derived compounds when the pathway is operating near saturation.

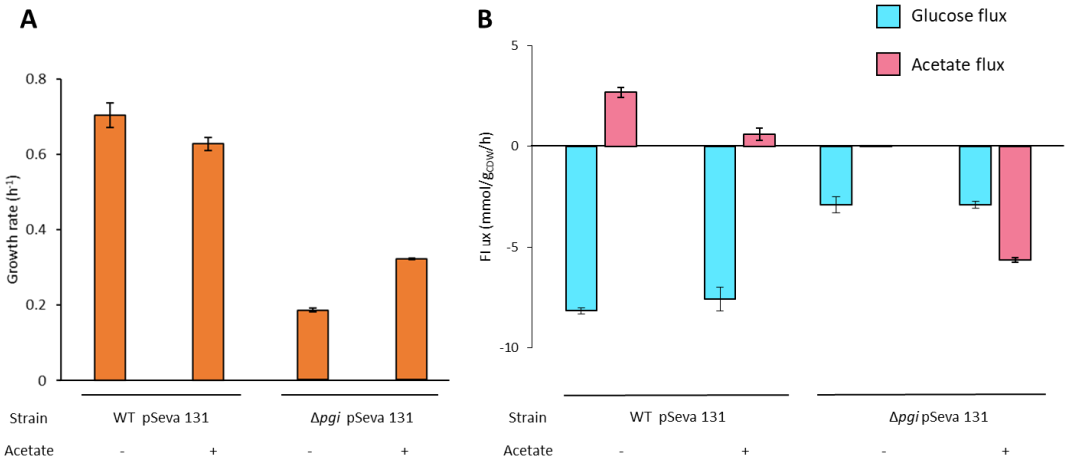


Figure 6. Impact of acetate with empty plasmid on (control experiment of figure 5). (A) Growth rate, (B) glucose and acetate fluxes

3. Discussion

Despite recent discoveries suggesting that acetate may benefit *E. coli*, it is still widely regarded as a problem in bioprocesses. In this chapter, we used kinetic modeling to explore acetate's potential in bioproduction. Our results indicate that while acetate is indeed detrimental to bioprocesses when glycolytic flux is high, it may be beneficial under low glycolytic flux conditions. Such conditions frequently occur in industrial bioprocesses due to intrinsically lower glucose uptake rates of engineered strains or to cultivation strategies that reduce the glycolytic flux (e.g., fed-batch and chemostat cultures) (Carneiro et al., 2013). These findings suggest that acetate may serve as a metabolic booster for many *E. coli*-based bioprocesses by optimizing the fundamental trade-off between growth and production, a major constraint on bioprocess performance (Mannan et al., 2025).

Simulations indicate that acetate's positive impact may arise from three distinct mechanisms: i) minimizing carbon loss from the biosynthetic pathway by reducing acetate production, ii) enhancing the bioproduction flux of acetyl-CoA-derived compounds by increasing acetyl-CoA concentration, and iii) improving volumetric productivity by promoting biomass accumulation.

Experimental results validate these mechanisms, demonstrating that they collectively enhance bioprocess efficiency. These findings are directly transferable to industrial bioprocesses based on *E. coli*.

The relative contribution of each mechanism to bioprocess improvement varies depending on the strain's genetic background and on the synthetic pathway. For acetyl-CoA sensitive pathways such as mevalonate production, all three mechanisms contributed to process improvement, with the predominant effects being the increase in biosynthetic flux, driven by reduced acetate accumulation and an elevated acetyl-CoA pool. The growth-promoting effect of acetate played only a minor role. In contrast, for acetyl-CoA insensitive pathways, such as 3HP production, no flux increase was observed in either the parental or Δ*pgi* producing strains, and the increase in productivity observed in the Δ*pgi* strain was solely due to acetate's positive effect on growth.

By understanding how enzyme saturation shapes production flux and its balance with microbial growth, we can strategically optimize bioproduction processes. Our findings demonstrate that acetate can help balance cell growth and production, addressing a common challenge in engineered strains. This benefit may extend beyond acetyl-CoA-derived bioproducts to other metabolic pathways, an area that warrants further investigation.

The modeling approach developed in this chapter serves as a valuable tool for the rational optimization of *E. coli*-based bioprocesses and can be extended to assess acetate's role in diverse metabolic contexts. Our findings demonstrate how acetate, traditionally seen as Mr. Hyde – sabotaging productivity – can be transformed into Dr. Jekyll, enhancing bioprocess efficiency. We hope this work helps reconcile its dual nature, which is key to understanding its role and unlocking its full potential in biotechnology. Since acetate can be sourced from various waste streams, its use as a metabolic booster for bioproduction will contribute to more sustainable and environmentally friendly processes.

4. Materials and Methods

4.1 Strains construction

Escherichia coli K-12 BW25113 was used as parental strain. Strains and plasmid used in this chapter are listed in Table 1.

Strain or plasmid	Genotype or description	Source
Plasmids		
pMevT	pMevT, Addgene plasmid # 17815 ; http://n2t.net/addgene:17815 ; RRID:Addgene 17815. ChlrR	(Martin et al., 2003)
pMevE	pMevT has been digested by HindIII and ligated to generate the empty plasmid. ChlrR	This chapter
p3HP	pSEVA 131 with *mcr* gene from *Chloroflexus aurantiacus* (GenBank: AAS20429, codon-optimized) under the control of an IPTG-inducible promoter (Ptrc) has been synthesized and subclone by genecust under the command number ZG220813. AmpR	This chapter
pSEVA131	Detailed in the source publication. AmpR	(Martínez-García et al., 2023)
Bacterial strains		
K12 - BW25113	*E. coli* K-12 BW25113 WT [F−λ− Δ*lacZ*4787(::*rrnB*-3) hsdR514 Δ(*araBAD*)567 Δ(*rhaBAD*)568]	(Baba et al., 2006)
K12 - Δ*pgi*	BW25113 Δ*pgi* strain from Keio collection, cured of kanamycin cassette (Datsenko and Wanner, 2000)	This chapter

Table 1. Strains and plasmid used in this chapter.

4.2. Cultivations

E. coli was grown in M9 minimal media (Millard et al., 2014) supplemented with 15 mM glucose. Sodium acetate (prepared as a 1.2 M solution at pH 7.0 by addition of potassium hydroxide) was added up to the required concentration, and IPTG (prepared as a 250 mM solution) was added at a final concentration of 1 mM. For isotope labeling experiments,

unlabeled acetate was replaced by U-$^{13}C_2$-acetate (Eurisotop, France). The cells were grown in shake flasks at 37°C and 200 rpm, in 20 mL of medium. Growth was monitored by measuring the optical density (OD) at 600 nm using a Genesys 150 ThermoScientific spectrophotometer. Biomass concentration was determined using a conversion factor of 0.42 g_{CDW}/L/OD unit.

4.3 Metabolomics

4.3.1 Exometabolome analysis.

Extracellular concentrations of glucose, acetate, mevalonate, and 3-hydroxypropionate were quantified during growth by 1D ^{1}H-NMR on a Bruker 500 MHz spectrometer equipped with a 5 mm TXI cryoprobe (Bruker, Germany). Briefly, 180 µL of filtered broth (0.2 µm, Sartorius, Germany) were mixed with 20 µL of D_2O containing TSPd4 (3-(trimethylsilyl)-1-propanesulfonic acid-tetra deuterated at a concentration of 10 mM, used as internal standard). A sequence using presaturation (ZGPR) was used for water signal suppression, with a 30° pulse and a relaxation delay between scans of 10 s to ensure full signal recovery. A total of 32 scans were accumulated (64 k data points with a spectral width of 16 ppm) after 4 dummy scans. From each spectrum, we quantified glucose, acetate, mevalonate, and 3-hydroxypropionate. Spectra were processed using TopSpin v4.1.4 (Bruker).

4.3.2 Intracellular acetyl-CoA quantification.

Cells were separated from the medium by fast filtration. Filters were washed with 1 mL of fresh medium containing the same carbon sources as the growth medium, quickly transferred into liquid nitrogen, and stored at -80 °C until metabolite extraction. Intracellular metabolites were extracted by incubating the filters for 1 h in 5 mL of extraction solution (MeOH:ACN:H_2O solution 40:40:20 with 0.5% formic acid) at -20°C, after adding 50 µL of a fully ^{13}C-labeled internal standard. The extracts were centrifuged at 12,000 g for 5 min, and the supernatants were evaporated under vacuum in a SpeedVac (Savant SC250EXP) overnight. The dried extracts were then resuspended in 200 µL of milliQ water. Samples were analyzed using liquid chromatography on a Dionex ICS 5000 coupled to a high-resolution Q-Exactive Plus mass spectrometer, as detailed in (Lajus et al., 2020). The raw data were processed using Skyline v24.1.0.

4.3.3 Isotopic analyses of mevalonate.

The ^{13}C-enrichment of extracellular mevalonate was measured in exometabolome samples (diluted 1000 times) using ionic chromatography on a Dionex ICS-5000 coupled to a high-resolution Q-Exactive Plus mass spectrometer, as detailed in (Pineda et al., 2018). The intensities of each mass fraction within the isotopic cluster of mevalonate were extracted from the raw data using Skyline v24.1.0. The mean ^{13}C-enrichment was calculated from these mass fractions after correction for naturally occurring isotopes and isotopic purity of ^{13}C-

labeled acetate (99%), using IsoCor v2.2.2 (Millard et al., 2019) (https://github.com/MetaSys-LISBP/IsoCor).

4.3.4 Extracellular flux calculations

Extracellular fluxes (i.e. glucose uptake, acetate flux, mevalonate production, 3-hydroxypropionate production, and growth rates) were determined from the time-course concentrations of biomass, substrates, and products using PhysioFit v3.4.0 (Le Grégam et al., 2024) (https://github.com/MetaSys-LISBP/PhysioFit).

4.3.5 Kinetic modeling

We used a published kinetic model of *E. coli* (Millard et al., 2021), available from the Biomodels database (https://www.ebi.ac.uk/biomodels; (Chelliah et al., 2015)) under identifier MODEL2005050001. This model was extended to include a bioproduction pathway which converts acetyl-CoA into an extracellular product, following an irreversible Michaelis-Menten kinetics (with V_{max} set to 10% of the maximal glucose uptake rate, and K_M = 5 mM or 5 µM). Simulations were performed as described in the text, using COPASI (Hoops et al., 2006) v4.39) with the CoRC package (Förster et al., 2021); COPASI R Connector v0.12, https://github.com/jpahle/CoRC) in R (v4.4.2, https://www.r-project.org). The R notebook used to run the simulations and generate the figures is provided at https://github.com/MetaSys-LISBP/glucose_acetate_bioproduction.

4.4 Statistical analyses

Comparisons between strains or conditions were performed using Student's t-tests with two-tailed distributions.

5. References

Baba, T., Ara, T., Hasegawa, M., Takai, Y., Okumura, Y., Baba, M., Datsenko, K.A., Tomita, M., Wanner, B.L., Mori, H., 2006. Construction of *Escherichia coli* K-12 in-frame, single-gene knockout mutants: the Keio collection. Molecular Systems Biology 2, 2006.0008. https://doi.org/10.1038/msb4100050

Bennett, B.D., Kimball, E.H., Gao, M., Osterhout, R., Van Dien, S.J., Rabinowitz, J.D., 2009. Absolute metabolite concentrations and implied enzyme active site occupancy in *Escherichia coli*. Nat Chem Biol 5, 593–599. https://doi.org/10.1038/nchembio.186

Carneiro, S., Ferreira, E.C., Rocha, I., 2013. Metabolic responses to recombinant bioprocesses in *Escherichia coli*. Journal of Biotechnology 164, 396–408. https://doi.org/10.1016/j.jbiotec.2012.08.026

Castaño-Cerezo, S., Chamas, A., Kulyk, H., Treitz, C., Bellvert, F., Tholey, A., Galéote, V., Camarasa, C., Heux, S., Garcia-Alles, L.F., Millard, P., Truan, G., 2024. Combining systems and synthetic biology for in vivo enzymology. EMBO J 43, 5169–5185. https://doi.org/10.1038/s44318-024-00251-w

Chelliah, V., Juty, N., Ajmera, I., Ali, R., Dumousseau, M., Glont, M., Hucka, M., Jalowicki, G., Keating, S., Knight-Schrijver, V., Lloret-Villas, A., Natarajan, K.N., Pettit, J.-B., Rodriguez, N., Schubert, M., Wimalaratne, S.M., Zhao, Y., Hermjakob, H., Le Novère, N., Laibe, C., 2015. BioModels: ten-year anniversary. Nucleic Acids Research 43, D542–D548. https://doi.org/10.1093/nar/gku1181

Chemler, J.A., Fowler, Z.L., McHugh, K.P., Koffas, M.A.G., 2010. Improving NADPH availability for natural product biosynthesis in *Escherichia coli* by metabolic engineering. Metabolic Engineering 12, 96–104. https://doi.org/10.1016/j.ymben.2009.07.003

Chohnan, S., Izawa, H., Nishihara, H., Takamura, Y., 1998. Changes in Size of Intracellular Pools of Coenzyme A and Its Thioesters in *Escherichia coli* K-12 Cells to Various Carbon Sources and Stresses. Bioscience, Biotechnology, and Biochemistry 62, 1122–1128. https://doi.org/10.1271/bbb.62.1122

Datsenko, K.A., Wanner, B.L., 2000. One-step inactivation of chromosomal genes in *Escherichia coli* K-12 using PCR products. Proc. Natl. Acad. Sci. U.S.A. 97, 6640–6645. https://doi.org/10.1073/pnas.120163297

Duncombe, G.R., Frerman, F.E., 1976. Molecular and Catalytic Properties of the Acetoacetyl-Coenzyme A Thiolase of *Escherichia coli*. https://doi.org/10.1016/0003-9861(76)90152-1

Eiteman, M.A., Altman, E., 2006. Overcoming acetate in *Escherichia coli* recombinant protein fermentations. Trends in Biotechnology 24, 530–536. https://doi.org/10.1016/j.tibtech.2006.09.001

Förster, J., Bergmann, F.T., Pahle, J., 2021. CoRC: the COPASI R Connector. Bioinformatics 37, 2778–2779. https://doi.org/10.1093/bioinformatics/btab033

Hoops, S., Sahle, S., Gauges, R., Lee, C., Pahle, J., Simus, N., Singhal, M., Xu, L., Mendes, P., Kummer, U., 2006. COPASI—a COmplex PAthway SImulator. Bioinformatics 22, 3067–3074. https://doi.org/10.1093/bioinformatics/btl485

Kyselova, L., Kreitmayer, D., Kremling, A., Bettenbrock, K., 2018. Type and capacity of glucose transport influences succinate yield in two-stage cultivations. Microb Cell Fact 17, 132. https://doi.org/10.1186/s12934-018-0980-1

Lajus, S., Dusséaux, S., Verbeke, J., Rigouin, C., Guo, Z., Fatarova, M., Bellvert, F., Borsenberger, V., Bressy, M., Nicaud, J.-M., Marty, A., Bordes, F., 2020. Engineering

the Yeast *Yarrowia lipolytica* for Production of Polylactic Acid Homopolymer. Front. Bioeng. Biotechnol. 8, 954. https://doi.org/10.3389/fbioe.2020.00954
Le Grégam, L., Guitton, Y., Bellvert, F., Heux, S., Jourdan, F., Portais, J.-C., Millard, P., 2024. PhysioFit: a software to quantify cell growth parameters and extracellular fluxes. Bioinformatics 40, btae488. https://doi.org/10.1093/bioinformatics/btae488
Lim, J.H., Jung, G.Y., 2017. A simple method to control glycolytic flux for the design of an optimal cell factory. Biotechnol Biofuels 10, 160. https://doi.org/10.1186/s13068-017-0847-4
Long, C.P., Antoniewicz, M.R., 2019. Metabolic flux responses to deletion of 20 core enzymes reveal flexibility and limits of *E. coli* metabolism. Metabolic Engineering 55, 249–257. https://doi.org/10.1016/j.ymben.2019.08.003
Mannan, A.A., Darlington, A.P.S., Tanaka, R.J., Bates, D.G., 2025. Design principles for engineering bacteria to maximise chemical production from batch cultures. Nat Commun 16, 279. https://doi.org/10.1038/s41467-024-55347-y
Martin, V.J.J., Pitera, D.J., Withers, S.T., Newman, J.D., Keasling, J.D., 2003. Engineering a mevalonate pathway in *Escherichia coli* for production of terpenoids. Nat Biotechnol 21, 796–802. https://doi.org/10.1038/nbt833
Martínez-García, E., Fraile, S., Algar, E., Aparicio, T., Velázquez, E., Calles, B., Tas, H., Blázquez, B., Martín, B., Prieto, C., Sánchez-Sampedro, L., Nørholm, M.H.H., Volke, D.C., Wirth, N.T., Dvořák, P., Alejaldre, L., Grozinger, L., Crowther, M., Goñi-Moreno, A., Nikel, P.I., Nogales, J., de Lorenzo, V., 2023. SEVA 4.0: an update of the Standard European Vector Architecture database for advanced analysis and programming of bacterial phenotypes. Nucleic Acids Research 51, D1558–D1567. https://doi.org/10.1093/nar/gkac1059
Millard, P., Delépine, B., Guionnet, M., Heuillet, M., Bellvert, F., Létisse, F., 2019. IsoCor: isotope correction for high-resolution MS labeling experiments. Bioinformatics 35, 4484–4487. https://doi.org/10.1093/bioinformatics/btz209
Millard, P., Enjalbert, B., Uttenweiler-Joseph, S., Portais, J.-C., Létisse, F., 2021. Control and regulation of acetate overflow in *Escherichia coli*. eLife 10, e63661. https://doi.org/10.7554/eLife.63661
Millard, P., Gosselin-Monplaisir, T., Uttenweiler-Joseph, S., Enjalbert, B., 2023. Acetate is a beneficial nutrient for *E. coli* at low glycolytic flux. The EMBO Journal 42, e113079. https://doi.org/10.15252/embj.2022113079
Millard, P., Massou, S., Wittmann, C., Portais, J.-C., Létisse, F., 2014. Sampling of intracellular metabolites for stationary and non-stationary ^{13}C metabolic flux analysis in *Escherichia coli*. Analytical Biochemistry 465, 38–49. https://doi.org/10.1016/j.ab.2014.07.026
Noor, E., Liebermeister, W., 2024. Optimal enzyme profiles in unbranched metabolic pathways. https://doi.org/10.1098/rsfs.2023.0029
Pineda, E., Thonnus, M., Mazet, M., Mourier, A., Cahoreau, E., Kulyk, H., Dupuy, J.-W., Biran, M., Masante, C., Allmann, S., Rivière, L., Rotureau, B., Portais, J.-C., Bringaud, F., 2018. Glycerol supports growth of the *Trypanosoma brucei* bloodstream forms in the absence of glucose: Analysis of metabolic adaptations on glycerol-rich conditions. PLoS Pathog 14, e1007412. https://doi.org/10.1371/journal.ppat.1007412
Snoeck, S., Guidi, C., De Mey, M., 2024. "Metabolic burden" explained: stress symptoms and its related responses induced by (over)expression of (heterologous) proteins in

Escherichia coli. Microb Cell Fact 23, 96. https://doi.org/10.1186/s12934-024-02370-9

Soriano, A., Radice, A.D., Herbitter, A.H., Langsdorf, E.F., Stafford, J.M., Chan, S., Wang, S., Liu, Y.-H., Black, T.A., 2006. *Escherichia coli* acetyl-coenzyme A carboxylase: Characterization and development of a high-throughput assay. Analytical Biochemistry 349, 268–276. https://doi.org/10.1016/j.ab.2005.10.044

Takamura, Y., Kitayama, Y., Arakawa, A., Yamanaka, S., Tosaki, M., Ogawa, Y., 1985. Malonyl-CoA: acetyl-CoA cycling. A new micromethod for determination of acyl-CoAs with malonate decarboxylase. Biochimica et Biophysica Acta (BBA) - Lipids and Lipid Metabolism 834, 1–7. https://doi.org/10.1016/0005-2760(85)90170-5

Vidra, A., Németh, Á., 2017. Bio-based 3-hydroxypropionic Acid: A Review. Period. Polytech. Chem. Eng. 62, 156–166. https://doi.org/10.3311/PPch.10861

Wang, C.-H., Hou, J., Deng, H.-K., Wang, L.-J., 2023. Microbial production of mevalonate. Journal of Biotechnology 370, 1–11. https://doi.org/10.1016/j.jbiotec.2023.05.005

Wang, H., Xue, J., Liu, C., Chen, Z., Li, C., Li, X., Zheng, T., Jiang, Q., Xia, C., 2023. CO2 electrolysis toward acetate: A review. Current Opinion in Electrochemistry 39, 101253. https://doi.org/10.1016/j.coelec.2023.101253

Zhuang, K., Yang, L., Cluett, W.R., Mahadevan, R., 2013. Dynamic strain scanning optimization: an efficient strain design strategy for balanced yield, titer, and productivity. DySScO strategy for strain design. BMC Biotechnol 13, 8. https://doi.org/10.1186/1472-6750-13-8

Chapter 4
Ethanol overflow of yeast: Toward the control of Crabtree effect?

Contributions: In this chapter, I conceived the study, experimental design, performed data acquisition, formal data analysis, interpretation of results, and visualization. I also conducted the literature review and wrote the original draft.

1. Introduction

In chapter 1, we discussed overflow metabolism as a possibly conserved metabolic phenomena in living organisms (Warburg, 1924; Pasteur, 1857; Harden, 1901). Chapter 2 and other studies (Millard et al, 2023, Enjalbert et al, 2017) demonstrate that *E. coli* is capable of simultaneously producing and consuming acetate, such that even during net acetate excretion, extracellular acetate feeds cellular metabolism and is incorporated into central metabolites and biomass components. This dynamic exchange suggests that acetate, far from being a toxic by-product, can actively contribute to carbon and energy homeostasis depending on environmental conditions (Millard et al, 2021, 2023; Enjalbert et al, 2017). When the glycolytic flux is lowered, acetate assimilation can even promote growth by buffering the carbon uptake (Millard et al., 2023). These findings collectively reveal a shared control of overflow metabolism modulated both by thermodynamics and by the metabolic state. Finaly, Chapter 1 showed that similar principles could also apply to eukaryotic microorganisms. In this chapter, I aim to experimentally evaluate this hypothesis in yeast.

Yeast species display remarkable diversity in how they partition carbon fluxes during aerobic growth on glucose (Christen & Sauer, 2011; Flores, 2000; Fiaux *et al*, 2003; Cannizzaro *et al*, 2004; Blank *et al*, 2005). Yeasts are classified in two main categories: Crabtree-positive species (e.g., *Saccharomyces cerevisiae*) which ferment glucose into ethanol even in the presence of oxygen, and Crabtree-negative species (e.g., *Komagataella phaffii*) which preferentially oxidize glucose fully through respiration and do not produce ethanol. These distinct metabolic strategies are translated into two different flux distributions: Crabtree-positive yeasts typically exhibit high glycolytic flux, high ethanol production, and reduced TCA activity, while Crabtree-negative yeasts show lower glycolytic fluxes with more carbon directed through respiration, enabling faster growth and reduced ethanol secretion (Christen & Sauer, 2011).

Whole-genome duplication, horizontal gene transfer, and other evolutionary events (such as the selection of glycolytic genes overexpression) have been proposed as a potential cause to this metabolic divergence (Seoighe & Wolfe, 1999; Conant & Wolfe, 2007; Merico *et al*, 2007; Piškur & Langkjaer, 2004; Van Hoek & Hogeweg, 2009). Despite extensive research, it remains unclear whether the Crabtree effect is caused by a limitation in respiratory capacity (Sonnleitner & Käppeli, 1986), the initiation of glucose-induced repression of respiration (De Deken, 1966; Kayikci & Nielsen, 2015), or merely an overflow of carbon flux at the pyruvate branchpoint (Vemuri *et al*, 2007) (Vemuri et al, 2007), though the underlying functional principles responsible for the Crabtree effect remain unresolved.

Using isotopic labeling with [U-^{13}C] ethanol, Xiao et al., shown that in *S. cerevisiae* (Crabtree positive) and *Issatchenkia orientalis* (Crabtree negative), exposure to labeled ethanol leads to the incorporation of labelling into TCA intermediates, even when ethanol is produced (Xiao *et al*, 2022). This demonstrates that ethanol flux in yeast is bidirectional, involving simultaneous production and consumption reactions occurring in the meantime. This behavior suggests that overflow metabolites like ethanol can function as recyclable intermediates rather than waste products like acetate for *E. coli*. In the same way, mutants with repressed glycolytic flux (Ma, 1989; Rose *et al*, 1991; Entian & Frohlich, 1984; Entian *et al*, 1985) (e.g., Δ*hxk2*) co-consume

ethanol and glucose (Raamsdonk *et al*, 2001). These observations suggest that, similarly to acetate in *E. coli*, ethanol may function not purely as a by-product, but as a dynamically exchanged metabolite whose flux depends on both extracellular concentration of ethanol and intracellular metabolic state. Furthermore, ethanol toxicity could also be conditional and not an intrinsic trait of ethanol. This is what we will try to verify in this chapter by addressing the following questions:

- Is the ethanol flux thermodynamically controlled by extracellular ethanol concentration?

- Is the switch from ethanol production to consumption governed by an interplay between glycolytic and TCA fluxes and overflow flux?

- Under metabolic perturbations (e.g., altered glycolysis or respiration), can ethanol become beneficial for yeast growth?

- Can we relate the principles proposed in Chapter 1 to the Crabtree effect?

2. Results

2.1 Is ethanol flux thermodynamically controlled by its extracellular concentration?

To answer this question, we exposed a Crabtree-positive yeast (e.g., *Saccharomyces cerevisiae*) to increasing ethanol concentrations (0, 40, or 100 mM) and monitored both growth and extracellular fluxes (Figure 2). If the ethanol flux is thermodynamically controlled by ethanol concentration, we expect a progressive decrease in ethanol production as extracellular ethanol concentration increases. Ultimately, this could possibly lead to a reversal of the ethanol flux, with glucose and ethanol being co-consumed.

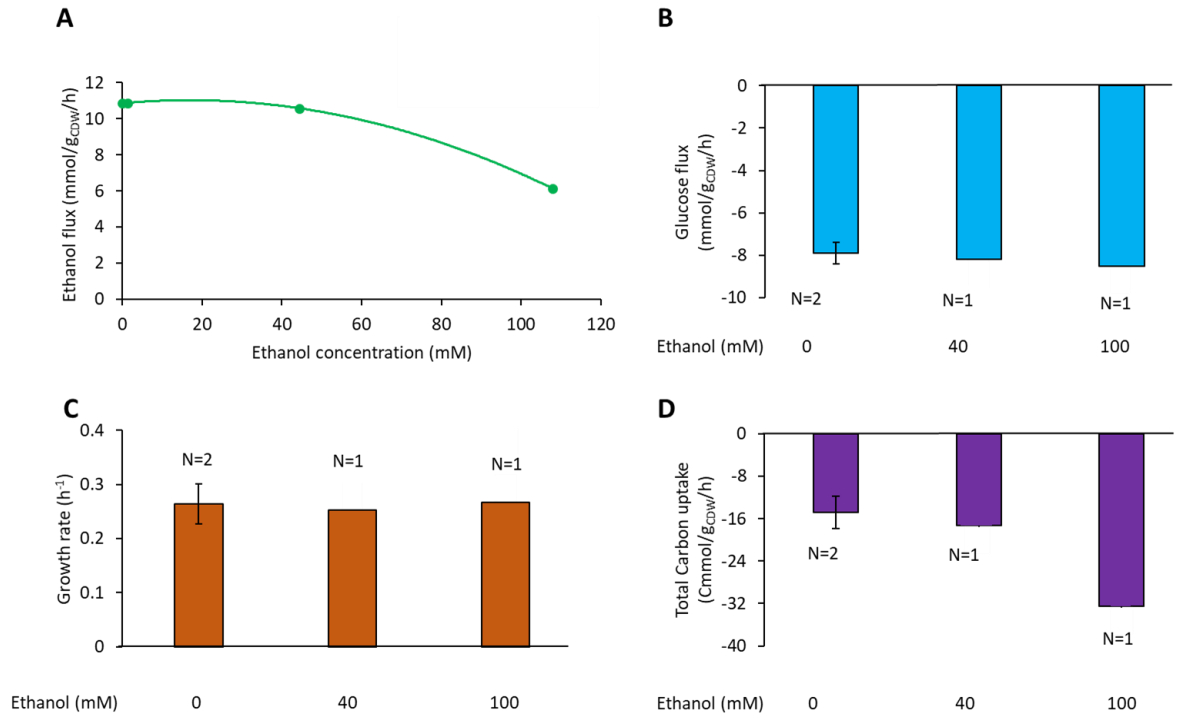


Figure 1. *S. cerevisiae* response to ethanol exposure. (A) Ethanol flux, (B) Glucose uptake flux, (C) Growth rate, and (D) Total carbon uptake.

At low to moderate ethanol concentrations (0–40 mM), the net ethanol production flux remained largely unchanged. However, at 100 mM ethanol, a marked decrease in ethanol production was observed, with flux reduced by up to 42% relative to the control (Figure 1A). Glycolytic flux is not affected by ethanol exposure (Figure 1B), and growth rate is stable along the different ethanol concentrations used here (Figure 1C). These observations support that ethanol flux in *S. cerevisiae*, like acetate in *E. coli*, may be thermodynamically controlled by extracellular ethanol concentration. Though, we don't observe in these conditions an inversion of ethanol flux (Figure 1A).

Although the data are consistent with a thermodynamic control of the ethanol flux by its extracellular concentration, additional experiments with more replicates and a broader range of ethanol concentrations are needed to confirm this conclusion. Interestingly, cells exposed to 100 mM ethanol exhibit increased carbon uptake despite a same growth rate (figure 1D). This is counterintuitive, as higher carbon uptake is typically associated with increased growth (Millard *et al*, 2023). One possible explanation is that the excess carbon is released as CO_2 via the TCA or the Pentose phosphate pathway, which was not measured in this experiment and though estimation of total carbon uptake is over-estimated. Testing this hypothesis using a genome-scale metabolic (GSM) model would be valuable, particularly to assess whether GSM simulations predict increased CO_2 efflux when growth rate is constrained to the experimentally observed values.

2.2 Is the switch from ethanol production to consumption governed by an interplay between glycolytic and overflow flux?

To address this question, we modulated the glycolytic flux and exposed yeast to different concentration of ethanol. To modulate glycolysis, we could have used (i) chemostat cultures to fix the growth rate (and thus the glycolytic flux); (ii) alternative carbon sources that are metabolized more slowly (e.g., galactose or glycerol); or (iii) glycolytic mutants (such as hxk2, a hexokinase 2 deletion mutant). Here, we chose to modulate the glycolytic activity by using 2-deoxyglucose (2DG), a non-metabolizable glucose analog that competitively inhibits hexokinase and hexose transporters thus slows down glycolytic flux (O'Donnell *et al*, 2015; Soncini *et al*, 2020). This strategy, which proved successful in *E. coli* (Chapter 2), allows fine-tuning of glycolytic inhibition by adjusting the inhibitor concentration.

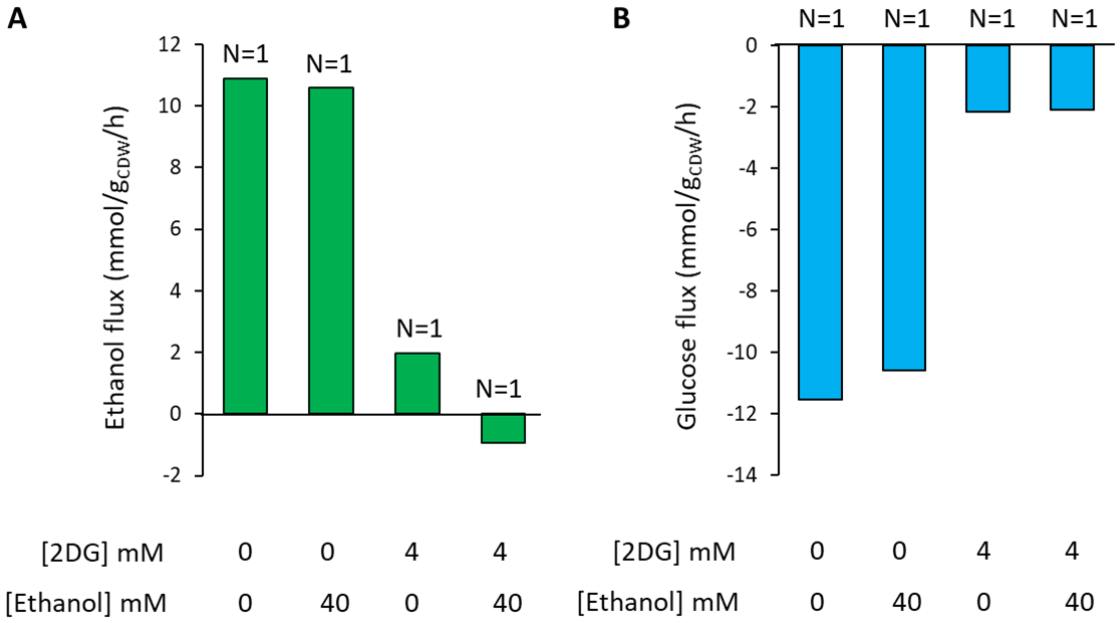


Figure 2. Glycolytic control of ethanol flux reversal. A, Ethanol flux or B, Glucose flux when BY 4741 is exposed to 40 mM of ethanol and/or 4 mM of 2DG

When 4 mM of 2DG was added to the culture medium, we observed a strong inhibition of ethanol production, with the overflow flux decreasing by fivefold (Figure 2A). This result is consistent with previous findings and further confirms the positive control of glycolysis on overflow metabolism in *S. cerevisiae* (Christen & Sauer, 2011; Heyland *et al*, 2009; van Hoek *et al*, 1998).

More interestingly, under these glycolysis-restricted conditions, the addition of 40 mM ethanol triggered a reversal in ethanol flux from net production (2.0 mmol/g_{CDW}/h) to net consumption (-1.0 mmol/g_{CDW}/h) clearly proving the yeast's capacity to assimilate ethanol even in the presence of glucose (Figure 2A). This finding is particularly striking given the

established model of glucose repression, which states that glucose inhibits the utilization of non-preferred carbon sources like ethanol during aerobic growth (Kayikci & Nielsen, 2015).

With the modulation of glycolytic flux (from -11 to -2 mmol/g_{CDW}/h) (Figure 2B), we observed a shift in ethanol flux, which transitioned from +10 mmol/g_{CDW}/h (net production) to –1 mmol/g_{CDW}/h (net consumption). This switch confirms that the balance between ethanol production and consumption is sensitive to the metabolic state of the cell and can be shifted simply by acting on the glycolytic flux.

These results reinforce the idea that ethanol overflow is not a straight, unidirectional process, but rather a flexible and dynamic feature of yeast metabolism, responsive to internal and external constraints. Furthermore, they highlight how environmental or chemical modulation of central pathways enable the co-utilization of multiple carbon sources, an insight of relevance both for metabolic engineering and for understanding adaptive strategies in fluctuating environments.

2.3 Under metabolic perturbations, can ethanol become beneficial for yeast growth?

To answer this question, we modulated the central carbon metabolism of the *S. cerevisiae* by deleting *hxk2 involved* in the uptake of glucose and measuring whether ethanol supplementation could improve growth.

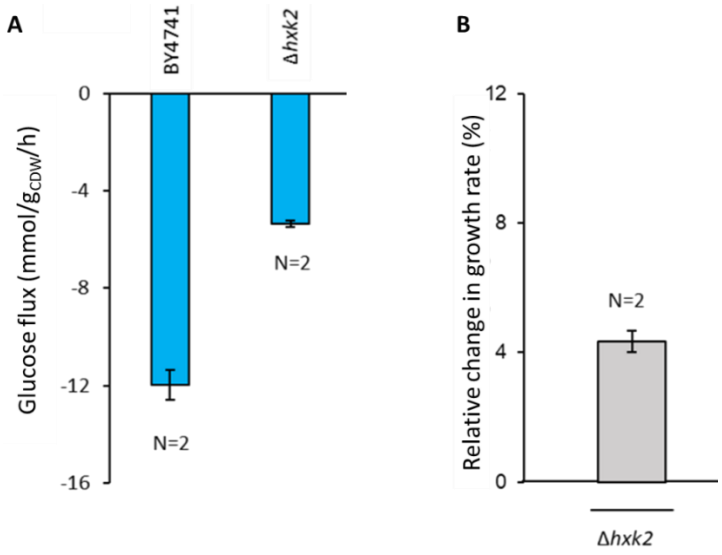


Figure 3. Ethanol effect on *Δhxk2* growth.
A. Impact of hxk2 deletion on glycolytic uptake compared to parental strain (BY4741), and wild type glycolytic uptake of *K. phaffi* (X33).

B. Growth rate difference between exposure or not with ethanol 40mM

In the strain *hxk2*, the glycolytic activity is strongly reduced compared to the parental strain. However, the presence of ethanol (40mM) appears to slightly enhance growth (Figure 3A) by 4%, as observed in *E. coli* (Chapter 2). This indicates that when glycolytic uptake is limited, ethanol can support cellular growth.

Our results clearly demonstrate the bidirectional and condition-dependent role of ethanol as both a by-product and a co-substrate. This suggests that ethanol is not merely a metabolic waste but can actively participate in central carbon metabolism and influence growth under specific conditions. This duality is further supported by the findings of (Xiao *et al*, 2022), who demonstrated that ethanol could act as a beneficial nutrient under oxidative stress an environmental condition that leads to a reduced glycolytic flux (Minard & McAlister-Henn, 2005; Grabowska & Chelstowska, 2003). They further argue that ethanol serves as an uncoupler of glycolysis and the TCA cycle, similarly to lactate in mammalian cells (Rabinowitz & Enerbäck, 2020), and as also observed in bacteria (Enjalbert *et al*, 2017).

2.4 Can we relate the principles proposed in Chapter 1 to the crabtree effect ?

Previous findings underscore that ethanol metabolism in *S. cerevisiae* is not merely a by-product of fermentative overflow, but a dynamic and reversible process, controlled by both the glycolytic flux and thermodynamicaly by the extracellular ethanol concentration. We show that ethanol can enhance growth under low glycolytic flux. To explore whether these principles are conserved beyond *S. cerevisiae*, we extended our investigation to other yeast species which went through distinct evolutionary and metabolic lineages. We selected *Komagataella phaffii*, a Crabtree-negative yeast known for its strong respiratory metabolism and minimal ethanol excretion under glucose-rich conditions (Karaoğlan *et al*, 2020).

Using the same experimental framework as for *S. cerevisiae*, we exposed *K. phaffii* to increasing concentrations of ethanol, ranging from 0 to 60 mM.

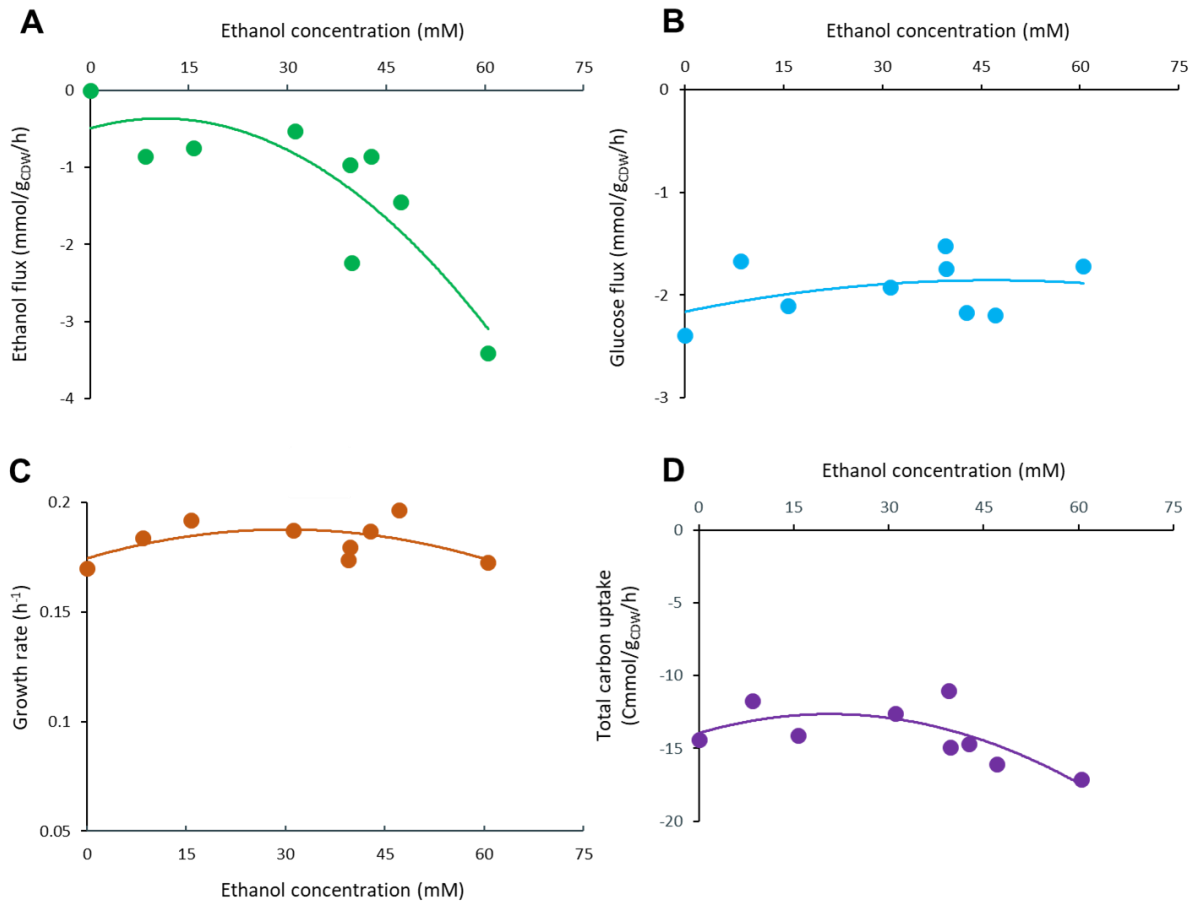


Figure 4. Impact of ethanol on *K. phaffi X33 strain* is exposed to increasing concentration of ethanol and exometabolome is calculated. (A) Ethanol flux, (B) Glucose flux, (C) Growth rate, (D) Total carbon uptake. The fits are a 2nd degree polynomial function fit.

As expected for strictly respiratory yeast, no ethanol production was observed in the absence of ethanol supplementation (Karaoğlan *et al*, 2020), consistent with its inherently low glycolytic flux and high respiratory capacity (Figure 4A). However, upon ethanol addition, we observed a progressive increase in ethanol uptake: from nearly zero at low concentrations, to approximately 0.5 mmol/g_{CDW}/h at 10–20 mM, and reaching 2–3 mmol/g_{CDW}/h at concentrations of 20 mM or higher (Figure 4A).

Increasing extracellular ethanol concentrations also led to a slight decrease in glucose uptake (~15–20%) (figure 4B). When calculating the total carbon uptake across this range of ethanol concentrations, we observed that carbon uptake remained stable up to 30 mM ethanol. Beyond this threshold, total carbon uptake increased by approximately 10% (figure 4D), which corresponds to a ~8% increase in growth rate (figure 4C). Since the increase in growth rate mirrors the increase in total carbon uptake, it is likely that the enhanced growth results directly from this elevated carbon assimilation. It could also be linked to increased availability of acetyl-CoA, as ethanol is metabolized through the acetaldehyde-to-acetate pathway, feeding into acetyl-CoA biosynthesis. This, in turn, fuels the TCA cycle, as demonstrated by (Xiao *et al*, 2022). This result also mirrors and confirms the previous findings obtained in

Δ*hxk2*, where both glycolytic uptakes are comparable (figure 3A and 4B) and lead to the same growth rate gain.

These results demonstrate that *K. phaffii*, despite not producing ethanol under aerobic conditions, retains a functional capacity to assimilate it in a concentration-dependent manner. This behavior contrasts with that of Crabtree-positive yeasts, where ethanol production dominates under glucose-rich conditions, and reinforces the idea that ethanol dynamics are not binary (production or consumption) but continuous and regulated along a spectrum shaped by environmental context.

Together, these cross-species comparisons reveal that ethanol metabolism can be shaped by a combination of intracellular flux control and environment. However, the balance between production and consumption is species-specific, reflecting the evolutionary tuning of metabolic networks.

3. Discussion

This chapter sheds light on the fundamental mechanisms governing overflow metabolism in yeast, with a particular focus on ethanol flux in crabtree positive yeast *S. cerevisiae* and its comparison to crabtree negative *K. phaffii*. By leveraging concepts derived from bacterial systems biology specifically from *Escherichia coli* we demonstrate that key principles such as thermodynamic constraints and the interplay between glycolysis and overflow metabolism are not only applicable to bacteria but may be broadly conserved across domains of life, as shown here for yeast.

Our results confirm that ethanol excretion in *S. cerevisiae* is a tightly regulated, bidirectional process influenced by both intracellular flux distribution and extracellular ethanol concentration. Strikingly, we observed that ethanol uptake can occur even in the presence of glucose under conditions of reduced glycolytic flux. This finding challenges the classical view of strict glucose repression and reveals a strong metabolic plasticity, allowing yeast to dynamically adapt to environmental fluctuations.

These insights support the idea that overflow metabolites are not merely waste products but act as modulators of central carbon metabolism contributing to redox balance as previously demonstrated (Xiao *et al*, 2022) and energy homeostasis.

This metabolic flexibility could provide an explanation for their evolution toward the adaptation of circadian rhythms of plants and microbiota. Yeast constantly adapts to its environment, which is often complex and dynamic. While various niches have been explored (Starmer and Lachance, 2011), plants and microbiota (Indu *et al*, 2021; Nenciarini *et al*, 2024) stand out as well-characterized ecosystems. During the day, plants are metabolically active and release a wide range of compounds, prompting yeast to adopt a metabolically responsive state. At night, when plant activity declines, yeast transitions to an alternative metabolic mode. Similar adaptive behavior should offer an advantage in interactions with commensal

microorganisms, where nutrient availability and competition fluctuate over time. These ecological interactions may have shaped yeast's capacity to exploit diverse carbon sources such as ethanol and adapt to fluctuating environments, allowing it to thrive in variable and resource-limited environments. In a more biotechnological view, the integrative consideration of the principal regulatory mechanisms and the dynamic interplay between them could provide us with the ability to effectively modulate the Crabtree effect. In Crabtree-positive yeasts, by tuning glycolytic flux or conversely, in Crabtree-negative yeasts, manipulating TCA cycle activity could elicit a comparable response to ethanol exposure (or other perturbations). The central question is whether these interventions would result in comparable growth rates. This approach aimed to reveal whether distinct metabolic routes could converge functionally, highlighting the plasticity of yeast metabolism, and to revisit the Crabtree effect not as a fixed metabolic state species dependant, but as a tunable outcome of flux balance and environmental context. Moreover, these results would further confirm that a given metabolic state can offer different functional responses (growth rate for instance), and more generally, that correlations between growth rate and overflow metabolism is often misleading, because the growth rate is a *consequence,* and not a *cause,* of the imposed restriction on the uptake rate of glycolytic substrates on glycolysis and/or TCA and by extension, other metabolic pathways. One major perspective of this work would be to investigate whether the functional principles elucidated in this study could be applied to the "negativisation" of Crabtree-positive yeasts for biotechnological applications, as suggested by (Guo *et al*, 2025). For instance, could co-feeding glucose and ethanol in wild-type or Δ*hxk2 S. cerevisiae* strains enhance the production of valuable biomolecules as acetate does for bacteria?

4. Materials and Methods

4.1 Strains, medium and cultivation conditions

The investigated yeast strains are listed in table 1.

Species	Genotype	Source
Saccharomyces cerevisiae - BY4741	MATa his3Δ1 leu2Δ0 met15Δ0 ura3Δ0	(Pan *et al*, 2004)
Saccharomyces cerevisiae - BY4741	MATa his3Δ1 leu2Δ0 met15Δ0 ura3Δ0 *hxk2*::Kan	(Pan *et al*, 2004)
Komagataella phaffii - X33	Wild Type	Invitrogen-Thermo Fisher Scientific

Table 1. Yeast species used in this chapter

All cultured yeast has been performed on YNB (Yeast Nitrogen Based) with 15 mM glucose and according to ethanol concentrations. After pre-cultivation on rich media (YPD), overnight YNB glucose medium, 25–50 mL cultures were inoculated to a starting OD_{600} nm of 0.1 and grown in 250-mL shake flasks at 30°C and 200 rpm. Aliquots were withdrawn and filtered sterilized during the exponential growth phase. For 2-deoxyglucose treatment, a concentrated stock 2-deoxy-glucose (1,2mM in H_2O) was first diluted 100× with water and added to the culture at a 100× dilution.

4.2 Biomass and extracellular metabolite concentrations

Growth was monitored by measuring the optical density (OD) at 600 nm using a Genesys 150 thermoscientific spectrophotometer. Biomass concentration was determined using a conversion factor of 0.37 $g_{CDW}/L/OD_{600}$ unit.

Extracellular concentrations of glucose and ethanol were quantified in 180 µL of filtered broth (0.2-µm syringe filter, Sartorius, Germany) by 1D ^{1}H-NMR on a Bruker Avance 500 MHz spectrometer equipped with a 5-mm z-gradient BBI probe (Bruker, Germany), as described previously (Millard *et al*, 2023).

4.3 Extracellular flux calculations

Extracellular fluxes (i.e. glucose uptake, ethanol flux and growth rates) were determined from the time-course concentrations of biomass, substrates, and products using PhysioFit v3.4.0 (Le Grégam *et al*, 2024).

5. References

Blank L, Lehmbeck F & Sauer U (2005) Metabolic-flux and network analysis in fourteen hemiascomycetous yeasts. *FEMS Yeast Res* 5: 545–558

Cannizzaro C, Christensen B, Nielsen J & Stockar UV (2004) Metabolic network analysis on Phaffia rhodozyma yeast using 13C–labeled glucose and gas chromatography-mass spectrometry. *Metab Eng* 6: 340–351

Christen S & Sauer U (2011) Intracellular characterization of aerobic glucose metabolism in seven yeast species by ^{13}C flux analysis and metabolomics: Flux response to Crabtree effect in yeast species. *FEMS Yeast Res* 11: 263–272

Conant GC & Wolfe KH (2007) Increased glycolytic flux as an outcome of whole-genome duplication in yeast. *Mol Syst Biol* 3: 129

De Deken RH (1966) The Crabtree Effect: A Regulatory System in Yeast. *J Gen Microbiol* 44: 149–156

Enjalbert B, Millard P, Dinclaux M, Portais J-C & Létisse F (2017) Acetate fluxes in *Escherichia. coli* are determined by the thermodynamic control of the Pta-AckA pathway. *Sci Rep* 7: 42135

Entian K-D & Frohlich K-U (1984) *Saccharomyces cerevisiae* Mutants Provide Evidence of Hexokinase Pll as a Bifunctional Enzyme with Catalytic and Regulatory Domains for Triggering Carbon Catabolite Repressiont. *J BACTERIOL* 158

Entian K-D, Hilberg F, Opitz H & Mecke D (1985) Cloning of Hexokinase Structural Genes from *Saccharomyces cerevisiae* Mutants with Regulatory Mutations Responsible for Glucose Repression. *MOL CELL BIOL* 5

Fiaux J, Çakar ZP, Sonderegger M, Wüthrich K, Szyperski T & Sauer U (2003) Metabolic-Flux Profiling of the Yeasts *Saccharomyces cerevisiae* and *Pichia stipitis*. *Eukaryot Cell* 2: 170–180

Flores C (2000) Carbohydrate and energy-yielding metabolism in non-conventional yeasts. *FEMS Microbiol Rev* 24: 507–529

Grabowska D & Chelstowska A (2003) The ALD6 Gene Product Is Indispensable for Providing NADPH in Yeast Cells Lacking Glucose-6-phosphate Dehydrogenase Activity. *J Biol Chem* 278: 13984–13988

Guo Y, Xiong Z, Zhai H, Wang Y, Qi Q & Hou J (2025) The advances in creating Crabtree-negative *Saccharomyces cerevisiae* and the application for chemicals biosynthesis. *FEMS Yeast Res* 25: foaf014

Harden A (1901) LXIV.—The chemical action of *Bacillus coli communis* and similar organisms on carbohydrates and allied compounds. *J Chem Soc Trans* 79: 610–628

Heyland J, Fu J & Blank LM (2009) Correlation between TCA cycle flux and glucose uptake rate during respiro-fermentative growth of *Saccharomyces cerevisiae*. *Microbiology* 155: 3827–3837

van Hoek P, Flikweert MT, van der Aart QJM, Steensma HY, van Dijken JP & Pronk JT (1998) Effects of Pyruvate Decarboxylase Overproduction on Flux Distribution at the Pyruvate Branch Point in *Saccharomyces cerevisiae*. *Appl Environ Microbiol* 64: 2133–2140

Indu B, Keertana T, Ipsita S, Jagadeeshwari U, Sasikala C & Ramana CV (2021) Uncovering the hidden bacterial ghost communities of yeast and experimental evidences demonstrates yeast as thriving hub for bacteria. *Sci Rep* 11: 9394

Karaoğlan M, Erden-Karaoğlan F, Yılmaz S & İnan M (2020) Identification of major *ADH* genes in ethanol metabolism of *Pichia pastoris*. *Yeast* 37: 227–236

Kayikci Ö & Nielsen J (2015) Glucose repression in *Saccharomyces cerevisiae*. *FEMS Yeast Res* 15: fov068

Le Grégam L, Guitton Y, Bellvert F, Heux S, Jourdan F, Portais J-C & Millard P (2024) PhysioFit: a software to quantify cell growth parameters and extracellular fluxes. *Bioinformatics* 40: btae488

Ma H (1989) The Residual Enzymatic Phosphorylation Activity of Hexokinase II Mutants Is Correlated with Glucose Repression in *Saccharomyces cerevisiae*. *MOL CELL BIOL* 9

Merico A, Sulo P, Piškur J & Compagno C (2007) Fermentative lifestyle in yeasts belonging to the *Saccharomyces* complex. *FEBS J* 274: 976–989

Millard P, Enjalbert B, Uttenweiler-Joseph S, Portais J-C & Létisse F (2021) Control and regulation of acetate overflow in *Escherichia coli*. *eLife* 10: e63661

Millard P, Gosselin-Monplaisir T, Uttenweiler-Joseph S & Enjalbert B (2023) Acetate is a beneficial nutrient for *E. coli* at low glycolytic flux. *EMBO J* 42: e113079

Minard KI & McAlister-Henn L (2005) Sources of NADPH in Yeast Vary with Carbon Source. *J Biol Chem* 280: 39890–39896

Nenciarini S, Renzi S, Di Paola M, Meriggi N & Cavalieri D (2024) Ascomycetes yeasts: The hidden part of human microbiome. *WIREs Mech Dis* 16: e1641

O'Donnell AF, McCartney RR, Chandrashekarappa DG, Zhang BB, Thorner J & Schmidt MC (2015) 2-Deoxyglucose Impairs *Saccharomyces cerevisiae* Growth by Stimulating Snf1-Regulated and α-Arrestin-Mediated Trafficking of Hexose Transporters 1 and 3. *Mol Cell Biol* 35: 939–955

Pan X, Yuan DS, Xiang D, Wang X, Sookhai-Mahadeo S, Bader JS, Hieter P, Spencer F & Boeke JD (2004) A Robust Toolkit for Functional Profiling of the Yeast Genome. *Mol Cell* 16: 487–496

Pasteur L (1857) Mémoire de L. Pasteur sur la fermentation alcoolique.

Piškur J & Langkjaer RB (2004) Yeast genome sequencing: the power of comparative genomics: Yeast comparative genomics. *Mol Microbiol* 53: 381–389

Raamsdonk LM, Diderich JA, Kuiper A, Van Gaalen M, Kruckberg AL, Berden JA & Van Dam K (2001) Co-consumption of sugars or ethanol and glucose in a *Saccharomyces cerevisiae* strain deleted in the HXK2 gene. *Yeast* 18: 1023–1033

Rabinowitz JD & Enerbäck S (2020) Lactate: the ugly duckling of energy metabolism. *Nat Metab* 2: 566–571

Rose M, Albig W & Entian K (1991) Glucose repression in *Saccharomyces cerevisiae* is directly associated with hexose phosphorylation by hexokinases PI and PII. *Eur J Biochem* 199: 511–518

Seoighe C & Wolfe KH (1999) Yeast genome evolution in the post-genome era. *Curr Opin Microbiol* 2: 548–554

Soncini SR, Chandrashekarappa DG, Augustine DA, Callahan KP, O'Donnell AF & Schmidt MC (2020) Spontaneous mutations that confer resistance to 2-deoxyglucose act through Hxk2 and Snf1 pathways to regulate gene expression and HXT endocytosis. *PLOS Genet* 16: e1008484

Sonnleitner B & Käppeli O (1986) Growth of *Saccharomyces cerevisiae* is controlled by its limited respiratory capacity: Formulation and verification of a hypothesis. *Biotechnol Bioeng* 28: 927–937

Van Hoek MJA & Hogeweg P (2009) Metabolic Adaptation after Whole Genome Duplication. *Mol Biol Evol* 26: 2441–2453

Vemuri GN, Eiteman MA, McEwen JE, Olsson L & Nielsen J (2007) Increasing NADH oxidation reduces overflow metabolism in *Saccharomyces cerevisiae*. *Proc Natl Acad Sci* 104: 2402–2407

Warburg VO (1924) Ober den Stoffwechsel der Carcmomzelle j.

Xiao T, Khan A, Shen Y, Chen L & Rabinowitz JD (2022) Glucose feeds the tricarboxylic acid cycle via excreted ethanol in fermenting yeast. *Nat Chem Biol* 18: 1380–1387

Chapter 5
Conclusion and Outlook

1. Chapter perspectives

Overflow metabolism refers to the excretion of partially oxidized metabolic by-products during growth on glycolytic substrates and, as highlighted in **Chapter 1**, appears to be a phenomenon conserved in many living organisms. Observed in *Escherichia coli*, *Saccharomyces cerevisiae* and mammalian cells, overflow is traditionally viewed as an inefficient metabolic phenomenon. However, through a comparative, holistic approach, this thesis proposes to re-conceptualize overflow metabolism from a wasteful process-which have to be mitigated in biotechnology (Eiteman & Altman, 2006; Mulukutla *et al*, 2012), or targeted in health (Warburg, 1924; Lemberg *et al*, 2022)-to an adaptative and controllable feature with several benefits for cellular metabolism (Millard *et al*, 2021, 2023; Enjalbert *et al*, 2017; Yasir *et al*, 2024; Alteri & Mobley, 2012).

In **Chapter 2**, focusing on *Escherichia coli*, we investigated the functional reversibility of acetate metabolism under varying glycolytic flux conditions. Traditionally considered a toxic byproduct of overflow metabolism, acetate was shown to play a more nuanced role: it can enhance growth when glucose uptake is limited, acting as a carbon and energy buffer rather than a mere waste metabolite. Through a system biology approach combining kinetic modeling and fluxomics, we demonstrated that the role of acetate as either a growth inhibitor or a beneficial nutrient is highly dependent on the cell's metabolic state and on the nutritional environment (Millard *et al*, 2023).

Specifically, under conditions of high glycolytic flux, acetate accumulation leads to growth inhibition (Luli & Strohl, 1990; Pinhal *et al*, 2019; Millard *et al*, 2023). In contrast, when glycolytic flux is lowered, acetate will enhance growth and buffer the total carbon uptake (Millard *et al*, 2023). These findings highlight the context-dependent role of overflow metabolites. This metabolic flexibility may offer a fitness advantage in fluctuating environments (e.g. the gut (Conway & Cohen, 2015; Pérez, 2021; Den Besten *et al*, 2013; Nakamoto *et al*, 2025), particularly under nutrient limitation or competition.

To further validate these findings and to estimate the involvement of gene regulation in this response, it would be highly informative to investigate the response of a *Δcrp* (cyclic AMP receptor protein knockout) strain of *E. coli* to acetate supplementation. CRP is a key regulator of catabolite repression, and its deletion is expected to broadly impact carbon source prioritization and metabolic flexibility (Deutscher, 2008; Diaz *et al*, 2019; Nakamoto *et al*, 2025). By removing the CRP-mediated repression, *E. coli* may gain increased access to alternative carbon sources such as acetate (Kumari *et al*, 1995), in particular in nutritionally rich environments.

Moreover, previous work has shown that *crp* deletion leads to improved survival in nutrient-scarce environments and improve the tolerance of *E. coli* to acetate (Nakamoto *et al*, 2025; Diaz *et al*, 2019; Chong *et al*, 2013), suggesting that this regulatory modification could confer

a selective advantage under stress or resource competition. Strengthening those results, it would also help identify potential metabolic engineering strategies aiming at enhancing robustness and resource utilization in industrial strains. Finally, the intermediate of acetate metabolism, known as acetyl-phosphate (acetyl-P), is known to acetylate or phosphorylate enzymes and/or transcription factors, thereby affecting their activity and/or the transcription of specific genes (Schastnaya *et al,* 2023). Investigating the acetylome and the phosphoproteome in our condition would be highly informative to explain the observed metabolic state.

Another perspective would be to investigate whether and how acetate affects the global energy and cofactor balance in *E. coli*. This could be explored through modeling, for example, by incorporating energy-related reactions into our existing kinetic model (which includes glycolysis, growth, and overflow metabolism). This approach would allow us to test whether acetate supplementation, under conditions where glycolysis is impaired, can enhance the overall energy status of the cells, highlighting the interplay between both glycolysis, acetate overflow and energy status. In order to get insights into the energetic response of *E. coli* to acetate, I have performed, in collaboration with Loïc Le Grégam from Metatoul platform, ^{13}C-fluxomics experiments to directly measure intracellular carbon and energy fluxes in response to perturbations of glycolytic activity and acetate concentration and the fluxes calculations are actually performed. Such information will be highly valuable for biotechnological applications, for instance to optimize the energy-dependent production of some chemicals

Taken together, these results support a shift in perspective: overflow metabolites such as acetate should not be viewed solely as undesirable byproducts, but as dynamically regulated metabolites whose roles vary according to metabolic and environment fluctuations. This insight has important implications for fundamental microbial physiology/metabolism understanding, applied bioprocess design (chapter 3) and health (Brooks, 2002; Dalile *et al*, 2019; Den Besten *et al*, 2013; Kim, 2023; Martinson & Walk, 2020), and should be explored further.

In **Chapter 3**, we demonstrate how those metabolic principles can be applied to optimize biotechnological processes. Specifically, we investigated the impact of acetate supplementation on the biosynthesis of acetyl-CoA-derived compounds, such as mevalonate (Martin *et al*, 2003; Yang & Guo, 2014) and 3-hydroxypropionate (Rathnasingh, 2012; Andreeßen *et al*, 2014; Lama *et al*, 2021) in engineered *Escherichia coli* strains. Metabolic modeling predicted that acetate co-feeding would enhance intracellular acetyl-CoA availability, particularly under low glycolytic flux, thereby improving glucose-based bioproduction in *E. coli*. These predictions were validated experimentally. In a lab bioproduction context, acetate supplementation led to increased biomass accumulation, higher product titers and flux for acetyl-CoA sensitive production pathway and even productivity (due to the improvement of growth rate) for acetyl-CoA insensitive production pathways. This improvement was largely attributed to the elevation of intracellular acetyl-CoA

levels. Our findings introduce a promising generic strategy in microbial bioproduction: the co-consumption of glucose and acetate can improve carbon efficiency use, sustainability and key bioproduction metrics (e.g. yield, flux, and productivity). Notably, this beneficial effect of acetate was observed even under conditions of metabolic burden, a common challenge in heavily engineered bacterial strains (Snoeck *et al*, 2024).

Given the central metabolic role of acetyl-CoA as a precursor to a broad range of industrially relevant molecules, it would be interesting to systematically assess the effect of acetate supplementation across a wider spectrum of target compounds using acetyl-CoA as a precursor (Zhu *et al*, 2022). Beyond acetyl-CoA-derived products, it would also be of great interest to explore whether the beneficial effects of acetate supplementation extend to the biosynthesis of compounds derived from other metabolic precursors, such as intermediates of the TCA cycle (Noh *et al*, 2018), upper glycolysis, or the pentose phosphate pathway (Ahn *et al*, 2011). In chapter 3, we have demonstrated that even when the production pathway is insensitive to precursor availability, the beneficial effect in growth rate still leads to enhanced 3HP productivity. This result is encouraging, as it confirms that the beneficial effect of acetate on bioproduction could be independent of increased precursor availability. Therefore, this productivity gain could possibly occur for the production of other biomolecules which do not use acetyl-CoA as precursors. Moreover, considering the concept of glycolytic and TCA uncoupling, presented in introduction, one should test whether the supplemented acetate may feed the TCA cycle, as previously suggested. Since this pathway is a key producer of energy and redox cofactors (NADH, NADPH, ATP), acetate could possibly increase their availability for the production of compounds that require cofactors for their biosynthesis.

Looking ahead, assessing the scalability and industrial relevance of the co-consumption strategy proposed in this thesis represents an opportunity for future research and development. In this thesis, I investigated the impact of acetate on bioproduction in batch cultures. However, alternative bioprocess strategies such as fed-batch or chemostat cultures are largely applied in industrial biotechnology, and the impact of acetate remains to be explored. In these setups, the glycolytic flux is typically regulated through the substrate feed rate (typically glucose or glycerol) and the dilution rate. We could develop a dual-feed strategy by co-feeding acetate with glycolytic substrates. Modulating the glucose and acetate concentration in the feed would enable fine-tuning the glycolytic and acetate flux in a producing strain and would enable the identification of optimal conditions for bioproduction.

Finally, the conserved nature of overflow metabolism across diverse biological systems suggests that the insights derived from this work could be transferable to other microbial hosts which are diverse and widely used in biotechnology (Demain & Adrio, 2008), including *Bacillus subtilis* (Halmschlag *et al*, 2023), *Lactococcus lactis* (Gaspar *et al*, 2004), *Corynebacterium glutamicum* (Xu *et al*, 2020), *Pseudomonas putida* (Weimer *et al*, 2024). In these microorganisms, as in *E. coli*, a part of the metabolic engineering work focuses on deleting or reducing overflow by-products accumulation. In many of these systems, attempts

to abolish overflow metabolism through strain engineering can be particularly challenging, especially in species with limited genetic modification tools or less characterized regulatory networks. In such cases, adopting a strategy of co-utilization of overflow by-products in synergy with glycolytic carbon sources may represent a solution to enhance production yields, biomass formation, or even carbon fixation. Such investigations could broaden the applicability of acetate co-feeding as a general strategy for improving microbial bioproduction.

Finally, in **Chapter 4**, we aimed to explore the principles highlighted in **Chapters 1 and 2** to yeast metabolism, focusing on the Crabtree effect and taking as models *Saccharomyces cerevisiae* (for Crabtree positive yeasts) and *Komagataella phaffii* (for Crabtree negative yeasts). Although further experiments are required to statistically validate the strength of these findings., preliminary Results indicate that ethanol flux in yeast is reversible and regulated by both the metabolic state and the extracellular ethanol concentration, much like the acetate flux in *E. coli*. Under conditions of reduced glycolytic flux (e.g., via HXK2 deletion or 2-deoxyglucose treatment or naturally low glycolytic flux yeast species such as *K. phaffi*), we observed ethanol consumption alongside glucose. These findings challenge the rigidity of glucose repression (Gancedo, 1998) and reveal that both Crabtree-positive and Crabtree-negative yeasts possess a latent capacity for ethanol co-utilization with glucose.

Moreover, we suggest that ethanol, like acetate, can be beneficial for growth under respiratory or glycolytic constraints. This supports the idea that overflow metabolism in yeast is a flexible, condition-dependent system evolved to cope with fluctuating environments.

A comparative analysis of ethanol response in Crabtree-positive and Crabtree-negative yeast species further illustrates how ethanol metabolism depends on the underlying metabolic state specifically the balance between TCA cycle activity and glycolysis. In Crabtree-positive yeast, which typically exhibits high glycolytic flux and low TCA activity (Christen & Sauer, 2011), ethanol exposure results in reduced growth (Brown *et al*, 1981). However, when glycolytic flux is lowered (Raamsdonk *et al*, 2001) (e.g., HXK2 deletion or *K. phaffi* with inherently low glycolytic flux), we observe a reversal of ethanol flux and concomitant growth-promoting effect of ethanol.

Interestingly, in Crabtree-negative yeast, which displays significantly higher TCA activity and lower glycolytic flux (Christen & Sauer, 2011), ethanol is consumed for way lower ethanol concentration than in Crabtree-positive strains. This difference in response toward ethanol should be due to the higher TCA activity of Crabtree negative yeasts (Christen & Sauer, 2011). To test this hypothesis, it would be interesting to perform ^{13}C-fluxomic experiments and monitor the labelling in TCA intermediates over this range of ethanol concentrations. This experiment would allow us to evaluate the direct contribution of TCA to ethanol response and better highlight the interplay between glycolysis and TCA cycle in determining ethanol flux.

It would also be highly informative to test the response of Crabtree-positive yeast to simultaneous exposure to ethanol and antimycin A (a known inhibitor of mitochondrial

respiration) (Potter & Reif, 1952; Liti *et al*, 2001). Such experiments could clarify the interplay of glycolysis and TCA activity within the same yeast species. To date, we have demonstrated the involvement of these two pathways independently in 2 different yeast species. Modulating TCA activity in Crabtree-positive yeast would thus help bridge the gap between Crabtree-positive and -negative phenotypes, thereby opening a new window on this historical phenomenon. Furthermore, a particularly valuable approach would be to investigate a broader diversity of yeast species that exhibit varying degrees of the Crabtree effect. This could include species with an intermediate or partial Crabtree effect such as *Saccharomyces bayanus*, *S. exiguus*, *Lachancea thermotolerans*, and *Kluyveromyces dobzhanskii* as well as Crabtree-negative yeasts like *Yarrowia lipolytica*, *Pichia angusta*, and *Candida rugosa*. Exposing these yeasts to a gradient of ethanol concentrations (e.g., from 0.1 to 80 mM) would provide strong evidence for the conservation of the underlying metabolic principles across the fungal kingdom and reveal the continuum that exists between different yeast species in terms of their resource allocation and overflow metabolism.

Considering recent advances in yeast metabolic engineering aiming at converting Crabtree-positive strains into Crabtree-negative ones (Guo *et al*, 2025) to reduce growth rate. It would be highly valuable to investigate whether modulating Crabtree-positive toward Crabtree negative metabolism and supplementing it with ethanol could enhance yeast bioprocesses similarly as acetate supplementation improves bacterial bioprocesses.

2. General perspective: Towards a unified theory of overflow metabolism

While this thesis explores the similarities of overflow metabolism across diverse organisms, these shared principles do not explain the root cause of overflow, for which various theories have been proposed. In this fundamental perspective, I reexamine the prevailing theories of overflow metabolism, focusing on those with potential relevance to all living organisms, in light of the outlined principles.

Cells operate under multiple universal biophysical constraints, some of which may drive overflow metabolism. These constraints may stem from resource allocation (Basan *et al*, 2015; Shen *et al*, 2024; Vazquez & Oltvai, 2016), intracellular crowding (Vazquez & Oltvai, 2016; Vazquez *et al*, 2010), cell geometry (Zhuang *et al*, 2011; Szenk *et al*, 2017), or limits on energy dissipation (Niebel *et al*, 2019; Saadat *et al*, 2020). Despite invoking distinct aspects of cells physiology, these theories converge on a common prediction: production of overflow metabolite occurs only at high glucose uptake rate. Therefore, they offer independent rationales for the emergence of overflow.

One particularly compelling set of theories links overflow metabolism to physical space constraints. Zhuang et al. (Zhuang *et al*, 2011) proposed that acetate overflow in *E. coli* results

from competition for membrane space between glucose transporters and respiratory chain components, forcing cells to favor overflow pathways when membrane space is limiting. Similarly, Szenk et al. (Szenk *et al*, 2017) hypothesized that when the bacterial membrane reaches full occupancy, cells shift from membrane-bound respiratory enzymes to cytosolic overflow pathways to maintain optimal energy production. Other studies suggest that compartment-specific macromolecular crowding also imposes a fundamental limit on how much oxidative metabolism a cell can sustain, potentially driving overflow in bacterial, yeast and mammalian cells (Vazquez & Oltvai, 2016; Vazquez *et al*, 2010; Elsemman *et al*, 2022). Together, these theories position overflow metabolism as a necessary adaptation for maximizing growth under space limitations, though the regulatory mechanisms underlying this shift remain to be identified.

Beyond structural constraints, metabolic economics may also drive overflow metabolism. Basan et al. (Basan *et al*, 2015) argued that bacterial oxidative metabolism, while energy-efficient, demands substantial enzyme investment due to its slow reaction rates, whereas overflow metabolism, though less efficient, requires fewer enzymes. This trade-off between pathway efficiency and enzyme cost could explain the emergence of overflow in *E. coli* (Basan *et al*, 2015). Recently, Kukurugya et al. (Kukurugya *et al*, 2024) suggested that this proteome allocation model may also apply to yeast and mammalian cells, but this remains a topic of active debate (Shen *et al*, 2024).

Another insightful perspective considers global thermodynamic constraints as the driving force behind overflow metabolism. Niebel et al. (Niebel *et al*, 2019) proposed that cells operate within a finite Gibbs energy dissipation rate, meaning that as substrate uptake rates increase, cells must eventually shift from respiration (high dissipation rate) to overflow pathways (low dissipation rate) once their energy dissipation threshold is reached (Niebel *et al*, 2019; Saadat *et al*, 2020). This theory successfully explains production of overflow metabolites in *S. cerevisiae* and *E. coli* cells, but its relevance to mammalian cells remains untested. Furthermore, the biophysical basis of this energy dissipation limit remains to be clarified (Niebel *et al*, 2019; Saadat *et al*, 2020; Losa *et al*, 2022; Yang *et al*, 2021).

All of the aforementioned theories assume that cells have evolved towards optimal growth, a strong assumption that remains controversial (Shen *et al*, 2024; Schuetz *et al*, 2012; Towbin *et al*, 2017; Basan *et al*, 2020; Mori *et al*, 2019). Alternative theories propose that overflow metabolism is not merely a consequence of growth optimization under biophysical constraints but confers broader evolutionary advantages. For instance, ethanol overflow in yeast may be an adaptive strategy to cope with fluctuating oxygen availability (Shen *et al*, 2024), while acetate overflow in *E. coli* may increase the number of offspring cells in nutrient-fluctuating environments (Rabbers *et al*, 2022). Other studies propose that overflow confers a competitive advantage by enabling cells to rapidly consume shared resources before competing species (Rozpędowska *et al*, 2011) or to limit the buildup of toxic reactive oxygen species (Brand, 1997).

Despite these significant advancements, no single theory is accepted as a universal cause of overflow, nor do these theories explicitly incorporate the functioning principles highlighted in this thesis. Notably, none of these models was developed with consideration for the reversibility of overflow pathways, the simultaneous utilization of overflow metabolites with glycolytic substrates, or the potential benefits of overflow metabolites to the producing cells. This raises fundamental questions about whether these theories can fully accommodate the outlined principles.

An alternative theory developed in *E. coli* suggests that thermodynamic gradients between the cells and their environment largely govern overflow metabolism (Enjalbert *et al*, 2017). This theory accurately predicts acetate secretion in *E. coli* in the absence of extracellular acetate and why increasing acetate concentrations can suppress or even reverse the acetate flux. Interestingly, the data presented in this study (Enjalbert *et al*, 2017) suggest that this theory may be applicable to yeast and mammalian cells, though further work is required to test this hypothesis in detail. While local thermodynamic forces are key drivers of flux reversal and co-utilization of overflow metabolites, enzymatic regulation remains equally critical, indicating that overflow metabolism is governed by a multi-layered regulatory system. Strengthening this view, a kinetic model accounting for both enzyme saturation and thermodynamic gradients fails to predict observed phenotypes in *E. coli* unless it also incorporates acetate-driven modulation of glycolytic and TCA cycle activities (Millard *et al*, 2021). This model provided a rationale for growth inhibition by acetate at high glycolytic flux, while also accurately predicting its beneficial effect at low glycolytic flux (Millard *et al*, 2021, 2023). To our knowledge, this is the only model that integrates both the regulation of the overflow pathway and the cellular response to overflow metabolites, two aspects that have historically been treated as separate phenomena. I have validated key predictions of this theory in *E. coli*, and transcriptomics data further supported the proposed regulatory interplay (Millard *et al*, 2021, 2023), though the underlying molecular regulatory network remains to be identified.

Ultimately, no single theory has yet been conclusively validated as a universal explanation for overflow metabolism. Even within a single organism, how these disconnected theories interrelate remains unknown. In an effort to compare existing theories, de Groot et al. (de Groot *et al*, 2020) reformulated multiple constraint-based models into a standardized mathematical framework and found that they all predict overflow metabolism whenever two growth-limiting constraints are reached – though the specific nature of these constraints remains unresolved. Determining whether current theories are mutually exclusive, complementary, or dependent on the organism or environmental conditions will require further studies. Clarifying how these theories align with the outlined principles will also be essential for challenging, refining, and integrating current hypotheses. For instance, the suppression of acetate production by *E. coli* supplemented with just a few millimolar acetate (Enjalbert *et al*, 2017; Millard *et al*, 2021, 2023), without significantly affecting growth, challenges theories asserting that rapid growth is inherently dependent on the production of

overflow metabolites. Similarly, the positive effect of overflow metabolites on growth questions theories that predict only negative impacts. Testing current theories under conditions where overflow metabolites are co-utilized with glycolytic substrates also presents an opportunity to uncover novel metabolic principles, as shown in this thesis.

A comprehensive re-evaluation and integration of the proposed theories, informed by the principles highlighted in this study, will be essential for uncovering the fundamental causes of overflow metabolism, clarifying its role, and understanding its regulation. Only by bridging these gaps can we move toward a unified theory – if one exists – for this widespread phenomenon across all domains of life.

3. References:

Ahn J, Chung BKS, Lee D-Y, Park M, Karimi IA, Jung J-K & Lee H (2011) NADPH-dependent pgi-gene knockout *Escherichia coli* metabolism producing shikimate on different carbon sources. *FEMS Microbiol Lett* 324: 10–16

Alteri CJ & Mobley HL (2012) *Escherichia coli* physiology and metabolism dictates adaptation to diverse host microenvironments. *Curr Opin Microbiol* 15: 3–9

Andreeßen B, Taylor N & Steinbüchel A (2014) Poly(3-Hydroxypropionate): a Promising Alternative to Fossil Fuel-Based Materials. *Appl Environ Microbiol* 80: 6574–6582

Basan M, Honda T, Christodoulou D, Hörl M, Chang Y-F, Leoncini E, Mukherjee A, Okano H, Taylor BR, Silverman JM, *et al* (2020) A universal trade-off between growth and lag in fluctuating environments. *Nature* 584: 470–474

Basan M, Hui S, Okano H, Zhang Z, Shen Y, Williamson JR & Hwa T (2015) Overflow metabolism in *Escherichia coli* results from efficient proteome allocation. *Nature* 528: 99–104

Brand K (1997) Aerobic Glycolysis by Proliferating Cells: Protection against Oxidative Stress at the Expense of Energy Yield.

Brooks GA (2002) Lactate shuttles in Nature. *Biochem Soc Trans* 30

Brown SW, Oliver SG, Harrison DEF & Righelato RC (1981) Ethanol inhibition of yeast growth and fermentation: Differences in the magnitude and complexity of the effect. *Eur J Appl Microbiol Biotechnol* 11: 151–155

Chong H, Yeow J, Wang I, Song H & Jiang R (2013) Improving Acetate Tolerance of Escherichia coli by Rewiring Its Global Regulator cAMP Receptor Protein (CRP). *PLoS ONE* 8: e77422

Christen S & Sauer U (2011) Intracellular characterization of aerobic glucose metabolism in seven yeast species by ^{13}C flux analysis and metabolomics: Flux response to Crabtree effect in yeast species. *FEMS Yeast Res* 11: 263–272

Conway T & Cohen PS (2015) Commensal and pathogenic *Escherichia coli* metabolism in the gut. *Microbiol Spectr* 3: 3.3.24

Dalile B, Van Oudenhove L, Vervliet B & Verbeke K (2019) The role of short-chain fatty acids in microbiota–gut–brain communication. *Nat Rev Gastroenterol Hepatol* 16: 461–478

Demain AL & Adrio JL (2008) Contributions of Microorganisms to Industrial Biology. *Mol Biotechnol* 38: 41–55

Den Besten G, Van Eunen K, Groen AK, Venema K, Reijngoud D-J & Bakker BM (2013) The role of short-chain fatty acids in the interplay between diet, gut microbiota, and host energy metabolism. *J Lipid Res* 54: 2325–2340

Deutscher J (2008) The mechanisms of carbon catabolite repression in bacteria. *Curr Opin Microbiol* 11: 87–93

Diaz CAC, Bennett RK, Papoutsakis ET & Antoniewicz MR (2019) Deletion of four genes in *Escherichia coli* enables preferential consumption of xylose and secretion of glucose. *Metab Eng* 52: 168–177

Eiteman MA & Altman E (2006) Overcoming acetate in *Escherichia coli* recombinant protein fermentations. *Trends Biotechnol* 24: 530–536

Elsemman IE, Rodriguez Prado A, Grigaitis P, Garcia Albornoz M, Harman V, Holman SW, Van Heerden J, Bruggeman FJ, Bisschops MMM, Sonnenschein N, *et al* (2022) Whole-cell

modeling in yeast predicts compartment-specific proteome constraints that drive metabolic strategies. *Nat Commun* 13: 801

Enjalbert B, Millard P, Dinclaux M, Portais J-C & Létisse F (2017) Acetate fluxes in *Escherichia. coli* are determined by the thermodynamic control of the Pta-AckA pathway. *Sci Rep* 7: 42135

Gancedo JM (1998) Yeast Carbon Catabolite Repression. *Microbiol Mol Biol Rev* 62: 334–361

Gaspar P, Neves AR, Ramos A, Gasson MJ, Shearman CA & Santos H (2004) Engineering *Lactococcus lactis* for Production of Mannitol: High Yields from Food-Grade Strains Deficient in Lactate Dehydrogenase and the Mannitol Transport System. *Appl Environ Microbiol* 70: 1466–1474

de Groot DH, Lischke J, Muolo R, Planqué R, Bruggeman FJ & Teusink B (2020) The common message of constraint-based optimization approaches: overflow metabolism is caused by two growth-limiting constraints. *Cell Mol Life Sci* 77: 441–453

Guo Y, Xiong Z, Zhai H, Wang Y, Qi Q & Hou J (2025) The advances in creating Crabtree-negative *Saccharomyces cerevisiae* and the application for chemicals biosynthesis. *FEMS Yeast Res* 25: foaf014

Halmschlag B, Völker F, Hanke R, Putri SP, Fukusaki E, Büchs J & Blank LM (2023) Metabolic engineering of *B. subtilis* 168 for increased precursor supply and poly-γ-glutamic acid production. *Front Food Sci Technol* 3: 1111571

Kim CH (2023) Complex regulatory effects of gut microbial short-chain fatty acids on immune tolerance and autoimmunity. *Cell Mol Immunol* 20: 341–350

Kukurugya MA, Rosset S & Titov DV (2024) The Warburg Effect is the result of faster ATP production by glycolysis than respiration. *Proc Natl Acad Sci* 121: e2409509121

Kumari S, Tishel R, Eisenbach M & Wolfe AJ (1995) Cloning, characterization, and functional expression of acs, the gene which encodes acetyl coenzyme A synthetase in *Escherichia coli*. *J Bacteriol* 177: 2878–2886

Lama S, Kim Y, Nguyen DT, Im CH, Sankaranarayanan M & Park S (2021) Production of 3-hydroxypropionic acid from acetate using metabolically-engineered and glucose-grown *Escherichia coli*. *Bioresour Technol* 320: 124362

Lemberg KM, Gori SS, Tsukamoto T, Rais R & Slusher BS (2022) Clinical development of metabolic inhibitors for oncology. *J Clin Invest* 132: e148550

Liti G, Wardrop FR, Cardinali G, Martini A & Walker GM (2001) Differential responses to antimycin A and expressions of the Crabtree effect in selected Klyuveromyces spp.

Losa J, Leupold S, Alonso-Martinez D, Vainikka P, Thallmair S, Tych KM, Marrink SJ & Heinemann M (2022) Perspective: a stirring role for metabolism in cells. *Mol Syst Biol* 18: e10822

Luli GW & Strohl WR (1990) Comparison of growth, acetate production, and acetate inhibition of *Escherichia coli* strains in batch and fed-batch fermentations. *Appl Environ Microbiol* 56: 1004–1011

Martin VJJ, Pitera DJ, Withers ST, Newman JD & Keasling JD (2003) Engineering a mevalonate pathway in *Escherichia coli* for production of terpenoids. *Nat Biotechnol* 21: 796–802

Martinson JNV & Walk ST (2020) *Escherichia coli* residency in the gut of healthy human adults. *EcoSal Plus* 9: ecosalplus.ESP-0003-2020

Millard P, Enjalbert B, Uttenweiler-Joseph S, Portais J-C & Létisse F (2021) Control and regulation of acetate overflow in *Escherichia coli*. *eLife* 10: e63661

Millard P, Gosselin-Monplaisir T, Uttenweiler-Joseph S & Enjalbert B (2023) Acetate is a beneficial nutrient for *E. coli* at low glycolytic flux. *EMBO J* 42: e113079

Mori M, Marinari E & De Martino A (2019) A yield-cost tradeoff governs *Escherichia coli*'s decision between fermentation and respiration in carbon-limited growth. *Npj Syst Biol Appl* 5: 16

Mulukutla BC, Gramer M & Hu W-S (2012) On metabolic shift to lactate consumption in fed-batch culture of mammalian cells. *Metab Eng* 14: 138–149

Nakamoto S, Kobayashi I, Watanabe K, Kikuta T, Imamura S & Shimada T (2025) Identification of a comprehensive set of transcriptional regulators involved in the long-term survivability of *Escherichia coli* in soil. *Sci Rep* 15: 4279

Niebel B, Leupold S & Heinemann M (2019) An upper limit on Gibbs energy dissipation governs cellular metabolism. *Nat Metab* 1: 125–132

Noh MH, Lim HG, Woo SH, Song J & Jung GY (2018) Production of itaconic acid from acetate by engineering acid-tolerant *Escherichia coli* W. *Biotechnol Bioeng* 115: 729–738

Pérez JC (2021) Fungi of the human gut microbiota: Roles and significance. *Int J Med Microbiol* 311: 151490

Pinhal S, Ropers D, Geiselmann J & de Jong H (2019) Acetate metabolism and the inhibition of bacterial growth by acetate. *J Bacteriol* 201

Potter VR & Reif AE (1952) Inhibition of an electron transport component by antimycin A. *J Biol Chem* 194: 287–297

Raamsdonk LM, Diderich JA, Kuiper A, Van Gaalen M, Kruckberg AL, Berden JA & Van Dam K (2001) Co-consumption of sugars or ethanol and glucose in a *Saccharomyces cerevisiae* strain deleted in the HXK2 gene. *Yeast* 18: 1023–1033

Rabbers I, Gottstein W, Feist AM, Teusink B, Bruggeman FJ & Bachmann H (2022) Selection for Cell Yield Does Not Reduce Overflow Metabolism in *Escherichia coli*. *Mol Biol Evol* 39: msab345

Rathnasingh C (2012) Production of 3-hydroxypropionic acid via malonyl-CoA pathway using recombinant *Escherichia coli* strains. *J Biotechnol*

Rozpędowska E, Hellborg L, Ishchuk OP, Orhan F, Galafassi S, Merico A, Woolfit M, Compagno C & Piškur J (2011) Parallel evolution of the make–accumulate–consume strategy in *Saccharomyces* and *Dekkera* yeasts. *Nat Commun* 2: 302

Saadat N, Nies T, Rousset Y & Ebenhöh O (2020) Thermodynamic Limits and Optimality of Microbial Growth. *Entropy* 22: 277

Schuetz R, Zamboni N, Zampieri M, Heinemann M & Sauer U (2012) Multidimensional optimality of microbial metabolism. *Science* 336: 601–604

Schastnaya E, Doubleday PF, Maurer L, Sauer U (2023) Non-enzymatic acetylation inhibits glycolytic enzymes in *Escherichia coli*.

Shen Y, Dinh HV, Cruz ER, Chen Z, Bartman CR, Xiao T, Call CM, Ryseck R-P, Pratas J, Weilandt D, *et al* (2024) Mitochondrial ATP generation is more proteome efficient than glycolysis. *Nat Chem Biol*

Snoeck S, Guidi C & De Mey M (2024) "Metabolic burden" explained: stress symptoms and its related responses induced by (over)expression of (heterologous) proteins in *Escherichia coli*. *Microb Cell Factories* 23: 96

Szenk M, Dill KA & de Graff AMR (2017) Why Do Fast-Growing Bacteria Enter Overflow Metabolism? Testing the Membrane Real Estate Hypothesis. *Cell Syst* 5: 95–104

Towbin BD, Korem Y, Bren A, Doron S, Sorek R & Alon U (2017) Optimality and sub-optimality in a bacterial growth law. *Nat Commun* 8: 14123

Vazquez A, Liu J, Zhou Y & Oltvai ZN (2010) Catabolic efficiency of aerobic glycolysis: The Warburg effect revisited. *BMC Syst Biol* 4: 58

Vazquez A & Oltvai ZN (2016) Macromolecular crowding explains overflow metabolism in cells. *Sci Rep* 6: 31007

Warburg VO (1924) Ober den Stoffwechsel der Carcmomzelle j.

Weimer A, Pause L, Ries F, Kohlstedt M, Adrian L, Krömer J, Lai B & Wittmann C (2024) Systems biology of electrogenic *Pseudomonas putida* - multi-omics insights and metabolic engineering for enhanced 2-ketogluconate production. *Microb Cell Factories* 23: 246

Xu J-Z, Ruan H-Z, Yu H-B, Liu L-M & Zhang W (2020) Metabolic engineering of carbohydrate metabolism systems in *Corynebacterium glutamicum* for improving the efficiency of l-lysine production from mixed sugar. *Microb Cell Factories* 19: 39

Yang J & Guo L (2014) Biosynthesis of β-carotene in engineered *E. coli* using the MEP and MVA pathways. *Microb Cell Factories* 13: 160

Yang X, Heinemann M, Howard J, Huber G, Iyer-Biswas S, Le Treut G, Lynch M, Montooth KL, Needleman DJ, Pigolotti S, *et al* (2021) Physical bioenergetics: Energy fluxes, budgets, and constraints in cells. *Proc Natl Acad Sci* 118: e2026786118

Yasir M, Thomson NM, Turner AK, Webber MA & Charles IG (2024) Overflow metabolism provides a selective advantage to *Escherichia coli* in mixed cultures. *Ann Microbiol* 74: 15

Zhu L, Zhang J, Yang J, Jiang Y & Yang S (2022) Strategies for optimizing acetyl-CoA formation from glucose in bacteria. *Trends Biotechnol* 40: 149–165

Zhuang K, Vemuri GN & Mahadevan R (2011) Economics of membrane occupancy and respiro-fermentation. *Mol Syst Biol* 7: 500

Annexes

Annex 1: MultiNMRFit: A software to fit 1D and pseudo-2D NMR spectra

Pierre Millard[1,2,*], Loïc Le Grégam[1,2], Svetlana Dubiley[1], Thomas Gosselin-Monplaisir[1], Guy Lippens[1], Cyril Charlier[1,*]

[1]Toulouse Biotechnology Institute (TBI), Université de Toulouse, CNRS, INRA, INSA, Toulouse, 31077, France

[2]MetaToul-MetaboHUB, National Infrastructure of Metabolomics and Fluxomics, Toulouse, 31077, France

Summary. Nuclear Magnetic Resonance (NMR) is widely used for quantitative analysis of metabolic systems. Accurate extraction of NMR parameters – such as chemical shift, intensity, coupling constants, and linewidth – is essential for obtaining information on the structure, concentration, and isotopic composition of metabolites. We present MultiNMRFit, an open-source software designed for high-throughput analysis of one-dimensional NMR spectra, whether acquired individually or as pseudo-2D experiments. MultiNMRFit extracts signal parameters by fitting the experimental spectra using built-in or user-defined signal models that account for multiplicity, providing high flexibility along with robust and reproducible results. The software is accessible both as a Python library and via a graphical user interface, enabling intuitive use by end-users without computational expertise. We demonstrate the robustness and flexibility of MultiNMRFit on datasets collected in metabolomics and isotope labeling studies.

Availability and Implementation. MultiNMRFit is implemented in Python 3 and was tested on Unix, Windows, and MacOS platforms. The source code and the documentation are freely distributed under GPL3 license at https://github.com/NMRTeamTBI/MultiNMRFit/.

Supplementary data. Supplementary data are available online.

Contact. Cyril Charlier (charlier@insa-toulouse.fr) and Pierre Millard (millard@insa-toulouse.fr)

1. Introduction

Nuclear Magnetic Resonance (NMR) spectroscopy is a powerful tool for investigating metabolism. Key applications include identifying and quantifying metabolites in metabolomics, determining the isotopic content of metabolites in ^{13}C-fluxomics, and identifying and characterizing protein-metabolite interactions [1–4]. Extracting meaningful information from NMR spectra requires precise characterization of each signal of interest, including their position (chemical shift), intensity (and area) and shape (coupling constants and linewidth) [5]. Signal parameters can be estimated by fitting spectra using various mathematical models that relate these parameters to the observed signals. This fitting step is often achieved with in-house scripts, which can be error-prone and lack the robustness and reproducibility necessary for comprehensive NMR studies of metabolic systems. Commercial software, such as TopSpin (Bruker) and Mnova (Mestrelab), are also available for this purpose, but these tools are limited to a few signal models and function as proprietary “black boxes”. Although open-source R and Python packages (such as *MetaboDecon1D* [6] and *BATMAN* [7,8]) have been developed, they are primarily designed for programmatic use and lack features essential for accessible and reproducible NMR data analysis by users without computational expertise. Such features include statistical methods for calculating confidence intervals for extracted parameters, a graphical user interface, and a logging system to save calculation parameters and process information along with the results. Furthermore, most existing tools treat each peak as an independent signal. However, in NMR, a single nucleus often provides signals comprising multiple peaks due to homo- and heteronuclear scalar couplings. These couplings are intrinsic properties of NMR signals and are crucial for identifying metabolites and quantifying their isotopic content. Signal multiplicity can also be leveraged to improve parameters estimation in case of overlapping peaks. Unfortunately, virtually none of the existing spectral processing tools account for multiplicity, making it challenging to extract and utilize this information effectively. As a result, the detailed analysis of NMR spectra remains a low throughput task, typically performed by expert users. This limitation also restricts the analysis of large datasets generated for instance in real-time NMR experiments. The lack of user-friendly, open-source software that accounts for signal multiplicity and allows for the flexible implementation of tailored signal models significantly hampers the scope, throughput, and reproducibility of NMR-based metabolic studies.

To address these challenges, we have developed MultiNMRFit, a versatile Python software for fitting one dimensional NMR spectra, whether acquired individually or as pseudo-2D datasets in time-course experiments. MultiNMRFit can be applied to any nucleus (^{1}H, ^{13}C, ^{15}N, ^{31}P, etc), any type of 1D or pseudo-2D NMR experiment, and any type of signal. MultiNMRFit includes built-in signal models for common multiplets and is easily extendable with user-defined models to process less conventional signals. MultiNMRFit is accessible both as a Python library and via a graphical user interface, allowing biologists without computational expertise to use it effectively. We demonstrate the robustness of MultiNMRFit on synthetic data and through its application to real-time metabolomics and isotope labeling experiments.

2. Methods and implementation

The general workflow of MultiNMRFit is shown in Figure 1. MultiNMRFit is a Python-based library that operates within common web browsers via a Streamlit-powered graphical user interface. Users can load 1D and pseudo-2D Bruker spectra pre-processed beforehand (*i.e.* referenced, phase-corrected and baseline-corrected). Spectra can also be provided as text files containing chemical shifts and intensities. MultiNMRFit performs automated peak picking within a specified spectral region, and users can add additional peaks manually. One or several peaks can then be grouped into a signal, and a model must be selected for each signal. As detailed in the next section, each model contains equations to simulate the corresponding signal based on parameters. MultiNMRFit automatically suggests a list of models based on the number of peaks (e.g., *doublet of doublet* and *quartet* for clusters containing four peaks) and initializes parameters based on the peak list. Note that a given peak can be included in multiple signals to account for overlapping peaks. For spectrum fitting, parameters p are estimated by minimizing the cost function $c(p)$, which is defined as the sum of squared residuals between the experimental intensities (a_i) and the values simulated by the model $y_i(p)$:

$$c(p) = \sum_i (a_i - y_i(p))^2$$

The cost function is minimized using the L-BFGS-B method [9], with an optional initial refinement step performed by the differential evolution algorithm [10]. Standard deviations

on parameters are estimated from the covariance matrix. For batch processing of multiple spectra, users can select a spectrum as reference to automatically initialize signals and parameters values for the next spectra, thereby automating the processing of several spectra for high-throughput analysis. Finally, MultiNMRFit provides a range of interactive plots for visual inspection of fitting results, and results can be exported as *csv* files containing *(i)* parameters values (with their confidence intervals) and *(ii)* chemical shifts and intensities of experimental and fitted spectra.

The complete process is automatically saved as a pickle file, which can be reloaded in MultiNMRFit to continue prior work or reanalyze calculation results. This file can also be shared, enabling collaborative analysis across multiple users and ensuring reproducibility. Detailed usage of MultiNMRFit can be found in the online documentation (https://MultiNMRFit.readthedocs.io).

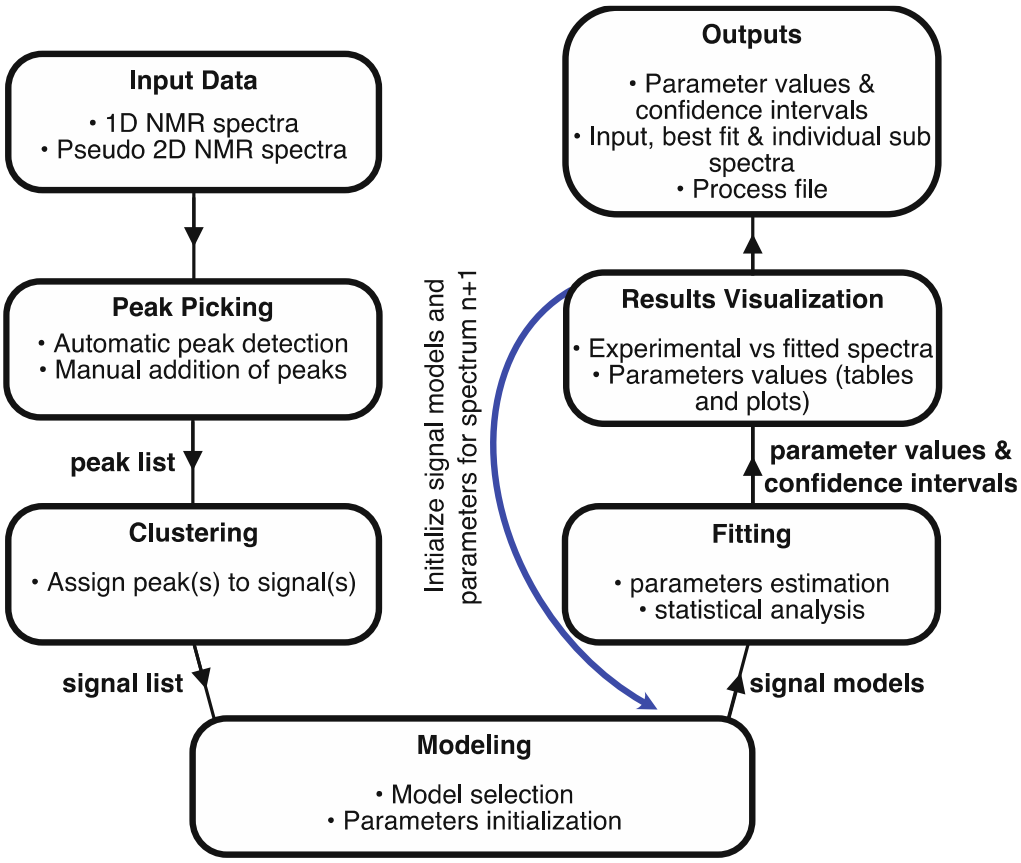


Figure 1. Flow chart of MultiNMRFit.

3. Signal models

A signal model consists of *(i)* equations that describe signal intensity as a function of chemical shift (used for simulations) and *(ii)* a list of parameters with their default values and bounds (used for optimization). Various mathematical functions, including Lorentzian, Gaussian, and Voigt functions, can be used to simulate the NMR spectrum of a given signal. For example, the intensity y_i of a doublet at chemical shift x_i can be described using the following Gaussian function:

$$y_i = I/2 \cdot \left(e^{-(x_i - x_0 + J/2)^2 / (2 \cdot {l_w}^2)} + e^{-(x_i - x_0 - J/2)^2 / (2 \cdot {l_w}^2)} \right)$$

with parameters x_0 (chemical shift of the signal), I (total signal intensity), J (coupling constant), and l_w (linewidth at half maximum). An NMR spectrum containing multiple signals can be simulated by summing the spectra of individual signals.

By default, MultiNMRFit provides mixed Gaussian-Lorentzian models for common multiplets, including singlet, doublet, triplet, doublet of doublet, and quadruplet. Advanced users can create custom models to handle less conventional signals, such as signals with other coupling patterns or described using alternative mathematical functions. A model template is included with MultiNMRFit for this purpose, and a tutorial on model construction is available in the documentation.

4. Validation and application to metabolomics and isotopic datasets

We validated MultiNMRFit using synthetic datasets (Supplementary data). Results confirm the capability of the software to handle complex spectral data and deliver robust parameter

estimation even under challenging conditions (such as low signal-to-noise ratio or significant signal overlaps).

Then, we used MultiNMRFit to monitor the dynamic conversion of glucose through the initial steps of glycolysis. Glucose was added to a buffer solution containing TSP (used as internal standard), ATP and the first three enzymes of glycolysis: glucokinase, glucose-6-phosphate isomerase, and phosphofructokinase (Figure 2A, Supplementary data). The time-course concentrations of glucose (GLC), glucose-6-phosphate (G6P), fructose-6-phosphate (F6P), fructose-1,6-bisphosphate (FBP), ATP and ADP were monitored in real-time using a pseudo-2D experiment consisting in 1024 1D ^{1}H spectra. All signal parameters were accurately extracted, including for overlapped signals of ADP and ATP (Figure 2B). The integrals of signals specific to each metabolite were normalized to the TSP signal (Figure 2C). A progressive decrease in GLC concentration was observed, accompanied by a transient accumulation of G6P and F6P, which were eventually converted into FBP. The high precision and resolution on the estimated dynamics illustrate the value of MultiNMRFit for high-throughput processing of large datasets, with the relative concentrations of the six metabolites of interest quantified in less than three hours for the 1024 spectra.

MultiNMRFit can also exploit the multiplicity resulting from the presence of isotopes in metabolites to quantify their isotopic content – a key capability for applications such as detecting counterfeit chemicals, identifying metabolic pathways, and quantifying metabolic fluxes. To demonstrate this, we conducted a ^{13}C-isotope labeling experiment by growing *Escherichia coli* on a mixture of glucose (15 mM, 80% 1-$^{13}C_1$-glucose + 20% U-$^{13}C_6$-glucose) and acetate (8 mM, 100% 2-$^{13}C_1$-acetate), and we collected samples each hour to quantify the dynamics of all isotopic forms of acetate (Supplementary data). In the ^{1}H NMR spectra, the methyl protons of acetate may give raise to nine peaks corresponding to the four isotopic species of this compound: a singlet for $^{12}C_2$-acetate, a doublet with a small (6 Hz) ^{2}J coupling constant for 1-$^{13}C_1$-acetate, a doublet with a large (127 Hz) ^{1}J coupling constant for 2-$^{13}C_1$ acetate, and a doublet of doublet for U-$^{13}C_2$-acetate. The results showed that the total acetate concentration remained stable throughout the experiment (8.5±0.1 mM), which could be interpreted as an acetate flux close to zero. However, while the provided isotopic form (2-$^{13}C_1$-acetate) initially represents 99% of the total acetate pool, its concentration decreased over time (from 8.5 to 6.5 mM). Concurrently, the concentration of the other labeled forms

(derived from glucose) increased (from 0.1 to 1.9 mM). In agreement with previous findings [12], these results confirm that acetate is continuously exchanged between cells and their environment, even in the absence of net acetate accumulation in the medium. Overall, this demonstrates the applicability of MultiNMRFit for extracting quantitative isotopic information on metabolites, providing meaningful biological insights.

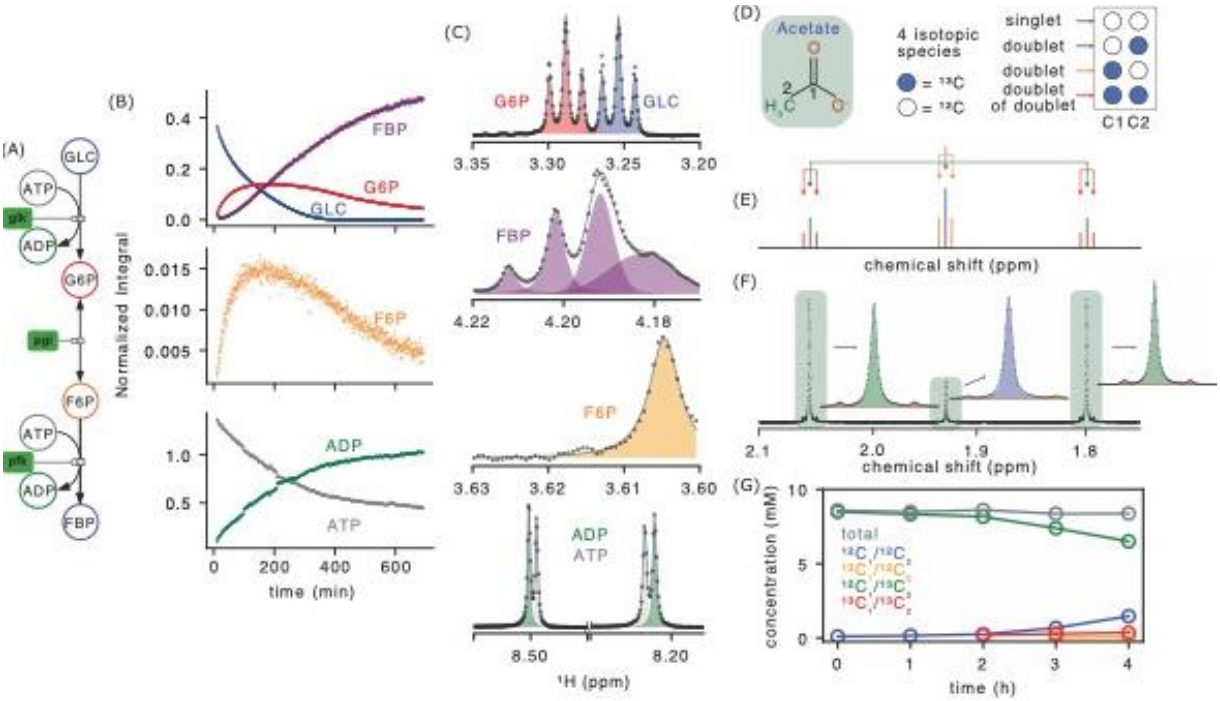


Figure 2. Applications of MultiNMRFit to metabolomics and isotope labeling studies. (A) Scheme of the biochemical reactions monitored in a real-time NMR experiment. **(B)** Dynamic of integrals of glucose (GLC, blue), glucose-6-phosphate (G6P, red), fructose-6-phosphate (F6P, orange), fructose-1,6-bisphosphate (FBP, purple), adenosine triphosphate (ATP, gray), and adenosine diphosphate (ADP, green). Integrals were normalized with the TSP signal. **(C)** Examples of signals processed with MultiNMRFit for each molecule of interest, where individual signals are shown by the shaded areas and the experimental and fitted spectra are represented by dots and lines, respectively. **(D)** Isotopic forms of acetate. **(E)** Theoretical ^{1}H spectrum of the methyl protons of acetate, with a singlet for $^{12}C_2$-acetate (blue), a doublet for 1-$^{13}C_1$-acetate (orange), a doublet for 2-$^{13}C_1$ acetate (green), and a doublet of doublet for U-$^{13}C_2$-acetate (red). **(F)** Example of spectrum processed with MultiNMRFit with the experimental spectrum shown as dots, the fitted spectrum as a line, and individual signals as shaded areas. **(G)** Time-course concentrations of the four isotopic forms of acetate (using the color code shown in panel E) and of the total acetate concentration (in grey).

Conclusion

We present MultiNMRFit, an open-source Python software designed to extract detailed quantitative parameters from NMR spectra. MultiNMRFit is applicable to spectra acquired from any nucleus, whether as 1D or pseudo-2D spectra, and can handle any type of multiplicity through a flexible system for implementing NMR signal models. MultiNMRFit is accessible to non-expert users through a graphical user interface and can also be used as a Python package, enabling seamless integration into metabolomics and fluxomics workflows.

Acknowledgements

We thank Marin Martin Mawah, Pauline Rouan and Dr. Valeria Gabrielli for testing previous versions of the software and for insightful discussions. We thank Dr. Edern Cahoreau and Lindsay Peyriga (MetaToul, Toulouse metabolomics & fluxomics facilities, www.metatoul.fr) for access to NMR facilities. MetaToul is part of MetaboHUB, the French National Infrastructure for Metabolomics and Fluxomics (www.metabohub.fr). This work was supported by a French government grant managed by the Agence Nationale de la Recherche under the Investissements d'Avenir program, reference ANR-18-EURE-0021.

Author contributions

PM & **CC** Software, Project administration, Supervision, Conceptualization, Writing - review & editing; **LL** Software**; SD** & **TM** Resources; **GL** Conceptualization, Writing - review & editing.

Competing interests

The authors declare that they have no conflict of interest.

References

[1] K.M. Koczula, C. Ludwig, R. Hayden, L. Cronin, G. Pratt, H. Parry, D. Tennant, M. Drayson, C.M. Bunce, F.L. Khanim, U.L. Günther, Metabolic plasticity in CLL: adaptation to the hypoxic niche, Leukemia 30 (2016) 65–73. https://doi.org/10.1038/leu.2015.187.

[2] S. Moco, Studying Metabolism by NMR-Based Metabolomics, Front. Mol. Biosci. 9 (2022) 882487. https://doi.org/10.3389/fmolb.2022.882487.

[3] S. Nargund, M.E. Joffe, D. Tran, V. Tugarinov, G. Sriram, Nuclear Magnetic Resonance Methods for Metabolic Fluxomics, in: H.S. Alper (Ed.), Systems Metabolic Engineering, Humana Press, Totowa, NJ, 2013: pp. 335–351. https://doi.org/10.1007/978-1-62703-299-5_16.

[4] M. Diether, Y. Nikolaev, F.H. Allain, U. Sauer, Systematic mapping of protein-metabolite interactions in central metabolism of *Escherichia coli*, Molecular Systems Biology 15 (2019) e9008. https://doi.org/10.15252/msb.20199008.

[5] A.S. Edison, M. Colonna, G.J. Gouveia, N.R. Holderman, M.T. Judge, X. Shen, S. Zhang, NMR: Unique Strengths That Enhance Modern Metabolomics Research, Anal. Chem. 93 (2021) 478–499. https://doi.org/10.1021/acs.analchem.0c04414.

[6] M. Häckl, P. Tauber, F. Schweda, H.U. Zacharias, M. Altenbuchinger, P.J. Oefner, W. Gronwald, An R-Package for the Deconvolution and Integration of 1D NMR Data: MetaboDecon1D, Metabolites 11 (2021) 452. https://doi.org/10.3390/metabo11070452.

[7] J. Hao, W. Astle, M. De Iorio, T.M.D. Ebbels, BATMAN—an R package for the automated quantification of metabolites from nuclear magnetic resonance spectra using a Bayesian model, Bioinformatics 28 (2012) 2088–2090. https://doi.org/10.1093/bioinformatics/bts308.

[8] J. Hao, M. Liebeke, W. Astle, M. De Iorio, J.G. Bundy, T.M.D. Ebbels, Bayesian deconvolution and quantification of metabolites in complex 1D NMR spectra using BATMAN, Nat Protoc 9 (2014) 1416–1427. https://doi.org/10.1038/nprot.2014.090.

[9] R.H. Byrd, P. Lu, J. Nocedal, C. Zhu, A Limited Memory Algorithm for Bound Constrained Optimization, SIAM J. Sci. Comput. 16 (1995) 1190–1208. https://doi.org/10.1137/0916069.

[10] R. Storn, K. Price, Simple and Efficient Heuristic for global Optimization over Continuous Spaces, Journal of Global Optimization 11 (1997) 341–359. https://doi.org/10.1023/A:1008202821328.

[11] N. Cox, P. Millard, C. Charlier, G. Lippens, Improved NMR Detection of Phospho-Metabolites in a Complex Mixture, Anal. Chem. 93 (2021) 4818–4824. https://doi.org/10.1021/acs.analchem.0c04056.

[12] B. Enjalbert, P. Millard, M. Dinclaux, J.-C. Portais, F. Létisse, Acetate fluxes in *Escherichia coli* are determined by the thermodynamic control of the Pta-AckA pathway, Sci Rep 7 (2017) 42135. https://doi.org/10.1038/srep42135.

Annex 2: Acetate promotes *Escherichia coli* metabolic adaptation

Lucas Devlin[a], Virginia Oudard[a], Manon Barthe[a], Thomas Gosselin-Monplaisir[a], Muriel Cocaign-Bousquet[a], Pierre Millard[a] and Brice Enjalbert[a#]

a. TBI, Université de Toulouse, CNRS, INRAE, INSA, Toulouse, France.

Author to whom correspondence should be addressed: Brice Enjalbert. E-Mail: brice.enjalbert@insa-toulouse.fr

Abstract:

Acetate is the most classic fermentation product of *Escherichia coli*. This overflow metabolite has long been described as a toxic compound for this model bacterium, albeit this perception was recently questioned. Here we demonstrate that acetate promotes the adaptation of *E. coli* when faced with a carbon substrate change. As low as 0.1 mM acetate is sufficient to reduce lag phase by several hours. This acetate is very early consumed through the acetyl-coA synthetase Acs. Metabolomic analysis proved that the small amount of acetate allows to replenish metabolic pools in the TCA cycle and the upper glycolysis, without detectable change in the cell energetic level. Finaly, single cell analysis revealed that acetate increases the fraction of cells able to switch to the new substrate. We conclude that excreted acetate is used by E. coli to facilitate metabolic adaptation by replenishing key metabolite pools such as Acetyl-CoA. This work sheds a new light on an unexpected role of acetate in the adaptation of *E. coli*, providing a brand-new understanding of the overflow metabolism.

Keywords: Acetate / Overflow / Adaptation / Metabolic transition / *Escherichia coli* / Sub-populations.

Running title: Acetate promotes Escherichia coli metabolic adaptation

Introduction

The life of microorganism such as the model Gram negative bacterium *Escherichia coli* is made of feast and famine, with short periods of substrate abundances and long periods of starvation. Metabolic adaptation, defined here as the capacity to alternate substrates, is a key feature to ensure the competitivity and hence survival of the species. Three main situations could necessitate this metabolic adaptation. The first is a resuming of growth after a period of arrest (i.e, when a carbon source is again available after a transient shortage). The second case is when the cells are transferred from one medium to another with a different carbon source. The third is the diauxic transition, when cells are growing on a mix of carbon substrates and sequentially consume them, requiring metabolic adaptation before using the next preferred resource. A transient growth arrest, the so-called lag plase, is generally observed during these adaptations (Madar Alon 2013, Moreno-Gamez Ackermann 2020). It was long considered as the amount of time required for the cells to reorganize their metabolism from one substrate to another (REF Monod). The recent emergence of single cell approaches has led to a new conception with lag being the time necessary for a subpopulation of adapted cells to emerge (Simsek Kim 2019 ; Moreno-Gamez Ackermann 2020). The matter is still subject to speculations (Heinemann Sauer 2020, Barthe Enjalbert 2020, Basan Sauer 2020).

Many processes are set up when the growth is stopped. First, there is an early drop in most central carbon metabolites (Enjalbert Portais 2013, Basan Sauer 2020). The stringent response is triggered by ppGpp (Chatterji and Kumar Ojha, 2001; Braeken et al., 2006; Potrykus and Cashel, 2008; Hauryliuk et al., 2015) and the pool of ribosomes is maintained but translationally inactive (Kohanim Alon 2018; Li Gitai 2018; Mori Hwa 2017). Energetic reserves such as ATP decrease (Morin Enjalbert 2017, Pu Bai 2019). Many works have explored the mechanisms dictating the resuming of growth and hence, the duration of lags, albeit seldom with matching conclusions. First, lag time appear to depend on specialized transcriptional factor to grow on the new substrate (Barthe Enjalbert 2020, Madar Alon 2013, Kaiser van Nimwegen 2018). Higher respiratory activity was proposed to reduce the lag duration albeit at the expense of the growth rate (Fuentes Zampieri 2021). These same authors also suggested valine, leucine and isoleucine to play a crucial role during the initial growth of bacteria after starvation (Fuentes Zampieri 2021). ATP-dependent protein disaggregation was

also reported to determine the lag time for bacterial regrowth (Pu Bai 2019). The reserve sugar glycogen has been described too as a key parameter in this process (Yamamotoya Matsuno 2012, Morin Enjalbert 2017, Sekar Sauer 2020). Carbon influx rate before the shift was proposed as a main determinant of lag duration (Basan Sauer 2020).

Acetate is produced by *E. coli* when the glycolytic flux is high such as during the growth on glucose. This mechanism is called metabolic overflow. While this production could be perceived as a loss of carbon, it is observed for most cells albeit with different small carbon molecules production (for examples, ethanol with yeast or lactate with mammal strains. After *E. coli* growth on glucose, a diauxic transition could be observed with the cell rerouting their metabolism toward acetate. This has become a classic condition for dynamic modelling efforts. However, a catabolic consumption of acetate with no growth is observed if the amount of acetate per cell is insufficient and the growth resuming could be prone to heterogeneity in the population. This led to question not only why *E. coli* secretes acetate but also why it is consumed without obvious benefit for the cells.

Here, we first compared the dynamic of diauxic transitions versus switching the cells between substrates. We found out that the former is faster and proved that this is not due to the mere presence of the second substrate during the diauxic shift but to the presence of acetate. Acetate was found out to efficiently reduced the lag even at concentrations hundred times lower than what the cell produces. We explore and discuss in this paper the metabolic reasons behind this newly described phenomenon, as well as its importance on *E. coli* lifestyle.

Results

Diauxic shift is faster than switch

Two experimental models are classicaly used to study metabolic adaptation, defined here as the capacity to change between two carbonated substrates : the diauxic shift where the cells grow in presence of both substrates and alternate when the prefered one is exhausted, and the switch where the cells are articifially moved from the first substrate medium to the second one. We compared the adaptive capacity, i.e the lag time, when cells have to change of carbon

substrate in both models. The experimental condition was the glucose to xylose transition as previously used (Barthe et al., 2020). Adaptation to xylose was impaired using plasmids with different copy numbers and carrying the xylA promoter, hence resulting in the titration of the xylose-specific transcriptional factor XylR and so longer lag times (Figure 1a). In these conditions, we observed that the lags are always significantly longer for the switches than for the diauxic transitions (in average, -45% ±25). The most obvious reason could have been a stress of the cells during the switch steps, but no lag at all were observed when the population is switched from glucose to glucose (data not shown). Our next hypothesis is that the presence of the second substrate during the first diauxic growth is somehow priming the cells to its following use. To challenge this hypothesis, we grew *E. coli* on a mix of glucose and xylose then switched the cells still growing on glucose to xylose (Figure 1a). This showed a moderate and non-significative benefit on the lag (in average, -11% ±11). We also found out through transcriptomic and cytometry approaches that the presence of xylose during growth on glucose has only a moderate and non-conclusive effect (Supp. Figure 1a and 1b). To know is the adaptive difference between switch and diauxie is a global population effect or is limited to a fraction of the cell, we used a pBR322 titration plasmid expressing a fluorescent reporter under control of the xylA promoter (Figure 1b and 1c). While the growth is performed here in well-controled bioreactor (Figure 1b), the same differences in lag time were observed than in the microplate system used for Figure 1a. Surprisingly, we observed that cells start to express the xylose-consumption reporter at the same time in both conditions. However, the rate of appearance of adapted cells is faster in the diauxic model than in the switch. We conclude that a compound other than xylose has to be present before glucose exhaustion to promote the diauxic adaptation and that the lost of this compound during the switch reduces the cells ability to use the xylose.

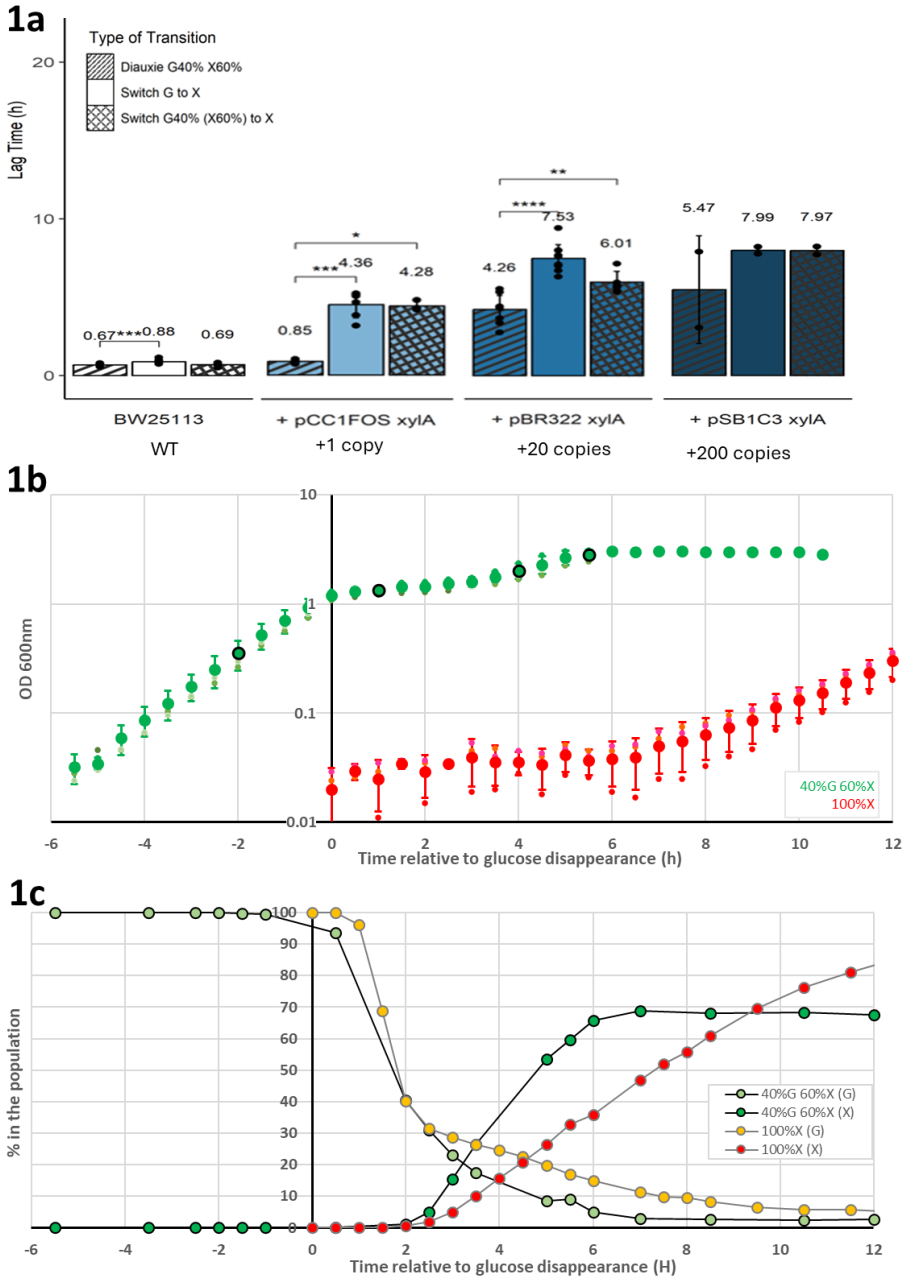


Figure 1: Glucose to xylose adaptation is faster during diauxic shift than artificial switch. 1A. lag times of *E. coli* strains with different degree of adaptation impairment. Resuming of growth on xylose is impaired by titration of the XylR factor with plasmids containing the XylR fixation sites from the *xylA* promoter (Barthe *et al*., 2020). BW25113 strain is the wild type without titration. Titration is created with different plasmids carrying the *xylA* promoter (pCC1FOS, pBR322 and pSB1C3). Expected copy number are indicated on the figure. First column of each series is the diauxic transition on a mix of glucose and xylose, second is the switch from glucose exponential phase to xylose, third is the switch from glucose exponential phase in presence of xylose to xylose alone. **1B**. Growth of the BW25113 strain carrying the pBR322-based titration plasmid in diauxic conditions (green) or artificial switch (red). Time 0 is set up on glucose exhaustion for the diauxie or the time of switch. **1C**. Cellular cytometric profiles during experiment 1B. The *xylA* promoter carried on the pBR322 plasmid is driving the expression of the red florescent reporter mRFP1. Fluorescent cells (i.e, metabolizing xylose) are defined as

"X" type (dark green for the diauxic shift, red for the switch), non-fluorescent cells are defined as "G" type (light green for the diauxic shift, yellow for the switch).

Acetate promotes metabolic adaptation.

Given the previous observations, we hypothesized that acetate could be the compound improving adaptation. Indeed, acetate is produced during the growth on glucose (ref) and so present during the diauxic growth and lost when the cells are switched on a fresh medium. We therefore tested if acetate addition in the new substrate medium reduces the lag time (Figure 2). Three conditions were selected : the previous glucose-xylose switch with the XylR-titrated strain (WT pBR322 on figure 2), but also galactose to fucose and or N-acetaylglucosamine (NAG) to malate models (two conditions known to present important lags for the wild type strain ; Devlin et al., xxx). When mimicking the quantity of acetate present in diauxic experiment (circum 2 mM), we observed an important reduction by half of the lag in comparison to the control without acetate addition for the three models (Figure 2). We then assessed the minimal quantity to observed this positive effect. Surprisingly, as low as 250 µM acetate is sufficient to obtain a significant effect and increasing the acetate concentration does not clearly further improved metabolic adaptation. The same results were observed in microplate and flask experiments (Supp. Figure 2). We conclude that acetate is indeed a booster of metabolic adaptation, even at very low concentration by far insufficient to promote growth.

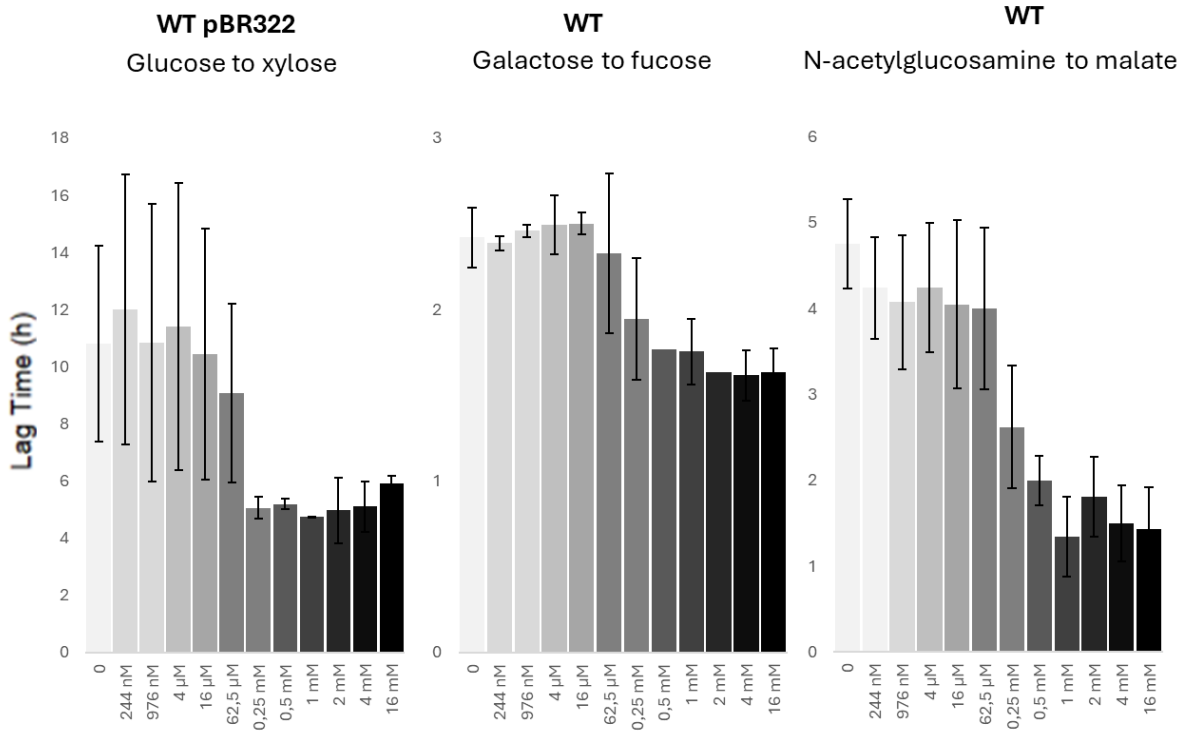


Figure 2: acetate promotes metabolic adaptation. Strain BW25113 carrying the titration plasmid pBR322 *PxylA*-mTagBFP was switched from glucose to xylose (left graph). Wild type BW25113 was switched from galactose to fucose (mid graph) or from N-acetylglucosamine to

malat (right part). 0 to 16 mM acetate was added in the second medium before adding the cells.

Acetate facilitates individual cells switch toward the next-substrate

Since the adaptation appears as heterogeneous (Figure 1c), we next explore the way acetate promotes adaptation in the cells population. The galactose-fucose switch was choosen since we previously validated a reporter fosmid rendering for fucose consumption in individual cells (Devlin *et al. xxx*). Using flow cytometry, we found out that acetate improved the speed of appearance of fucose comsumming cells, with a situation 60 min after the switch from galactose to fucose matching these at 120 min without acetate. This confirms the previous results from figure 1c and demonstrates that acetate is improving the fraction of cells able to adapt to the next substrate.

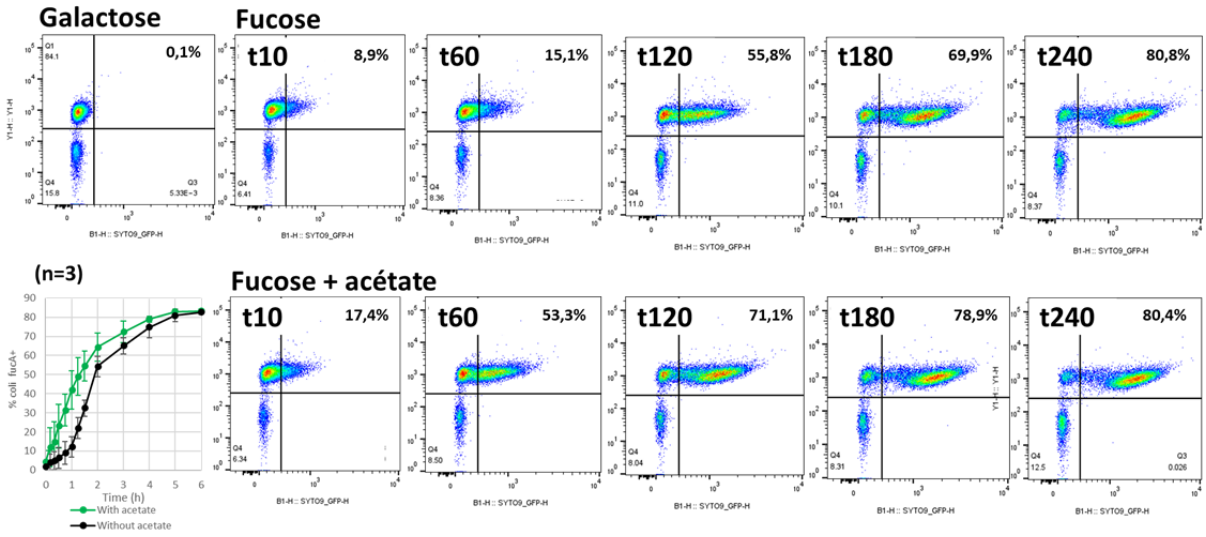


Figure 3: cytometric profile of BW25113 pCC1FOS *PfucA*-mNeonGreen *Pj23119*-mScarlet cells switched from galactose to fucose without (top lane) **or with** (bottom lane)**.** Cells distributions are represented in two dimensions (x-axis: green fluorescence from inducible mNeonGreen; y-axis: pink fluorescence from constitutive mScarlet). Upper left quadrant encompassed “galactose signature” cells, upper right lasso for the “fucose signature cells, lower left quadrant for artefacts and cells having lost the plasmid. A graph summarizing the results from three independent experiments is provided.

Acetate is early consumed during metabolic adaptation.

Since acetate boost the early adaptation to the new substrate, we investigated the timing of its consumption. For this, we measured the evolution of extracellular metabolites by NMR after the switch. The NAG to malate switch was chosen here as it presents longer lags for the wild type strain (Figure 4). We observed that acetate is readily consumed in the first hours

after the switch, well before cells resume and observable growth. Increasing the inoculate size of cells from an initial OD of 0.1 to 0.6 ended up in the 0.5 mM acetate consumption in less than 30 minutes but nonetheless a dramatic reduction of the lag time from 16.47 h to 3.57 h. Increasing the acetate concentration in the new medium from 0.5 to 3 mM improved further this lag time to 1.09 h, meaning that the ratio between acetate amount and cells quantity is important.

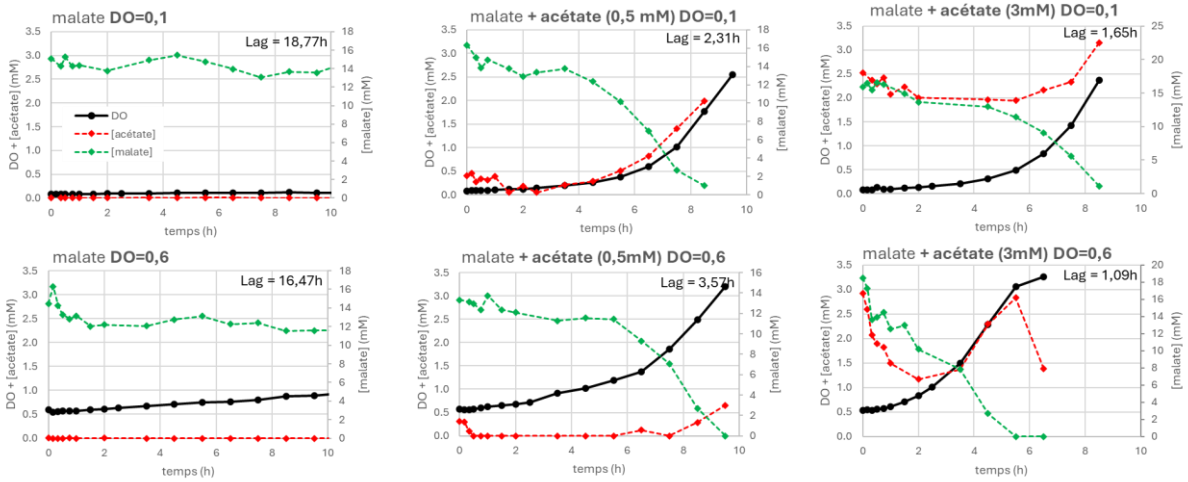


Figure 4: extracellular metabolites during switches from N-acetylglucosamine to malate. Biomass (Optical Density; black dot), acetate concentrations (red dots) and malate concentrations (green dots) are plotted against the time. Upper lane: inoculation at OD 0.1. Lower lane: inocaulation at OD 0.6. Left graph: no acetate addition in the malate medium. Mid graph: switch to malate plus 0.5 mM acetate. Right graph: switch to malate plus 3 mM acetate.

The acetyl-coA synthetase gene acs is essential to the acetate booster effect.

We next wondered about the metabolic pathway involved in the acetate consumption. The PTA-ACKA pathway (Figure 5) has previously been demontrated to be central to acetate production and consumption (Enjalbert *et al,* 2017), raising questions about the fonction of the alternative ACS pathway. We thus challenged the booster effect of acetate during the NAG to malate adaptation in mutants of these pathways. The results clarly showed that only the *acs* loss of function abolished the booster effect of acetate (Figure 5). Acs presents a higher affinity for acetate than the PTA-ACKA pathway (ref) and it has been previously described as induced after glucose exhaustion (Enjalbert *et al*., 2013 & 2015). Our finding are thus attributing a clear role to Acs in the early consumption of small amount of acetate to improve metabolic adaptation to a new substrate.

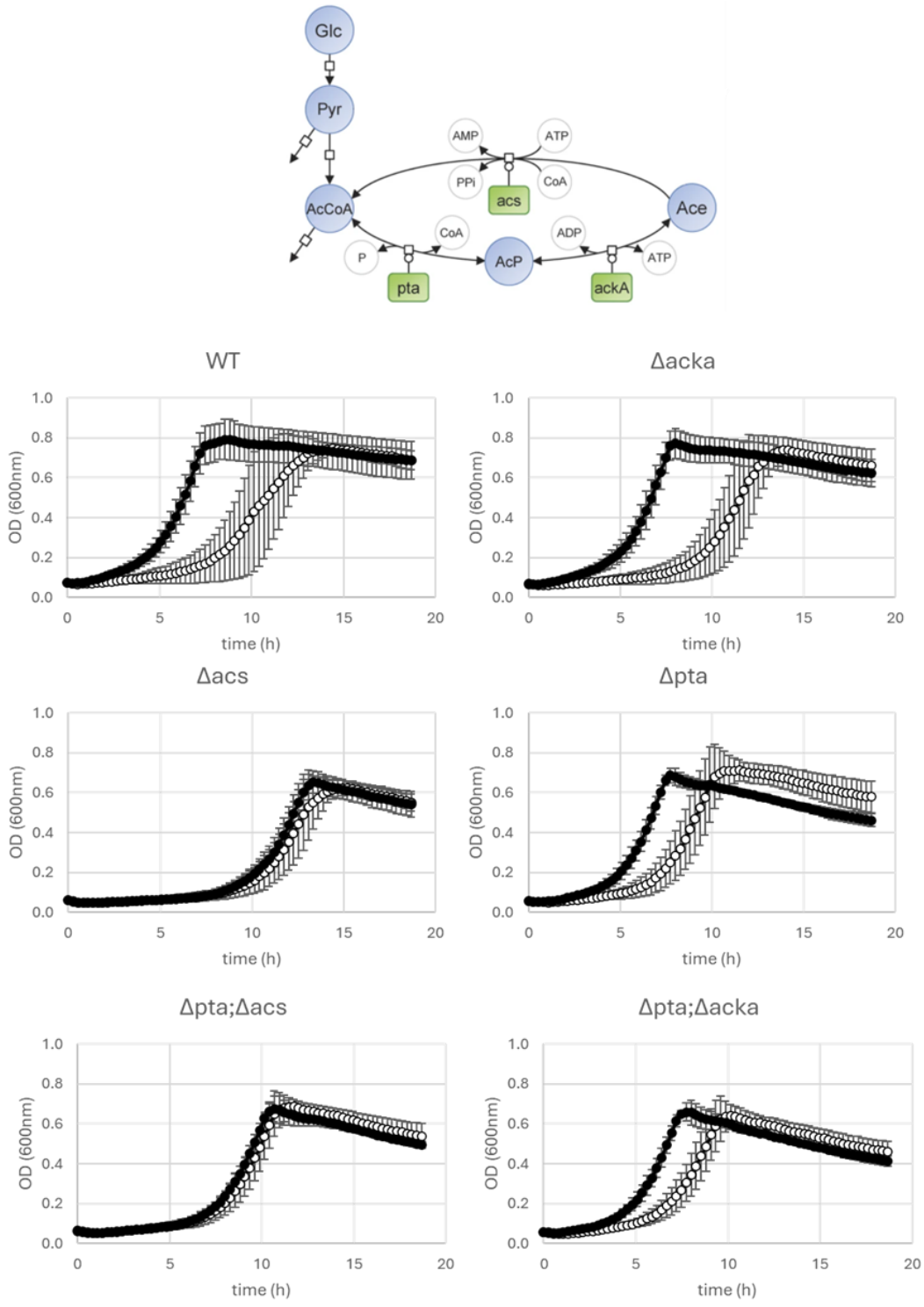


Figure 5: *acs* is necessary to the acetate booster effect. The graphs represent the raw biomass evolution after a switch from N-acetylglucosamine to malate for the wild type strain and various single or double mutants for acetate metabolic pathways (represented on top of the figure), with acetate (black circles) or without acetate addition (open circles).

Acetate allows replenishing the TCA metabolite pools.

The remaining question is how acetate boost metabolic adaptation. To answer this, we performed a metabolomic analysis to found out if acetate modify the intracellular pools of metabolites and/or the energetic content of cells. We found out that acetate significantly increased the pool of acetyl-CoA and citrate early during the adaptation from NAG to malate (Figure 6). Other less significant effects were observed in the TCA and the upper glycolysis. No positive effect were observed on ATP content (Figure 5) or the adenylate energetic charge (Supp. Figure 3). We conclude that acetate act by boosting the acetyl-CoA pool in the first minutes of the switch, repleneshing this way key metabolites pools in the cells to relaunch the central carbon metabolism.

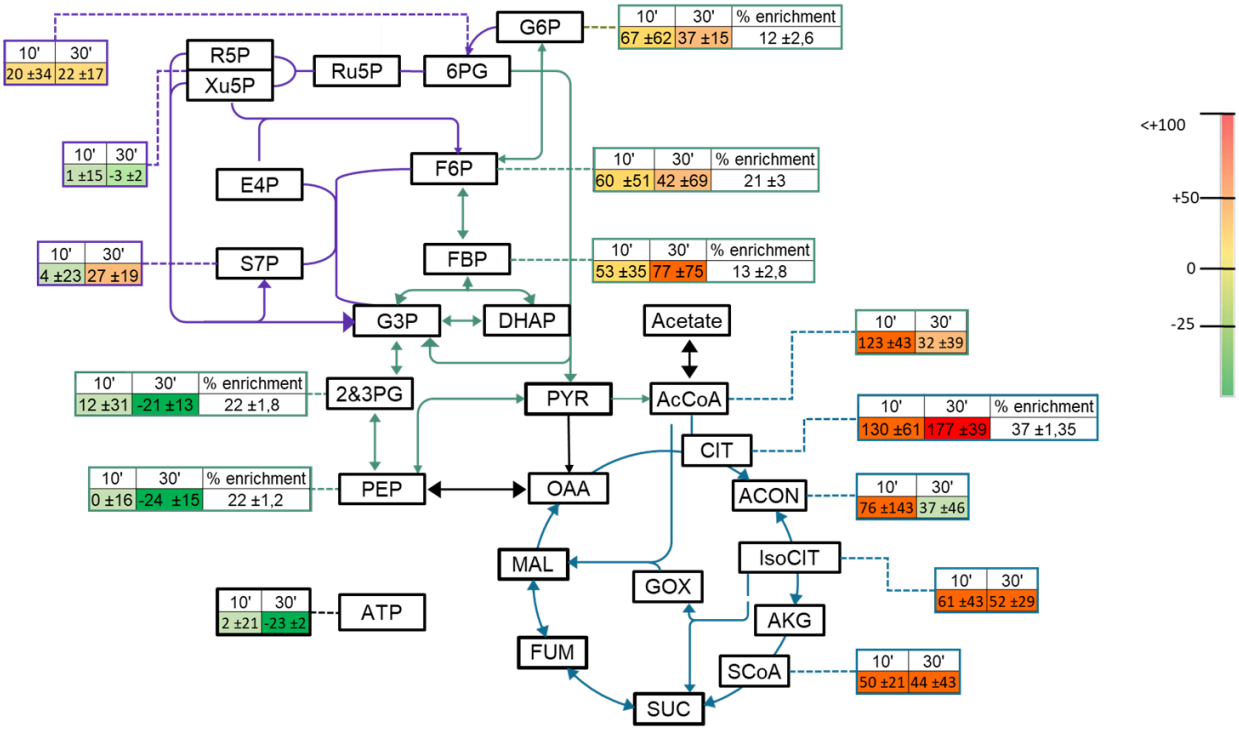


Figure 6: metabolic pools comparison with versus without acetate in the central carbon metabolism. Differences are indicated in term of percentages at 10 and 30 minutes after the switch from N-acetylglucosamine to malate of the wild type strain (color scale with higher content in red, lower content in green and no evolution in yellow). This is the results of three independent experiments. Standard deviation is provided under each value.

Discussion

In this work, we shed a brand-new light on the role of acetate as a facilitator of metabolic adaptation. We demonstrated that very small amounts of acetate are sufficient to promote adaptation to a new substrate. This positive effect is related to the metabolization of acetate by the acetyl-CoA synthetase Acs allowing a rapid replenishing of Acetyl-CoA and hence a faster restart of the central carbon metabolic activity. This incidentally explains why diauxic lags are shorter than switch related lags. A chronology of events can therefore be drawn, with a faster higher expression of Acs after glucose exhaustion, a rapid reconsumption of this acetate to replenish the central pool of acetyl-CoA and from there the other metabolites to prime the central carbon metabolism. These pools likely facilitate the production of the machinery necessary to the next substrate consumption, a step that seems the main lock since the fraction of cells succeeding here could be low depending on the metabolic transition. This fraction of cells will then catabolize the new substrate, proliferate and allow the resuming of growth.

Acetate has a notorious bad reputation because of its acknowledged toxicity in biotechnological processes (ref). We previously described that acetate could act positively on the growth depending on the glycolytic flux rate (Millard *et al.*, 2023). Here again, we highlight another unexpected positive role of acetate, this time on the metabolic adaptation of *E. coli*. One of pour most surprising finding is that what one could consider as mere trace of acetate could have a massive impact on metabolic lags. This reinforces the complex scheme of interplay between acetate and *E. coli*. Our perception is that acetate act as an external carbon reserve for this bacterium, allowing sharing the carbon surplus at the population scale to both facilitates the growth resuming after starvation or during a change of substrate, and to reinforce the growth in conditions not as optimal as a laboratory set-up.

As detailed in the introduction, many parameters have been found out to affect metabolic lags, gene expression, stringent response, energetic levels to mentioned only a few. When we underwent the metabolomic analysis, we were rather convinced to find a difference in energetic level with or without acetate. However, only the carbon apport of acetate seems to prevail here. A previous conclusion of the team of Uwe Sauer stated that the carbon influx rate before the shift is a main determinant of lag duration (Basan Sauer 2020). A conciliating explanation could be that the previous carbon influx rate rather influences the production of acetate, and hence the lag.

In a nutshell, this work has both fundamental and applicative importance. In term of application, our findings offer a very easy way to reduce lag times by simply adding minimal amount of acetate to the new medium. We showed that this lag reduction could be massive and thus with consequences on fermentation process rentability and sustainability.

Fundamentally, it further changes our conception of the relationship between *E. coli* and acetate. Since similar overflow mechanisms exist in yeast (with ethanol) or mammal cells (with lactate), it will be of a tremendous interest to investigate if the boost function of acetate is also observed with other metabolic products in *E. coli* but also for other model prokaryotic and eukaryotic organisms.

Acknowledgements

This work was granted by the ANR project JANUS (ANR-19-CE43-0004-01). TWB (Toulouse White Biotechnology) and its staff members are gratefully acknowledged for allowing us access to their cytometry facilities. C.Graham, S. Méléard and N. Thibeau-Sutre were supported by the Chair « Modélisation mathématique et Biodiversité » of Veolia-Ecole polytechnique-Muséum national d'Histoire naturelle-Fondation X and by a French government grant managed by the Agence Nationale de la Recherche under the Investissements d'Avenir program, reference ANR-18-EURE-0021.

Materials and Methods

Strains and plasmids

All the strains used in this study are listed in Table 1.

Table 1: *Escherichia coli* strains used in the study

Strain	Phylo Group	Description	Source or Reference
BW25113	A	K-12 derivative laboratory strain	(55)
MG1655	A	K-12 derivative laboratory strain	(55)

All the plasmids used in this study are listed in Table 2.

Table 2: Plasmids used in this study

Plasmids	Relevant characteristics	Reference
pSB1C3 mRFP1	Cloning vector of this study. pUC19-derived pMB1 ori, chloramphenicol resistance, with mRFP1(FPbase ID:5YCFA) coding sequence	iGEM part BBa_E1010
pSB1C3 mTagBFP	Cloning vector. pUC19-derived pMB1 ori, chloramphenicol resistance, with mTagBFP (FPbase ID:BFJKS) coding sequence	iGEM part BBa_K592100
pSB1C3 P_{ihfBA}-mTagBFP	pSB1C3 plasmid containing mTagBFP under the control of *ihfB* promoter	This study
pSB1C3 P_{xylA}-mRFP1	pSB1C3 plasmid containing mRFP1 under the control of *xylA* promoter	This study
pSB1C3 P_{xylA}-*mut*-mRFP1	pSB1C3 plasmid containing mRFP1 under the control of a mutated *xylA* promoter, mutations were introduced in xylR binding sites	This study
pSB1C3 P_{xylA}-mRFP1 P_{ihfB}-mTagBFP	pSB1C3 plasmid containing mTagBFP under the control of *ihfB* promoter and mRFP1 under the control of *xylA* promoter	This study
pSB1C3 P_{xylA}	pSB1C3 plasmid containing *xylA* promoter	This study
pMET219	Plasmid pBR322 with tetR but ampR replaced by cmR. Negative control of the plasmid pMET219	Gift from Sébastien Nouaille
pMET219 P_{cysG}-*xylR*	Plasmid pMET219 with tetR replaced by *xylR* under control of *cysG* promoter	This study

All the plasmids based on the pSB1C3 backbone were constructed through digestion and ligation. The *xylA* promoter was obtained by amplification of 800 bp of the regulatory area of the gene upstream of its ATG from genomic DNA of the BW25113 strain. The *xylA* mutated promoter was designed as described in Supplementary data file S5 and obtained as a synthetic gene (Eurofins). E*coR*I and X*ba*I restriction sites at 5 'and S*pe*I restriction site at 3' were used

for cloning on the chassis plasmid. Primers (Supplementary data file S6) were designed from the sequences in the Ecocyc database obtained from Eurofins (France). For the construction of the double fluorescence plasmid, the pSB1C3 P_{ihfBA}-mTagBFP was digested with E*coR*I and *SpeI* to be ligated in the pSB1C3 P_{xylA}-mRFP1 linearized with E*coR*I and X*ba*I digestion. The plasmids based on pBR322 were constructed by DNA HiFi assembly (New England Biolab). Fragments were amplified from *E. coli* DNA or plasmid purification with 20 bp of homology between each fragment. For all constructions, transformants were selected on LB plates containing 40 mg/L of chloramphenicol. The plasmids were checked by sequencing (Eurofins). Plasmids were then transformed into *E. coli* BW25113 strain.

Growth media

The culture were grown in M9 medium containing 33.7 mM Na_2HPO_4, 22 mM KH_2PO_4, 8.55 mM NaCl, 9.35 mM NH_4Cl, 1 mM $MgSO_4$, 0.3 mM $CaCl_2$, 13.4 mM EDTA, 3;1 mM $FeCl_3$-$6H_2O$, 0.62 mM $ZnCl_2$, 76 µM $CuCl_2$-$2H_2O$, 42 µM $CoCl_2$-$2H_2O$, 162 µM H_3BO_3, 8.1 µM $MnCl_2$-$4H_2O$, 1 $\mu g.L^{-1}$ thiamine and carbon sources at 90 mMeqC (100% glucose, 100% xylose, 80% glucose + 20% xylose, 60% glucose + 40% xylose, 40% glucose + 60% xylose, or 20% glucose + 80% xylose). For the culture of strains containing plasmids, M9 medium was supplemented with 20 $mg.L^{-1}$ chloramphenicol.

Lag calculation

The term “lag” is used to describe the time necessary for the cell population to reach exponential phase after an event (Enjalbert Létisse 2015, Barthe Enjalbert 2020, Basan Sauer 2020).

Microplate cultivation

Cells were pre-grown overnight in 5 mL tubes with M9 glucose medium at 37 °C with agitation at 150 rpm. Overnight cultures were centrifuged at 5 000 rpm for 3 min and pellets were suspended in M9 glucose medium or M9 xylose medium at an initial OD_{600nm} of 0.05. The 96-well microplates were inoculated in triplicate with 200 µL of the cell suspensions or 200 µL of medium as control. Microplates with lids were read at OD_{600nm} at 17-minute intervals for 24 h with a Versamax microplate reader (Molecular devices, USA). Maximum growth rates μ_{max} were determined during the exponential growth phase, and estimated using the coefficient of the linear regression of the curve representing ln(OD) versus time.
Regrowth lag times were considered as the difference in time needed to reach the same OD point in the exponential phase between growth with a time lag and growth that started immediately at the maximum growth rate, as defined by Enjalbert (Enjalbert *et al.*, 2015). Diauxic lag was considered as the time lost in comparison to hypothetical growth in which the first exponential phase is immediately followed by a second exponential phase. Formulas and demonstrations of how the lag was calculated are provided in supplementary data file S7.

Statistical validation was based on paired two-tailed Student's t tests, assuming equal or unequal variances according to the F test. Means were calculated from three biological replicates with three technical replicates each (n=9).

Batch cultivation

Bioreactor batch cultures were performed in a Sartorius Biostat B plus bioreactor in 1 L of M9 medium with 90 mMeqC of glucose and/or xylose mixes. The temperature was set at 37 °C and pH at 7. Non-limiting aeration conditions were obtained with an air flow set at 0.35 $L.min^{-1}$ and adaptation of stirring to maintain pO2 > 20%. Growth was assessed by OD_{600nm} measurement at 30-min intervals with a LibraS4 spectrophotometer (Biochrom, UK). Glucose, xylose and acetate concentrations were quantified by HPLC (Agilent, USA) with an HPX 87H Ion exclusion column (Biorad) as described in (Morin *et al.*, 2017).

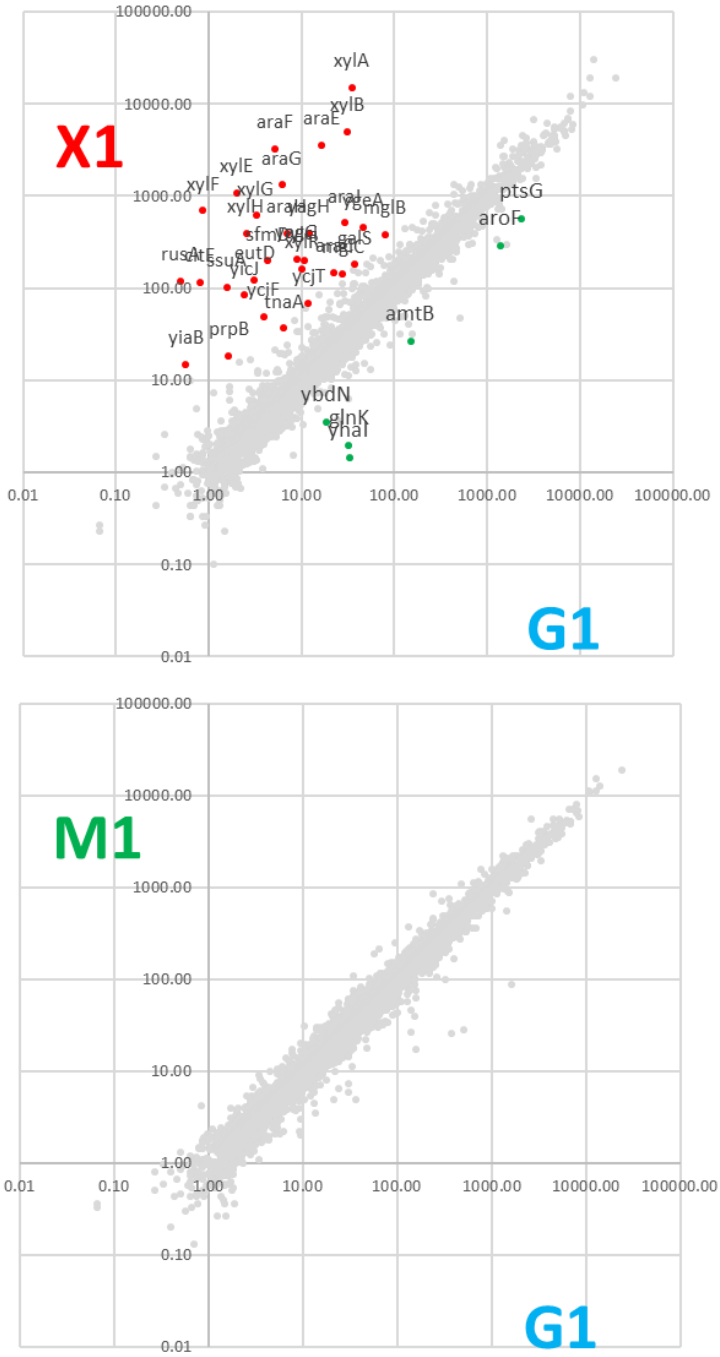
Flow cytometry

Cells were sampled at 30-min intervals and immediately frozen at -20 °C, tests showed that freezing has no influence on the level of fluorescence. After thawing and diluting in filtered 0.9% NaCl to obtain a cell concentration of $1x10^6$ $cells.mL^{-1}$, fluorescence intensities were measured with a Masquant VYB cytometer (Miltenyi Biotec, Germany) equipped with a 561 nm yellow laser for excitation of mRFP1 and a 405nm purple laser for mTagBFP. Data acquisition was set at 40 000 events per sample. FlowJo X software was used for cytometry data analysis. A gate was created in the dot plot of the forward scatter channel (FSC-H) versus the side scatter channel (SSC-H) to distinguish bacteria from technical noise. A second gate was created in the dot plot of the SSC-H versus the SSC-A to select single cells. The mTagBFP fluorescence emissions were analyzed with the V1-H channel (BP450/25nm) and the mRFP1 emissions with the Y2-H channel (BP615/10 nm). The OD600nm subpopulation was extrapolated from the total OD600nm population and the percentage of each subpopulation obtained in flow cytometry, based on blue and red fluorescence.

Mathematical modeling

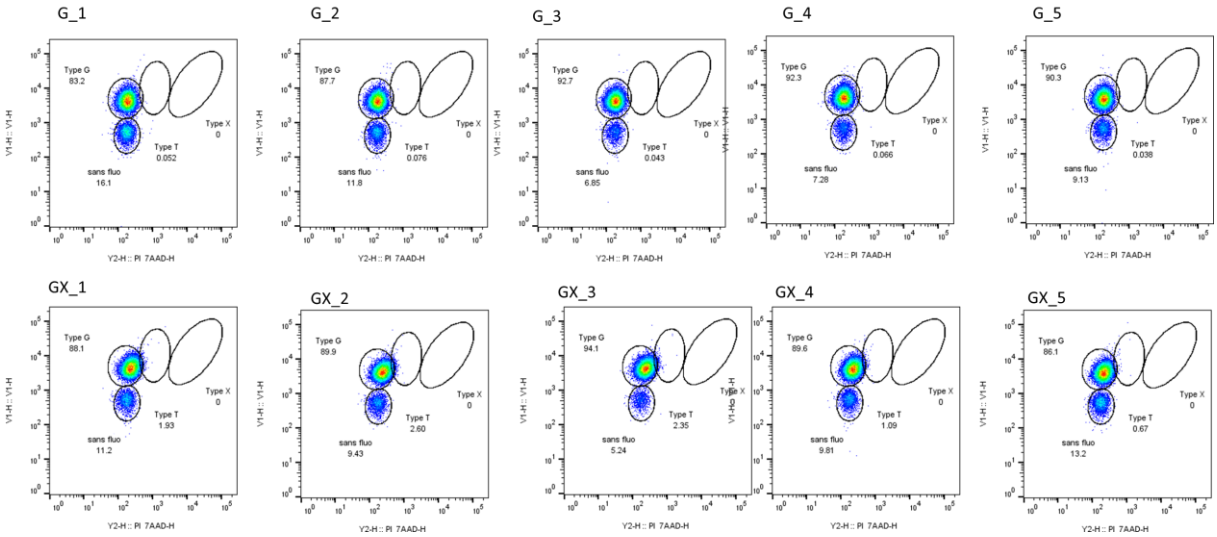
A detailed description of the model, including its rationale, parameters, and code, is provided in supplementary data file S8.

Supplementary data files

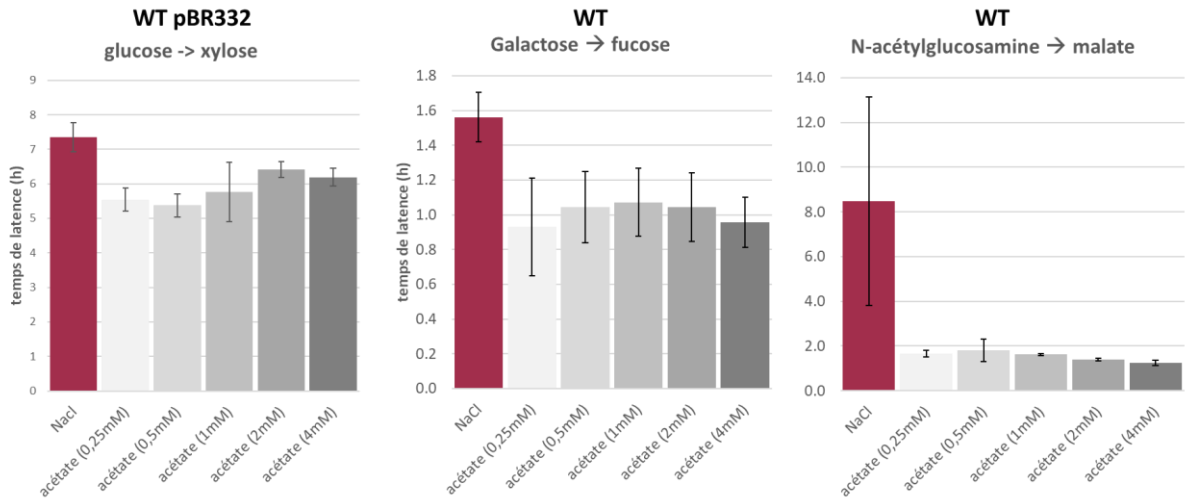


TMM_Fe	commo	M1/G1	Pvalue
b4677	yobI	6.00	1.E+00
b4671	ykgR	5.00	1.E+00
b0989	cspH	4.81	4.E-01
b1729	ydjN	3.46	8.E-01
b2424	cysU	3.35	1.E+00
b2425	cysP	3.28	1.E+00
b3704	rnpA	3.19	1.E+00
b4098	phnJ	3.10	1.E+00
b3088	alx	2.95	1.E+00
b1565	ydfV	2.78	1.E+00
b2423	cysW	2.76	1.E+00
b0365	tauA	2.68	5.E-01
b0113	pdhR	2.65	1.E+00
b4341	yjiS	2.56	1.E+00
b3175	secG	2.38	1.E+00
b3471	yhhQ	2.33	1.E+00
b2422	cysA	2.31	8.E-01
b1821	mntP	2.27	1.E+00
b2912	fau	2.27	1.E+00
b0874	ybjE	2.25	1.E+00
b2886	ygfS	2.22	1.E+00
b0398	sbcD	2.18	1.E+00
b3452	ugpA	2.17	1.E+00
b3565	xylA	2.15	4.E-01
b3568	xylH	2.14	1.E+00
b4177	purA	2.12	1.E+00
b0957	ompA	2.11	1.E+00
b0413	nrdR	2.11	1.E+00
b4062	soxS	2.09	1.E+00
b1689	ydiL	2.08	1.E+00
b4345	mcrC	2.07	1.E+00
b4115	adiC	2.07	1.E+00
b4423	ldrC	2.06	1.E+00
b0446	cof	2.06	1.E+00
b2583	yfiP	2.06	1.E+00
b1433	ydcO	2.05	1.E+00
b0468	ybaN	2.04	1.E+00
b4246	pyrL	2.04	1.E+00
b4557	yidD	2.02	1.E+00
b3633	waaA	2.02	1.E+00
b1627	rsxA	2.02	1.E+00
b2764	cysJ	2.01	1.E+00
b0813	rhtA	2.01	1.E+00
b3707	tnaC	2.00	1.E+00
b3566	xylF	2.00	1.E+00
b2003	yeeT	2.00	1.E+00

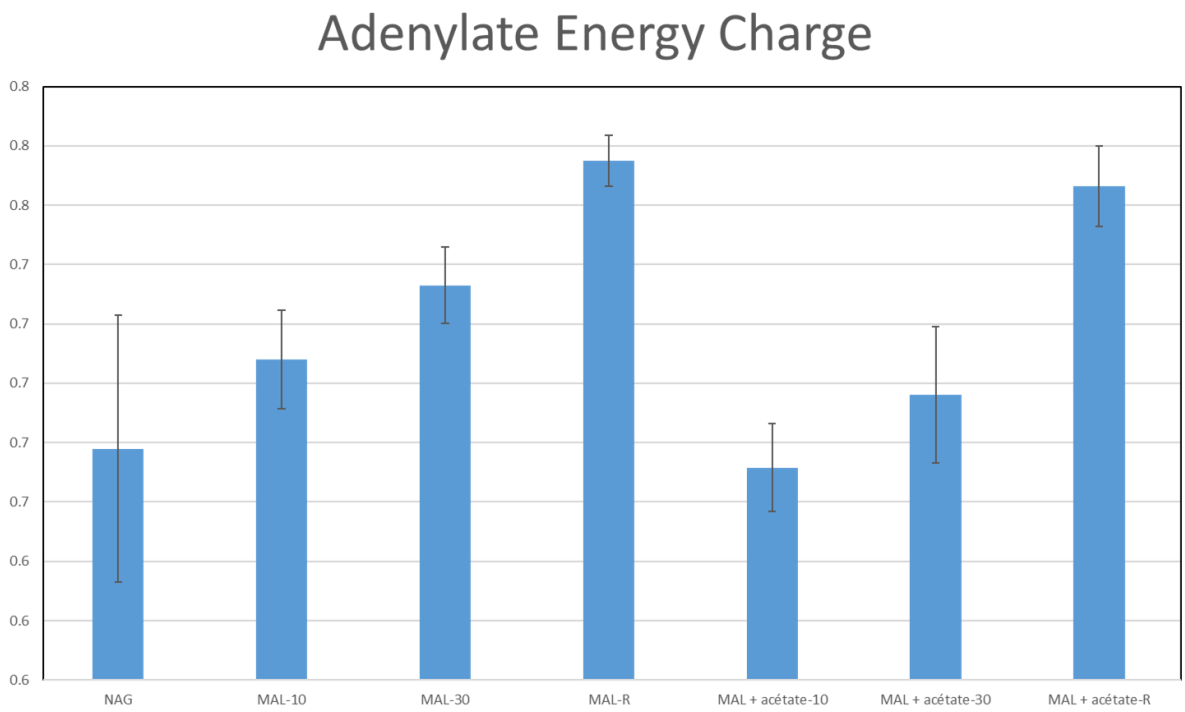
Supplementary Figure 1a: transcriptome of exponentially growing BW25113 strain carrying the pBR322 P*xylA*-mRFP1 plasmid. Upper part: xylose (X) versus glucose (G). Lower part: glucose+xylose (M; during the first exponential phase on glucose) versus glucose (G). Right part: most differentially expressed genes between M versus G. Significativity is provided in the p-value column (none of these genes are significatively differentially expressed).



Supplementary Figure 1b: cytometric profile of BW25113 pBR322-*PxylA*-mRFP1 *PihfB*-mTagBFP cells maintained in exponential phasis on glucose (top lane) **and glucose in presence of xylose** (bottom lane) during X days**.** Cells distributions are represented in two dimensions (x-axis: red fluorescence from inducible mRFP1; y-axis: blue fluorescence from constitutive mTagBFP). Upper left lasso encompassed “glucose signature” cells, upper right lasso for the “xylose signature cells, and the mid one for the cells in transition. The lower lasso corresponds to artefacts and cells having lost the plasmid. One can observe a slight increase in red fluorescent on the substrate mix versus glucose alone.



Supplementary figure 2: acetate promotes metabolic adaptation in Erlen-Meyer flask. Strain BW25113 carrying the titration plasmid pBR322 *PxylA*-mTagBFP was switched from glucose to xylose (left graph). Wild type BW25113 was switched from galactose to fucose (mid graph) or from N-acetylglucosamine to malat (right part). 0 to 16 mM acetate was added in the second medium before adding the cells.



Supplementary figure 3: adenylate energy charge comparison during malate adaptation (wild type strain). NAG: exponential growth on N-acetylglucosamine, MAL-10: 10 minutes after the switch from N-acetylglucosamine to malate. MAL-30: 30 minutes after the switch from N-acetylglucosamine to malate. MAL-R: XXX minutes after the switch from N-acetylglucosamine to malate (i.e, when the cells are resuming growth). Data for the same three conditions but with XX mM acetate addition are represented on the right. This is the results of three independent experiments.

Annex 3: Support for International Mobility 2024 – Report

First Name: Thomas **Last Name:** Gosselin-Monplaisir

Laboratory: University of Basel, department of biomedicine, Mattia Zampieri Lab

Year of PhD: 3rd year

Dates of stay abroad: From 3 of march to 17 of march

Destination: 8, Mattenstrasse, Basel, Switzerland

Initial objectives/ Introduction

Acetate as a Central regulator in *E. coli* Metabolism: Insights and Research Goals

Acetate is one of the most abundant by-products of glycolytic metabolism in *Escherichia coli* (Harden, 1901). Historically, it was considered a toxic compound that inhibits microbial growth (Pinhal *et al.*, 2019). However, our recent studies reveal that acetate can also act as a nutrient, enhancing *E. coli* growth under conditions of low glycolytic flux (Millard *et al.*, 2023). While acetate production remains a significant challenge in industrial biotechnology, it also holds promise as a valuable carbon source in sustainable bioprocesses (Kiefer *et al.*, 2021).

Importantly, *E. coli* resides in highly dynamic environments (Conway and Cohen, 2015), such as the gut microbiota and industrial bioreactors, where it must constantly adapt to fluctuations in availability of acetate and glycolytic substrates. This work aims at understanding the role of acetate in metabolic adaptation of *E. coli* and at providing insight into how *E. coli* adapts to its natural and industrial environments.

Current Understanding of Acetate's Role in *E. coli* Metabolism

Through a systems biology approach that combines isotope labeling experiments with a kinetic model of *E. coli* metabolism, we have demonstrated that glycolytic and acetate metabolisms are tightly interconnected:

- **Co-substrate of Glucose**: At high concentrations, acetate functions as a co-substrate of glucose, exerting regulatory effects on *E. coli* metabolism and physiology, including motility and growth (Enjalbert *et al.*, 2017).
- **Thermodynamic Regulation**: The Pta-AckA pathway, which governs acetate metabolism, is thermodynamically controlled, suggesting that acetate's effects involve direct metabolic regulation (Enjalbert *et al.*, 2017).
- **Gene Expression Regulation**: At high glycolytic flux, acetate downregulates the expression of most glycolytic and TCA cycle genes, potentially explaining its "toxic" effects on growth. Conversely, under low glycolytic flux, acetate positively regulates gene expression and enhances growth (Millard *et al.*, 2021, 2023).

- **Fluxome-Transcriptome Correlation**: Analysis of steady-state transcriptomic and fluxomic data suggests that acetate controls metabolic fluxes via both metabolic and transcriptional mechanisms. Specifically, acetate appears to inhibit gene expression, which in turn reduces protein activity and metabolic flux.

Advancing the Understanding of Acetate Regulation

To unravel the timing and mechanisms of acetate regulation, we developed an innovative approach that simultaneously measures intracellular metabolite and transcript concentrations from a single ~40 µg biomass sample. Using this method, we analyzed the dynamic responses of the *E. coli* metabolome and transcriptome to an acetate pulse during exponential growth on glucose. Transcriptomic analysis (e.g., RNA-seq) was performed at various time points (before and at 2, 5, 10-, 20-, 40-, and 90-minutes post-pulse), revealing significant gene expression changes after 5–10 minutes.

Key Findings:

- The timing of acetate's regulatory effects occurs on the scale of minutes.
- Several previously proposed regulatory mechanisms were ruled out.
- Gaps remain in our understanding of the integrated response of *E. coli* to acetate.

Research Questions to Address

1. What is the regulatory network involved in the response of *E. coli* to acetate?
2. What are the principal targets involved in this response?
3. How *E. coli* adapt to her environment in time?

Research Goals with Mattia Zampieri's Lab

Mattia Zampieri's lab focuses on the adaptation of *Escherichia coli* to changing environments and has developed a diverse set of computational tools to integrate large datasets into models in order to obtain physiological understanding. Three of these tools are particularly valuable for this work:

- **ULM (Univariate Linear Model):** A method designed to infer transcription factors activity from omics data by leveraging prior knowledge through a linear modeling approach. It systematically integrates regulatory interactions and weights to estimate regulator activities, offering a balance between interpretability and performance (Badia-i-Mompel *et al.*, 2022).

- **iSIM (Inference of Similarity by Integrative Modeling):** This computational method compares omics datasets (such as gene expression or metabolomics) to identify similarities. It does this by using statistical tests to detect patterns of shared regulation. In application, it gives a similarity score between different conditions (such as the metabolome at a given time compared to the disruption of a gene, or after addition of a given chemical) (Anglada-Girotto *et al.*, 2022).

- **CCM Kinetic Perturbation Model:** A computational approach that simulates the modulation of central carbon metabolism (CCM) enzyme activity and predicts the resulting dynamics of intracellular metabolite levels. This method provides insights into metabolic adaptations by integrating enzyme kinetics and regulatory interactions.

The goal of this collaboration is to use these tools to deepen our understanding of the mechanisms involved in acetate regulation by integrating the dynamic metabolomics and transcriptomics data already obtained by the MetaSys and Metatoul team.

By addressing these questions, we aim to uncover the regulatory network that governs the response of *E. coli* to acetate. This work will not only provide fundamental insights into the impact of acetate in microbial physiology but also leverage its potential for biotechnological applications.

Results

- Identification of transcriptomic regulatory network

To achieve this, Alexandra Evelyne Huber and Mattia Zampieri suggested me to use a regulon matrix from RegulonDB, which provides information on transcription factors, their target genes, and the directionality of their regulatory effects (activation or inhibition). Following their advices, I refined the matrix by removing poorly defined or conflicting interactions. This included cases where:

- A gene was reported as both activated and inhibited by the same transcription factor.
- The interaction had a low confidence level.

I then applied ULM (Univariate Linear Model) to transcriptomic data at each time point. To assess transcription factor activity, I randomly selected 80% of the regulon matrix and repeated this process 200 times. This allowed me to infer the dynamic activity of transcription factors over time (Figure 1). The t-value of the slope was used as an activity score:

- Positive t-value → Indicates an active transcription factor.
- Negative t-value → Suggests inhibition.

Out of 318 transcription factors in the RegulonDB matrix, I filtered for those with a mean transcription activity above 1. This resulted in 48 transcription factors identified as being involved in *E. coli's* response to acetate.

Most of these transcription factors exhibited activity consistent with previous transcriptomic observations, typically becoming active 5–10 minutes after the acetate pulse. However, one transcription factor, GlaR, showed unexpected behavior: it appeared to be involved immediately at the onset of the acetate pulse.

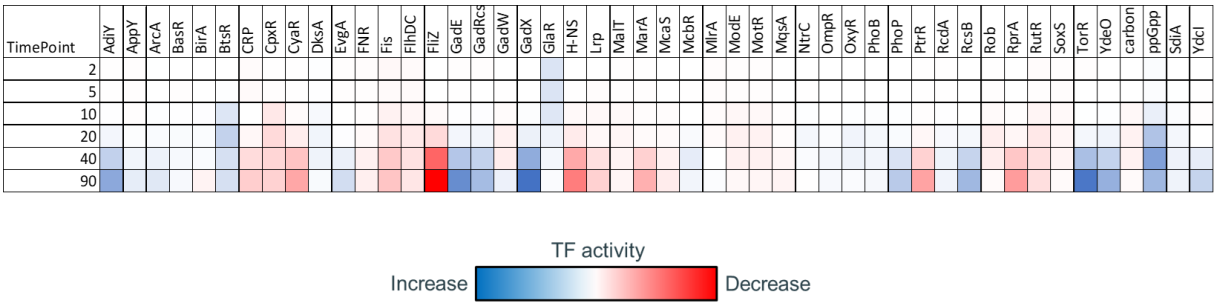


Figure 1. Transcription factors activity inferred from transcriptomics data

Further investigation of these transcription factors could provide valuable insights into the cellular processes underlying *E. coli*'s response to acetate. An interesting next step would be to delete the GlaR gene and assess whether the same response is observed. This experiment could clarify its precise role in the regulatory network and determine whether it has a direct influence on *E. coli*'s adaptation mechanisms to acetate.

- Identification of key targets of *E. coli* response to acetate

In this section I present two strategies tested in order to identify which is/are the main target(s) (eg. metabolite(s), enzyme(s), gene(s)) of the regulation imposed by the acetate pulse.

a) iSIM (Inference of Similarity by Integrative Modeling)

As introduced earlier, iSIM is a tool that evaluates the similarity between different conditions using hypergeometric tests on various types of input matrices. Here, with the help of Laurentz Schuhknecht and Mattia Zampieri, I used iSIM to compare the metabolomic data obtained at each time point to two different reference datasets: the CRISPRi and chemical perturbation banks (Anglada-Girotto *et al.*, 2022). These two datasets were generated by measuring the metabolome of all CRISPRi bank mutants or by exposing the parental strain (BW25113) to a library of drugs.

Figure 2A shows the similarity of each time point's metabolome to that of a CRISPRi mutant library. The Cstle score represents the similarity score multiplied by the p-value (the higher it is, the stronger the similarity). Through this approach, I identified metabolic similarities

between our conditions and several downregulated genes from the CRISPRi bank, including dnaX, ftsH, infB, lptE, lptF, metA, pheT, nusG, and ubiJ. These genes are involved in essential cellular processes such as DNA replication (dnaX), protein synthesis (infB, pheT, nusG), membrane biogenesis (lptE, lptF), and metabolism (metA, ubiJ). The observed similarities suggest that acetate exposure might trigger metabolic responses overlapping with the inhibition of these specific genes. Further investigation into their functions and regulatory networks will help us determine which pathways and targets are most relevant to acetate stress.

Figure 2B presents a comparison of the metabolome at each time point to a chemical perturbation library. While this analysis revealed several chemicals that induce a metabolomic response similar to that of acetate including methyl benzethonium chloride, benzethonium chloride, imipenem, 5-azacytidine, cefpiramide, aminacrine, cladribine, fleroxacin, rifabutin, grepafloxacin, florfenicol, and sulfamethoxypyridazine the underlying molecular links between acetate and these perturbations remain unclear. To refine this approach, we propose applying the iSIM analysis using datasets obtained from different carbon sources to identify acetate-specific responses. Additionally, we plan to investigate common molecular targets among these chemicals using databases such as DrugBank, ChEMBL, and BindingDB, which could provide insights into acetate-related regulatory mechanisms.

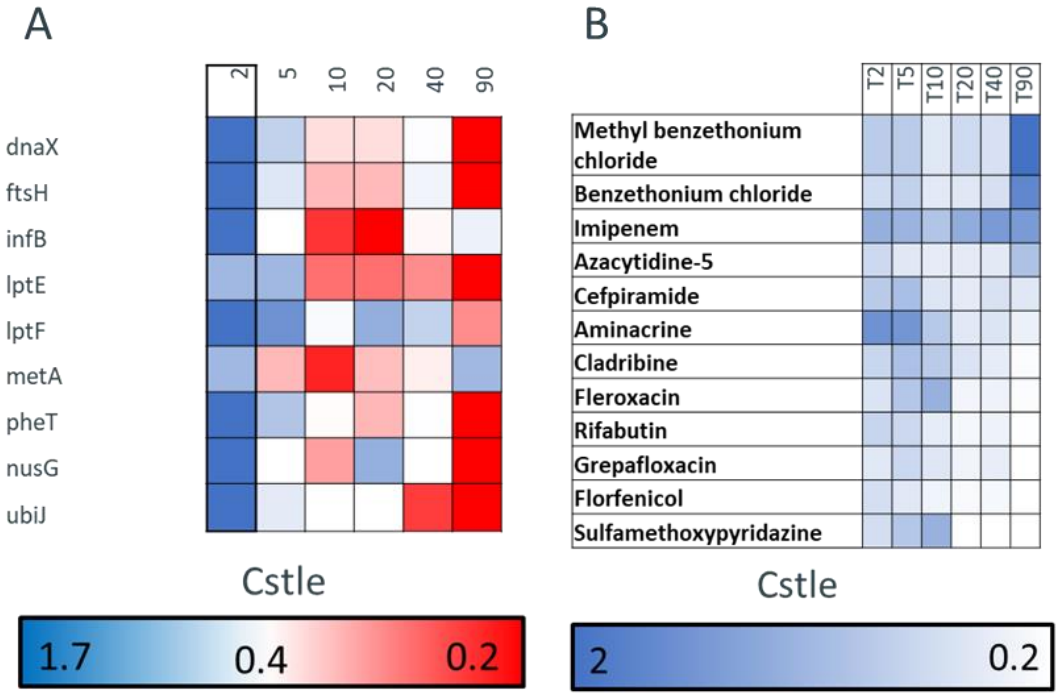


Figure 2 Metabolic similarity between acetate perturbation and gene inhibition or chemical perturbation

A. iSIM results for comparison of metabolome evolution from 2 to 90 min after acetate pulse to the CrisprI bank (DOI:10.1038/s41589-022-00970-3)

B. iSIM results for comparison of metabolome evolution from 2 to 90 min after acetate pulse to the chemical perturbation bank (DOI:10.1038/s41589-022-00970-3)

b) CCM kinetic perturbation model:

The final approach I conducted was testing the **CCM (Central Carbon Metabolism) kinetic perturbation model developed and used in the team by Terezia Dorcakova.** As previously introduced, this model predicts the intracellular evolution of metabolites through iterative modulation of enzyme activity. Using this method, I aim to identify which enzyme inhibition could explain the best our metabolomic experimental results. Since the computational process is time-consuming and I was working within time constraints, we decided with Terezia Dorcakova to focus on two enzymes that were among the most likely to be modulated: **GpmA** and **GapA**.

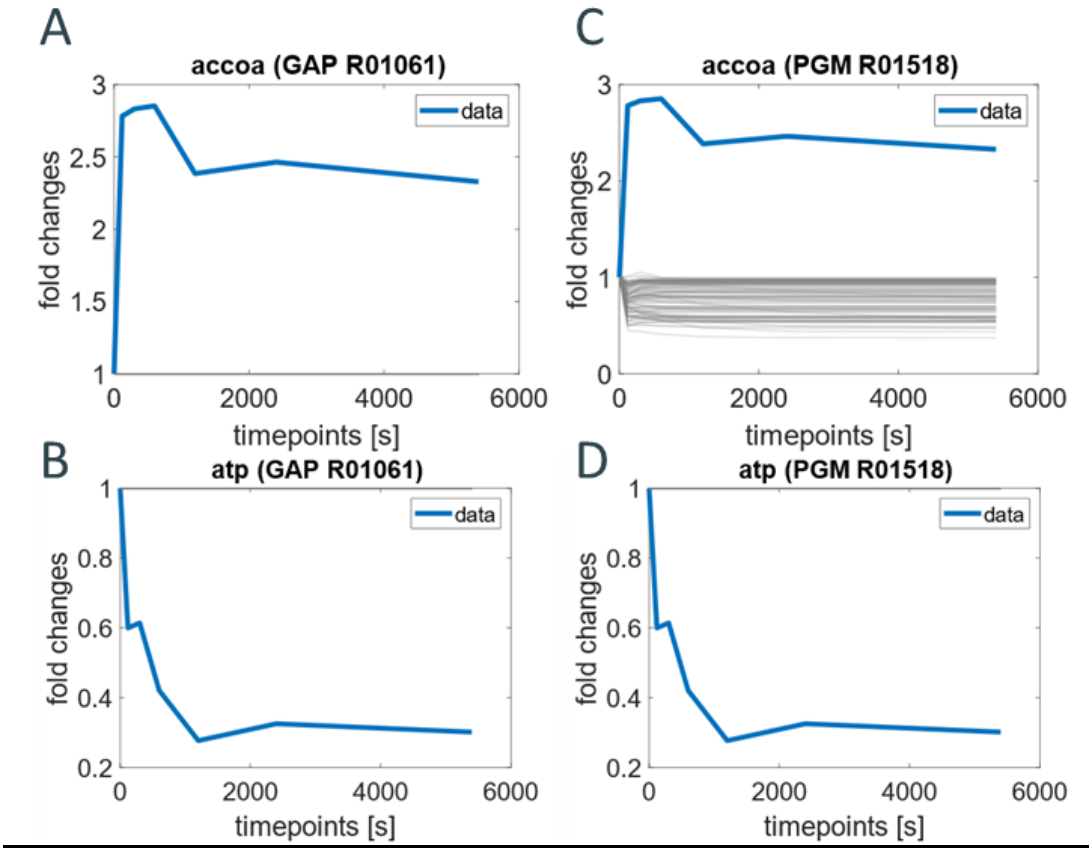


Figure 3 Prediction of metabolites evolution after inhibition of Gap or GpmA vs experimental data after acetate pulse

A,B : Simulated evolution of Acetyl-coA pool or ATP when GAP in inhibited by 80% (blue lines represents experimental data and grey lines represents the model simulations)

C, D: Simulated evolution of Acetyl-coA pool or ATP when GpmA in inhibited by 80% (blue lines represents experimental data and grey lines represents the model simulations)

We so predicted the evolution of all intracellular metabolites across the central carbon metabolism (CCM) network after perturbation of GapA or GpmA. However, for clarity, I presenting only a portion of the data. Despite this, the interpretation of the results remains consistent for each metabolite.

The experimental metabolite evolution (blue line) does not align with the model-based predictions (grey lines). This discrepancy indicates that, using this approach, we cannot conclusively determine whether GapA or GpmA are involved in the regulation.

To improve this analysis, an iterative testing approach for each enzyme in the network would be highly valuable. Additionally, the metabolites currently used in the model represent only 20% of the total metabolites in the network. As suggested by Tobias Fuhrer, expanding the dataset using Orbitrap mass spectrometry to detect more metabolites would help reduce the degrees of freedom in the model, ultimately refining our conclusions. Moreover, a major drawback of this approach is that it involves inhibiting only one enzyme at a time. However, the response to enzyme inhibition is likely a systemic process, engaging multiple enzymes simultaneously.

Extraction of metabolites from raw orbitrap data:

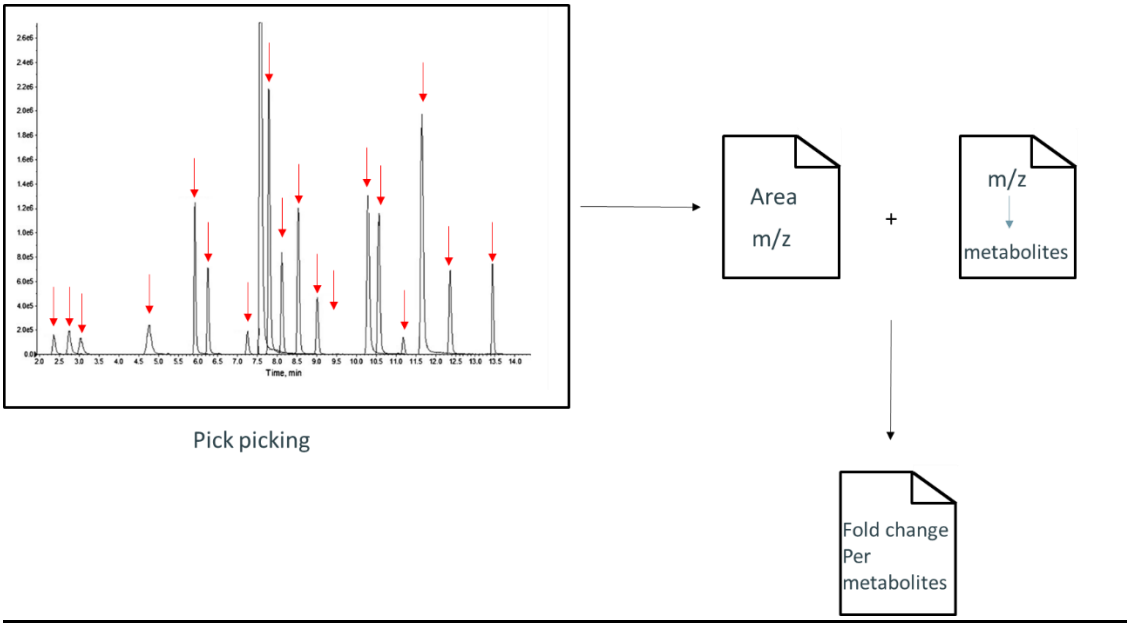


Figure 4: Extraction of metabolites fold change from raw orbitrap data

To enhance the stringency, robustness, and precision of previous tests, we sought to extract as much information as possible from the available mass spectrometry data. To achieve this, I adapted a workflow developed by Tobias Fuhrer for extracting peak areas from Orbitrap mass spectrometry (MS) data.

In earlier approaches, we relied solely on a targeted set of metabolites, which may have restricted the number of metabolites available for similarity and perturbation tests. To overcome this limitation, we aimed to maximize metabolite coverage, allowing us to re-evaluate these approaches with a broader dataset. This expansion would help identify additional targets and strengthen confidence in those already identified.

To support this effort, I developed a Python script that extracts metabolite names based on their m/z values from the detected peaks. This script enables the calculation of fold enrichment for metabolites using the extracted data. However, I was unable to re-run these tests before the conclusion of my stay.

Conclusion

Through a combination of transcriptomic and metabolomic analyses, we investigated the dynamic response of *E. coli* to an acetate pulse. With the help of Alexandra Evelyne Huber and using ULM, we inferred transcription factor activities over time, confirming that transcriptional regulation becomes significant after 5–10 minutes, the transcription factors identified needs to be investigated in order to understand the global regulatory network involved in the response of *E. coli* to acetate. Interestingly, GlaR/CsiR was identified as an early responder, suggesting a potential role in acetate direct adaptation that warrants further investigation.

With the help of Laurentz Schuhknecht, I then applied iSIM to compare metabolomic data with two reference datasets. The first, a CRISPRi mutant library, revealed similarities between key time points and several genes (*dnaX, ftsH, infB, lptE, lptF, metA, pheT, nusG,* and *ubiJ*), highlighting potential regulatory networks. The second, a chemical perturbation library, identified chemicals that induce similar metabolic responses to acetate. Future work will focus on identifying common molecular targets among these chemicals using databases such as DrugBank, ChEMBL, and BindingDB.

Third, with the help of **Terezia Dorcakova**, we tested the CCM kinetic perturbation model to predict intracellular metabolite evolution under enzyme activity modulation. However, experimental data did not align with model-based predictions, preventing us from drawing conclusions about the involvement of GapA and GpmA in acetate regulation. Expanding the dataset using Orbitrap mass spectrometry to detect a broader range of metabolites could refine the model and improve confidence in the identified targets.

Finally, I adapted a pipeline initially developed by Tobias Fuhrer with another Python script to extract metabolite names based on m/z values from MS data, enabling fold enrichment calculations. This tool will facilitate future re-analysis with an expanded metabolite dataset to strengthen our findings.

This mobility stay was a valuable opportunity to advance my PhD project by providing a fresh perspective on acetate regulation in *Escherichia coli*. Scientific discussions and access to new methodological approaches allowed me to explore complementary approaches to the work conducted in my home laboratory.

Beyond scientific progress, this stay also fostered collaborative interactions with the host team, paving the way for future joint projects. This dynamic could lead to collaborative research efforts and, on a personal level and open opportunities for a postdoctoral position.

Acknowledgements:

I would like to express my sincere gratitude to all those who contributed to this collaboration.

First, I extend my thanks to EurBioeco for funding this mobility. I am also deeply grateful to Pierre Millard and Stéphanie Heux for their invaluable supervision.

A special thank you to Mattia Zampieri and the University of Basel for their warm welcome, supervision, availability, and guidance throughout this project. I also appreciate Alexandra Evelyne Huber for her hospitality, insightful advice, access to resources, and keen interest in the project.

A big thank you to Tobia Fuhrer for both his resource allocation and his (occasional) French bashing! Finally, I would like to acknowledge Laurentz Schuhknecht for his valuable assistance in using MATLAB scripts.

References:

Anglada-Girotto, M. *et al.* (2022) 'Combining CRISPRi and metabolomics for functional annotation of compound libraries', *Nature Chemical Biology*, 18(5), pp. 482–491. Available at: https://doi.org/10.1038/s41589-022-00970-3.

Badia-i-Mompel, P. *et al.* (2022) 'decoupleR: ensemble of computational methods to infer biological activities from omics data', *Bioinformatics Advances*. Edited by M.L. Kuijjer, 2(1), p. vbac016. Available at: https://doi.org/10.1093/bioadv/vbac016.

Conway, T. and Cohen, P.S. (2015) 'Commensal and pathogenic *Escherichia coli* metabolism in the gut', *Microbiology Spectrum*. Edited by T. Conway and P. Cohen, 3(3), p. 3.3.24. Available at: https://doi.org/10.1128/microbiolspec.MBP-0006-2014.

Enjalbert, B. *et al.* (2017) 'Acetate fluxes in *Escherichia. coli* are determined by the thermodynamic control of the Pta-AckA pathway', *Scientific Reports*, 7(1), p. 42135. Available at: https://doi.org/10.1038/srep42135.

Harden, A. (1901) 'LXIV.—The chemical action of *Bacillus coli communis* and similar organisms on carbohydrates and allied compounds', *Journal of the Chemical Society, Transactions*, 79(0), pp. 610–628. Available at: https://doi.org/10.1039/CT9017900610.

Kiefer, D. *et al.* (2021) 'From acetate to bio-based products: underexploited potential for industrial biotechnology', *Trends in Biotechnology*, 39(4), pp. 397–411. Available at: https://doi.org/10.1016/j.tibtech.2020.09.004.

Millard, P. *et al.* (2021) 'Control and regulation of acetate overflow in Escherichia coli', *eLife*, 10, p. e63661. Available at: https://doi.org/10.7554/eLife.63661.

Millard, P. *et al.* (2023) 'Acetate is a beneficial nutrient for *E. coli* at low glycolytic flux', *The EMBO Journal*, 42(15), p. e113079. Available at: https://doi.org/10.15252/embj.2022113079.

Pinhal, S. *et al.* (2019) 'Acetate metabolism and the inhibition of bacterial growth by acetate', *Journal of Bacteriology*. Edited by W.W. Metcalf, 201(13). Available at: https://doi.org/10.1128/JB.00147-19.